BEHAVIOUR AND UPTAKE OF ENGINEERED GOLD NANOPARTICLES IN AQUATIC SYSTEMS

SUJUNG PARK

PhD

University of York

September 2014

Abstract

Nanotechnology is a rapidly growing industry of global economic importance. However, there is concern that the unique properties of engineered nanoparticles (ENPs) which can make them useful to society could mean that they pose a risk to the natural environment. There are still many uncertainties around the behaviour of ENPs in aquatic systems, their capacity to be taken up by aquatic organisms, and their potential toxic effects. This study therefore used four different surface functionalised gold (Au) nanoparticles as exemplars and explored their behaviour in various aquatic systems and their uptake into aquatic organisms. Studies into the behaviour of the study ENPs in standardized ecotoxicity test media showed that the particles exhibit very different aggregation behaviour depending on the test media type, the chemical composition of the test media and surface capping of the nanoparticles. Based on the results of the aggregation studies in a range of natural waters, a series of methods to predict size of Au particles in different water chemistries were developed. Results showed that there would likely be big differences in the aggregation of the different Au nanoparticle types in UK water types which implies that aggregation of ENPs will vary widely across surface waters. The uptake of the four Au nanoparticles into the aquatic invertebrate, *Gammarous pulex*, did not show obvious relationship between the aggregation state in a treatment and uptake suggesting that the widely accepted assumption that ENP uptake is related to particle size does not hold for the range of aggregation states studied. The results of this thesis showed that the degree of aggregation of ENPs and uptake into aquatic organisms would vary depending on the surface functionalisation of the ENPs and water chemistry. The results imply that aggregation of ENPs will vary widely across surface waters which make assessment of risks a challenge. Additionally, the uptake data indicate that factors other than particle size determine uptake of ENPs into organisms. Therefore, it may be necessary to develop new paradigms and models for risk assessment of ENPs.

List of contents

List of Tables

List of Figures

Acknowledgments

I would like to thank the numerous people who have support me during the course of this thesis and were instrumental in its success and completion. First, and foremost, I would like to say huge thank you to my best supervisor Prof. Alistair Boxall who led me to complete successful PhD. Your encouragement and consistently positive outlook were a true inspiration to me and were the major driving force behind this study. I also would like to thank James Woodhall at FERA who helped me to get the fund and made possible to continue my PhD.

Next, I would like to thank past and present group members who supported and helped me in many ways; Rungnapa Tagun, Tom Bean, Samuel Thompson, Dr. Laura Cater, Dr. Agnieszka Dudkiewicz, Dr. Beatrice Hernout, Dr. Annika Agatz, Jiahua Guo, Shuo Sun and Kyoduk Koo.

I also appreciate Prof. Kyungho Choi and his group, ENVITOX at Seoul National University for their support and encouragement.

Great thanks to all members of Korean church and Pastor Sunjin Kim and his wife, Hyeyouen Jo for the spiritual support.

I would like to great thank you my family, my dad and mum, my brother Byoungchul Park, sister-in-law, Eunseon Oh and my lovely niece and nephew, Haewon Park and Hyunsuk Park. Without your unconditional support and understanding, it was absolutely impossible to finish this long journey for PhD. I owe many thanks to you.

Author's declaration

The work in this thesis was undertaken as a PhD student at University of York. This research was by partly supported by the seed corn funding from the Department of Environment, Food and Rural Affairs, UK. Additional funding was provided by the Cefic Long Range Research Initiative under Project N2 'Fate and uptake of engineered nanoparticles in aquatic systems'.

The papers (Chapter 2 to chapter 5) have been written by the candidate as leading author. However, it should be noted that the papers have gained in quality through suggestions, advice and editing from the co-authors. Chapter 2 and Chapter 5, which are published papers, have also benefited from the comments of the anonymous referees as part of the review process. The candidate has co-authorship on the paper presented in the appendices.

Table 1. Status of the papers presented in this thesis with respected to the publication process

Chapter	Authors	Title	Status	Journal
2	**Park S**, Woodhall J, Ma G, Veinot JG, Cresser MS, Boxall AB.	Regulatory ecotoxicity testing of engineered nanoparticles: are the results relevant to the natural environment?	Published	Nanotoxicology, 2014, 8(5):583-592
3	Park S, Woodhall J, Thompson SR, Ma G, Veinot J G, Cresser MS, Boxall AB.	Aggregation of metal nanoparticles in the environment: does the core matter?	In preparation	
4	Park S, Woodhall J, Williams RJ, Ma G, Veinot JG, Cresser MS, Boxall AB.	Estimating the Aggregation Behaviour of Functionalised Gold Nanoparticles in Natural Waters	In preparation	
5	**Park S**, Woodhall J, Ma G, Veinot JG, Cresser MS, Boxall AB.	Does particle size and surface functionality affect uptake and depuration of gold nanoparticles by aquatic invertebrates?	Accepted	Environmental Toxicology and Chemistry
Appendix 1	P Luo, I Morrison, A Dudkiewicz, K Tiede, E Boyes, P O'Toole, **S Park**, A B Boxall	Visualization and characterization of engineered nanoparticles in complex environmental and food matrices using atmospheric scanning electron microscopy.	Published	Journal of Microscopy, 2013, 250 (1): 32-41

Chapter 1

Review: Occurrence, behaviour and ecotoxicity of engineered nanoparticles in aquatic environment

Introduction

Nanotechnology uses engineered nanoparticles (ENPs) which are manufactured to have specific properties and which have at least one dimension less than 100 nm (SCENIHR, 2005, Nowack and Bucheli, 2007; Christian *et al.*, 2008). The small size of ENPs gives a large mean surface area, high reactivity and potentially a high surface charge. These unique properties have allowed ENPs to be used in a wide range of industrial applications (Farré *et al.*, 2009). For example, nano-textiles synthesised with titanium dioxide (TiO_2) nanoparticles or carbon nanotubes (CNTs) are applied in waterproof sports or outdoor clothing (Siegfried and Som, 2007). Application of nanotechnology in the sports field provides ultralight and high strength sports equipment made of carbon nanotubes (Esawi and Farag, 2007). TiO_2 and zinc oxide (ZnO) become transparent to visible light when formed at the nanoscale; however, they are able to absorb and reflect UV light, so these are currently being used in sunscreens and in the cosmetic industry. Nanotechnology could be applied in the elimination of pollutants and for water remediation. The development of nanotechnology allows us to do new things in almost every conceivable technological discipline.

As the markets for nanotechnology grow the production volume of ENPs is also increasing. For example, it was reported that the total annual production of nickel (carbon-coated) powders was 3,500 tonnes/year between 2006 and 2007 and this was expected to increase by at least three times by 2014 (UNEP, 2007). Potential production of TiO_2 is likely to be almost 2.5 million metric tons per year by 2025 (Robichaud $et\ al.$, 2009). With the increasing use of ENPs, there is increased likelihood of their release to the environment. Concerns about their safety and the potential risks posed to human health and the environment have therefore been raised by many (Banfield and Zhang, 2001; Simonet and Valcarcel, 2009). Consequently, the public are now aware of nanotechnology meaning that quantification and regulation of the risks are a priority (Seaton $et\ al.$, 2009). The U.S. Environmental Protection Agency (EPA) is currently developing and combining regulatory interventions such as the Toxic Substances Control Act (TSCA), as one key scheme to regulate nanotechnology (Gibson and Pula, 2009). Under TSCA, EPA intends to publish a significant new use rule (SNUR) for certain, as yet undetermined, nanoscale materials (nanoscale silver, TiO_2, and ZnO). This rule asks to provide not only specific information concerning production volumes, methods manufacture and processing but also health effects, ecological effects, and environmental fate (Sayre $et\ al.$, 2011). The European Chemical Agency has attempted to control uses of ENPs under the REACH (Registration, Evaluation, Authorization and Restriction of Chemicals) regulation number EC 1907/2006 (European Commission, 2006). Under the REACH regulation, information of physico-chemical properties, human health effects, environmental effects and environmental fate of a substance should be provided in order to register a substance. However, for nanomaterials, not only data requirements for the substance but also information on the specific properties of the substances at nanoscale including size, number concentration, surface area, charge and overall surface reactivity and aggregation/agglomeration status may be required (Emerging and Risks, 2007). The inclusion of ENPs in the regulations indicates that the human health and environmental risk are major issues to be discussed and the safety of ENPs could be a crucial factor

of trade restrictions or global communication after enforcement of the regulation. There are various regulations for ENPs but environmental data; namely data on the fate, exposure and hazard/risk are yet to be properly quantified and knowledge is still lagging far behind. Therefore, in this introduction, an overview of types of ENPs and the occurrence and behaviour of ENPs in the aquatic environment is provided, followed by a summary of potential effects on aquatic organisms. Finally, the main aims and objectives of the research performed in this thesis are defined.

Types and properties of engineered nanoparticles

Types of engineered nanoparticles

Fullerenes and carbon nanotubes

A fullerene is any molecule composed of carbon. Carbon-based nanomaterials are well known carbon allotropes including a hollow sphere or a tubular structure (Aitken *et al.*, 2006). Spherical fullerenes are known as buckminster fullerenes or 'buckyballs'. Fullerenes have chemically and thermally stable properties so they can be used in several different applications. They can be dissolved in solvents, purified, functionalized, sublimed, polymerized, or act as excellent electron acceptors (Murayama *et al.*, 2005). If fullerenes are functionalized with more hydrophilic functional groups such as -OH, -COOH, and $-NH_2$, the biological and pharmacological activity could be increased so these materials could be used in medical and pharmaceutical applications (Bosi *et al.*, 2003). Following the discovery of fullerenes, CNTs have been in the spotlight as an impressive nanomaterial. CNTs are fibrous fullerenes composed of rolled-up graphene sheets and are capped with pentagonal carbon rings (Terrones, 2003; Ajayan and Zhou, 2001). There are two types of carbon tubes: single-walled nanotubes (SWNTs) which consist of a single layer or individual cylinders of 1-2 nm diameter and multi-walled nanotubes (MWNTs) which have multiple concentric tubes. CNTs are not only lightweight but also have high tensile strength and unique electronic properties (Aitken

et al., 2006). The main applications of CNTs include use in electrochemical devices, microelectronics industry, energy storage (e.g. Li-ion batteries, solar cells and fuel cells) and sensing elements utilizing their electrical, electrochemical or optical properties (Endo *et al.*, 2008).

Quantum dots

Quantum dots (QDs) are spherical nano-sized (2-10 nm) crystals. QDs are semiconductors with characteristics closely related to the size and shape of their individual crystals. QDs have a colloidal core enclosed by one or more surface coating shell which helps to improve their optical properties and solubility in aqueous media (Zhang and Monteiro-Riviere, 2009; Ghasemi *et al.*, 2009). QDs can emit light at different wavelengths due to their size and chemical composition. These unique fluorescence properties of QDs coupled with their surface functionalisation make them useful in cell imaging, immunohistochemistry, and cancer targeting (Ghasemi *et al.*, 2009). Other applications of QDs include imaging and therapeutic functions. Many researchers are exploring the use of QDs for drug delivery and to aid the understanding of pharmacokinetics in cells and animals (Qi and Gao, 2008).

Metal and metal oxide nanoparticles

Metal and metal oxide (MeO) nanoparticles are normally categorized as single element (e.g. silver (Ag), gold (Au), Copper (Cu), iron (Fe), *etc,*), compounds (e.g. silicon carbide (SiC), silicon nitrade (Si_3N_4), *etc.*) and single metal oxides (e.g. Aluminum oxide (Al_2O_3), TiO_2, ZnO, Cerium Oxide (CeO_2), *etc.*) (Joner *et al.*, 2008). MeO nanoparticles can be synthesized from a variety of materials in different shapes and sizes, resulting in nanoparticles with a range of different physical properties. Additionally, MeO nanoparticles have been reacted with polymers, ligands, ionic liquids to assist with stabilization (Bigall and Eychmüller, 2010; Chaudret and Philippot, 2007) so these are regarded as useful materials in many chemical industries. TiO_2 and ZnO nanoparticles

are used in sunscreens, cosmetics, and bottle coatings because of their ability to block ultraviolet light (Klaine *et al.*, 2008; Chaudret and Philippot, 2007). CeO_2 is used as a combustion catalyst in diesel fuels to improve the quality of the emissions. CeO_2 nanoparticles are also used in solar cells, gas sensors, oxygen pumps and metallurgical and glass/ceramic applications (Chaudret and Philippot, 2007; Park *et al.*, 2008). Ag nanoparticles are used in fabric softeners, washing machines and toothpaste for their antimicrobial activity properties (O'Brien and Cummins, 2011). Au nanoparticles are applied to biological imaging, electron microscopy and therapeutics due to their plasmon resonance properties (Rayavarapu *et al.*, 2007; Jain *et al.*, 2008; Murphy *et al.*, 2005).

Dendrimers

Dendrimers are particles which have diameters ranging from 2 to 10 nm. Dendrimers are based on a class of polymeric materials comprising an inner core molecule surrounded by a series of branches. Due to the molecular composition of dendrimers, they have improved physical and chemical properties (Klajnert and Bryszewska, 2001; Sakthivel and Florence, 2003). The special magnetic, optical, and electronic properties of dendrimers means they are well suited to biomedical applications such as use as an active therapeutic agents, as vectors for targeted delivery of drugs, or as peptides and oligonucleotides (Bronstein and Shifrina, 2009; Duncan and Izzo, 2005).

Properties of engineered nanoparticles

ENPs have special functionalities such as high chemical stability, hydrophobic or hydrophilic properties which make them different to the bulk material of the same chemical composition (Wigginton *et al.*, 2007). Additionally, properties such as particle size, shape, surface charge and associated changes in surface charge and modified electronic characteristic make ENPs novel and important.

The small size and large surface area of ENPs is the main characteristic that distinguishes ENPs from other materials. ENPs have greater specific surface area than material made out of ordinary material of the same chemical composition. The specific surface area is the ratio of surface area to the mass (Aitken *et al.*, 2006). The surface area of ENPs increases dramatically as particle size decreases because of reactive sites on the surface of ENPs (Suttiponparnit *et al.*, 2011; Navarro *et al.*, 2008a). The reactivity of ENPs is increased by a higher ratio of surface-to-core atoms and a greater number of corner and edge atoms (Feldheim, 2007). Reactivity of ENPs and surface properties can be exploited by manufacturers for use in a variety of consumer products (Stone *et al.*, 2010).

The morphology of ENPs is an important factor in determining the properties of an ENP due to changes in colloidal stability and composition of the materials themselves (Qu *et al.*, 2004; Christian *et al.*, 2008). For example, the shape of ENPs can affect shape dependent toxicity to organisms (Chithrani *et al.*, 2006; Simon-Deckers *et al.*, 2009). Chithrani *et al.* (2006) observed rod shaped nanoparticles were less taken up due to larger contact area with the cell membrane receptors than the spherical nanoparticles.

The surface properties of ENPs can be functionalized with small molecules, surfactants or polymers (Christian *et al.*, 2008). The surface property is the most important factor in determining ENP behaviour due to the way it affects how ENPS interact within organisms and how the ENP behaves in the environment (Nowack and Bucheli, 2007; El Badawy *et al.*, 2011). Surface properties also affect surface area, charge at the surface and any surface modifications (Jiang *et al.*, 2009a). Therefore, the surface property of ENPs is a very important factor which must be considered in risk assessments for human and environmental health.

Occurrence and behaviour of engineered nanoparticles in the aquatic environment

Occurrence engineered nanoparticles in the aquatic environment

ENPs can be released into air, soil and aquatic systems either during the manufacturing process, during product use or when their use has ended through either accidental or deliberate release. For example, Ag nanoparticles can be released from textiles during washing and then enter sewage systems. Once the sewage is treated, the nanoparticle can potentially enter aquatic environments in wastewater effluents (Benn and Westerhoff, 2008; Geranio *et al.*, 2009). Large quantities of TiO_2 nanoparticles in paints can be washed from the exterior of buildings by rainfall and end up in surface waters. Weathering and photochemical and oxidation reactions can further contribute to the release of TiO_2 from paint into the environment (Kaegi *et al.*, 2008).

The pathways releasing ENPs to the environment are interconnected (Figure 1). Understanding the pathways of ENPs between each environmental compartment could be difficult. However, what we do know is that the aquatic environment is likely to be the sink where a large number of ENPs end up; therefore understanding the sensitivity of aquatic organisms to ENPs is a key knowledge gap that needs to be bridged (Schaller and Fan, 2009; Scown *et al.*, 2010; Farré *et al.*, 2009).
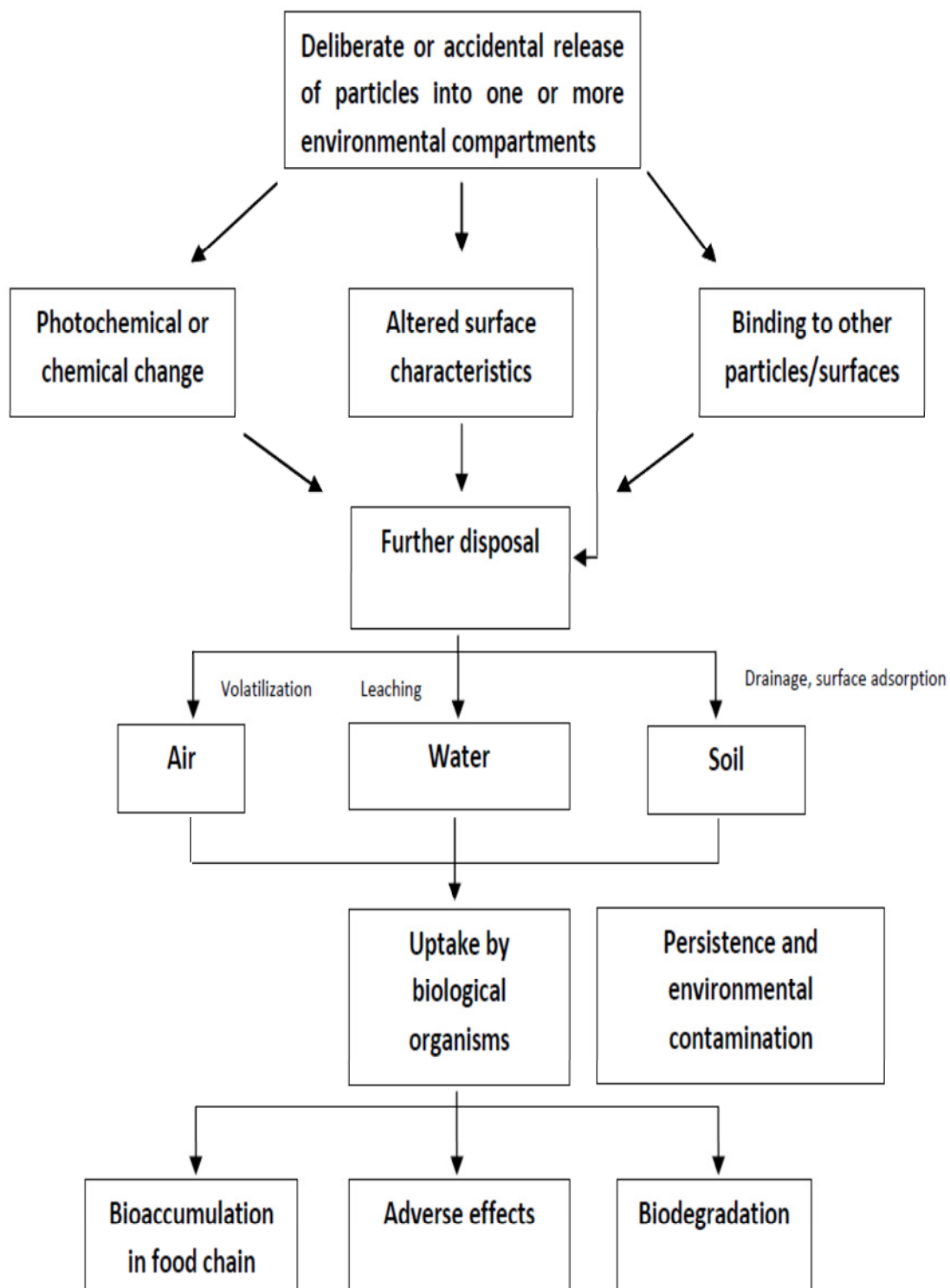
Figure 1. Fate of nanoparticles in the environment (SCENIHR, 2005).

Although the aquatic environment is a compartment of importance for ENP risk, the lack of suitable analytical methods makes determining concentrations of ENPs in the aquatic environment difficult (Hassellöv *et al.*, 2008). To this end, there have been a number of predictive modelling approaches developed to predict environmental concentrations of ENPs (Table 2). For example, Mueller and Nowack (2008) calculated the predicted environmental concentrations (PECs) of Ag nanoparticles, TiO_2 nanoparticles and carbon nanotubes (CNT) using a realistic exposure scenario and a high exposure scenario including worst-case assumptions. The PECs for CNTs, Ag nanoparticles, and TiO_2 nanoparticles ranged from 0.0005 to 0.0008 µg/L, 0.03 to 0.08 µg/L and 0.7 to 16 µg/L, respectively. Gottschalk *et al.* (2010) used Monte Carlo and Markov Chain Monte Carlo simulations combined with sensitivity and uncertainty analysis to derive PECs for Ag nanoparticles, TiO_2 nanoparticles and CNT. The model assumed that the most dominant ENPs transfers were from products to sewage treatment plants (STP), waste incineration plant (WIP) and landfill sites. In surface waters, the PECs for these ENPs were up to 0.021 µg/L. For STP, PECs were much higher than surface waters (up to 4.3 µg/L). Boxall *et al.* (2007) estimated potential concentration of metal nanoparticles and metal oxdie such as aluminium oxide (AlO_3 nanoparticles), silica oxide (SiO_2 nanoparticles) and ZnO nanoparticles and calculated PECs up to 76 µg/L in surface water under the modelling. While the data generated by these studies will understandably include many limitations, they provide a good starting point for predicting exposure concentrations of ENPs in the aquatic environment. The main limitations of the modelling studies include the uncertainty of estimating and quantifying the production of ENPs in a year, as no quantitative data are available on ENPs emissions during manufacturing process. In addition, the lack of data on dispersion states for ENPs in the environment is a major limitation of the models which potentially could lead to large discrepancies between the modelled and measured values. Research efforts need to focus on quantifying these factors which are at present unknown but potentially could play a major role in deciding the fate of ENPs in the environment.

Table 2. Predicted Environmental Concentrations of Engineered Nanoparticles in surface waters

	Silver Nanoparticle	Titanium dioxide	Carbon nanotube
STP effluent[1]	0.0298-0.127	3.5-16.3	0.0076-0.0191
STP[2]	2-18	N.A	N.A
Surface water[1,3,5]	0.56×10^{-4} - 0.08	0.016 – 24.5	0.28×10^{-6} - $0.000.810^{-3}$
River water[2,4]	0.04 - 0.32	0.25	N.A

µg/L. NA= no data available,

1) Gottschalk *et al.* (2010),

2) Blaser *et al.* (2008),

3) Mueller and Nowack (2008)

4) Johnson *et al.* (2011)

5) Boxall *et al.* (2007)

Behaviour of engineered nanoparticles in aquatic suspensions

Specific functionalised capping agents such as inorganic or organic compounds can be applied to ENPs to enhance their stability and mobility in suspension (Ju-Nam and Lead, 2008). However, due to the interactions between the surface properties of ENPs and the chemical properties in the aquatic environment, they can change formation or dispersion status once in the environment. This change in formation or dispersion status could be due to aggregation, which is an attachment via particle-surface and particle-particle interactions, adsorption and dissolution, which is transformation of the nanoparticulate form of a chemical compounds to the dissolved ionic form (Petosa *et al.*, 2010; Quik *et al.*, 2010). Aggregation into larger particle sizes is a common behaviour of ENPs in the aquatic environment and can result in particle elimination from the water column to sediment by changing particle settlement rates (Keller *et al.*, 2010; Nowack and Bucheli, 2007; Navarro *et al.*, 2008a; Christian *et al.*, 2008; Klaine *et al.*, 2008). The aggregation state of an ENP can also cause size-dependent toxic responses and alter the uptake routes of ENPs into aquatic organisms (Alkilany and Murphy, 2010). Therefore, understanding the behaviour of ENPs, especially aggregation, in aquatic environments, is essential if we are to determine the fate and potential to cause adverse effects in aquatic species.

The aggregation and dispersions of nanoparticles can be explained by the theory of Derjaguin-Landau-Verwey-Overbeck (DLVO). The DLVO theory uses the sum of attractive (van der Waals attractive) and repulsive forces (electrostatic double layer (EDL) potential) acting on two closely adjacent particles (Hotze *et al.*, 2010). The charge of the EDL on the surface of the particle can be controlled by the ionic strength (IS) in the solution. At a low IS, the EDL could extend far out from the particle while at higher IS, the additional charge screening of the surface compresses the EDL (Hotze *et al.*, 2010; Handy *et al.*, 2008b).

Figure 2 demonstrates the aggregation of Au nanoparticles in different conditions. In distilled water, the ENPs are stabilised (Figure. 2 (a)). However, in $CaCl_2$ solution and natural lake water and, the particles stick together to form an aggregate (Figure. 2 (b) and (c)) (Tiede, 2008).

(a)   (b)   (c)
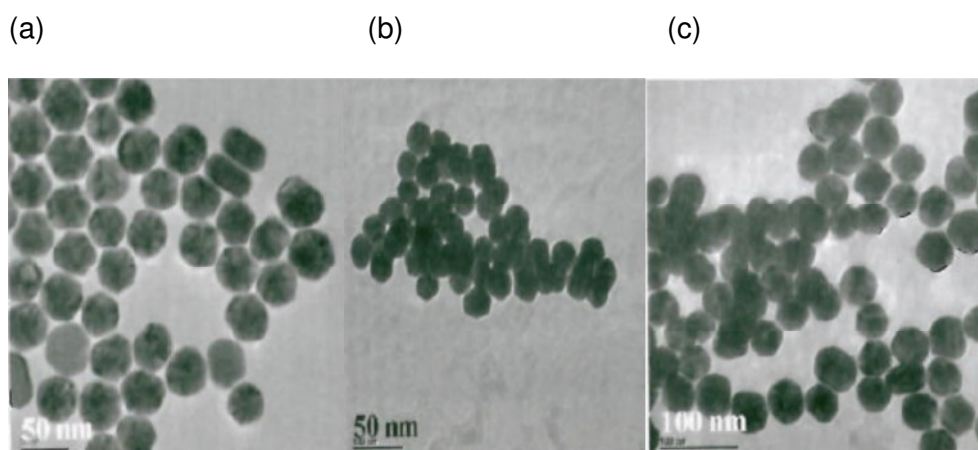
Figure 2. Transmission electron microscopy (TEM) images of gold nanoparticles (50 nm) in different aquatic systems. (a) Distilled water, (b) $CaCl_2$ and (c) lake water. There was particle destabilization in $CaCl_2$ and natural waters compare to in distilled water due to high IS and divalent cations. Reproduced with permission from Tiede (2008).

Particle aggregation is also strongly influenced by other environmental factors and many studies have investigated the effects of environmental properties on particle stabilisation (Nowack and Bucheli, 2007). One of these major factors is the presence of natural organic matter (NOM) including humic and fulvic acids in natural waters. NOM has different interactions with ENPs depending on the surface charge of the particles. Zhang *et al.* (2009) observed the impact of NOM on stabilization of MeO nanoparticles such as TiO_2 and ZnO. In the absence of NOM, MeO nanoparticles showed induced aggregation while significant stabilisation of particles was observed in the presence of NOM. The stabilisation behaviour of MeO nanoparticles were caused by adsorption of NOM onto the surface of nanoparticles and the negative charge of the functional groups of NOM which makes the negative charged ENPs to be more electronegative. The more electronegative ENPs are more stable than before their interactions with the NOM functional groups and are more likely to be involved in repulsion reactions with NOM (Dickson *et al.*, 2012; Chen and Elimelech, 2007; Navarro *et al.*, 2008a). Baalousha *et al.* (2008) also have observed the effects of NOM on destabilization of iron oxide nanoparticles. The positive surface charge of iron oxide nanoparticles was neutralized by the adsorption of the negatively charged NOM. After adsorption, the surface layer of the iron oxide became thicker, this influenced the increasing particle hydrodynamic diameter.

The presence of divalent cations affects particle aggregation through the interaction with the surface charge of ENPs. For example, citrate coated Ag nanoparticles and Au nanoparticles showed faster aggregation with increasing concentration of $CaCl_2$ and NaCl. The cations in the solution change the negative surface charge of citrate effectively by neutralising the coating by the specific interactions with carboxyl groups of citrate molecules (Huynh and Chen, 2011; Liu *et al.*, 2012). However, if positively charge ENPs are in the solution containing divalent cations, steric repulsion forces will be dominant and lead to electrostatic stabilisation (El Badawy *et al.*, 2012).

The variability of particle stabilisation and aggregation between ENPs could further be affected by pH. As pH increases, the concentration of OH^- also increases and causes

the surface charge of ENPs to become more negative (El Badawy *et al.*, 2010). Liu *et al.* (2012) have observed the aggregation of Au nanoparticles coated with citrate and 11-mercaptoundecanoic acid at low pH by neutralization of the surface charge by protonation of the carboxyl functional groups in NaCl solution. However, at higher pH values, citrate coated Au NP (negatively charged) were electrostatically stabilised by the deprotonated carboxylic acid group.

The aggregation of ENPs in natural aquatic environments will be determined by a combination of the environmental factors described above and studies have been done to explore the effects of combinations of parameters on aggregation. Stankus *et al.* (2011) observed the aggregation behaviour of Au nanoparticles in a solution containing NOM and divalent cations. The particle size of Au nanoparticles was enhanced at high concentrations of IS with the NOMs through cation binding, adsorption and reducing steric interactions while stabilised particles were seen at lower IS in the presence of NOM. Aggregation studies using natural water samples have shown stabilization of the ENPs at high concentrations of dissolved organic carbon (DOC) and low IS whereas high concentrations of divalent ions caused particles to aggregate (Lin *et al.*, 2010; Sillanpää *et al.*, 2011; Keller *et al.*, 2010; Hoecke *et al.*, 2011; Ottofuelling *et al.*, 2011). In natural waters, ENPs can interact with clays, minerals and other natural colloids and may form heteroaggregates. Since the number of natural particles is likely to be much higher than ENPs in natural systems, heteroaggregation is likely to occur more frequently than homoaggregation (i.e. the attachment two similar nanoparticles). Therefore, heteroaggregation is also an important factor to be considered when predicting the fate and behaviour of ENPs in the aquatic environment.

Acute and chronic effects of engineered nanoparticles

A variety of aquatic species have been used in the ecotoxicological assessment for ENPs. Table 3 summarises some of the acute and chronic effects data for both metal and MeO nanoparticles. Most studies have followed standard test methods from the Organisation for Economic Co-operation and Development (OECD), EPA guidelines and American Society for Testing and Materials (ASTM). The exposure durations of these tests generally ranged from 24 h to 96 h for acute studies and were 21 d for chronic tests. In acute toxicity tests, the EC/LC_{50} of TiO_2 nanoparticles on aquatic invertebrates (*Daphnia magna* and *Ceriodaphnia dubia*) was highly variable between studies, ranging from 0.73 mg/L (Dabrunz *et al.*, 2011) to over 100 mg/L (Wiench *et al.*, 2009). In chronic toxicity tests, the EC_{50} were 0.46 mg/L (Zhu *et al.*, 2010) and 66.1 mg/L in a 21 day longer term test (Wiench *et al.*, 2009). The lowest toxicity values were reported for metal oxides on algal growth inhibition (*Pseudokirchneriella subcapitata*), with values of 0.42 mg/L for ZnO nanoparticles and 0.72 mg/L for copper oxide (CuO) nanoparticles, respectively (Aruoja *et al.*, 2009).

The effects of metallic nanoparticles on various aquatic organisms have been reported by a number of researchers (Griffitt *et al.*, 2008; Gaiser *et al.*, 2011; Chae *et al.*, 2009). For aluminum nanoparticles, *C. dubia* had an LC_{50} of 0.42 mg/L but no effects were seen on *Danio rerio* at the highest exposure concentration (10 mg/L) (Griffitt *et al.*, 2008). The most sensitive organism to Ag nanoparticles exposure was *Oryzias latipes* which had an LC_{50} of 0.035 ± 0.9 mg/L (96 h). The LC_{50} of daphnids and algae at 48 h for Ag nanoparticles were 0.04 mg/L and 0.19 mg/L, respectively (Griffitt *et al.*, 2008; Gaiser *et al.*, 2011).

The homogenous dispersion that is currently recommended for ecotoxicological tests could be difficult to apply to risk assessments of nanomaterials or bulk substance. The current test methods for ENPs may not accurately reflect the behaviours of ENPs in the natural environment such as agglomeration and aggregation after which precipitation is likely to occur. Additionally, reactions of ENPs with other (naturally occurring)

substances that may attach themselves to the surface of nanomaterials are not accounted for (Pronk *et al.*, 2009). Several preparation methods are therefore applied to maintain homogenous dispersion or enhance particle stabilization (Table 3). Some of the studies referenced in Table 3 were performed under semi-static or flow-through methods (Zhu *et al.*, 2010; Chae *et al.*, 2009) while others used centrifugation (Hoecke *et al.*, 2008) or filtration (Chae *et al.*, 2009) to remove aggregated particles before the particles were dispersed into the test media. The method by which the nanoparticles are prepared could affect different biological effects. It is therefore necessary to select appropriate nanoparticle preparation methods for the ecotoxicoloigical assessment of ENPs. In particular, the ecotoxicity test media that are typically used contain $CaCl_2 \cdot H_2O$, $MgSO_4 \cdot 7H_2O$, $NaHCO_3$, KCl and $CaSO_4 \cdot H_2O$ (U.S. EPA, 1991; OECD, 2011; OECD, 2004) which would have a large influence on particle aggregation. It is questionable whether the methods listed above are effective to prevent particles aggregation or to maintain particles in a stable state. In addition, particle aggregation will strongly influence exposure routes, toxicity effects and bioavailability in the test organisms (Baun *et al.*, 2008a). It is therefore not only important to consider toxicity based on values such as EC/LC_{50} derived by a dose-response relationship, but other metrics such as combinations of specific surface area, particle size, zeta potential, and shape might be better suited to quantify adverse effects across nanomaterials.

Table 3. Examples of acute and chronic effects of ENPs on aquatic organisms

Organisms	Test methods	Particle treatment	Particle size (nm)	Endpoints	Reference
Metal oxides- TiO_2					
Daphnia magna	OECD TG 202	N.A	101	96 h EC_{50}=0.73 mg/L, Mortality and reduce molting rate	Dabrunz *et al.* (2011)
Daphnia magna	OECD TG 202 and OECD TG 211	sonicate for 10 min	21	72 h EC_{50}= 1.62 mg/L 21 d EC_{50}=Chronic: 0.46 mg/L, severe growth retardation, mortality	Zhu *et al.* (2010)
Daphnia magna	U.S EPA	sonicate solution	30	48 h EC_{50}= 5.5 mg/L, no changes to feeding and hopping rate and heart rate	Lovern and Klaper (2006)
Daphnia magna *Ceriodaphnia dubia* *Danio rerio*	ASTM	sonication	20.5 ± 6.7	48 h LC_{50} >10 mg/L for daphnids and adult and Juvenile fish	Griffitt *et al.* (2008)

Table 3. Continued

Organisms	Test methods	Particle treatment	Particle size (nm)	Endpoints	Reference
			Metal oxides- TiO_2		
Daphnia magna	OECD TG 202	sonication and stirring	Length: 50, Width: 10	48 h EC_{50} >100 mg/L 21 d EC_{50}= 66.1 mg/L effects on reproduction	Wiench *et al.* (2009)
Desmodesmus subspicatus	ISO8692, OECD TG 201 and DIN 38412-33	Stirring for 19 h	25	72 h EC_{50}= 44 mg/L, growth inhibition	Hund-Rinke and Simon (2006)
			Metal oxides- CeO_2		
Pseudokirchneriella subcapitata	OECD TG 201	Stirring	90.8-97.7	24 h EC_{50}= 2.4–29.6 mg/L, inhibition cellular function	Rodea-Palomares *et al.* (2011)

Table 3. Continued

Organisms	Test methods	Particle treatment	Particle size (nm)	Endpoints	Reference
Metal oxides- ZnO					
Daphnia magna	OECD TG 202	sonication and stirring	<200	1.0 ->100 mg/L	Wiench *et al.* (2009)
Daphnia magna	other	sonication for 30 min	50–70	48 h LC_{50}= 3.2 ± 1.3 mg/L, mortality	Heinlaan *et al.* (2008)
Pseudokirchneriella subcapitata	OECD TG 201	sonication for 30 min	30	72 h EC_{50}= 0.42 (0.036-0.049) mg/L, growth inhibition	Aruoja *et al.* (2009)
Metal oxides- CuO					
Daphnia magna	other	sonication for 30 min	~30	48 h LC_{50}= 3.2 ± 1.6 mg/L, mortality	Heinlaan *et al.* (2008)
Pseudokirchneriella subcapitata	OECD TG 201	sonication for 30 min	30	72 h EC_{50}= 0.710 (0.556-1.092) mg/L, growth inhibition	Aruoja *et al.* (2009)

Table 3. Continued

Organisms	Test methods	Particle treatment	Particle size (nm)	Endpoints	Reference
Metal oxides-SiO$_2$					
Pseudokirchneriella subcapitata	OECD TG 201	centrifuge for 15 min	12.5±0.2 27.0±0.5	72 h E$_r$C$_{20}$ = 20.0 ± 5.0 mg/L for 12.5 ±0.2 nm particle 72 h E$_r$C$_{20}$ =28.8 ± 3.2 mg/L for 27.0±0.5 nm particle	Hoecke *et al.* (2008)
Metal nanomaterials-Al					
Daphnia pulex *Ceriodaphnia dubia* *Danio rerio* *Pseudokirchneriella subcapitata*	ASTM	stirring for 48 h	41.7 ± 8.1	48 h LC$_{50}$ >10 mg/L for *Danio rerio* and *Daphnia pulex* 48 h LC$_{50}$= 0.419 mg/L for *Ceriodaphnia dubia* 96 h LC$_{50}$= 8.30 mg/L for *Pseudokirchneriella subcapitata*	Griffitt *et al.* (2008)

Table 3. Continued

Metal nanomaterials- Ag

Organisms	Test methods	Particle treatment	Particle size (nm)	Endpoints	Reference
Daphnia pulex					
Ceriodaphnia dubia				48 h LC_{50}= 0.040 mg/L for *Daphnia pulex*,	
Danio rerio	ASTM	stirring for 48 h	26.6 ± 8.8	48 h LC_{50}= 0.067 mg/L for *Ceriodaphnia dubia*	Griffitt *et al.* (2008)
Pseudokirchneriella subcapitata				96 h LC_{50}= 0.19 mg/L for *Pseudokirchneriella subcapitata*	
Oryzias latipes	US EPA	filtering	49.6	96 h LC_{50}=0.035 ± 0.9 mg/L	Chae *et al.* (2009)
Danio rerio	ASTM	stirring for 48 h	26.6 ± 8.8	48 h LC_{50}=7.07 mg/L for adult, 7.20 mg/L for juvenile	Griffitt *et al.* (2008)
Ceriodaphnia dubia	US EPA	sonication	26.8	48 h LC_{50}= 0.067 for *Ceriodaphnia dubia*	Gaiser *et al.* (2011)
Daphnia pulex				48 h LC_{50}= 0.04 mg L *for Daphnia pulex*	

Uptake routes and effects of engineered nanoparticles on the aquatic organisms

Cellular level

At the cellular level, plants, bacteria, and fungi are surrounded by a semipermeable cell wall (Fabrega *et al.*, 2011). Uptake across this semi-permeable membrane is highly dependent upon the type of ENP involved. ENPs that are readily soluble can either release ions inside the cell after passing through the cell membrane, attach to the cell surface or diffuse across an algal cell layer (Cronholm *et al.*, 2013; Miao *et al.*, 2010). Solid particles can be taken up inside the cell *via* processes such as endocytosis, phagocytosis and pinocytosis and show particle internalisation (Miao *et al.*, 2010; Nowack and Bucheli, 2007; Klaine *et al.*, 2008). If the pore size of the cell is larger than particle size, most semipermeable cell walls would allow small particles to penetrate and reach the plasma membrane. After ENPs penetrate the cell membrane, the cells can produce new pores which are larger than normal causing more internalization of ENPs which further affects the way the cell membrane functions (Navarro *et al.*, 2008a; Fabrega *et al.*, 2011; Jiang *et al.*, 2008).

The surface charge of ENPs is also an important factor for determining uptake into algae and bacteria. For example, in *Bacillus* species, carboxyl, phosphate and amino groups are present in the cellular membranes which are negatively charged. This causes high repulsion between negatively charged particles and so negatively charged particles may be taken up less and cause less toxic effects. However, positively charged ENPs can be attracted to the cell membranes and this attraction could result in damage to cell membranes through the formation of reactive oxygen species which can lead to cell death (El Badawy *et al.*, 2011).

ENPs can also interact with biomolecules, such as proteins. Proteins strongly adsorb to the surface of nanoparticle forming a protein layer, commonly referred to as a 'protein

corona' (Lynch *et al.*, 2008). The protein corona can have various effects on the physiological responses of a cell to an ENP including the stimulation of agglomeration, cellular uptake, transport, accumulation and toxicity (Rahman *et al.*, 2013).

Table 4 presents the results from studies looking at the effects of metal and MeO ENPs on algae. For CeO_2 ENPs, there was a weak physical interaction between single or aggregated CeO_2 ENP and a *P. seudokirchneriella* cell. It resulted in cellular damage and membrane disruption but no uptake or strong adsorption to the cell wall were seen (Hoecke *et al.*, 2009; Rodea-Palomares *et al.*, 2011). There was adsorption of SiO_2 ENPs to the outer surface of the algal cell. However, uptake effects were not observed in TEM analysis (Hoecke *et al.*, 2009). Unlike the results for CeO_2 ENPs and SiO_2 ENPs, CuO ENPs penetrated into *Microcystis aeruginosa* cell wall and internalised into the cell (Wang *et al.*, 2011). The internalisation of ZnO ENPs was also observed in the cells of *Euglena gracilis* (Brayner *et al.*, 2010). Ag nanoparticles have been found to internalise in *Ochromonas danica*. The internalisation of Ag nanoparticles could be due to cell membrane permeability or a break in the membrane that resulted in the passive uptake of Ag nanoparticles (Miao *et al.*, 2010)

Table 4. Summary of studies that have been performed to explore the uptake of ENPs into algae

ENPs	Organisms	Test conditions	Effects	Reference
CeO_2 (14, 20, 29 nm)	*Pomaderris subcapitata*	3.2, 5.6, 10, 18, and 32 mg/L for 72 h	Weak physical interaction aggregation between CeO_2 and algal cells.	Hoecke *et al.* (2009)
CeO_2 (90.8-97.7nm)	*Pomaderris subcapitata*	Up to 100 mg/L for 96 h	Damaged cell walls and membrane damage.	Rodea-Palomares *et al.* (2011)
SiO_2 (12.5 and 27 nm)	*Pomaderris subcapitata*	2.2 to 460 mg/L for 72 h	Considerable adsorption to the outer surface of the cell but no uptake effect	Hoecke *et al.* (2008)
CuO	*Microcystis aeruginosa*	0.5 mg/L for 12 h	Internalization were observed	Wang *et al.* (2011)
ZnO	*Euglena gracilis*	0.06 and 0.6 mol/L	Internalization were observed	Brayner *et al.* (2010)
Ag (1–10 nm)	*Ochromonas danica*	3, 10, 15, 20 and 30 mg/L	Internalization into the cells	Miao *et al.* (2010)

Crustaceans

Crustaceans, especially daphnia species such as *D. magna* and *C. dubia* species, are commonly used to assess hazardous materials or chemicals under regulatory testing schemes. These species are also recommended for ENP risk assessment (Baun *et al.*, 2008a) so many studies have been done to explore the uptake of ENPs into daphnids. *D. magna* is one of many filter feeding organisms which gather food particles by direct interception through the interaction between single filter-fibres and particles. The filter mesh size of daphnids ranges from 0.24 to 0.64 µm, therefore, ENPs in this size range can be readily ingested by daphnids and may show effects on the organism (Geller and Muller, 1981; Burns, 1968; Rosenkranz *et al.*, 2009). Larger size particles may penetrate into the filter chamber less readily than those that are in the size range of filter mesh. After ENPs are ingested by daphnids, ENPs typically accumulate in the digestive tract which is the main place where foods are stored. In the gut of daphnids, there is a peritrophic membrane which protects the gut epithelium and controls the exchange of nutrients and enzymes (Heinlaan *et al.*, 2011). The gut epithelium contains well-developed microvilli lines which are regarded as important in the adsorption of ENPs (Zhu *et al.*, 2009).

ENPs also transfer into the large spherical storage cells which contains lipids or lipid-like cytoplasmic along the epithelial lining of the digestive tract. The storage cells are the area where vitellogenin and yolk globules are synthesised (Rosenkranz.., 2009; Heinlaan *et al.*, 2011; Goulden and Hornig, 1980). The high lipid fraction in the egg yolk sac of foetuses shows high levels of accumulation of lipophilic fullerene (C_{60}) (Tao *et al.*, 2009). Rosenkranz *et al.* (2009) also found carboxylated fluorescent polystyrene beads (size 20 nm and 1000 nm) crossed the epithelial barrier and accumulated in the oil storage droplets of daphnids very quickly within 30 minutes of exposure. After being taken up, the aggregated ENPs require high amounts of energy to remove them from

the gut which can ultimately result in growth inhibition and reduced fecundity (Lovern *et al.*, 2008; Li and Huang, 2010).

Several studies have investigated the uptake and translocation of CNTs (MWNTs, SWNTs and C_{60} nanoparticles), QD, CuO nanoparticles, Ag nanoparticles and Au nanoparticles in *D. magna* and *C. dubia* (Table 5). Petersen *et al.* (2009) observed that carbon nanotubes attach to *D. magna*'s carapace, appendages and antennae. TEM analysis showed that most CNTs were located in the organisms' gut and were not absorbed into cellular tissues. Depuration of the CNTs was not observed after the organisms were moved to clean water. Li and Huang (2011) observed the uptake of CNTs following different physical-chemical treatments e.g. ozonation and ultrasound treatment. After exposure, the gut of *C. dubia* were filled with ultrasound treated CNTs (around 86%). The results indicated that surface treatment influenced the aggregate size and led to the ENPs being accumulated in the digestive tract. Roberts *et al.* (2007) treated the coating of CNTs to enhance solubility and observed the effects to *D. magna*. The organisms ingested soluble CNTs as a food source and excreted insoluble CNTs only.

Baun *et al.* (2008b) observed the influence of C_{60} on the uptake of other environmental contaminants such as atrazine, methyl parathion, pentachlorophenol (PCP), and phenanthrene on uptake in*to D. magna*. Faster uptake of phenanthrene was observed when it was absorbed onto C_{60}, however, the phenanthrene without C_{60} was also rapidly eliminated when the organisms were moved to clean water.

The uptake of amphiphilic polymer coated CdSe/ZnS QDs were examined using *D. magna*. QDs were found not only in the digestive tracts of daphnia but also in the carapace, antennae, and thoracic appendages. After the animals were moved to clean water, QDs in the digestive tracts were not removed with around 53% of the initial amount taken up remaining in the organism (Lewinski *et al.*, 2010).

Heinlaan *et al.* (2011) compared the uptake of CuO nanoparticles and bulk CuO in *D. magna*. Both CuO nanoparticles and bulk CuO were taken up and observed in the midgut of *D. magna*. Nanoparticulate CuO was observed to have caused ultrastructural

changes in the midgut epithelium of the organisms; this effect wasn't apparent after exposure to bulk CuO. This strongly suggests that the adverse effect to the daphnids was caused by a size-related effect.

Zhao and Wang (2010) observed the uptake of Ag nanoparticles in different test conditions using different ENP concentrations and feeding condition. At lower exposure concentrations, the uptake rate was lower than that of Ag free ions. However, at higher concentrations, the uptake of Ag nanoparticles increased significantly after 8 h exposure. Greater uptake of the Ag nanoparticles was observed in the presence of food (i.e. algae) compared to a no food treatment.

Lovern *et al*. (2008) found that the uptake of Au nanoparticles into the gut of organisms depends on exposure time. At the beginning of the exposure, there were no visible particles in the gut of *D. magna*, however, after 6 h exposure, Au nanoparticles were found not only in midgut but also in mouth and the tail regions of digestive systems of the organisms. Following the depuration phase of the experiments, the accumulated Au nanoparticles were observed to remain in the gut tissue for some time.

Table 5. Studies that have investigated the uptake of fullerene, metal oxide and metal nanoparticles on daphnia species

ENPs	Organisms	Test conditions	Effects	Reference
Carbone nanotube (30 to 70 nm)	Daphnia magna (<24 h old)	0.04, 0.1, or 0.4 µg/mL of CNTs for 48h	Remained in the organisms' guts but adsorbing into the organism tissue was not associated. No depuration was observed.	Petersen et al. (2009)
Carbone nanotube (14.1 to 59.2 nm)	Ceriodaphnia dubia (<24 h old)	10 mg/L of ozone and ultrasound treated MWNTs for 60 min	Interacted with the body tissue and ingested and accumulated in the digestive tract and brood vessel.	Li and Huang (2011)
Carbone nanotube (1.2 nm) C_{60}	Daphnia magna (<24 h old)	0, 0.1, 0.25, 0.5, 1, 2.5 mg/L for 20 h	Readily ingested and stayed in the gut tract in daphnids.	Roberts et al. (2007)
(Adsorption of phenanthrene onto C_{60})	Daphnia magna (4 d old)	49ug/L 14C-phenanthrene + 3.0 mg/L C_{60} for 48 h	Fast uptake of phenanthrene with C_{60} in the animal and found in the digestive tract but fast clearance was shown.	Baun et al. (2008b)

Table 5. Continued

ENPs	Organisms	Test conditions	Effects	Reference
CdSe/ZnS QDs	*Daphnia magna* (neonates)	7.7 nM (4.63 × 10^{12} particles/mL) for 24 h uptake and 24 h depuration	Accumulate within the digestive tracts	Lewinski *et al.* (2010)
CuO (31 ±12.8 nm)	*Daphnia magna* (neonates)	4.0 and 175 mgCuO/L for 48 h	Filled with CuO nanoparticles in posterior midgut.	Heinlaan *et al.* (2011)
Ag (≤20 nm)	*Daphnia magna* (≤3 d old)	highest Ag nanoparticles conc. : 500 µg/L, for 8 h	Uptake rate increased by algal food within Ag nanoparticles in the daphnids.	Zhao and Wang (2010)
Au (17-20 nm)	*Daphnia magna* (adult)	500 ppb for 24 h	Found in the mouth, midgut, and tail regions of the digestive system.	Lovern *et al.* (2008)

Fish

Contaminants can enter fish from the water *via* the gills, ingestion of food and by dermal absorption (Clark *et al.*, 1990). Uptake through the gills is considered as the primary site of uptake for contaminants due to the optimized function for exchange of solutes between blood of fish and water, a large surface area and the existence of a thin epithelial barrier (Farkas *et al.*, 2011; Kleinow *et al.*, 2008). There is an unstirred layer which is made up of water and layers of mucus on the gill surface. The functional layers which are in between epithelial cell surfaces and the unstirred layers act like cell membrane charge barriers and lead to metal ion mobility, exchange and diffusion. They also have defence mechanisms which occur in the unstirred layer; the mucus provides protection from chemicals penetrating into the epithelia cell by trapping and aggregating the contaminants on the gill surface (Handy *et al.*, 2008a; Kleinow *et al.*, 2008; Smith *et al.*, 2007).

The extent to which ENPs are absorbed from the gastrointestinal tract of fish varies depending on the size and surface chemistry of the ENPs in question. Small sized nanoparticles cross the colonic mucus layer in the gut within a short time (2 min for 14 nm latex nanoparticle) while larger particles (e.g. >1000 nm) cannot pass this layer. Lipophilic ENPs can be taken up through endocytosis in the gut or diffuse directly through the cell membrane. Again, the surface charge of ENPs is important for uptake as the positively charged particles can be trapped in the negatively charged mucus whereas negatively charged particles diffuse across the mucus layer and interact with epithelial cells (Handy *et al.*, 2008a; Buzea *et al.*, 2007).

In terms of dermal uptake, the skin of fish acts like a barrier to separate internal and external environments. It maintains the internal environment with ionic and osmotic integrity and protects it from the external environment and pathogens. The skin consists of two major layers, an outer layer (epidermis) and an inner layer (dermis). Like the gill and the gut, the mucus is produced from goblet cells which help to protect

the epidermis by trapping ENPs or other environmental contaminants (Kleinow *et al.*, 2008; Coello and Khan, 1996; Handy *et al.*, 2008a).

Table 6 summarises ENP uptake studies for fish. In these studies, most of the accumulated ENPs were observed mainly in the gut and gill (Smith *et al.*, 2007; Farkas *et al.*, 2011; Griffitt *et al.*, 2009; Peyrot *et al.*, 2009). After fish embryos were exposed to ENPs, the ENPs would either attach or adsorb to the surface of the chorion of fish egg and then penetrate into the chorionic space through the chorion pore canals by passive diffusion. Once inside the embryo, the ENPs could interact with incoming nanoparticles and then form larger particles. Due to these interactions, the chorion pore canals might be blocked and influence particle bioaccumulation or induced abnormalities to developing embryos (Fent *et al.*, 2010; Lee *et al.*, 2007; Kashiwada, 2006).

Table 6. Studies that have investigated the uptake of fullerene, metal oxide and metal nanoparticles into fish

ENPs	Organisms	Test conditions	Effects	Reference
SWCNTs (<5 nm)	Oncorhynchus mykiss (juveniles)	0.1, 0.25, 0.5 mg/L for 10 d	Ingested and resulted in precipitated SWCNT in the gut lumen and intestinal pathology and gill irritation and brain injury.	Smith et al. (2007)
TiO₂ (<100 nm)	Oncorhynchus mykiss	50, 500, or 5000 µg/L for	Internalization in gill tissue	Johnston et al. (2010)
SiO₂ (fluorescent core-shell, ~60 and ~200 nm)	Danio rerio (<6 hpf)	~60 nm: 0.0025 to 25mg/L from < 6 hpf to 96 hpf ~200 nm: 0.25to 200 mg/L from < 6 hpf to 96 hpf	Adsorbed on the chorion of eggs for all size but no uptake effects.	Fent et al. (2010)
Fluorescent (39.4 - 42,000 nm)	Oryzias latipes (fertilized eggs and adult fish)	Fertilized eggs: 39.4 nm particles in ERM (up to 30 mg/L) for 3 d. Adult fish: 39.4 nm particles at 10 mg/L in 500mL ERM for 7d	Adsorbed to the chorion of medaka eggs and accumulated in the oil droplets, gill, intestine, brain, testis, liver, and blood and penetrated into the yolk and gallbladder.	Kashiwada (2006)

Table 6. Continued

ENPs	Organisms	Test conditions	Effects	Reference
Ag (citrate and PVP coated, 12.3±8 nm and 7.3±3.7 nm)	*Oncorhynchus mykiss* (juveniles, gill cell)	20 mg/L of citrate coated Ag nanoparticles for 48 h 10 mg/L of PVP coated Ag nanoparticles for 48 h	Citrate coated Ag nanoparticles were readily taken up into the gill cell monolayers, mainly in nuclei	Farkas *et al.* (2011)
Ag (11.6± 3.5 nm)	*Danio rerio* (embryo)	From 0.04 to 0.71 nM from cleavage stage to 120 hpf	Penetrated into the chorion pore canals of developing embryos and caused abnormalities.	Lee *et al.* (2007)
Ag (26.6 ± 8.8 nm) and Cu (26.7 ± 7.1 nm)	*Danio rerio* (adults)	1000 µg/L 100 µg/L and for 48 h	Found in gill and whole body tissue.	Griffitt *et al.* (2009)

In summary, various environmental parameters determine the behaviour of ENPs and their uptake and toxic impacts in aquatic systems. However, there are still many uncertainties around the behaviour and effects of these materials in the environment and this makes it difficult to establish the risks of ENPs in natural systems. Many reviews have therefore highlighted the importance of in-depth knowledge for nanoparticle characterization, fate and effects of ENPs in experimental or environmental media in order to more fully understand the observed effects (Handy *et al.*, 2008b; Hassellöv *et al.*, 2008; Baun *et al.*, 2008a).

Conclusion and aim for future work

This review shows that various environmental parameters are likely to affect the behaviour of ENPs. Many studies in aquatic organisms have been conducted to investigate the effects of ENPs on the aquatic environment and demonstrated a wide range of biological effects. However, relating exposure concentration of ENPs to their effects is challenging as the traditional use of mass or mass per unit volume alone is unlikely to be appropriate for risk assessment of ENPs. Conducting risk assessments of ENPs using traditional methods fails to consider the interactions and dynamic behaviours of ENPs that are likely to occur in the natural environment. Thus the aims of this study were threefold (1) Develop an improved understanding of the factors affecting the aggregation behaviour of ENPs in aquatic systems; (2) observe the factors affecting uptake of ENPs into aquatic organisms; and (3) based on the knowledge gained, to provide recommendations on how the environmental risks of ENPs could be better assessed in the future.

These aims were achieved through the following specific objectives:

1. To compare the behaviour of ENPs between standardised test media which are commonly applied to ecotoxicity test and natural waters.
2. To identify key physicochemical properties of ENPs which influence their behaviour.

3. To develop a model to predict aggregation and size distribution of ENPs in river systems through the UK.

4. To explore the effects of aggregation state on the uptake of ENPs into aquatic organisms.

5. Based on the knowledge gained in objectives 1 to 4, to provide recommendations as to how future risk assessments of ENPs can more accurately reflect conditions of natural aquatic environments.

The aims and objectives described above have been addressed in 4 experimental Chapters and one discussion Chapter:

Chapter 2 describes studies to assess the fate study of gold nanoparticles, with different surface functionalisation, in standard ecotoxicity test media and natural waters. The study explores behaviour in standard tests reflects the likely behaviour of these ENPs in the natural environment. The effects of one environmental factor (dissolved organic matter) and the presence/absence of test organisms on particle aggregation are also explored.

Chapter 3 describes studies to assess whether the particle core affects the behaviour of ENPs. In this chapter, the behaviour of silver and gold nanoparticles with equivalent size and surface functionality are compared.

Chapter 4 develops relationships between particle aggregation and water chemistry. These relationships are then used to predict particle size distributions for a range of gold nanoparticle with different surface functionalities in river systems through the UK.

Chapter 5 describes studies to explore the uptake of gold nanoparticles into aquatic invertebrate. The studies were performed using *Gammarus pulex* and gold nanoparticles coated with different surface functionalities under different environmental conditions.

Chapter 6 provides the overall conclusion and recommendations for how to take this work forwards.

Chapter 2

Regulatory ecotoxicity testing of engineered nanoparticles: are the results relevant to the natural environment?

Introduction

As a result of their exquisitely tunable properties, ENPs are being, or have the potential to be, used in many sectors including defence, energy storage and generation, agriculture, as well as environmental remediation (Aitken *et al.*, 2006). The increased prevalence of ENPs means their release into the aquatic environment is inevitable (Scown *et al.*, 2010; Handy *et al.*, 2008b). Available exposure estimates for surface waters indicate that concentrations of silver ENPs are likely to range from 0.72 - 30 ng/L; TiO_2 ENP concentrations will range from 0.021 - 16 µg/L; and concentrations of CNTs will range from 0.0033 – 0.8 ng/L (Mueller and Nowack, 2008; Gottschalk *et al.*, 2010). Even though the concentrations of ENPs in the environment are predicted to be low, the risk of ENPs cannot be ignored. Over the past few years a wide range of acute and chronic ecotoxicological studies have therefore been performed to better understand the potential risks of ENPs to the aquatic environment (e.g. Hoecke *et al.*, 2008; Griffitt *et al.*, 2008; Wiench *et al.*, 2009; Dabrunz *et al.*, 2011).

Most published ecotoxicity studies follow traditional test method guidelines such as those developed by OECD or U.S. EPA (e.g. Dabrunz *et al.*, 2011; Wiench *et al.*, 2009; Lovern and Klaper, 2006; Rogers *et al.*, 2010). These studies employ standardised test

media designed primarily to support the test organism and to provide consistency across studies. For traditional chemical contaminants, where toxicity is related to mass concentration, the use of standardised media is probably appropriate; this is particularly true if exposure concentrations are characterised throughout the duration of the study. However, this may not be the case for ENPs, for which bioavailability and toxicity are not only affected by mass or particle number concentration but also by the degree of aggregation of the ENPs and the resulting particle size distribution (French *et al.*, 2009; Kümmerer *et al.*, 2011; Sharma, 2009; Lin and Xing, 2008). Aggregation and disaggregation are highly dependent on environmental factors, such as the pH, electrolyte valence and presence of NOM (Hyung *et al.*, 2007; Stankus *et al.*, 2011; Jiang *et al.*, 2009b). If the degree of aggregation in standard test media is not representative of aggregation in the natural environment then, if used for environmental risk assessment purposes, existing standard ecotoxicity test methodologies could either over- or under-estimate the risk of an ENP in natural systems. Differences in ENP behaviour across standardized media will also make it difficult to develop an understanding of the relative sensitivity of different species to a particular ENP.

Although the effects of individual environmental parameters and particle characteristics on ENPs aggregation have been well studied (Keller *et al.*, 2010; Hyung *et al.*, 2007; French *et al.*, 2009; Thio *et al.*, 2011), we currently do not know whether ENPs behaviour in standard ecotoxicity experiments accurately reflects behaviour in the natural environment. The present study was performed to explore the behaviour of a set of model Au nanoparticles with different surface functionality in a range of standardised test matrices and to determine whether behaviour in standard tests reflects the likely behaviour of these ENPs in the natural environment. The effects of the presence/absence of test organisms and the addition of NOM to the standardised media were also explored.

Material and methods

Study materials

Citrate capped Au nanoparticles (Au-citrate nanoparticles; d~30 nm) were prepared in aqueous media by heating a solution of $HAuCl_4\cdot2H_2O$ (0.25 mM, 3.75 mM tribasic salt, 1 liter) to 90 ^{o}C. The solution was heated for 1 h over which time its colour gradually changed to gray and finally purple/red. The Au nanoparticles solutions were subsequently purified by dialysis. Dialysis was done on 1000 mL of stock solution which was divided into two 500 mL fractions and placed in Lot Number 3244650 dialysis tubing (approximate molecular weight cut off = 8,000 Daltons). The filled tubes were submerged in distilled water for 4 d and the bath water was changed at 12 h intervals. Mercaptoundecanoic acid capped particles (Au-MUDA nanoparticles; d~30 nm) were prepared by addition of 500 mL fraction of 30 nm citrate capped Au nanoparticles stock solution directly to an ethanol solution of 11-mercaptoundecanoic acid (0.12 g, 3 mL). The mixture was stirred in subdued light for one week. The resulting solution was then purified by dialysis using the procedure outlined above. The chemical structures of MUDA and citrate are shown in Figure 3.

'Positive' amino PEG thiol-capped (Au-PEG-NH$_2$ nanoparticles) and 'neutral' PEG-capped (Au-PEG nanoparticles) Au nanoparticles were obtained from Nanocs Inc (Boston, United States). Humic acid sodium salt (CAS No. 68131-04-4) was used to explore effects of NOM, this was obtained from Sigma Aldrich (Poole, Dorset, United Kingdom).
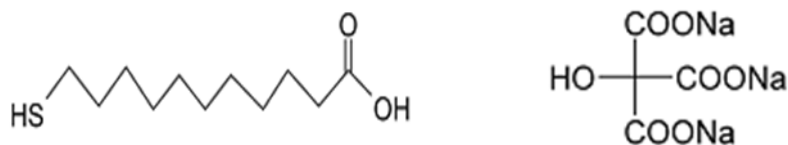
Figure 3. Test gold nanoparticles coated with; (a) 11-mercaptoundecanoic acid (MUDA) gold nanoparticles, (b) sodium citrate tribasic dehydrate (citrate) gold nanoparticles.

Prior to testing, all model study particles were characterised by TEM operating at 200kV (JEOL-JEM 2011) and nanoparticle tracking analysis (NTA) using a NanoSight 2.2 LM 10 instrument. NTA follows individual nanoparticles in the liquid phase moving under Brownian motion and records their movement as a video on a frame-by-frame basis. After recording for a given time, hydrodynamic diameter of individual particles is calculated using the Stokes-Einstein equation (Malloy and Carr, 2006):

$$d_p = \frac{kT}{3\pi\eta D} \qquad \text{(Equation 2.1)}$$
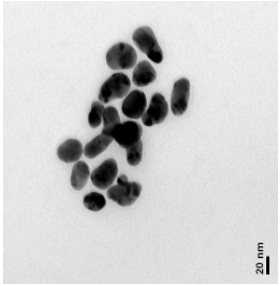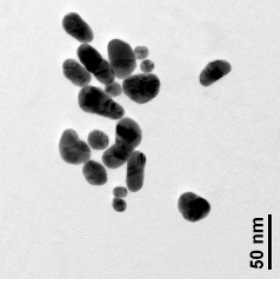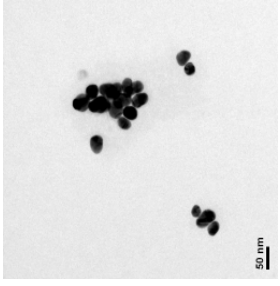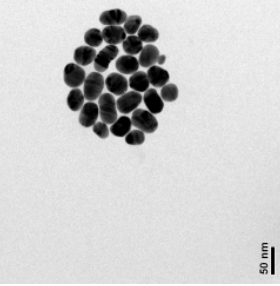
d_p is hydrodynamic diameter (nm), k is the Boltzmann constant (J K^{-1}), T is the absolute temperature (K), η is the viscosity of the medium (kg m^{-1} s^{-1}) and D is diffusion coefficient

The Au-MUDA and Au-citrate nanoparticles were also characterised by FTIR and XPS analysis. The characteristics of the study particles and exposure concentrations are summarised in Table 7 and the results of the FTIR and XPS analysis are given in the Appendix 2.

Standardised test media

A range of commonly used standard ecotoxicity media was studied, specifically: artificial pond water (APW) (Naylor *et al*., 1989), OECD *Daphnia* M4 media (OECD, 2004), algae media (Kuhl and Lorenzen, 1964), Gamborg's B-5 basal medium, artificial salt water (ASW) at 35 ‰ salinity (Kester *et al*., 1967), and US EPA hard (HW), moderate hard (MHW) and soft (SW) waters (U.S. EPA, 1991). Information on the general characteristics of the test media is described in Table 8. Zeta potential (NanoSight NS500, NanoSight Ltd, Amesbury, United Kingdom) were measured for each test ENPs in each test media except in ASW, M4 and Lemna media where the NS500 was unable to produce reliable zeta measurements (Table 7).

Table 7. Physical and chemical characteristics of the ENPs

	Au-MUDA nanoparticles	Au-citrate nanoparticles	Au-PEG-NH$_2$ nanoparticles	Au-PEG nanoparticles
Coating	mercaptoundecanoic acid	citric acid	amino polyethylene glycol thiol	neutral polyethylene glycol
Surface property	Amphoteric	negative	positive	neutral
Bond type	Covalent	covalent	N.A	N.A
D$_{TEM}$ (nm)	29.4±7.8	23.6±9.6	33.3±6.8	36.4±6.0
D$_{NTA}$ (nm)	33.1±14.9	43.6±35.1	50.8±33.2	61.9±36.4
ξ-potential $_{pH\,7}$ (mV)				
APW	-15.3±13.8	-10.7±16.5	-11.6±12.6	-11.6±14.1
M4	N.A	N.A	N.A	N.A
ASW	N.A	N.A	N.A	N.A
Lenma media	N.A	N.A	N.A	N.A
Algae media	-17.2±33.9	-13.4±41.4	8.5±26.8	-5.2±37.2
HW	-19.4±17.5	-13.8±18.8	-19.0±13.8	-13.3±16.7
MHW	-22.4±16.5	-15.1±13.8	-17.8±17.4	-17.0±13.8
SW	-15.9±16.4	-7.2±18.1	-21.1±13.3	-23.0±13.1
Exposure concentration	0.5 mg/L	0.5 mg/L	1 mg/L	1 mg/L
TEM image				

D$_{TEM}$ (nm): mean±standard deviation, D$_{NTA}$ (nm): mean±standard deviation, ξ-potential (mV): mean±standard deviation, N.A: not available

Table 8. Characteristics of the standard ecotoxicity media used in the aggregation studies

Test media	Tests where media used	Example of test orgnaisms	pH	Conductivity (μS/cm)	Ionic strength (mM)	Major elements
Artificial pond water	Naylor *et al.* (1989)	Fish, Gammarids	7.47	651	11.1	$CaCl_2 \cdot H_2O$, $MgSO_4 \cdot 7H_2O$, $NaHCO_3$, KCl
M4 media	OECD TG 202	Daphnids sp.	7.29	645	7.99	$CaCl_2 \cdot H_2O$, $MgSO_4 \cdot 7H_2O$, $NaHCO_3$, KCl, combined vitamin
Algae media	Kuhl and Lorenzen, 1964	Green algae	6.17	1,272	17.2	$CaCl_2 \cdot 2H_2O$, $MgSO_4 \cdot 7H_2O$, KNO_3, $NaH_2PO_4 \cdot 1H_2O$, $NaH_2PO_4 \cdot 2H_2O$
Lemna media	N.A.	Lemna sp.	6.50	4,200	N.A	-
Artificial salt water	N.A.	Marine organisms	7.74	47,100	N.A	-
EPA hard water			7.82	464	7.39	
EPA moderate hard water	USEPA 1991	Freshwater organisms	7.69	494	3.70	Different concentrations of $NaHCO_3$, $CaSO_4 \cdot H_2O$, $MgSO_4$, KCl
EPA soft water			7.98	293	1.85	

N.A.: Not available, pH and conductivity are measured. IS is calculated.

Natural waters

Forty nine samples, ranging in pH from 3.79 – 7.90, were obtained from rivers in the north of England. The samples were selected to provide a broad representation of surface water chemistry (pH, conductivity, dissolved organic carbon content and cation and anion concentrations) for UK systems. Following collection, samples were filtered using 2.5 μm cellulose filter papers and then stored at 4 ºC prior to use. The characteristics of the samples are summarised in Table 9. The details of natural water analysis methods are given in Chapter 4, 'Collection and characterization of natural water samples'.

Test organisms

Three aquatic organisms, *D. magna*, *G. pulex* and *Lemna minor*, were chosen to observe the effects of test organisms on aggregation. *D. magna* were obtained from an in-house culture maintained at 21 ± 1 ºC in M4 on a diet of algae under a 16 h light: 8 h dark cycle. *G. pulex* were collected from Bishop Wilton, East Yorkshire, United Kingdom and were maintained in the laboratory at room temperature in APW for at least 10 d under s 12 h light:12 h dark cycle on a diet of horse chestnut leaves (*Castanea sativa*) prior to testing. *L. minor* were obtained from an in-house culture maintained in Gamborg's B-5 basal medium at 20 ± 1 ºC under 10000 lux light intensity. For the study, 5 day old *D. magna* and adult *G. pulex* were used.

Table 9. Summary of the characteristics of the 49 natural water samples used in the aggregation studies

Parameters	unit	Mean	Minimum	25%	75%	Maximum
pH	N.A	6.13	3.79	4.55	7.3	7.90
Conductivity	µS/cm	278.40	46.1	85.9	245.50	1239.00
Ammonia-N	µg/mL	0.17	0.003	0.03	0.16	1.25
Nitrate-N	µg/mL	0.71	0.00	0.075	1.17	2.27
DOC	mg/L	14.71	1.84	5.42	7.74	49.3
Ionic strength	mmole/L	2.38	0.08	0.37	2.47	11.41
SO_4^{2-}	mmole/L	0.07	0.01	0.02	0.10	0.23
Cl^-	mmole/L	0.21	0.02	0.08	0.29	0.71
NO_3^-	mmole/L	0.02	0.00	0.01	0.03	0.06
PO_4^{3-}	mmole/L	0.00	0.00	0.00	0.01	0.01
F^-	mmole/L	0.00	0.00	0.00	0.00	0.03
K^+	mmole/L	0.07	0.00	0.01	0.15	0.31
Na^+	mmole/L	0.55	0.01	0.05	0.44	3.57
Ca^{2+}	mmole/L	0.67	0.00	0.02	0.82	3.61
Mg^{2+}	mmole/L	0.23	0.01	0.03	0.23	1.25
Hardness*	mg/L	90.89	1.56	5.77	103.55	484.69

N.A : Not available, *: calculated value

Behaviour of gold nanoparticles

Test media and natural waters

The behaviour of the study nanoparticles in each artificial test medium was monitored over 48 h using NTA. Prior to the aggregation studies, the stock solutions were ultra-sonicated for 15 min and duplicates of 0.5 mg/L of Au-MUDA nanoparticles and citrate and 1 mg/L of Au-PEG-NH$_2$ nanoparticles and Au-PEG nanoparticles then prepared from the stock solution. Following addition of the ENPs, samples (1 mL) were taken for NTA analysis from each duplicate 1, 2, 4, 6, 8, 24 and 48 h after addition of the ENPs to the media. The same test concentrations were used for the natural water studies. In these studies Au-MUDA nanoparticles was dispersed into all water samples while for the other particle types only twenty six water samples were used. The test duration was also shorter with samples being taken for NTA analysis 1, 2, 4, 6 and 8 h after addition of the ENPs. Samples of media and natural water, without ENPs, were also taken for NTA analysis and these analyses showed the 'background' nanoparticle concentrations in the test media were lower than or close to the NTA limits of detection.

Effects of test organism

In three of the media, the influence of the presence of a test organism on aggregation of Au-MUDA nanoparticles was also assessed over 24, 48 or 96 h, the media/organism/exposure time combinations were: M4 media /*D. magna* /48 h, APW /*G. pulex* /96 h, and Gamborg's media /*Lemna minor* /24 h. The organism loadings for *D. magna* and *L. minor* were based on OECD guidelines 202 and 211 (OECD, 2004; OECD, 2006) while the loading for *G. pulex* was based on the method of (Meredith-Williams *et al.*, 2012). For *D. magna,* there were four replicates of 5 animals in 30 mL of test solution; for *G. pulex,* there were three replicates of 10 animals in 500 mL of media. For *L. minor* colonies, there were 3 replicates of 4 colonies in 100 mL of test

solution. For the invertebrates, samples (1 mL) of media were taken 0, 1, 2, 4, 6, 8, 24, 48 and 96 h for NTA analysis and for the macrophyte, samples were taken at 0, 1, 4, 6, 8 and 24 h.

Effects of humic acid

To investigate the effects of dissolved organic carbon, duplicate 0.5 mg/L dispersions of Au-MUDA nanoparticles, citrate and PEG-NH$_2$ were prepared in either deionised water or deionised water containing 1 mg/L or 5 mg/L of HA. Samples of dispersions were taken 0, 1, 2, 4, 6 and 8 h after spiking for characterisation of particle size distributions by NTA.

Statistical analyses

Statistical analysis of the data was performed using PASW (v 19; SPSS Inc.). Data were evaluated for normality by a Shapiro-Wilk or a Kolmogorov-Smirnov test and homogeneity was then confirmed. For the *D. magna* results, two-way ANOVA was used and for the HA results for Au-MUDA nanoparticles and Au-PEG-NH$_2$, a non-parametric analysis (Kruskal-Wallis) test was used to evaluate differences in behaviour between treatments and de-ionised water. A nonparametric analysis (Scheirer-Ray-Hare (SRH) test), was used to assess the differences in aggregation of Au nanoparticles for all the other treatments (i.e. standard media and behaviour in the presence of *L. minor* and *G. pulex*) compared to deionised water. The Scheirer-Ray-Hare test is non-parametric analysis equivalent of a two way ANOVA with replication and extension of the Kruskal- Wallis test (Dytham, 2011). The significance level was *p* < 0.05.

Results

Behaviour in standardised test media

The behaviour of the studied nanoparticles depended upon particle surface chemistry and the type of test media. Aggregation was typically observed within 1 - 6 h after which time the mean particle sizes stabilised (Figure 4). No significant increase in mean size of the Au-PEG-NH$_2$ was seen in any test media compared to deionised water (SRH, $p > 0.05$). With the exception HW, there was also no significant difference in the aggregation of Au-PEG nanoparticles in any of the standard media compared to deionised water (SRH, $p > 0.05$). In contrast, significant aggregation was seen for the Au-MUDA nanoparticles in all test media compared to deionised water (SRH, $p < 0.05$). For the Au-citrate nanoparticles, increased aggregation was seen in all test media (SRH, $p < 0.05$) except in MHW and SW (SRH, $p > 0.05$).
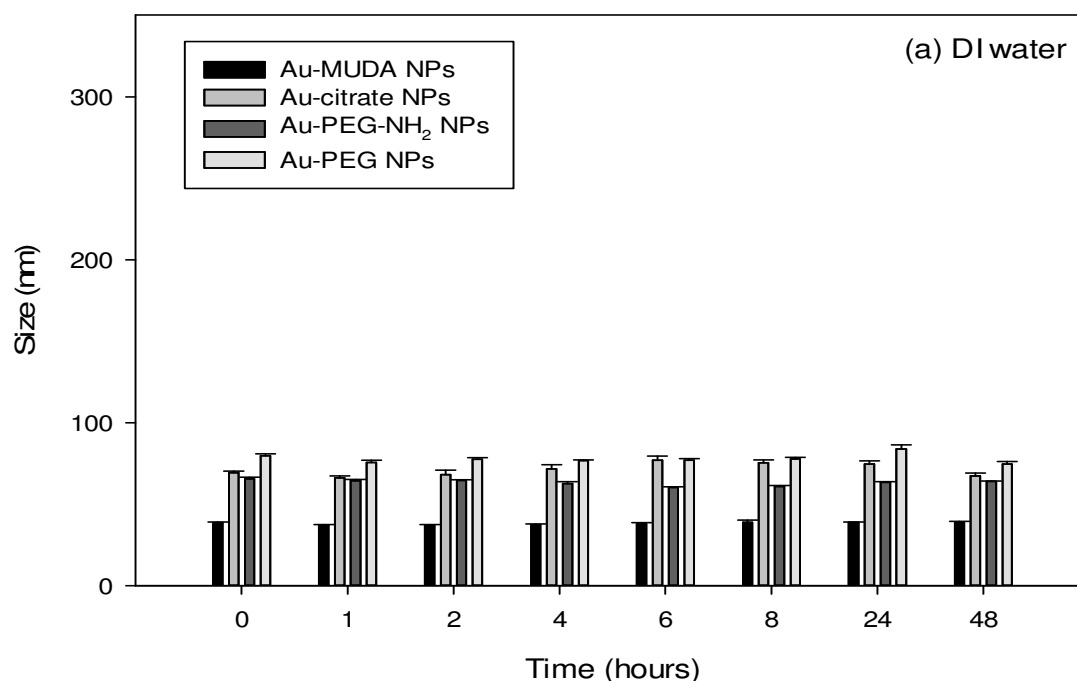
Figure 4. Change in mean particle size of four types of Au ENPs in standard test media. (a) DI water, (b) APW, (c) M4 media, (d) ASW, (e) Algae media, (f) Lemna media, (g) HW, (h) MHW and (i) SW.
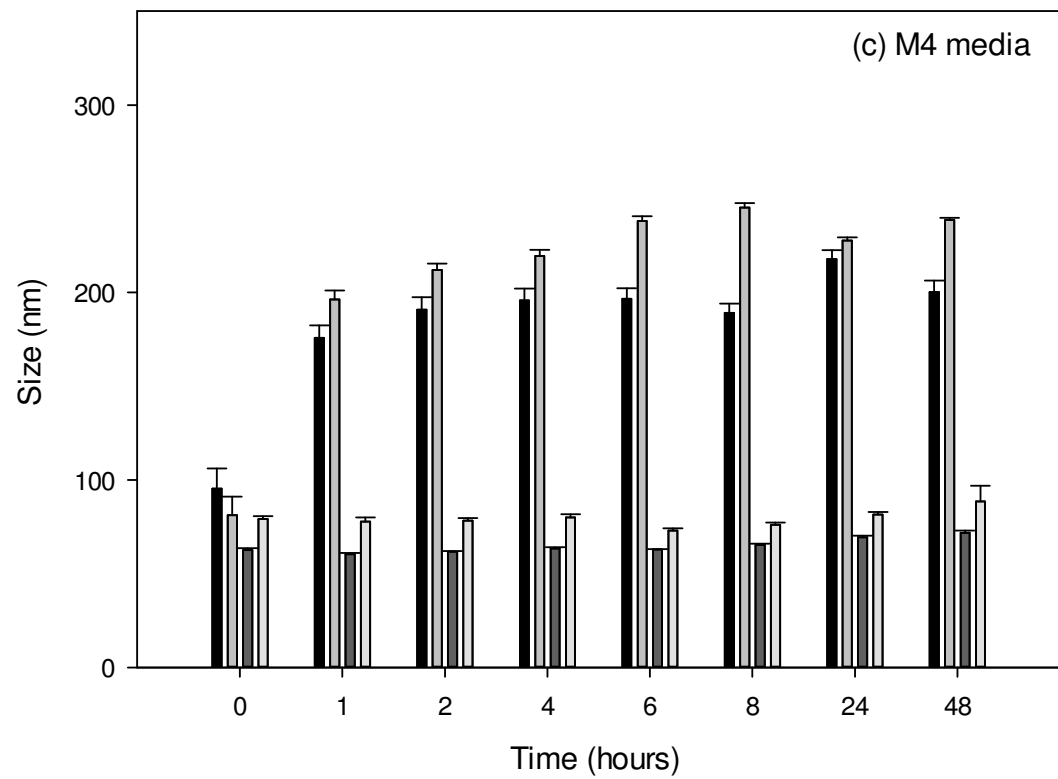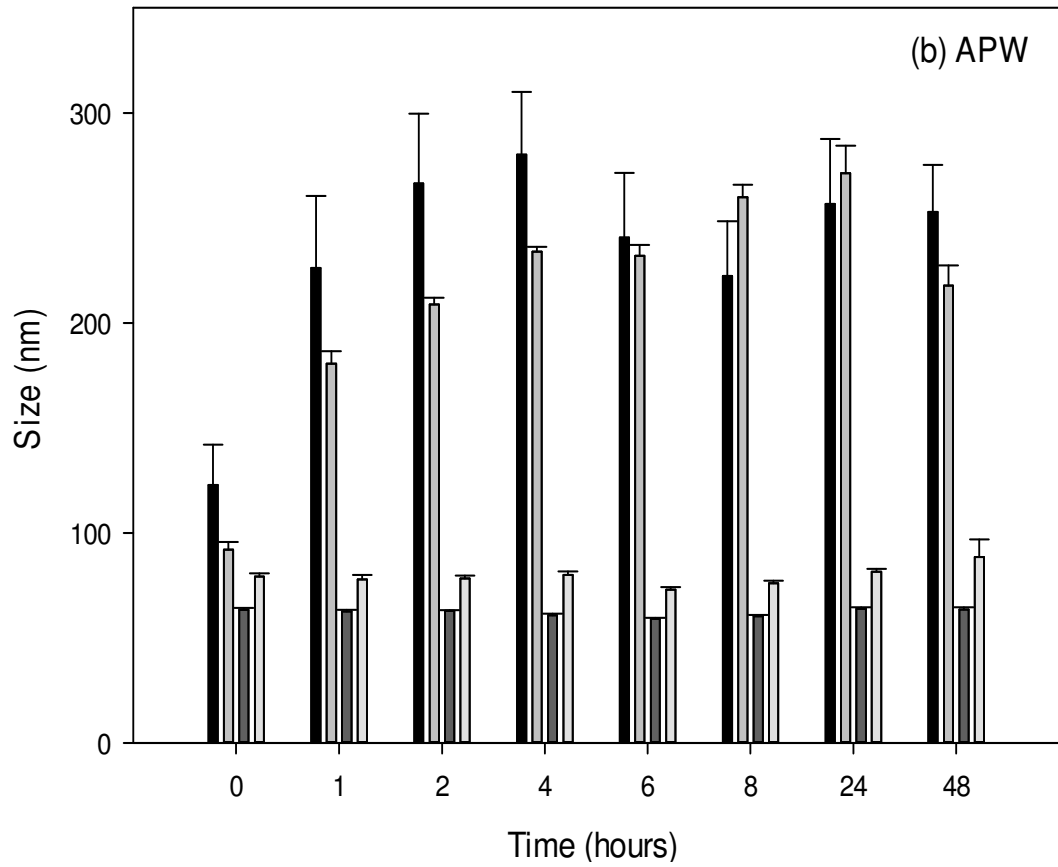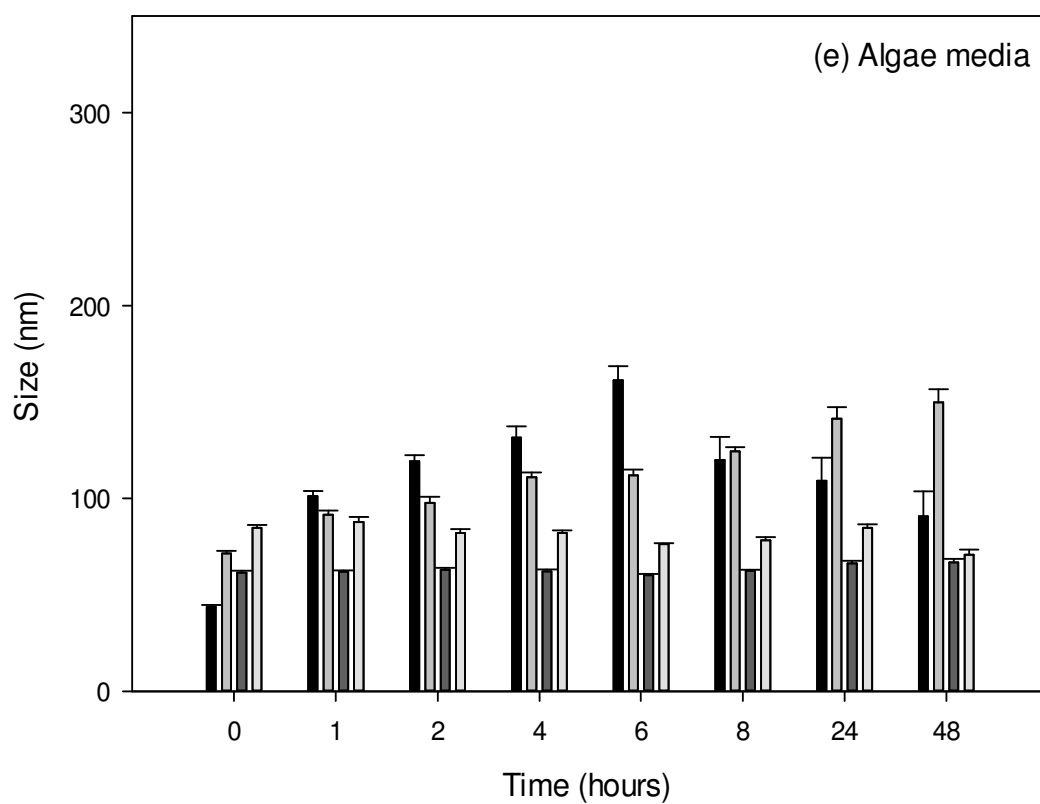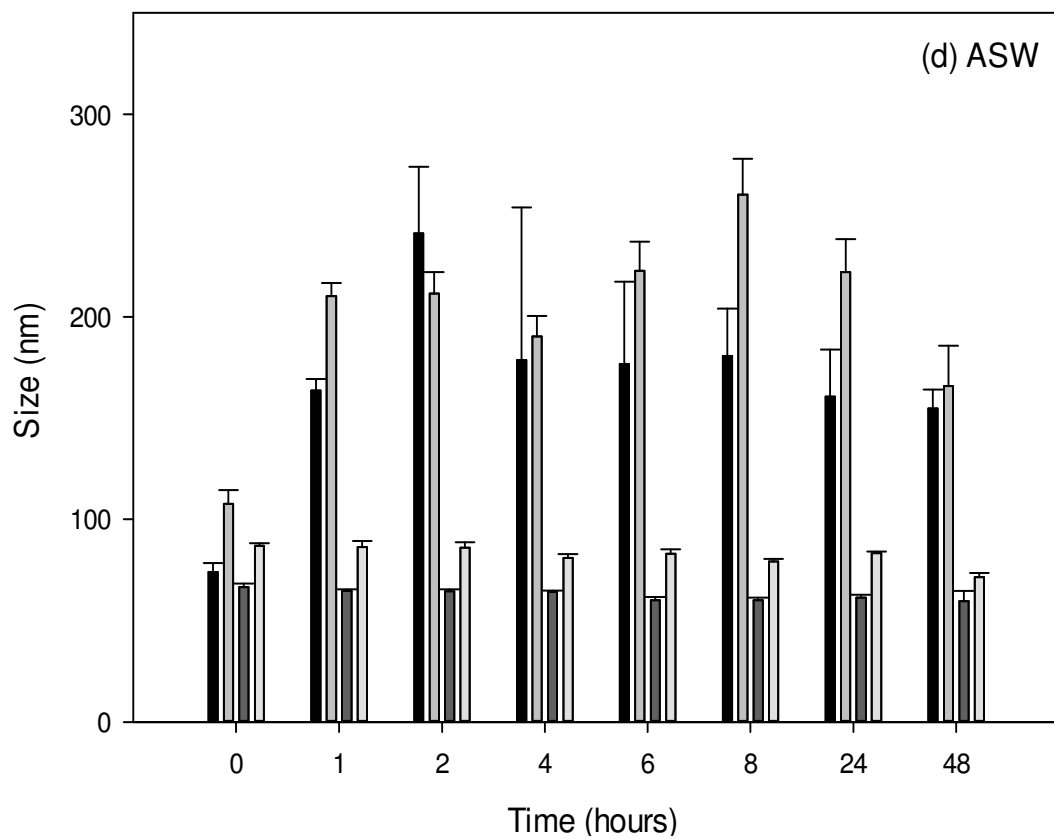
Figure 4. Continued.

Figure 4. Continued.

(f) Lemna media

(g) HW

Figure 4. Continued.

(h) MHW

(i) SW
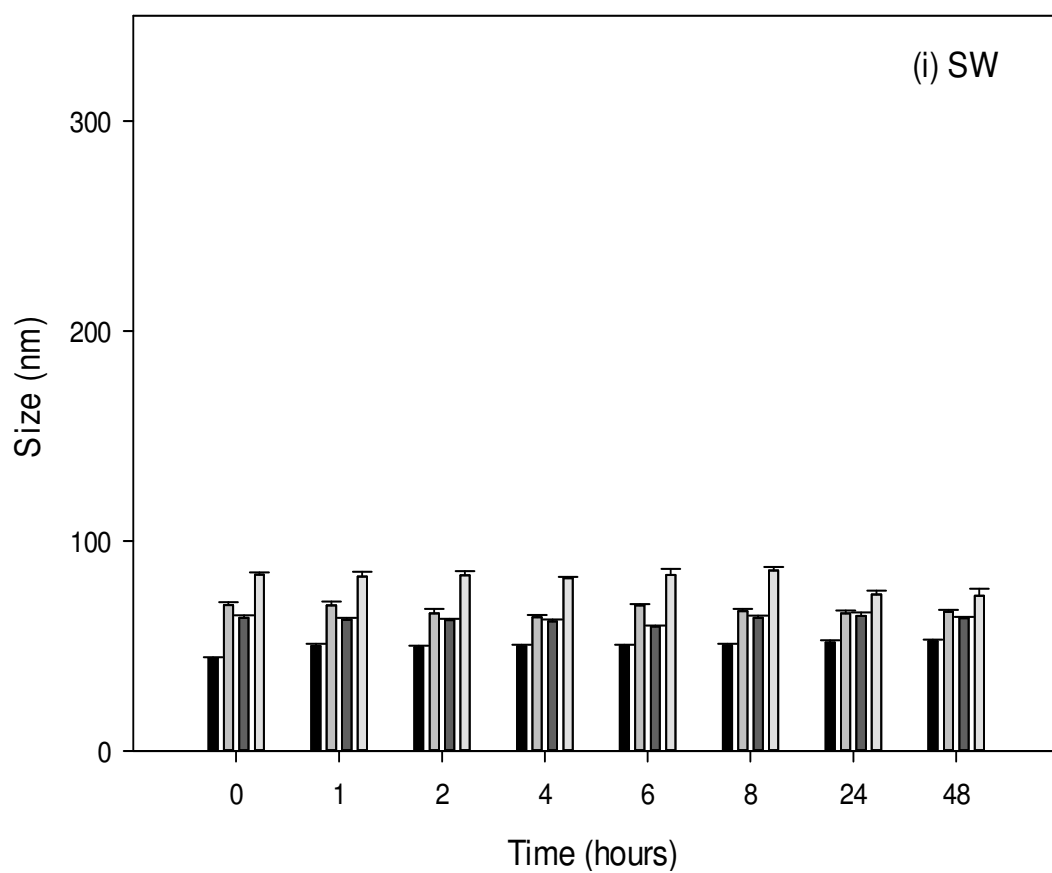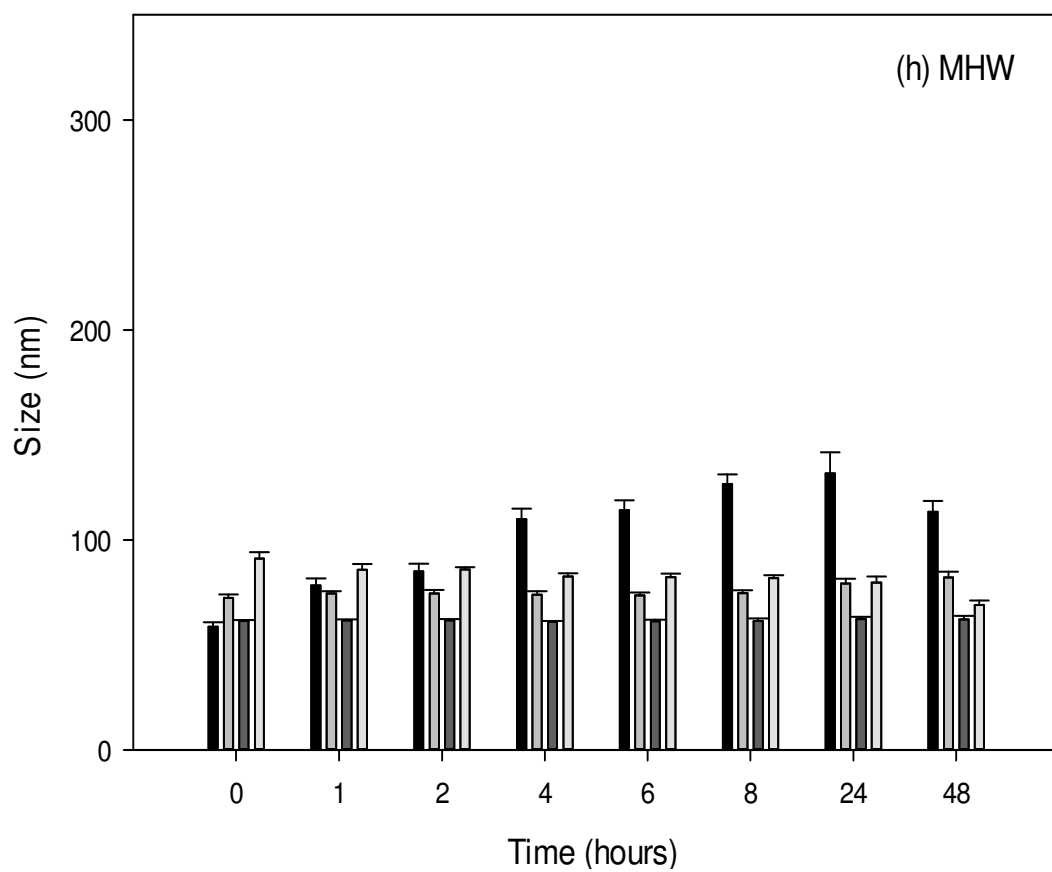
Figure 4.Continud

Effects of test organisms on aggregation

As the Au-MUDA nanoparticles were found to be unstable in the majority of test media, studies were performed to assess the effects of three organism/media combinations on the behaviour of these nanoparticles only. In the absence of test organisms, the nanoparticles aggregated with mean particle sizes at the end of the study being 3 (Lemna media) to 10 times greater than the starting mean particle size of the stock solution. However, the presence of *D. magna* and *G. pulex* significantly reduced the degree of aggregation in M4 and APW (Figure 5a and 5b; two-way ANOVA and SRH, *p* < 0.05). The presence of *L. minor* had no effect on aggregation (Figure 5c; SRH, *p* > 0.05) although particles were observed to sediment out in the presence of the macrophyte.

Behaviour in natural waters

There was large variability in the behaviour of the study nanoparticles in the natural water samples with mean particle sizes varying by a factor of 2 (Au-PEG-NH$_2$) to 6 (Au-MUDA nanoparticles) between samples (Figure 6 (c) and (a)). The Au-PEG-NH$_2$ and Au-PEG nanoparticles were found to be less stable in the natural waters (sized from 72 nm to 245 nm) than in the artificial test media (mean size range of between 56.3 nm and 86 nm) (Figure 6 (c) and (d)). Au-MUDA nanoparticles were generally less aggregated in natural waters compared to standard media (Figure 6 (a)). Substantial variation was seen in the aggregation of Au-citrate nanoparticles in natural waters with these ENPs appearing to be stable in some samples and unstable in others (Figure 6 (b)).
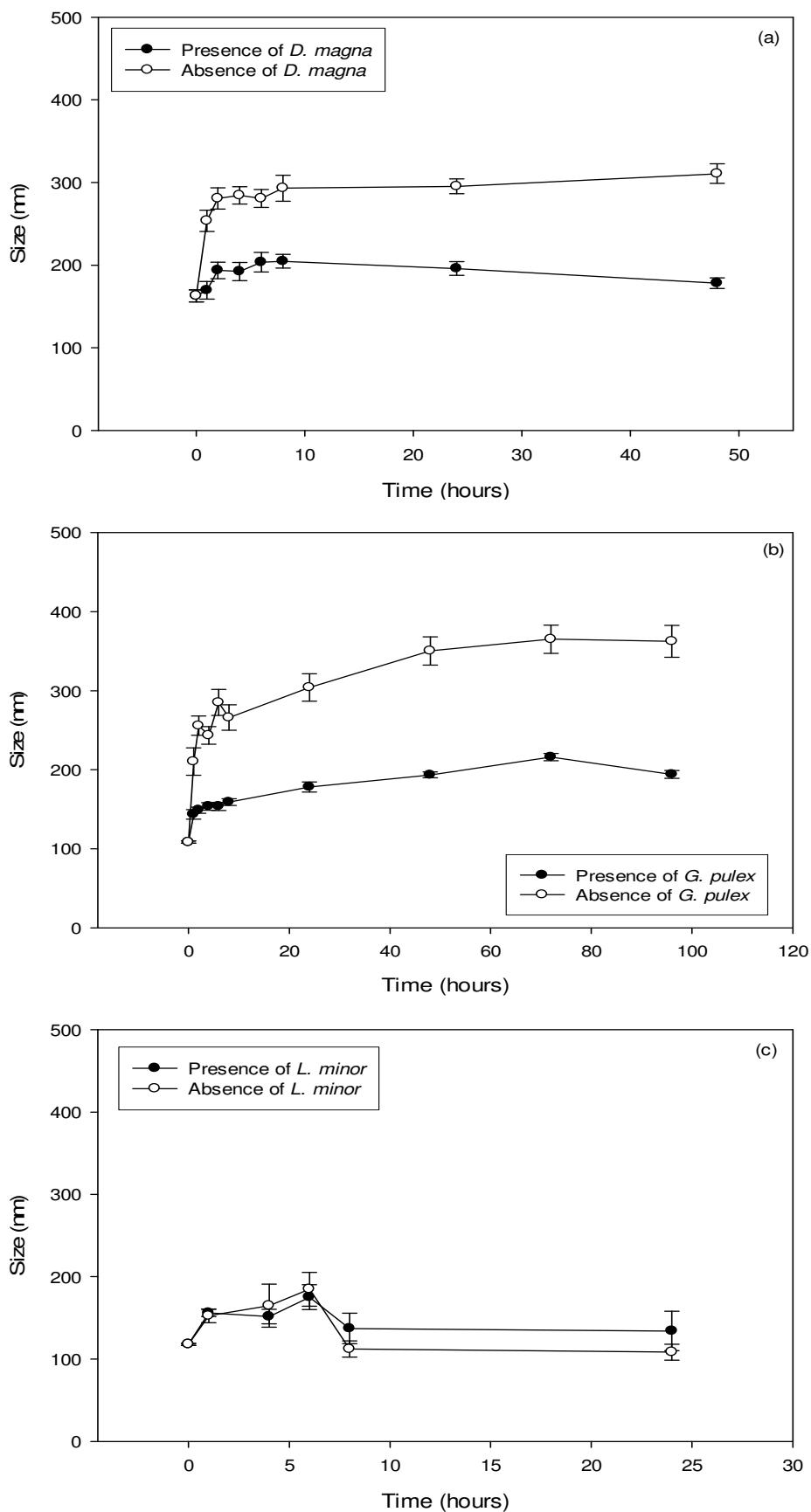
Figure 5. Change in particle size (mean values with standard errors) cross section area over time for Au-MUDA particles in the presence and absence of test organisms. (a) *Daphnia magna* (b) *Gammarus pulex* and (c) *Lemna minor*.
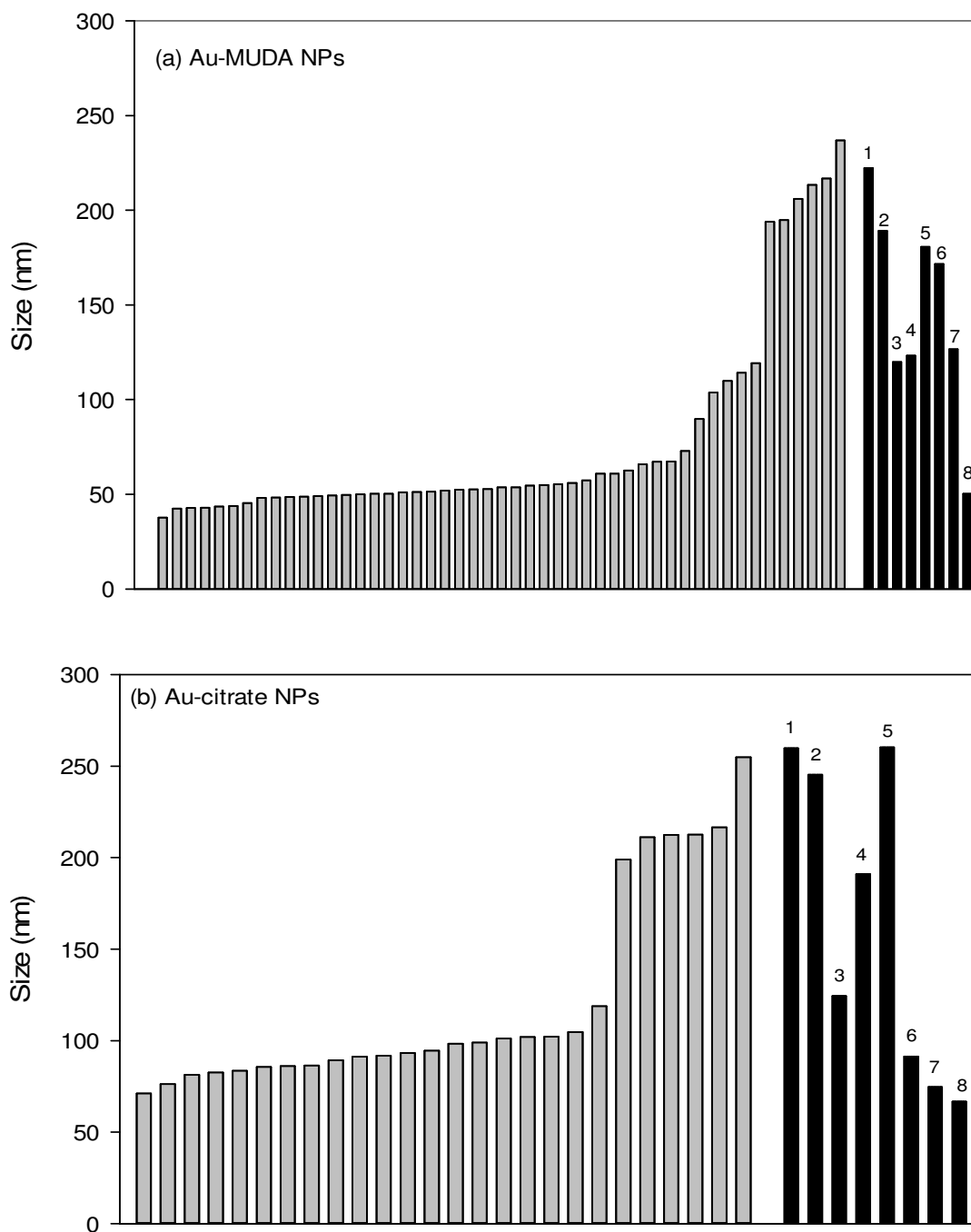
Figure 6. Comparison of mean particle size of four type of Au nanoparticles between natural waters (grey bars) and standard ecotoxicity test media (black bars) at 8 h after dispersion. 1: artificial pond water, 2: M4 media, 3: artificial salt water, 4: algae media, 5: Lemna media, 6: EPA hard water, 7: EPA moderate hard water and 8: EPA soft water.
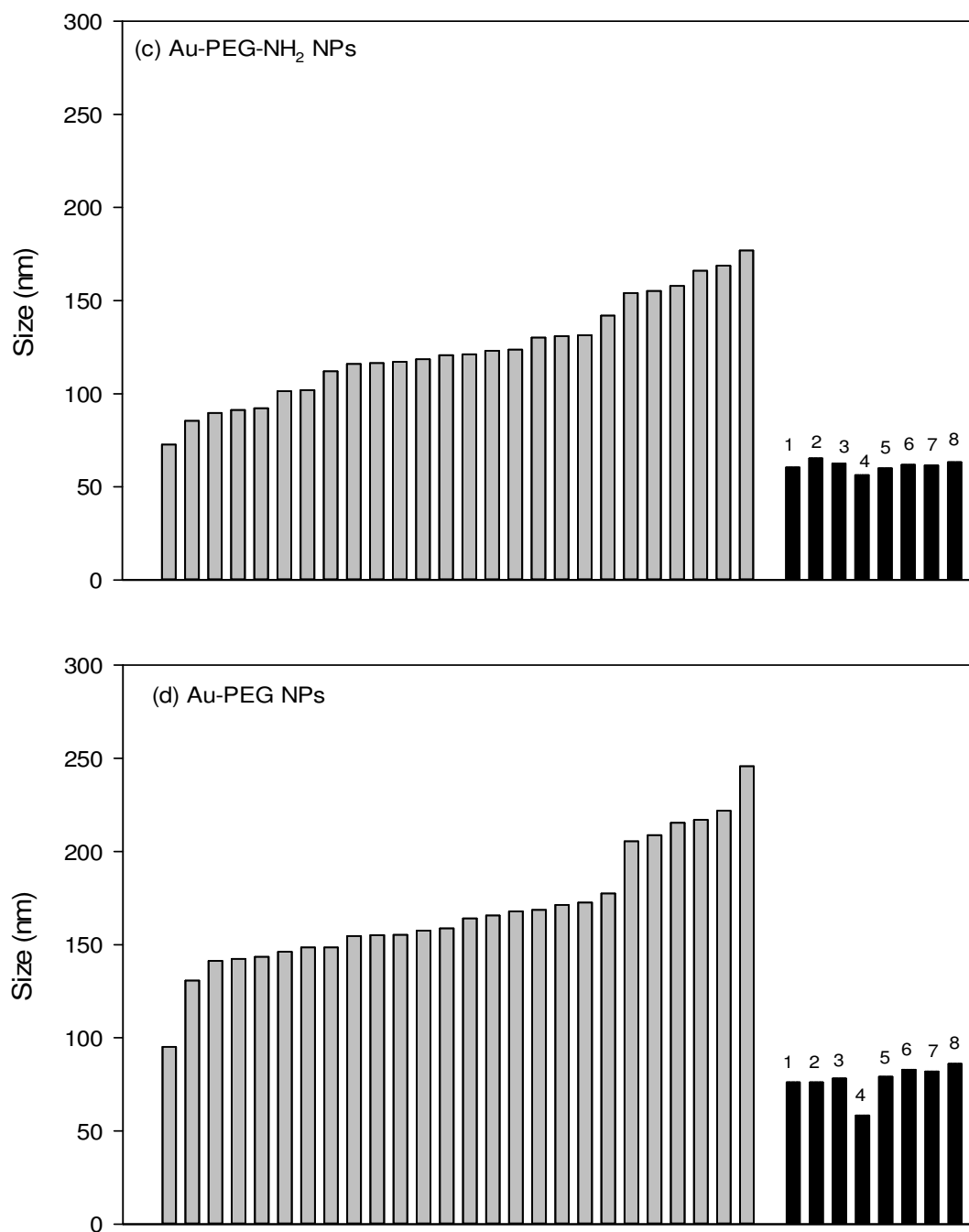
Figure 6. Continued.

Effects of humic acid on aggregation

It is well known that the presence of dissolved organic material stabilises some ENPs (Chen and Elimelech 2007; Hyung *et al.* 2007) and that this depends on the surface charge or coating agents of nanoparticles (Baalousha 2008). When Au-PEG nanoparticles were added to humic acid solutions, there were few particles detected. In these exposures, aggregates of the Au-PEG particles were visually observed to settle out which is explains the lower level of detection. It was only possible to explore the effects of humic acid on the behaviour of other three study nanoparticles. A small, but significant increase in mean particle size was seen with increasing humic acid concentrations in DI water for all Au nanoparticles (Figure 7 (a); Kruskal-Wallis and one-way ANOVA, $p < 0.05$). With the exception of M4 media, addition of humic acid significantly reduced the mean particle size of Au-MUDA nanoparticles in all test media compared to the media only treatment (Figure 7 (a); Kruskal-Wallis, $p < 0.05$). While a small but significant increase in mean particle size was seen for the Au-citrate nanoparticles in the algal media and Lemna media (Figure 7 (b); Kruskal-Wallis and one-way ANOVA, $p < 0.05$), HA addition had no effect on mean particle size in the other test media (Figure 7 (b)). For the Au-PEG-NH$_2$ nanoparticles, a significant increase in mean particle size was seen with increasing HA concentration for all media (Figure 7 (c), Kruskal-Wallis, $p<0.05$).
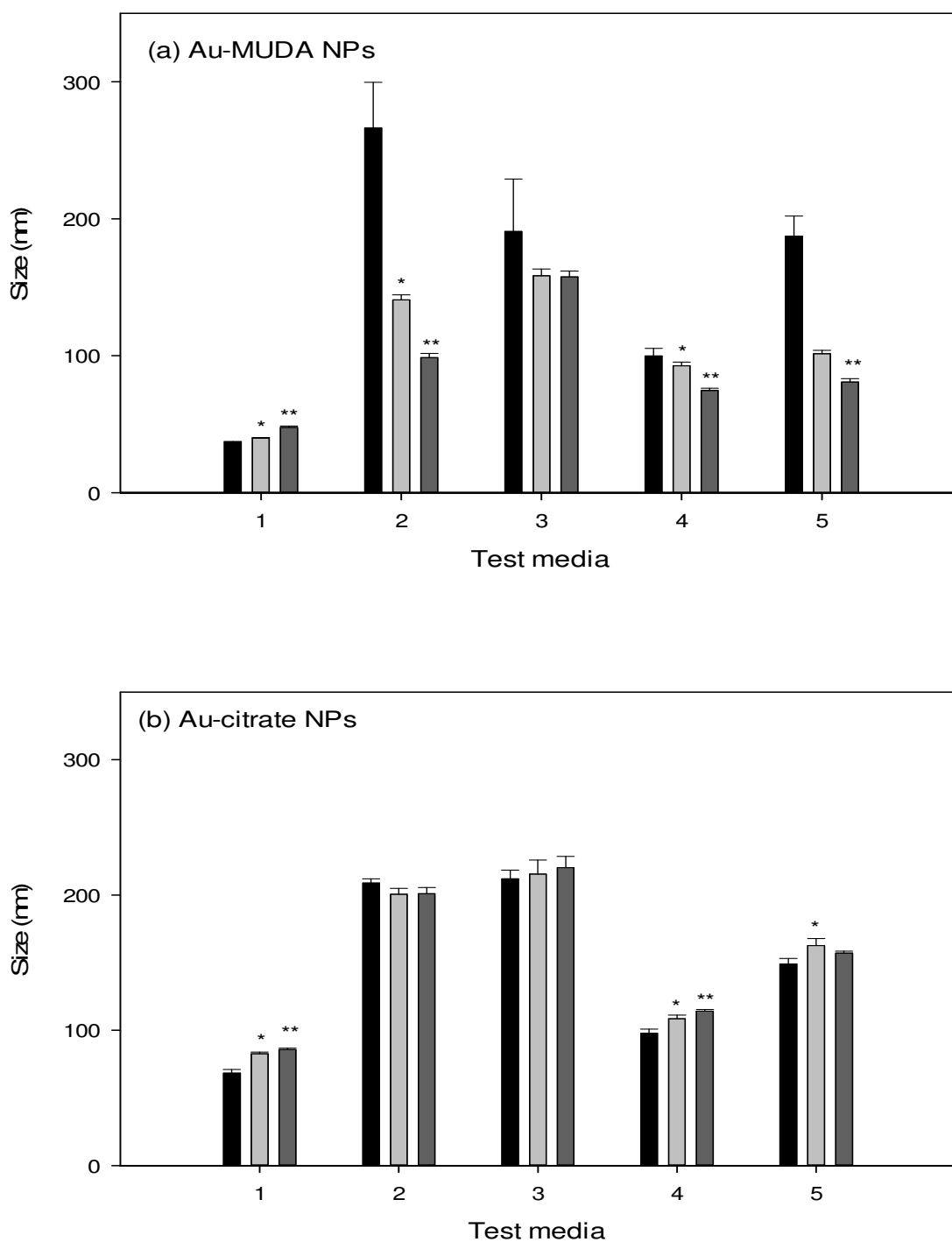
Figure 7. The effects of humic acid on aggregation of three types of Au ENPs in different test media after 2 h disperse. Error bars indicate standard errors of mean size of particle. 1: DI water, 2: APW, 3: M4 media, 4: Algae media and 5: Lemna media.
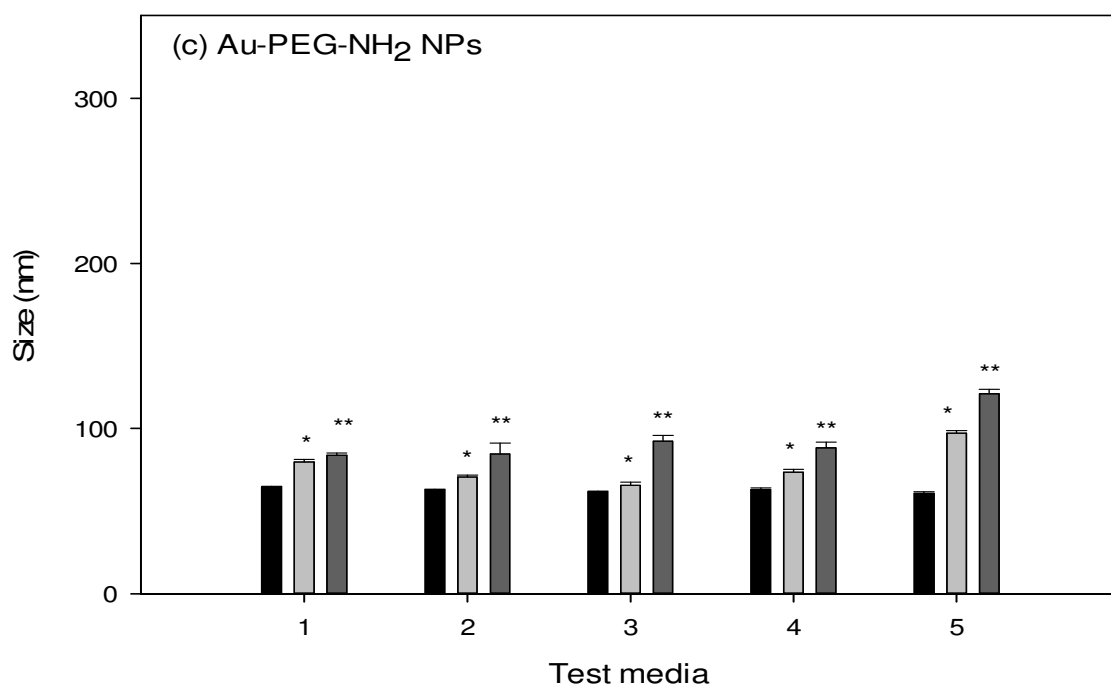
Figure 7. Continued.

Discussion

Behaviour in test media

Aggregation of the study nanoparticles was assessed in a wide range of ecotoxicity media that have previously been used by other workers to assess the effects of a range of metal-based nanoparticles on different aquatic organisms (Table 10). M4 media and MHW, in particular have been used in these investigations. While the nanoparticle mass concentrations used in this study were high compared to concentrations expected in the natural environment, comparison with concentrations used in ecotoxicity studies (Table 10) indicate that they are similar or lower than concentrations of metal and MeO nanoparticles that have been previously tested.

The aggregation behaviour of all Au nanoparticles in the test media varied according to the surface coatings of the particles and composition of test media. The 'positive' Au-PEG-NH$_2$ and 'neutral' Au-PEG nanoparticles were stable in most test media. Similar results were found by Stankus *et al.* (2011) who showed that 'neutral' polyvinyl pyrrolidone capped Au particles are stable across a range of solutions of different IS and that aggregation of 'positive' mercaptopentyl (trimethylammonium) capped Au particles does not occur in 10mM of CaCl$_2$ and MgCl$_2$. The stability of the 'neutral' Au-PEG nanoparticles is reasonably explained by steric repulsion arising from interactions of the capping agent whereas the stability of the Au-PEG-NH$_2$ nanoparticles is understood in the context that these particles are positively charged in the test media and that adjacent particles will repel each other (French *et al.* 2009; Stankus *et al.* 2011).

Table 10. Engineered metal nanoparticles that have been studied in published ecotoxicological studies and the type of test media employed in these studies

Particle types	Coating	Test concentration ranges	Test media						
			M4	Algae media	Lemna media	HW	MHW	SW	Others
Aluminium		3.6 - 27.8 mg/L					2[1,2]		
Cobalt		3.6 - 27.8 mg/L					1[1]		
Copper		100 µg/L - 27.8 mg/L					1[1]		1[3]
Gold		500 µg/L - 30 mg/L		1[4]			2[5]		
Gold	Citrate	1.3, 2.6, and 5.2 mg/L				1[6]	1[6]	1[6]	
Gold	Dodecane thiol coated	~ 50 mg Au/L		1[7]					
Nickel		3.6 - 27.8 mg/L					1[1]		
Silver		0.1 µg/L - 100 mg/L	3[8,9,10]		1[11]	2[13,14]	3[1,12,15]		
Silver	Citrate	0.625 µg/L - 400 mg/L	2[16,17]		1[18]		3[19,21,22]	1[21]	
Silver	Poly vinyl pyrrolidone	0.45 - 50 µg/L					1[20]	1[22]	

1) Griffitt et al. (2008), 2) Griffitt et al. (2011), 3) Shaw et al. (2011), 4) Hartmann et al. (2012), 5) Lovern et al. (2008), 6) Lee and Ranville (2012), 7) Hoecke et al. (2011),
8) Park and Choi (2010), 9) Zhao and Wang (2011), 10) Wang et al. (2012), 11) Kim et al. (2011), 12) Gaiser et al. (2012), 13) Laban et al. (2010), 14) Chae et al. (2009),
15) Jo et al. (2012), 16) Asghari et al. (2012), 17) Römer et al. (2011), 18) Gubbins et al. (2011), 19) Allen et al. (2010), 20) Bilberg et al. (2011), 21) Croteau et a., (2011),
22) Poynton et al. (2012)

In contrast to the positive and neutral particles, the stability of the 'negative' Au-citrate and 'amphoteric' Au-MUDA particles varied considerably with greatest aggregation generally being seen in the media with highest IS. Similar relationships between IS and aggregation have been seen in other studies with Au-citrate and Au-MUDA capped particles (Stankus *et al*. 2011; Liu *et al*. 2012) and citrate capped Ag nanoparticles (El Badawy *et al*. 2010). The instability of the negative and amphoteric particles at higher IS are probably explained by the compression of the electrostatic double layer on the particle surface which reduces the degree of electrostatic repulsion (e.g. Stankus *et al*. 2011).

The observed behaviour of the Au-citrate and Au-MUDA nanoparticles in the different systems highlights the problem of performing ecotoxicity studies with standard media. The large differences in particle size distribution across media demonstrates that if a suite of ecotoxicity studies were performed on these particles, the exposure of the test organisms would be very different, meaning that results would not be at all comparable. This raises a significant challenge for the environmental risk assessment process.

Effects of organisms

The presence of *D. magna* and *G. pulex* significantly reduced the degree of aggregation of the Au-MUDA nanoparticles. Even though *L. minor* is a photosynthetic aquatic macrophyte which will affect the pH of the test media over time (in this study pH was observed to drop from 6.5 to 6.0), this species had no effect on aggregation. The observed effects for the invertebrates might be explained by effects of the organisms on water movement, the physical breakdown of aggregates by the test organisms and/or chemical modification of the particles within the invertebrates. Previous work has shown that greater aggregation of CuO nanoparticles occurs in low flow velocity environments compared to higher flow velocity systems (Jeong and Kim, 2009).

Studies with *D. magna* using lipid coated nanotubes showed that, following ingestion, the animals are able to modify the solubility of the particles, probably as a result of the digestion of the surface coating (Roberts *et al.*, 2007) while *D. hyalina* has been shown to reduce the aggregation of mineral colloids in lake water and this is thought to be due to action of the filter mesh of the organism (Filella *et al.*, 2008). Other invertebrates have been shown to increase the aggregation of nanoparticles. For example, the freshwater crustacean *Thamnocephalus platyurus* enhances aggregation of C_{60} fullerenes (Patra *et al.*, 2011). The results highlight the need to better understand the effects of organisms on the properties and speciation of nanoparticles and that biological effects on nanoparticles behaviour should be considered when assessing the exposure and effects of nanoparticles in the natural environment.

Natural waters vs. test media

The behaviour of the study nanoparticles varied across the natural waters. Comparison of the results for natural waters with observed behaviour in the standardised test media shows that the Au-PEG-NH$_2$ and Au-PEG nanoparticles behave very differently in the natural waters compared to the standard media. In natural waters, these particles are aggregated to different degrees whereas in the standardised media, the particles are stable (Figure 6). Limited aggregation of the Au-MUDA and Au-citrate nanoparticles was seen for the majority of the natural waters tested whereas these particles were found to aggregate in the standardised media (Figure 6). The different behaviours of Au nanoparticles between natural waters and standard media might be explained by differences in the dissolved organic carbon concentration and IS of the different samples (Keller *et al.* 2010). The IS of the test media (mean = 8.21 mmol/L) was generally higher than in the natural waters (mean = 2.38 mmol/L) and DOC was present in the natural waters (mean = 14.7 mg/L) while in standard media no DOC was present.

Previous studies have shown that humic substances can adsorb onto Au-MUDA and citrate nanoparticles leading to electosteric repulsion in natural waters (Gao *et al.* 2009). Humic acids have also been shown to change the surface charge of Au-PEG-NH$_2$ nanoparticles and Au-PEG NP to either a negative charge or to neutral (Ottofuelling *et al.*, 2011) resulting in aggregation of the particles depending on the amount of cations in natural waters (Zhang *et al.*, 2009). To explore whether DOC addition could be used as a refinement to standard ecotoxicity testing procedures in order to provide more environmental realism, studies were performed in a selection of the standard media using HA addition.

Effects of natural organic matter

The presence of humic acid significantly reduced the aggregation of the Au-MUDA particles and significantly increased the aggregation of the Au-PEG-NH$_2$ nanoparticles but had limited impact on the stability of the Au-citrate nanoparticles. The results for the Au-PEG-NH$_2$ nanoparticles are probably explained by the neutralisation of the NP surface charge by the humic acid (Dickson *et al.*, 2012). Previous studies with Au-MUDA nanoparticles contrast with our observations and show that natural organic matter had no effect on the aggregation rates of the 30 nm Au-MUDA particles (Liu *et al.*, 2012). However, studies with mercapto(ethoxy)ethanol (MEE) capped gold nanoparticles, which are structurally similar to MUDA particles, indicate that NOM does have a stabilising effect on the particles (Stankus *et al.*, 2011). Data from the humic acid addition experiments indicated that for positive and amphoteric nanoparticles, addition and dissolved organic carbon to standardised ecotoxicity media may help bridge the gap between behaviour in laboratory-based studies and behaviour of these particles in natural systems.

Overall, these results indicate that the behaviour of nanoparticles in standardised media can be very different from behaviour in the natural environment, particularly for neutral and positive nanoparticles, this therefore brings into question the broader

environmental relevance of many of the studies that have been performed to date into the effects of metal-based nanoparticles on aquatic organisms.

Conclusion

This study shows that ENPs had very different behaviours in various types of standardized test media depending on the particle type. The aggregation of ENPs was also affected by existence of test organisms and DOC. The behaviour of nanoparticles in natural waters was completely different from behaviour in laboratory media. The mismatch between behaviour of ENPs in standard media and natural systems raises questions around the relevance of standard ecotoxicity experiments for use in the risk assessment of nanoparticles. Therefore, for the risk assessment of ENPs, it is crucial that appropriate test media be selected for the ecotoxicity testing. In the short term, it may be appropriate to use a range of real river water samples that represent the range water characteristics seen in the natural environment, for ecotoxicity tests. Such an approach might provide a better characterisation of the risks of ENPs in natural systems. In the longer term, as our knowledge of ENP fate and toxicity develops, it may be possible to tailor testing based on the properties of the ENP being studied. Overall, there is a pressing need to develop ecotoxicity tests that provide test conditions which are environmentally relevant. Such testing should probably be tailored to the surface properties of the ENP under investigation.

The work described in this Chapter explored the behaviour of Au ENPs with different surface functionalities. In the next Chapter we explore whether particles with a different core but the same functionality behave in the same way.

Chapter 3

Aggregation of metal nanoparticles in the environment: does the core matter?

Introduction

In the previous Chapter, we explored the degree of aggregation experienced by Au nanoparticles with various surface functionalisation across a range of standardised test media and natural waters. The particle size was found to be principally dependent on the surface functionalisation and the water type. These studies were done with Au particles so the applicability of the developed relationships to other particles with other metals as cores is unknown. The core material of ENPs is not only an important descriptor for their application and use (Ghosh Chaudhuri and Paria, 2011) but also is strongly related to nanoparticle toxicity (Christian *et al.*, 2008). One study showed that Ag nanoparticles caused rapid inhibition of algal photosynthesis in, the freshwater alga *Chlamydomonas reinhardti,* which was meditated by the release of Ag^+. Furthermore, results showed that algae could mediate the release of Ag^+ from the nanoparticles (Navarro *et al.*, 2008b). Franklin *et al.* (2007) exposed ZnO nanoparticles to the freshwater green alga *P. subcapitata,* and found adverse effects could be attributed to dissolved Zn (II) originating from the ZnO nanoparticles. This study showed that the

effect was not caused by nanoparticulate form of ZnO, but rather attributed it to the presence of ZnO in the tests.

Although the core material could play an important role, whether particle aggregation is affected by core material has seldom been considered. The objective of this study described in this Chapter was therefore to investigate whether the core material influences particle aggregation of metal ENPs. The studies described in this Chapter employed Ag nanoparticles coated with citrate and 11-mercaptoundecanoic acid cappings to observe aggregation in standardized test media. The results were then compared to the results obtained for the equivalent Au nanoparticles which are reported in Chapter 2.

Material and methods

Study materials

Studies were done on Ag nanoparticles with an average particle size of 30 nm. Two different capping agents were used, namely 'Amphoteric' 11-mercaptoundecanoic acid-capped (MUDA) and 'negative' sodium citrate tribasic dehydrate-capped (citrate). Citric acid capped Ag nanoparticles were prepared in aqueous solution by mixing AgNO3 and citric acid in the molar ratio citric acid/$AgNO_3$ = 12 (0.25 mM of $AgNO_3$, 3.0 mM tribasic salt, 1 L). Two drops of 4M NaOH base solution were added after stirring the citric acid/$AgNO_3$ solution for 10 minutes, and then the solution was heated to 70 ºC for 1 h. During heating the solution gradually changed to dark yellow consistent with the formation of Ag nanoparticles. MUDA passivated Ag nanoparticles were prepared by a ligand exchange reaction of MUDA. MUDA readily displaces the surface citric acid on Ag-citrate nanoparticles. An ethanol solution of MUDA (0.12 g, 3 mL) was added drop wise to 1 L of citric acid capped Ag nanoparticles aqueous stock solution with rapidly stirring. The mixture was kept in subdued light and was stirred for one week. All silver nanoparticles were purified using dialysis. The stock solution (200 mL) of choice was

poured into a dialysis tube. The filled tubes were submerged distilled water (4 L capacity beaker) for 4 d (bath water was changed at regular 5 h intervals). The results of the TEM and UV-Vis spectrum analysis are given in the Appendix 3.

Detailed information on the preparation of the Au nanoparticles is given in Chapter 2.

Standardised test media

Test media commonly used in ecotoxicity testing were used in this study: artificial pond water (APW) (Naylor *et al.*, 1989), OECD Daphnia M4 media (OECD, 2004), Gamborg's B-5 basal medium (Lemna media), artificial salt water (ASW) at 35 ‰ salinity (Kester *et al.*, 1967), and U.S. EPA hard (HW), moderate hard (MHW) and soft (SW) waters (USEPA, 1991). The test media ranged in pH from 6.17 to 7.98 and in IS from 1.85 to 17.2 mM (Park *et al.*, 2014).

Particle aggregation study of silver nanoparticles

Aggregation studies of Ag nanoparticles were performed using the methodology described in Chapter 2. Prior to the aggregation studies, the stock solutions were ultra-sonicated for 15 min to break down any existing agglomerated particles. Solutions of the study nanoparticles were then prepared in duplicate at a concentration of 0.1 mg/L. Samples (1 mL) were then taken 1, 2, 4, and 7 h after dispersion and analysed three times using nanoparticle tracking analysis (NTA) using a NanoSight 2.2 LM 14 instrument (NanoSight Ltd, Amesbury, UK). NTA follows individual nanoparticles in the liquid phase moving under Brownian motion and records their movement as a video on a frame-by-frame basis. After recording for a given time, hydrodynamic diameter of individual particles is calculated using the Stokes-Einstein equation (Malloy and Carr, 2006):

$$d_p = \frac{kT}{3\pi\eta D} \qquad \text{(Equation 3.1)}$$

d_p is hydrodynamic diameter (nm), k is the Boltzmann constant (J K^{-1}), T is the absolute temperature (K), η is the viscosity of the medium (kg m^{-1} s^{-1}) and D is the diffusion coefficient.

The particle aggregations of Ag nanoparticles were compared with that of Au nanoparticles in Chapter 2 to investigate effect of core materials on aggregation.

Statistical analyses

Statistical analysis of the data was performed using SPSS (v 21; SPSS Inc.). Data were evaluated for normality by a Shapiro-Wilk or a Kolmogorov-Smirnov test and homogeneity was then confirmed. One-way ANOVA and Mann-Whitney tests were applied to determine differences in aggregation between different core materials in each test media. The significance level was $p < 0.05$.

Attachment efficiency method

Attachment efficiency (sometimes also referred to as 'inverse stability ratio') is a measure of the propensity of nanoparticles to adhere to each other; it is the fraction of collisions between particles that result in aggregation. Calculation of attachment efficiency from single-particle tracking data (like that acquired by the NanoSight) requires knowledge of 1) the number of primary particles that go to form a given aggregate (and hence the number of successful collisions that must have taken place), and 2) the rate at which the nanoparticles are colliding.

Attachment efficiency was estimated by looking principally at the primary particles, since these constituted the majority of the particles in the samples. By considering their hydrodynamic radii r, a collision cross-section σ between two particles can be

calculated. The mean free paths *l* of particles can be estimated by assuming that the Brownian motion of the nanoparticles can be described adequately by a Maxwell distribution. A Maxwell distribution is used in physics to describe the distribution of energy between particles in thermal equilibrium. The mean free path may be calculated using Equation (3.2), where *n* is the number of particles per unit volume. It is possible to rearrange the Stokes-Einstein equation to extract a mean particle drift speed, $\bar{v}$ from the other parameters, as shown in Equation (3.3), where *T* is the absolute temperature in Kelvin, k_B is the Boltzman constant, and η is the viscosity of the suspending medium (in this case water).

$$l = \frac{1}{\sqrt{2}\sigma n}$$ (Equation 3.2)

$$\bar{\upsilon} = \sqrt{\frac{2Tk_B}{6\pi\eta r}}$$ (Equation 3.3)

The second step involves estimating the number of successful collisions that must have occurred in the time period in order to create aggregates of the size observed. For these purposes, the fractal dimension (which in this case can be used as a measure of the porosity) of the aggregates was assumed to be about 2, halfway between the 1.7 observed in diffusion-limited (fast) aggregation, and 2.3 observed in reaction-limited (slow) aggregation (He *et al.*, 2013).

Once the necessary adhesion rate has been calculated, it is then trivial to take the ratio, which will be the fraction of collisions that resulted in adhesion of particles. This is the attachment efficiency. The results match well with other experimental values reported in the literature (Chen and Elimelech, 2007; Tufenkji and Elimelech, 2004). Two possible means of improving this method would be introducing derivatives to account for the opposing factors that as particles aggregate, there are fewer particles in the suspension to collide, and that as particles aggregate, the size increases, as does the collision cross-section.

Results and Discussion

Effect on aggregation by surface functionalisation and core materials

Overall, the aggregation behaviour of all study Ag and Au nanoparticles were highly dependent upon test media but comparable within each test media. The most aggregation for both core types was observed in APW, M4 media and ASW while the least aggregation was observed in MHW and SW compared with those in DI water after 7 and 8 h exposure.

Comparisons of stabilisation of each particle by surface functionalisation in the test media are described in Figure 8. For Ag nanoparticles coated with MUDA and citrate, the most aggregation was seen in APW, at a mean size of 260 ± 14.76 nm, and 189.83 ± 52.47 nm, respectively. The most stabilisation of those particles was observed in SW, which showed similar particle size with those in DI water. Neither surface functionalized Ag nanoparticles showed significant particle size differences in most test media, except ASW, MHW and SW (One way-ANOVA and Mann-Whitney tests, $p < 0.05$) (Figure 8 (a)). Both of the tested Au nanoparticles behaved similarly to both Ag nanoparticles in the test media. The most aggregation of both Au nanoparticles was seen in APW and the least aggregation occurred in SW. Significant differences in particle size between MUDA coated Au nanoparticles and citrate Au nanoparticles were seen in DI water, Lemna media, HW, MHW and SW (One way-ANOVA and Mann-Whitney tests, $p < 0.05$) (Figure 8 (b)).

(a) Ag NPs
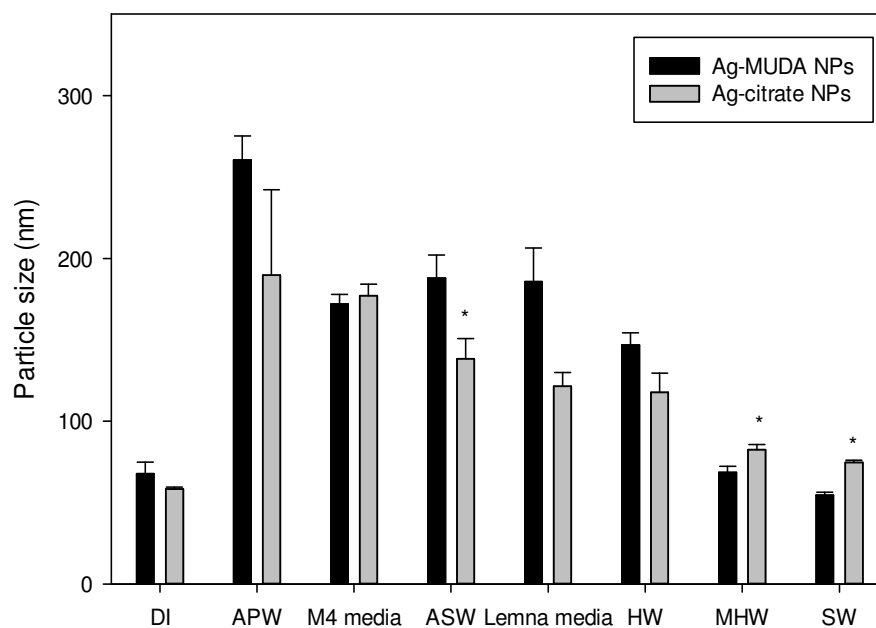
(b) Au NPs
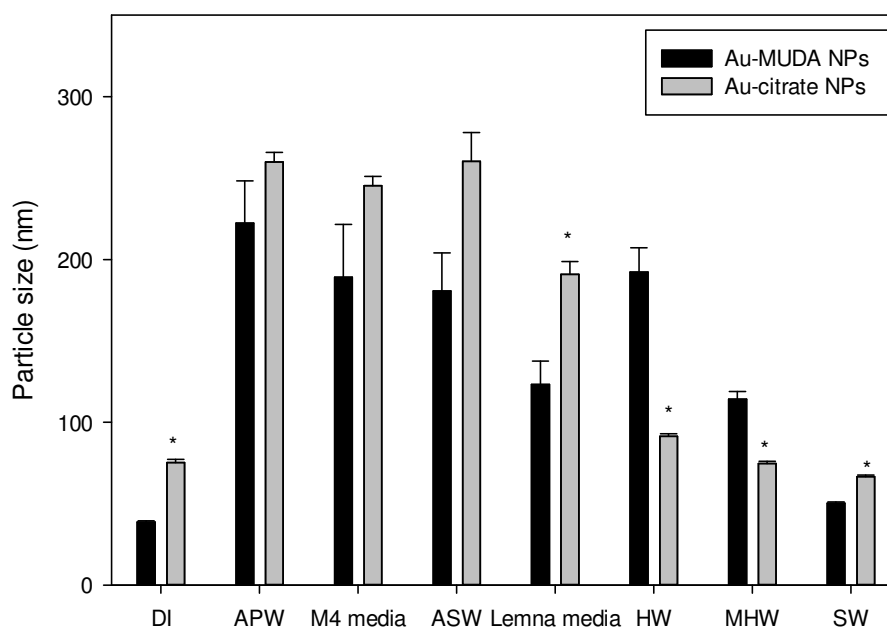
Figure 8. Comparison of mean size of Au nanoparticles and Ag nanoparticles by surface functionalisation at 7 and 8 h dispersed into the test media (a) MUDA and citrate coated Ag nanoparticles and (b) MUDA and citrate coated Au nanoparticles. All data are mean ± standard error. * $p < 0.05$

A comparison of particle aggregation between different core materials in the test media is shown in Figure 9. The greatest aggregation of MUDA coated Ag and Au nanoparticles was seen in APW and the most stable particles were observed in SW, compared with those in DI water (Figure 9 (a)). The significant differences in particle size of both particles were seen in DI water, Lemna media, HW and MHW (One way-ANOVA and Mann-Whitney tests, $p < 0.05$). In contrast to the MUDA coated Ag and Au nanoparticles, the stability of citrate coated Ag and Au nanoparticles was found to be significantly different in most test media except in APW and HW (One-way ANOVA and Mann-Whitney test, $p < 0.05$) (Figure 9 (b)).

To confirm the effects of surface functionalisation and core materials on particle stabilisation, particle attachment efficiencies were derived in the test media depending on IS of the test media (Figure 10). The attachment efficiencies of Ag and Au nanoparticles increased with increasing IS, of which the lowest and highest IS was 1.85 mM in SW and 11.1 mM in APW respectively. It is well known that attachment efficiency of ENPs is highly correlated with surface charge or surface functionalisation and IS (Chen and Elimelech, 2006). Liu *et al.* (2012) observed the significance of effects of IS on the stability of Au nanoparticles coated with MUDA and citrate in various concentrations of NaCl, suggesting an electrostatic mechanism. French *et al.* (2009) also found fast aggregation from nano-sized particles to micron-sizes of TiO_2 with increasing IS. These aggregation studies have addressed the effect of the relationship of IS and electronic double layer on nanoparticle behaviour. At low IS, the influence of the EDL forces could extend far out from the particles and thus cause strong electrostatic repulsion between particles (Hotze *et al.*, 2010; Laaksonen *et al.*, 2006). However, at high IS, the EDL could be compressed, reducing the degree of electrostatic repulsion and increasing attractive force between particles. This results in unstable and highly aggregated agglomerated particles (Jiang *et al.*, 2009a).

(a) MUDA coated Ag and Au NPs
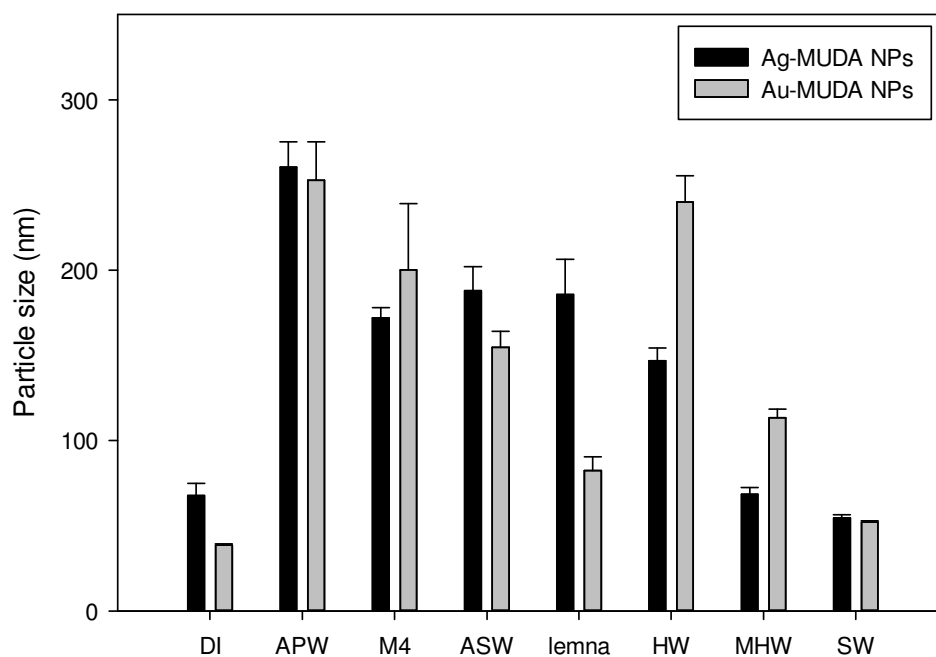
(b) Citrate coated Ag and Au NPs
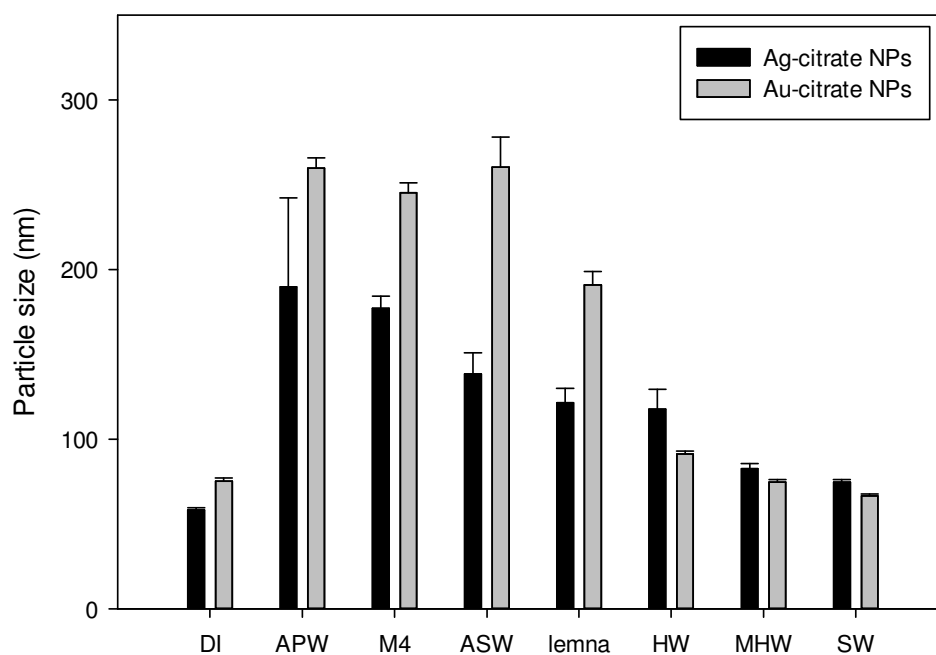
Figure 9. Comparison of mean size Au nanoparticles and Ag nanoparticles by core materials at 7 and 8 h dispersed into the test media. (a) Ag nanoparticles and Au nanoparticles coated with MUDA and (b) Ag nanoparticles and Au nanoparticles coated with citrate. All data are mean ± standard error. * $p < 0.05$.
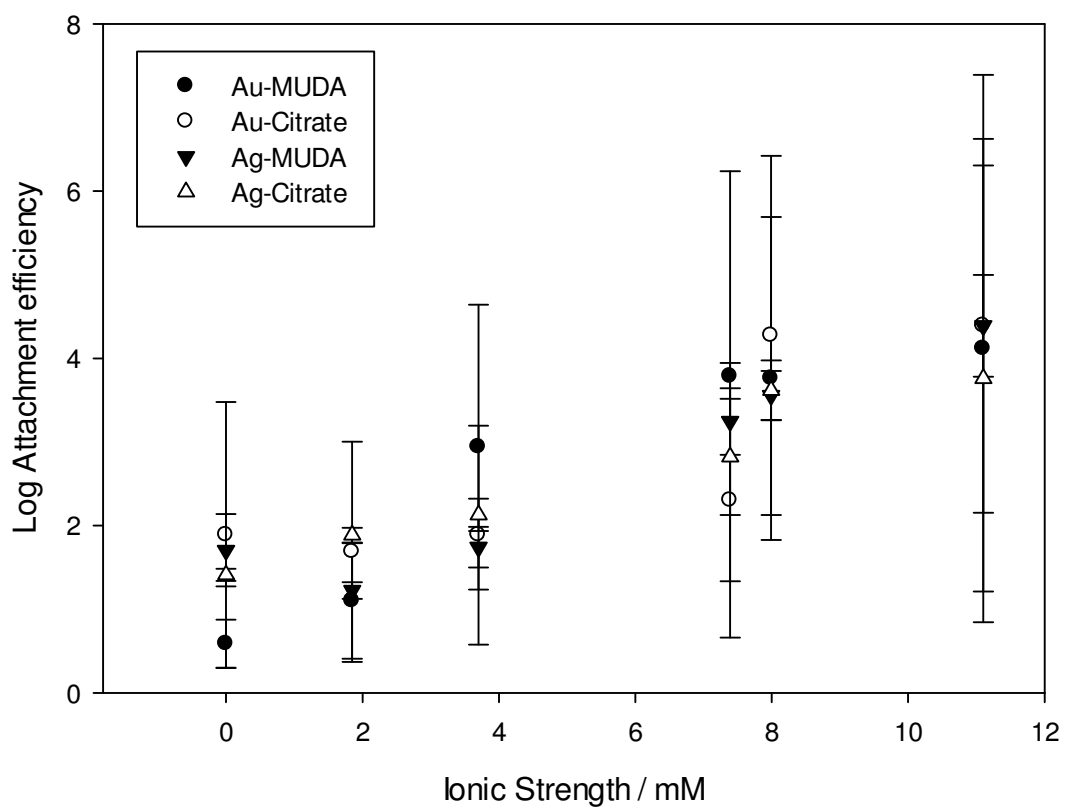
Figure 10. Attachment efficiency of all study particles in various test media. The IS were 1.85 mM (SW), 3.70 mM (MHW), 7.39 mM (HW), 7.99 mM (M4 media) and 11.1 mM (APW).

There are only a few studies that have been done to observe the effects of core material of ENPs on aggregation behaviour. El Badawy *et al.* (2010) and Liu *et al.* (2012) observed particle attachment efficiency in various concentrations of NaCl using citrate coated Ag and Au nanoparticles, respectively. Both citrate coated Ag and Au nanoparticles showed increasing degree of aggregation with increasing concentration of NaCl. Those studies indicated that particle aggregation was caused by the interactions of surface functionalisation of ENPs and divalent cations in the test solution, which acted a major factor to control particle stabilisation rather than being significantly influenced by core materials (Liu *et al.*, 2012). The aggregation behaviour in the studies of El Badawy *et al.* (2010) and Liu *et al.* (2012) were in a good agreement with our results which compared core material effects on particle stabilisation, shown in Figure 9. The core material is a less significant factor affecting particle aggregation. Conversely, aggregation of ENPs affects dissolution of core materials. Mudunkotuwa *et al.* (2011) and Bian *et al.* (2011) observed a decrease in the extent of dissolution of ZnO cores with increased aggregation rate. This decrease was caused by reduced reactive surface area of nanoparticles by aggregation (Mudunkotuwa *et al.*, 2011). In one study, the aggregation of ENPs started immediately and completed aggregation within short time (Park *et al.*, 2014) so fewer ions would be released into the test media. Li and Lenhart (2012) have reported that citrate coated Ag nanoparticles could not release silver ions due to rapid aggregation at an early stage of the experiment and reached a comparable concentration with control group after 15 d exposure. The OECD guideline recommended experiment durations for acute toxicity tests are between 48 h and 96 h (OECD, 2004; OECD, 1992), which could be insufficient time to release core material. Therefore the effects caused by core materials to aquatic organisms could be less than usually estimated.

Conclusion

This study has demonstrated the importance of the surface functionalisation for the aggregation behaviour of functionalized Au and Ag nanoparticles. Increasing aggregation rate and attachment efficiency were seen with increasing IS of test media. The core material of Au and Ag nanoparticles showed weaker influence on particle aggregation. The effect of surface functionalisation on environmental fate and behaviour of ENPs is therefore a critical parameter that should be explored in future research. Although the core material was less relevant to particle aggregation, it cannot be ignored for the purposes of risk assessment of ENPs. Further investigation is needed to address a role of core material and the relationship between particle aggregation and dissolution of core material, and develop a tool for quantification of ENPs in the aquatic environment.

The aggregation studies in this chapter were performed in idealised lab conditions, which made it possible to clarify what factors influenced particle aggregation. However, there are considerably more variables in the real environment, so it would be salient to extend a future study to a wider and more representative range of conditions.

In the next chapter, we explore the aggregation of Au nanoparticles with different functionalisation in the natural waters and develop methods to predict the stability of Au nanoparticles in UK river systems.

Chapter 4

Estimating the stability of Functionalised Gold Nanoparticles in Natural Waters

Introduction

For exposure assessment of 'normal chemical substances', it is common that environmental concentration is predicted using mathematical models or determined in real environmental samples using analytical methods (Tiede *et al.*, 2009). Since the environmental concentration is strongly associated with the toxic effects on aquatic organisms, measuring or predicting environmental concentration of a substance is important for risk assessment (Solomon *et al.*, 2000).

Unlike 'normal' substances in solution in aquatic systems, ENPs can occur in different states of aggregation and this will be influenced by a range of environmental parameters including pH, DOC concentration and IS on their fate after exposure (French *et al.*, 2009). Chapter 2 and Chapter 3 have demonstrated the strong influence of environmental factors on stability of Ag and Au nanoparticles in various test media. If environmental parameters vary across environmental water bodies, the degree of aggregation of an ENP across surface waters in the natural environment can therefore vary greatly (Park *et al.*, 2014). For the assessment of the environmental risks of ENPs, it would therefore be beneficial to develop an understanding of the relationships between particle properties and water parameters and aggregation.

In a recent study, Liu *et al.* (2013) described the application of an *in vitro* testing approach for estimating stability of gold ENPs across water bodies in continental Europe. They demonstrated that the use of *in-vitro* multi-parameter matrix testing approach alongside hydrochemistry data for European streams is a valuable tool for understanding the aggregation, transport, and fate of functionalized ENPs on a broad scale and indicated how the method provides a template for predicting the stability of ENPs in aqueous media that can be implemented in exposure modelling. However, this approach does require experimental testing of an ENP under a wide range of conditions. The development of mathematical models relating particle stability to water chemistry of natural waters might be an attractive alternative to the *in-vitro* tests.

Therefore in this study we build upon the concept of Liu *et al.* (2013) and use the data from Chapter 2 to develop a series of models for predicting the aggregation behaviour of ENPs with different surface functionalities in real water systems. We then illustrate how the models can be used to estimate the spatial stability of ENPs taking the UK as a case study and discuss how the concept and results of the spatial assessments could be applied in environmental risk assessment of ENPs in the future.

Material and methods

Study material

Four different types of Au nanoparticles (average 30 nm) were used: 'amphoteric' 11-mercaptoundecanoic acid-capped (Au-MUDA nanoparticles); 'negative' sodium citrate tribasic dehydrate-capped (Au-citrate nanoparticles); 'positive' amino PEG thiol-capped (Au-PEG-NH$_2$ nanoparticles); and 'neutral' PEG-capped (Au-PEG nanoparticles). Au-MUDA and citrate nanoparticles were prepared at the University of Alberta using the methodologies described in Chapter 2. 'Au-PEG-NH$_2$ nanoparticles and Au-PEG nanoparticles were purchased from Nanocs Inc (Boston, USA). Before each

aggregation study began, all Au nanoparticles stock solutions were ultra-sonicated for 30 minutes each to ensure dispersion.

Collection and characterisation of natural water samples

A total of 49 fresh water samples with different pH values ranging from 3.79 to 7.90 were collected from various sites across the north of England in August 2011 (Table 11) and March 2012 (Table 12) for use in the aggregation studies to support the model development work. An additional set of four samples was collected in July 2013 for use in aggregation studies for model evaluation (Table 12). The details of sampling time, sampling site and water chemistry were shown in Appendix 4.

After collection, the samples were filtered through cellulose filter papers (2.5 µm) and stored at 4 ºC. The pH (FG2 – FiveGo™ pH, Mettler-Toledo, Inc.) and conductivity (SG7 – SevenGo pro™ conductivity, Mettler-Toledo, Inc.) were measured at the sampling point.

Nitrate and ammonia were analysed by an auto analyser (Bran + Luebbe Auto Analyser 3 from Seal Analytical, Fareham, UK). Aqueous standard solutions of five different concentrations (0, 0.5, 1.0, 1.5, and 2.0 mg/L) were analysed and the correlation of coefficients (R^2) of the calibration curves were higher than 0.99.

The detection limits of nitrate and ammonia were 0.06 mg/L and 0.04 mg/L, respectively. All of the relative standard deviation (RSD, %) were well below 5% showing that this method is very precise.

To determine chloride, fluoride, nitrate, sulphate and phosphate, the water samples were filtered with 0.25 µm and were analysed by chromatography (ICS 2000 series Dionex Ion Chromatograph System, USA). To generate calibration curves, from 0.5 mg/L to 2.5 mg/L for fluoride, nitrate and phosphate were prepared and ranging from 5 mg/L to 25 mg/L for chloride and sulphate were set. A standard reference material containing 1.5 mg/L of fluoride, nitrate and phosphate and 5 mg/L of chloride and sulphate were also prepared and analysed. Linear regressions were performed on the

standards (R^2=0.99) and used in analysis of the standard reference material which showed recoveries ranged from 99 % to 100%. The limits of detection were from 0.5 µg/L to 0.21 mg/L and range of % RSD were from 0.03 to 1.47.

To analyse DOC in the samples, samples were filtered 0.45 µm filters again and analysed by a TOC analyser (liqui TOC, Elementar). The standards for calibration were set 1, 5, 10, 20, 35 and 50 mg/L and correlation coefficients (R^2) were higher than 0.99. The detection limit was 0.18 mg/L and %RSD was well below 5 %.

Metal concentrations (calcium, magnesium, sodium and potassium) were determined using an atomic absorption spectrophotometer (AA-6300, Shimadzu). The correlation coefficients (R^2) of calibration curve were higher than 0.99 and recovery ranged from 99 % to 100%. The detection limits were ranged from 2 µg/L to 1 mg/L and less than 5% of RSD were shown.

Hardness was calculated based on the measured concentrations of calcium and magnesium ions in the water samples and expressed in terms of calcium carbonate equivalents. Concentration of cations and anions in the natural water were used to estimate IS (IS = $1/2 \times \Sigma C_i \times Z_i^2$; where C_i= concentration of the ith species, Z_i^2=valence (or oxidation) number of the ith species).

Table 11. Characteristics of a range of natural water samples for Au-MUDA nanoparticles only

Parameters	unit	Mean	Minimum	25%	75%	Maximum
pH	N.A	5.61	3.79	4.03	7.23	7.90
Conductivity	µS/cm	235.13	54.1	85.9	238	883.00
Ammonium-N	µg/mL	0.14	0.01	0.03	0.15	0.85
Nitrate-N	µg/mL	0.60	0.01	0.07	0.78	1.74
Ionic strength	mmole/L	2.89	0.08	0.37	2.47	11.41
DOC	mg/L	23.18	6.61	7.81	39.51	49.38
SO_4^{2-}	mmole/L	0.07	0.01	0.02	0.10	0.23
Cl^-	mmole/L	0.21	0.02	0.08	0.29	0.71
NO_3^-	mmole/L	0.02	0.0001	0.01	0.03	0.06
PO_4^{3-}	mmole/L	0.004	0.001	0.001	0.007	0.01
F^-	mmole/L	0.01	0.002	0.003	0.007	0.02
K^+	mmole/L	0.07	0.00	0.01	0.15	0.31
Na^+	mmole/L	0.55	0.01	0.05	0.44	3.57
Ca^{2+}	mmole/L	0.67	0.00	0.02	0.82	3.61
Mg^{2+}	mmole/L	0.23	0.01	0.03	0.23	1.25
Hardness*	mg/L	68.13	1.56	2.28	100.39	317.06

N.A : Not available, *: calculated value

Table 12. Characteristics of a range of natural water samples for all types of Au nanoparticles

Parameters	unit	Mean	Minimum	25%	75%	Maximum
pH	N.A	6.60	4.29	5.88	7.29	7.64
Conductivity	µS/cm	316.68	46.10	56.85	388.50	1239.00
Ammonium-N	µg/mL	0.19	0.01	0.03	0.16	1.25
Nitrate-N	µg/mL	0.82	0.24	0.58	1.38	2.28
DOC	mg/L	7.22	1.84	4.04	10.34	17.65
Ionic strength	mmole/L	2.93	0.37	0.42	5.75	11.41
SO_4^{2-}	mmole/L	0.01	0.08	0.06	0.13	0.23
Cl^-	mmole/L	0.25	0.09	0.15	0.39	0.53
NO_3^-	mmole/L	0.03	0.002	0.02	0.04	0.06
PO_4^{3-}	mmole/L	0.003	0.001	0.001	0.004	0.01
F^-	mmole/L	0.006	0.003	0.004	0.008	0.01
K^+	mmole/L	0.05	0.01	0.01	0.09	0.20
Na^+	mmole/L	0.71	0.08	0.14	0.58	3.57
Ca^{2+}	mmole/L	0.83	0.01	0.04	2.13	3.61
Mg^{2+}	mmole/L	0.28	0.03	0.06	0.32	1.25
Hardness*	mg/L	111.02	4.06	10.01	175.81	484.69

N.A : Not available, *: calculated value

Aggregation studies of gold nanoparticles in natural waters

Aggregation studies were performed in duplicate in each of the test waters at a concentration of 0.5 mg/L for the Au-MUDA and citrate nanoparticles and 0.1 mg/L for the Au-PEG-NH$_2$ and PEG nanoparticles. Following addition of Au nanoparticles to water, 1 mL of samples were taken from each duplicate at 0, 1, 2, 4, 6 and 8 h and analysed three times. For model validation, samples for each Au nanoparticles were prepared at 0.2 mg/L using additional four natural water samples. 1 mL of each Au nanoparticles were sampled from three replicates at 0 h and 24 h and analysed two times. All samples for aggregation study and model validation were analysed by a NanoSight 2.2 LM 14, nanoparticle tracking analysis (NTA) instrument (NanoSight Ltd, Amesbury, UK). NTA records the movement of individual nanoparticles in the water samples under Brownian motion and then calculates the hydrodynamic diameter of particles (nm) using the Stokes-Einstein equation (Malloy and Carr, 2006). All natural water samples without Au nanoparticles were also taken for NTA analysis and these analyses showed that the 'background' NP concentrations in the natural waters were lower than or close to the NTA limits of detection. The stability of Au-MUDA nanoparticles was explored in all water samples whereas the stability of the other particles was assessed in 30 water samples (26 model development and 4 model validation).

Statistical analysis

To explore the differences in aggregation behaviour over time, statistical analysis of the data was performed using SPSS (v 21; SPSS Inc.). One-way ANOVA and a non-parametric analysis (Kruskal-Wallis) were used to assess the differences in aggregation of Au nanoparticles between 0 h and 8 h. The significance level was $p < 0.05$.

Model developing and evaluation

Models for estimating ENP stability were developed for each study ENP from the mean particle size of each material at 8 h. Models were developed using multiple linear regression by SPSS v21 (SPSS Inc). Water quality data from natural waters, including pH, DOC, IS and individual or sum of cations (Ca^{2+}, Mg^{2+}, Na^+ and K^+) and anions (Cl^-, SO_4^{2-} and NO_3^-) were used as regression parameters in the method and the enter method in multiple liner regression was applied. The level of significance for all analyses was set at 0.05. The best prediction model equations were selected based upon adjusted R^2 values. For model evaluation, water quality data for four additional water samples for Au-MUDA and citrate nanoparticles and three additional samples for Au-PEG-NH$_2$ and PEG nanoparticles were used in the models to predict particle sizes of the Au nanoparticles. The predicted particle sizes were then compared to experimentally determined values to evaluate adequacy the model.

Assessment of particle stability across the UK

The developed models were used alongside data on water chemistry for a range of UK rivers to develop stability maps for the study particles for the UK landscape. The chemical species required for calculation of the regression equations were taken from five data sources: 1) routine monitoring carried out by the Environment Agency of England and Wales, 2) The Thames initiative research platform of the Centre for ecology and Hydrology, 3) The Ribble/Wyre observatory, 4) The UK Acid Waters Monitoring Network data report and 5) The Land Ocean Interaction Study (Neal *et al.*, 2012). Despite using multiple data sets, only 233 sites were found that had values for the chemical species required to apply the particle size regression equations.

Most of the data from the 233 sites, mainly freshwater river sites, were obtained from monitoring studies performed over the last ten years, (data from the Thames initiative and the Environment Agency were taken from the last 3 years of measurement). The

extracted environmental parameters (mean concentration) from the data were pH, DOC, cations (Ca^{2+}, Mg^{2+}, Na^+ and K^+) and anions (Cl^-, SO_4^{2-}, NO_3^-). IS was calculated from the cation and anion concentrations using the methodology described earlier. Water parameters for each site were input to the stability equations to estimate the mean particle size for each particle at each site, assuming the same exposure concentration as used in the aggregation studies.

Particle stability maps

The particle sizes estimated by the equations using the average values of the collected natural water data were plotted as particle stabilisation maps using ArcMap 10.1 (ESRI inc. Redlands, CA, USA). The location of each sampling site was defined by a six figure UK National Grid reference.

Results and discussion

Stability of gold nanoparticles in natural water

Aggregation of the Au nanoparticles varied across surface functionalities and water types (Figure 11). Au-MUDA nanoparticles were stable in the majority of water samples over an 8 h period although significant aggregation was seen in a few water samples with a mean particle size of 236 ± 7.93 nm being measured in once sample at the end of the study (Figure 11 (a)). For Au-citrate nanoparticles, rapid aggregation (i.e. before the first sampling point) was seen in all water samples and, in most waters, only a small change in size was seen over the remainder of the study although in some sample, significant further aggregation was observed. Mean particle sizes of the Au-citrate after 8 h ranged from 71.17 ± 3.23 nm to 254.83 ± 5.84 nm (Figure 11 (b)). For Au-PEG-NH$_2$ nanoparticles, rapid aggregation was seen and the mean particle sizes then only changed slightly over the remainder of the study. The mean particles sizes of the Au-PEG-NH$_2$ nanoparticles ranged from between 72.67 ± 2.17 nm and 117 ± 3.80

nm (Figure. 11 (c)). Rapid aggregation was also observed for the Au-PEG nanoparticles with then little change in mean particle sizes over the remainder of the study. Mean particle sizes for the Au-PEG nanoparticles after 8 h ranged from 95.17 ± 6.79 nm to 254.83 ± 15.87 nm, respectively (Figure. 11 (d)).

Au-MUDA nanoparticles in most water samples did not show remarkable particle size differences compare with aggregation in DI water. However, Au-citrate, PEG-NH$_2$ and PEG nanoparticles showed rapid and greater aggregation in the water samples than those in DI water at 0 h and 8 h exposure. According to our previous study (Chapter 2) the aggregation could be occurred immediately after exposure by the interactions with water chemistry and surface charge of Au nanoparticles. For Au-citrate nanoparticles, it could be explained that divalent cations (e.g. Ca^{2+} and Mg^{2+}) affected on changing negative surface charge to neutral through the interactions with the carboxyl group of citrate and reduced electrostatic repulsion between particles (Huynh and Chen, 2011). In addition, compression electrical double layer of Au-citrate nanoparticles by IS, it caused different degree of aggregation in the water samples depending on concentration of IS (Nason *et al.*, 2012). The presence of DOC could be a main contributor to induce aggregation of Au-PEG-NH$_2$ and PEG nanoparticles by altering the surface charge to either negative or neutral resulting in more aggregation by the interaction with divalent and monovalent cations in the water (Zhang *et al.*, 2009; Ottofuelling *et al.*, 2011).The least aggregation of Au-MUDA nanoparticles in most water samples were caused by DOC which coated the surface of Au-MUDA nanoparticles immediately and enhanced electrostatic repulsion and then induced particle stabilisation. However, if the concentration of IS increased, there would be divalent cation bridging between divalent cations and surface charge. It could lead reducing electrostatic interaction between particles and increasing aggregation rate (Stankus *et al.*, 2011).

Some studies also have addressed the particle aggregation in natural waters by the combined effects of environmental factors for TiO$_2$ (Keller *et al.*, 2010; Sillanpää *et al.*, 2011; Ottofuelling *et al.*, 2011), CeO$_2$ (Van Hoecke *et al.*, 2011; Keller *et al.*, 2010),

multiwalled CNTs (Lin *et al.*, 2010) and QDs (Navarro *et al.*, 2009). These studies have pointed out increasing particle stabilization with increasing concentration of DOCs and decreasing amount of divalent cations in natural waters.
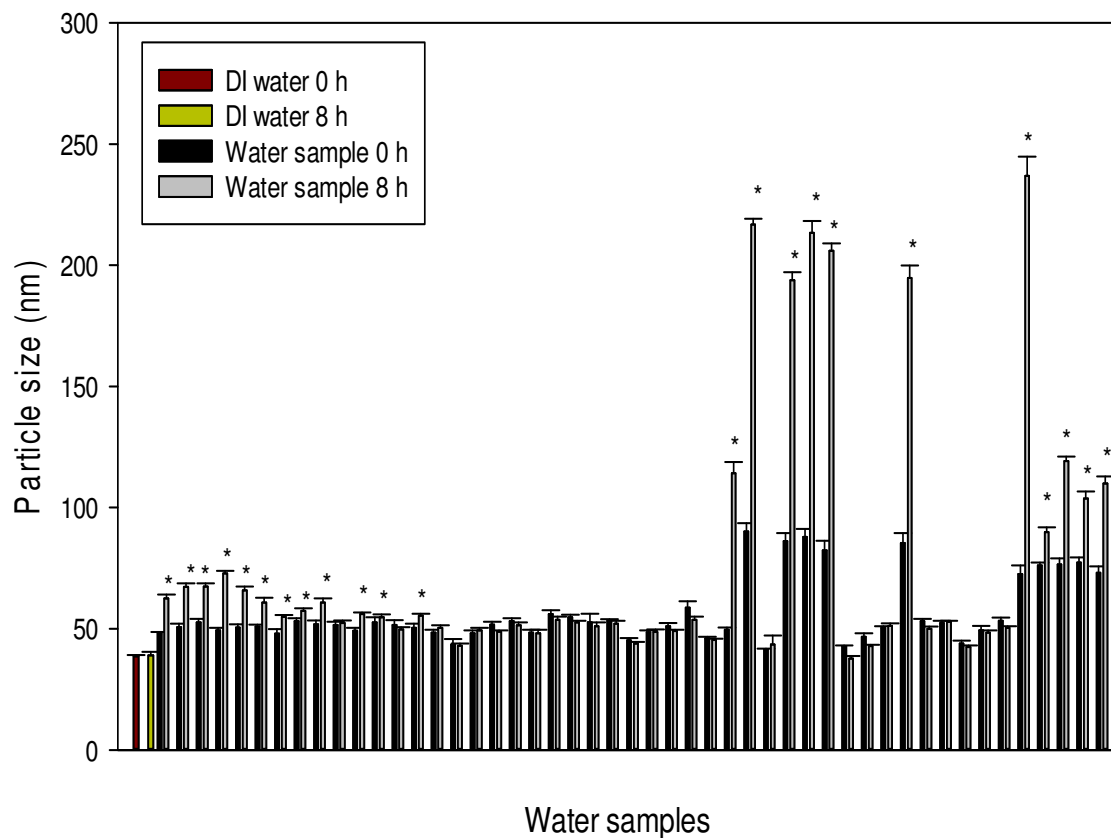
Figure 11. Aggregation of All types of nanoparticles in natural water samples after dispersion at 0 h and 8 h. The water samples were categorised by pH. The particles sizes are mean ± standard errors. (a) Au-MUDA nanoparticles, (b) Au-citrate nanoparticles, (c) Au-PEG-NH$_2$ nanoparticles and (d) Au-PEG nanoparticles.

(b) Au-citrate NPs
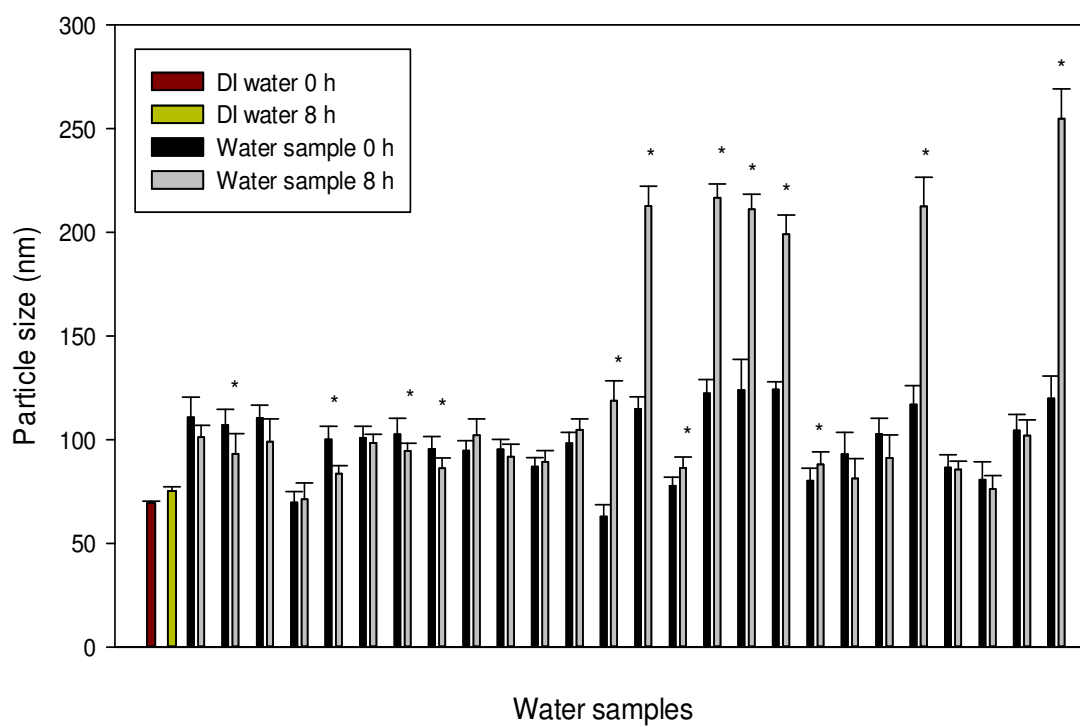
(c) Au-PEG-NH$_2$ NPs
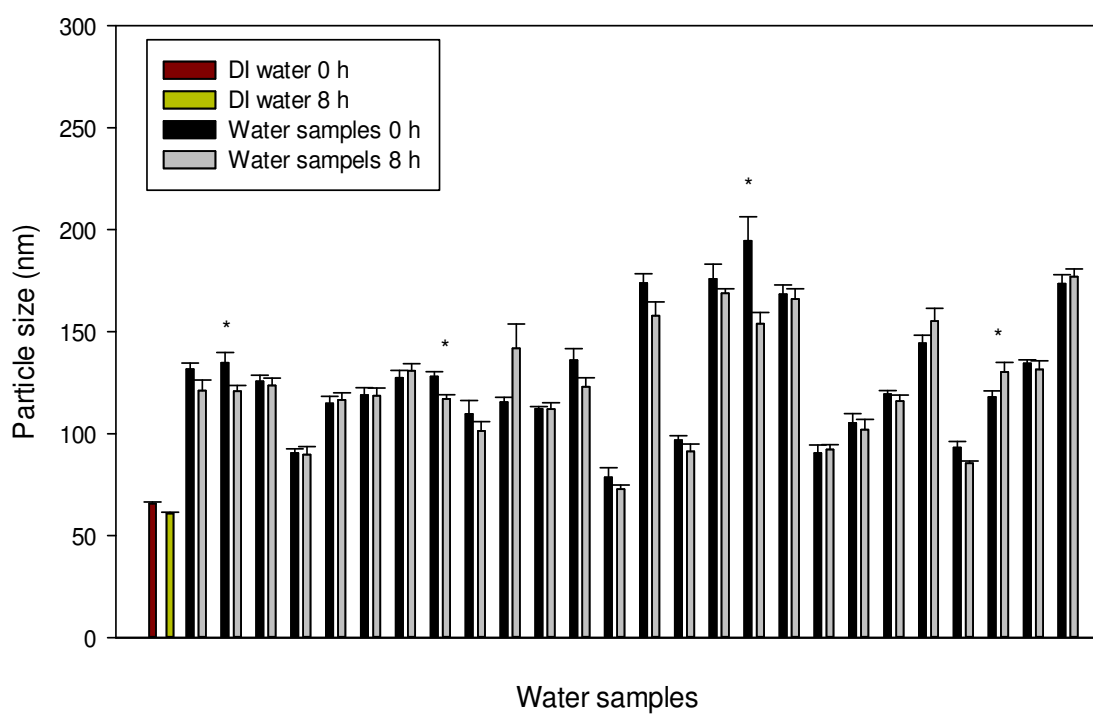
Figure 11. Continued.

(d) Au-PEG NPs
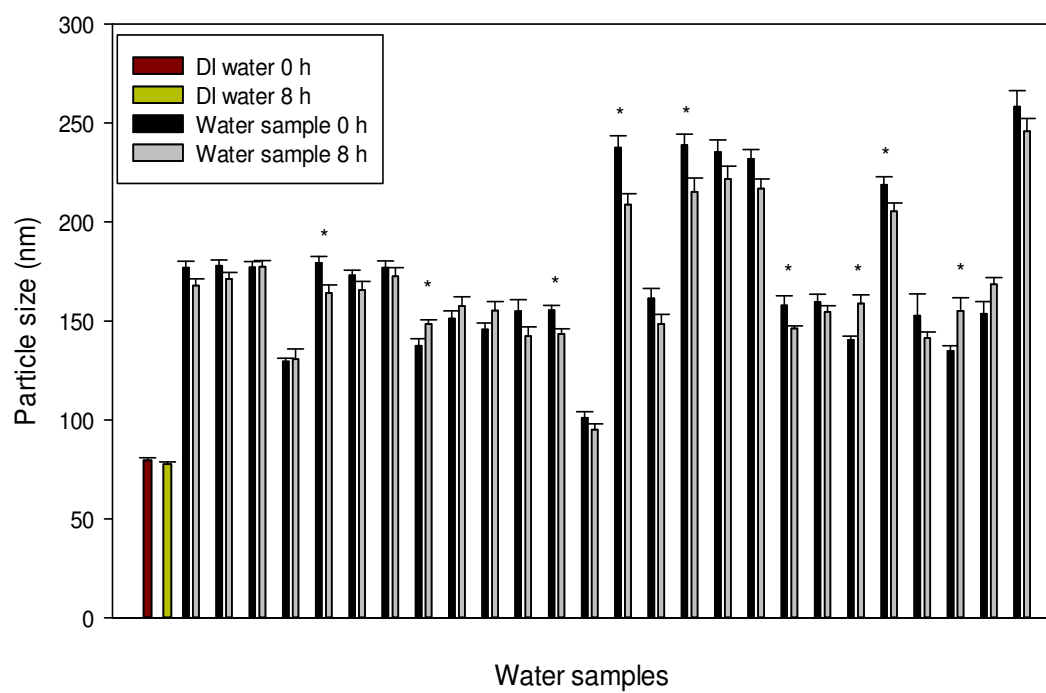
Figure 11. Continued.

Development and evaluation of model to predict aggregation

To develop models to predict aggregation of Au nanoparticles, multiple linear regression analysis were performed using several combination of natural water chemical properties. The multiple linear regression analysis resulted in strong and statistically significant relationships between mean particle size and pH, DOC and IS of the natural waters which showed high correlation coefficients (R^2) of ranged from 0.61 to 0.93 (Equations 4.1- 4.4; $p < 0.05$). In equation 4.1, a negative correlation was found with pH, however, DOC and IS were positively related to particle aggregation of Au-MUDA nanoparticles. In equations from 4.2 to 4.4, all of three water parameters are positively correlated to stability of Au-citrate, PEG-NH$_2$ and PEG nanoparticles.

Size of Au-MUDA nanoparticles at 8 h (0.5 mg/L)

$= 84.89 - 8.72 \times pH + 0.23 \times DOC + 17.86 \times IS$ ($R^2 = 0.88$)   (Equation 4.1)

Size of Au-citrate nanoparticles at 8 h (0.5 mg/L)

$= 39.80 + 3.48 \times pH + 2.25 \times DOC + 14.31 \times IS$ ($R^2 = 0.93$)   (Equation 4.2)

Size of Au-PEG-NH$_2$ nanoparticles at 8 h (0.1mg/L)

$= 59.23 + 4.35 \times pH + 2.91 \times DOC + 5.03 \times IS$ ($R^2 = 0.61$)   (Equation 4.3)

Size of Au-PEG nanoparticles at 8 h (0.1mg/L)

$= 67.64 + 7.92 \times pH + 4.30 \times DOC + 5.98 \times IS$ ($R^2 = 0.71$)   (Equation 4.4)

To confirm the model's ability to predict particle size in natural waters, the model was evaluated by applying it to the equations to estimate aggregation in additional water samples and comparing the predictions with aggregation measurements for these samples (red dots). There was fair to good agreement between the predictions and

measurement with correlation coefficients (R^2) for measured vs predicted sizes being 0.99 for Au-MUDA nanoparticles, 0.83 for Au-citrate nanoparticles, 0.79 for Au-PEG-NH_2 nanoparticles and 0.69 to PEG nanoparticles (Figure 12). After evaluation of the model, the equations were also applied to observe the correlation between measured and predicted particle size for Au-MUDA nanoparticles in 49 water samples and for Au-citrate, PEG-NH_2 and PEG nanoparticles in 26 water samples (Black dots). It also showed high correlations for measured and predicted particle size (R^2= 0.76 to 0.94).
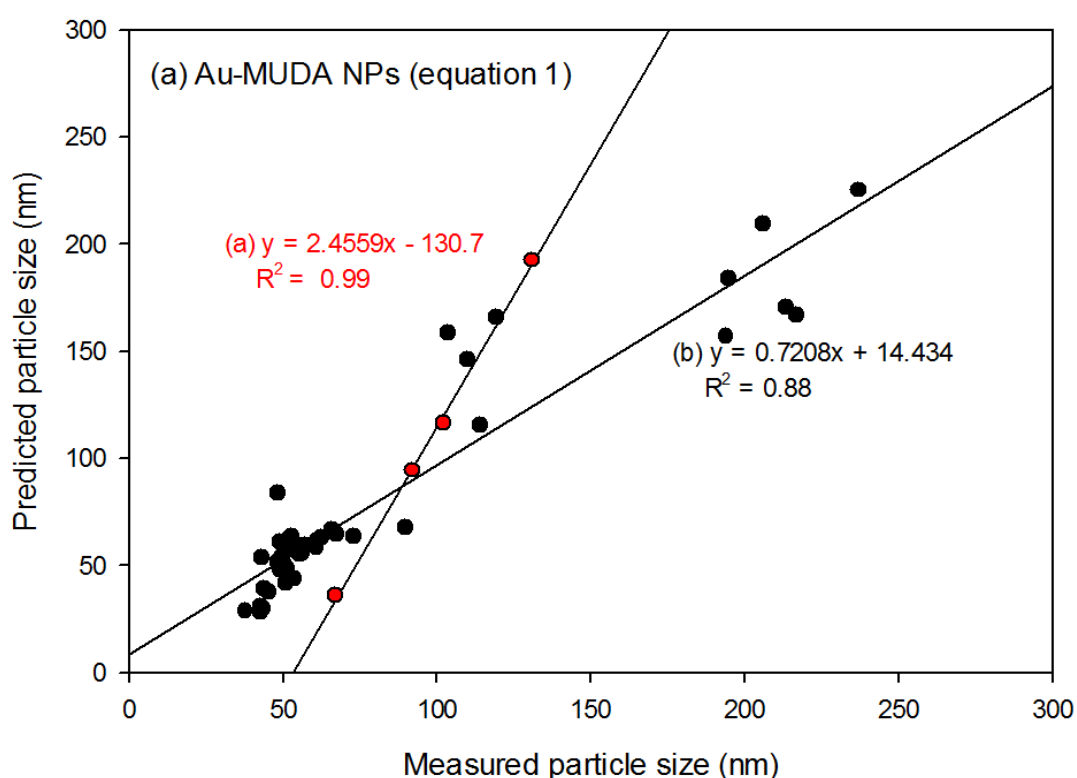
Figure 12. Correlation between measured and predicted particle size of each Au NP (Black dots) and model evaluation of the model (red dots) (a) Au-MUDA nanoparticles, (b) Au-citrate nanoparticles, (c) Au-PEG-NH_2 nanoparticles and (d) Au-PEG nanoparticles.

(b) Au-citrate NPs (equation 2)

(a) y=1.8333x - 81.396
R^2 = 0.8345

(b) y= 0.9408x + 7.181
R^2 = 0.94

Predicted particle size (nm) / Measured particle size (nm)

(c) Au-PEG-NH$_2$ NPs (equation 3)

(b) y = 0.7668x + 27.381, R^2 = 0.76

(a) y= 0.8756x -3.4559, R^2=0.79

Predicted particle size (nm) / Measured particle size (nm)

Figure 12. Continued

Figure 12. Continued

Predicted particle size distribution in UK

Based on the developed equations, the stability of the study particles was predicted using surface water chemistry data for the UK. For Au-MUDA nanoparticles, 33% of sites would be expected to have the most stable particles (below 50 nm) and 43.9% of sites would have a mean particle size of 50 nm - 100 nm. In 22.2 % of sites, the Au-MUDA nanoparticles were predicted to be unstable (100 nm - 300nm). For Au-citrate, around 49 % of sites were predicted to result in moderate stability (50 nm -100 nm) and at 51 % of the sites, the particles were predicted to be unstable through the UK. Au-PEG-NH$_2$ particles were predicted to be unstable in most sites except some area in Wales and North of England. Most Au-PEG nanoparticles were expected to be unstable in all study areas of UK. The overall predicted particle sizes of Au nanoparticles were geographically divided into four areas and described as particle size distribution maps for each particle type (Figure 13). In addition, Box and whisker plots with mean, median, interquartile ranges and minimum and maximum values for each particle size in UK waters are provided in Figure 13. Due to lack of water chemistry information it was only possible to estimate the stability of the study ENPs at a few sites in the Midlands of England, Scotland and Ireland so we have focused our discussion on regional differences in behaviour between Wales, South West, South East and London, and the North of England.

The most stabilised Au-MUDA nanoparticles were distributed mainly in 91% of Wales (Figure 13 (a)). The most aggregated Au-MUDA nanoparticles were predicted in South East and London area (56.0%), which ranged in a mean particle size from 116.49 nm to 174.92 nm (Figure 13 (a)). For Au-citrate nanoparticles, distribution of the moderate stable particles were in Wales (a mean particle size of 84.52 ± 2.54 nm) but unstable particles were distributed in South West area (a mean particle size of 102.31 ± 3.55 nm), South East and London area (a mean particle size of 155.82 ± 6.30 nm) and North of England (a mean particle size of 119.39 ± 5.38 nm) (Figure 13 (b) and Figure 14 (b)). Most unstable Au-PEG-NH$_2$ and PEG nanoparticles were seen in most areas

(Figure 13 (c) and (d)) and the mean sizes ranged from 103.31 nm to 134.19 nm for Au-PEG-NH$_2$ NP and from 140.30 nm to 179.47 nm for Au-PEG nanoparticles (Figure 14 (c) and (d)).

The different ranges of predicted particle size were strongly related to environmental factors, especially depending on amount of IS and DOC in each area. The most stabilisation of Au-MUDA nanoparticles and moderate stable of Au-citrate nanoparticles in Wales were caused by low concentration of IS (0.94 mmol/L) and high amount of DOC (3.23 mg/L). In contrast, unstable Au-MUDA and citrate nanoparticles were predicted in South East and London area, and North of England due to much higher concentration of IS (from 5.60 mmol/L to 6.79 mmol/L). The similar particle stabilisations of Au nanoparticles were also observed in study of Liu *et al.* (2013). They has predicted particle stabilisation of MUDA and citrate coated Au nanoparticles by IS and DOC through European countries. MUDA and citrate coated Au nanoparticles were predicted rapid aggregation in regions that high concentration of divalent cations. In contrast to aggregation resulted by divalent cations, significant stabilization by DOC on MUDA and citrate coated Au nanoparticles were in most parts of European streams.
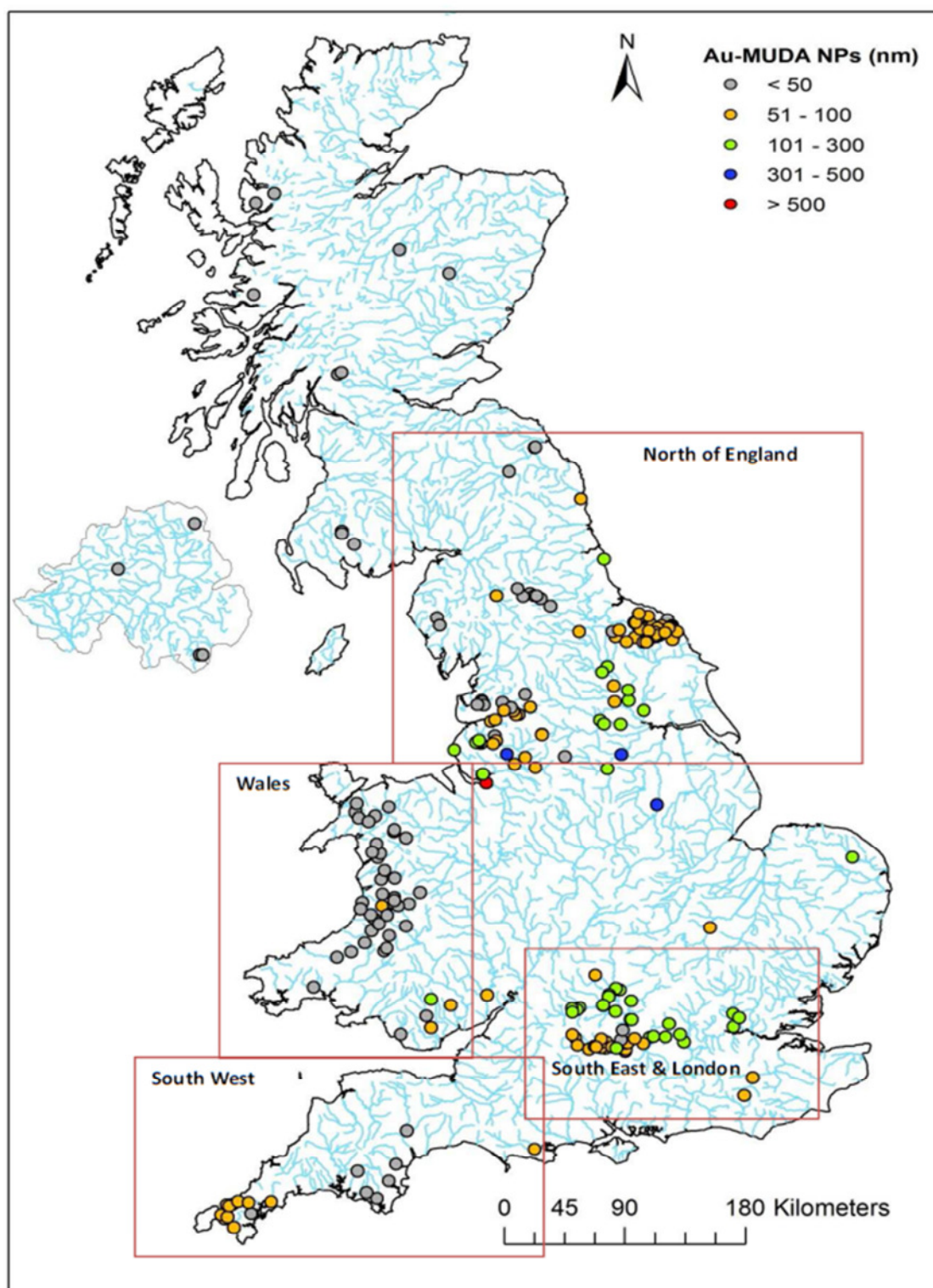
Figure 13. Estimated mean particle sizes for different gold particles in rivers in England and Wales based on an initial concentration of 500 µg/ L and 100 µg/L of 30 nm particles. (a) Au-MUDA nanoparticles, (b) Au-citrate nanoparticles (c) Au-PEG-NH$_2$ nanoparticles and (d) Au-PEG nanoparticles.
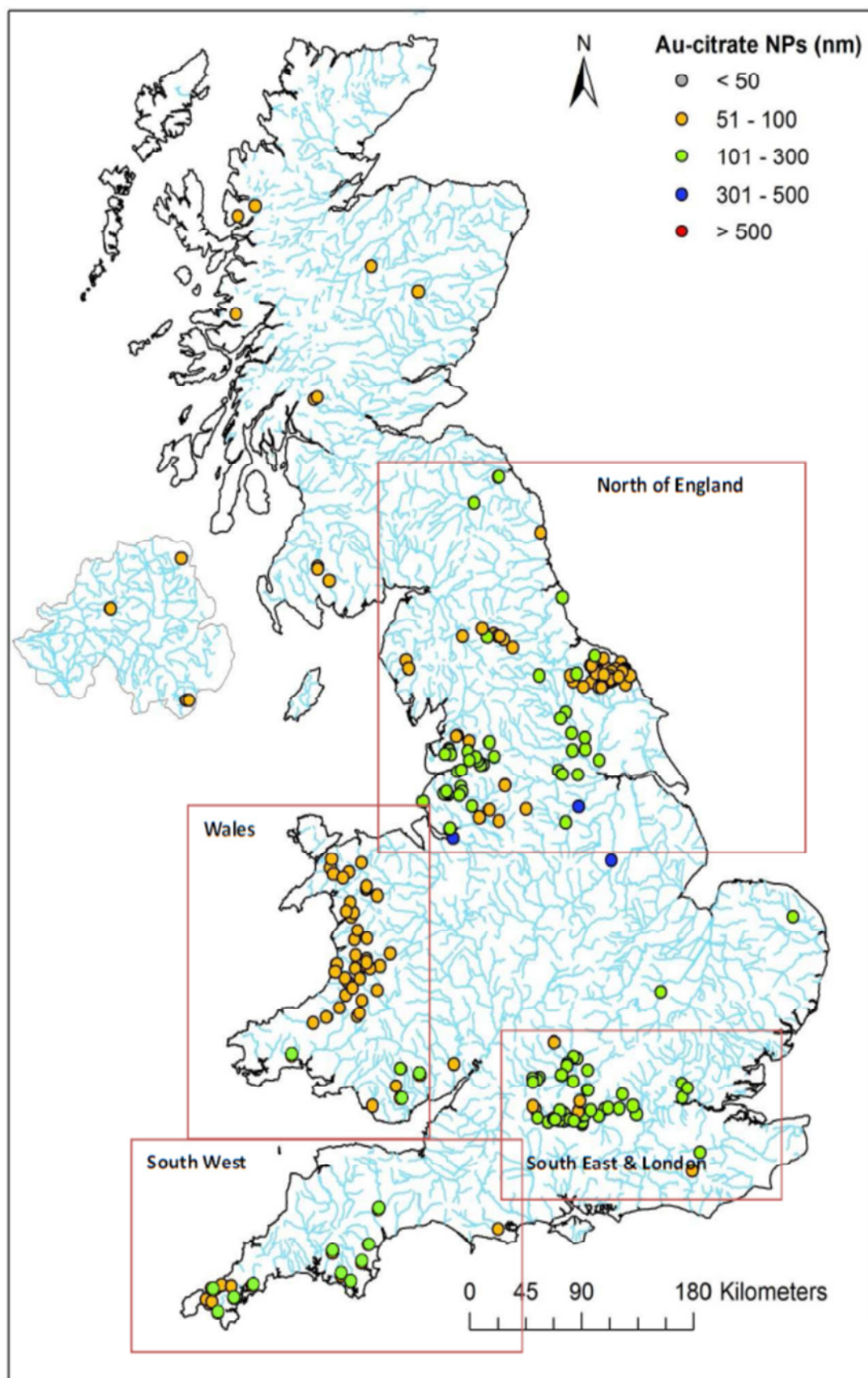
Figure 13. Continued.
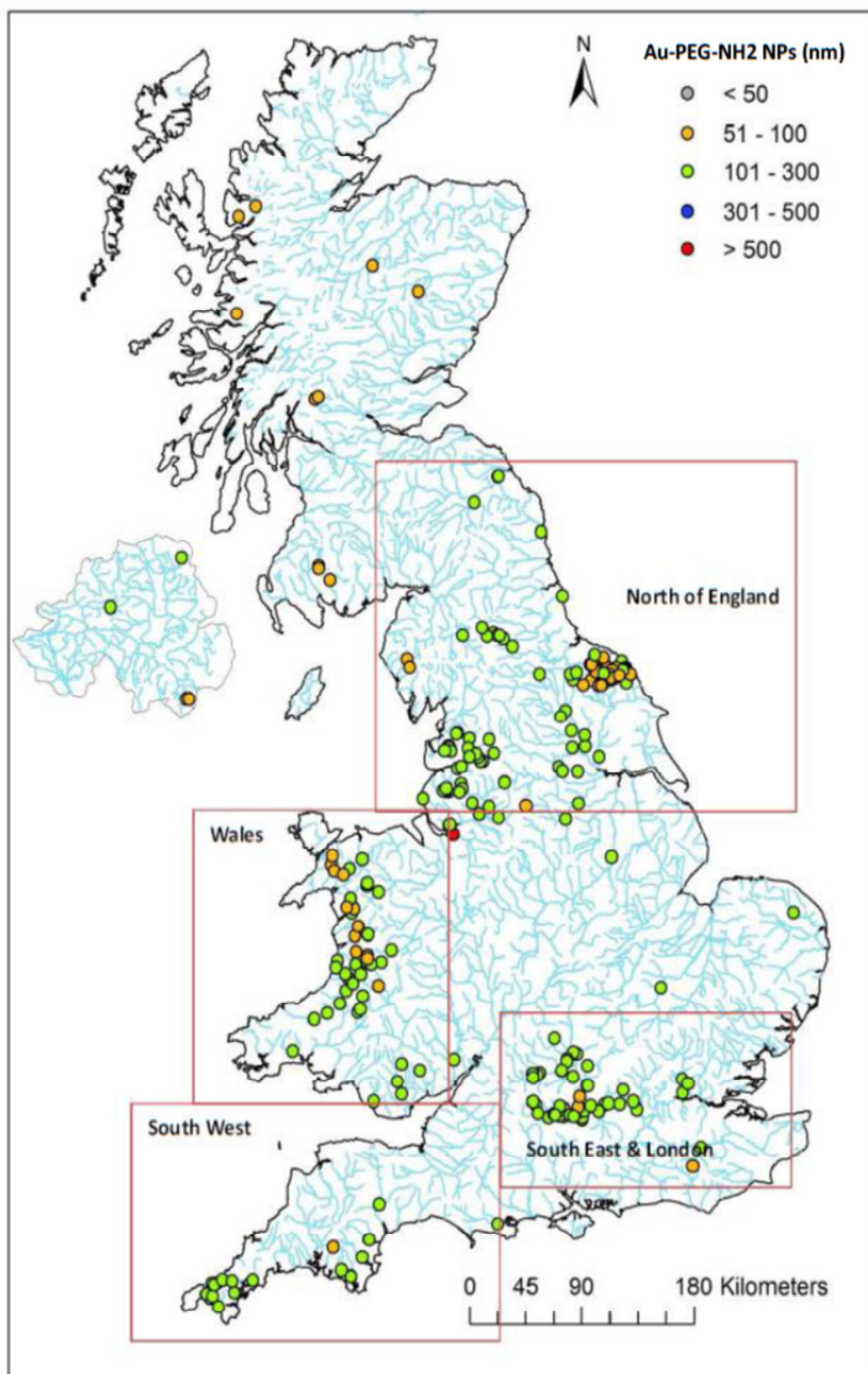
Figure 13. Continued.
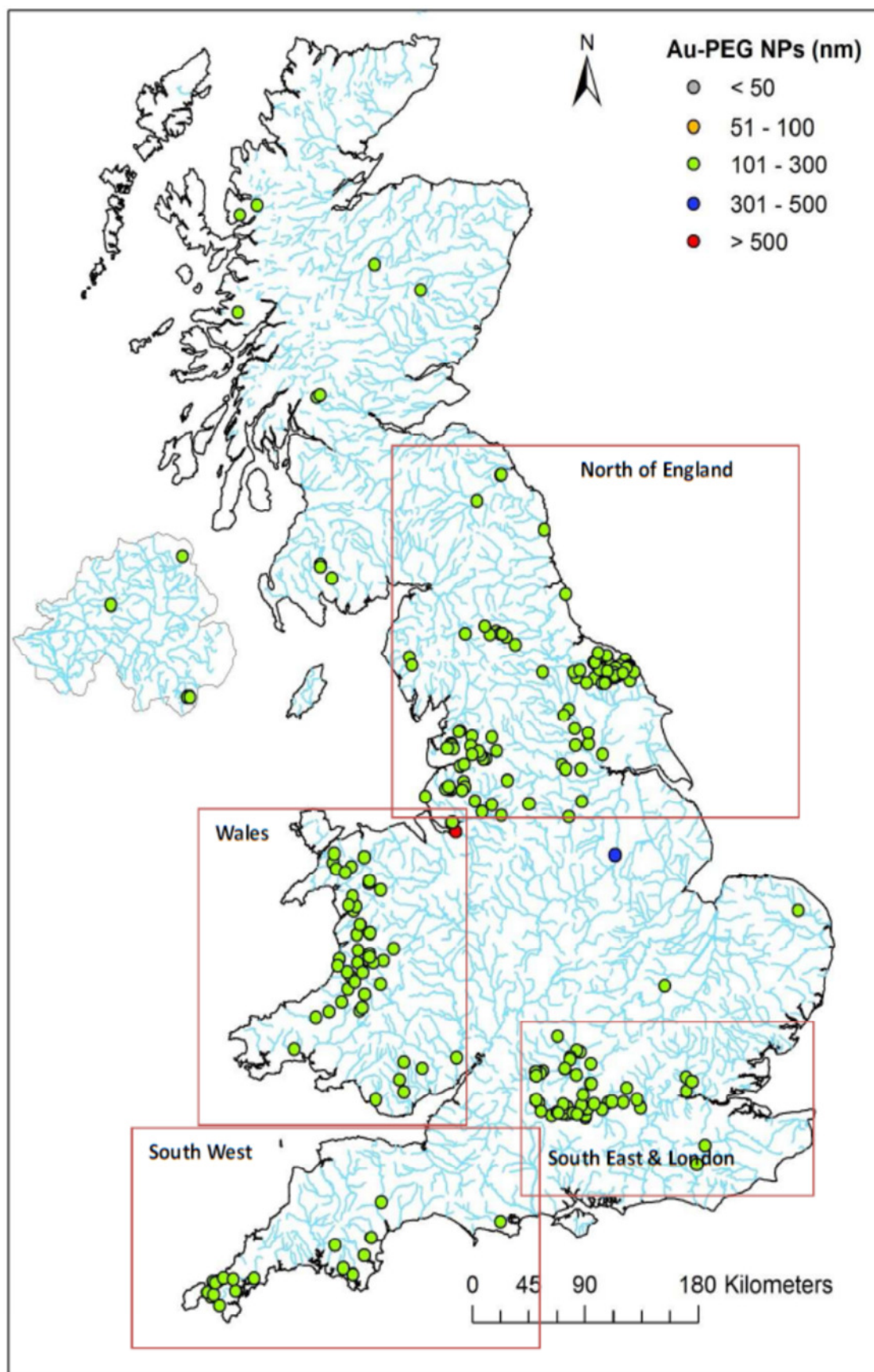
Figure 13. Continued.
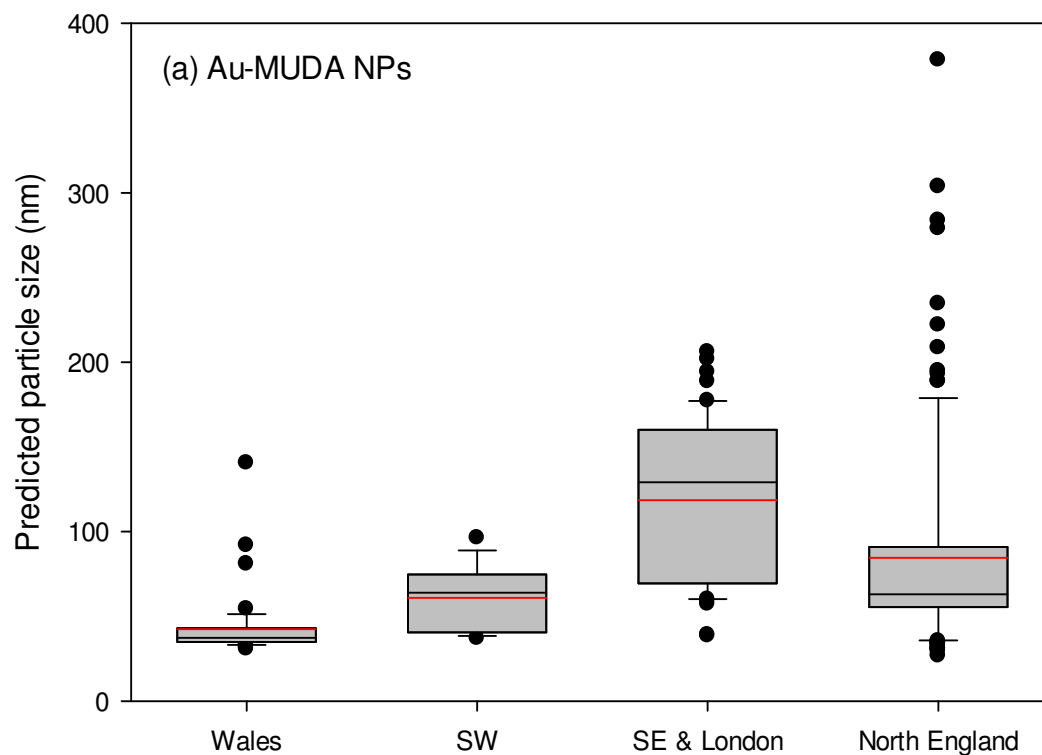
Figure 14. Box and whisker plot of mean particle size distributions of Au nanoparticles in rivers in different regions of the UK. The central box represents the lower and upper quartiles (25 and 75 percentile) and the red line is mean value. Two horizontal bars denote the minimum and the maximum predicted particle size. (a) Au-MUDA nanoparticles, (b) Au-citrate nanoparticles, (c) Au-PEG-NH$_2$ nanoparticles and (d) Au-PEG nanoparticles.
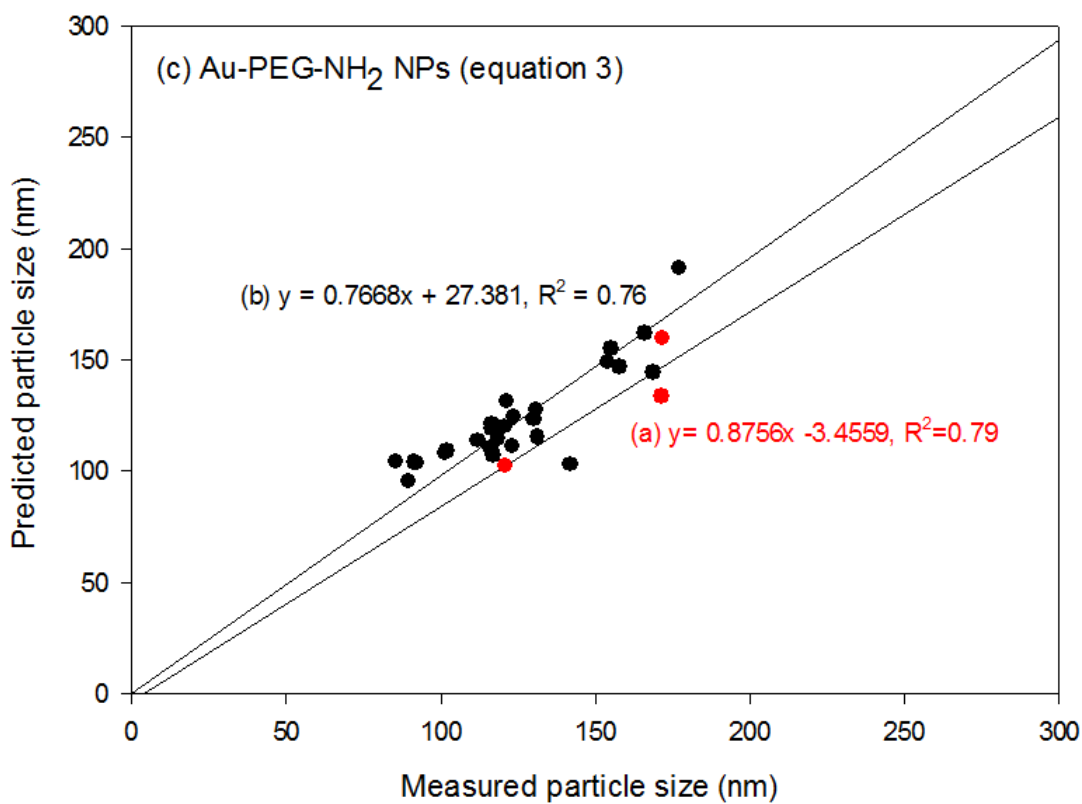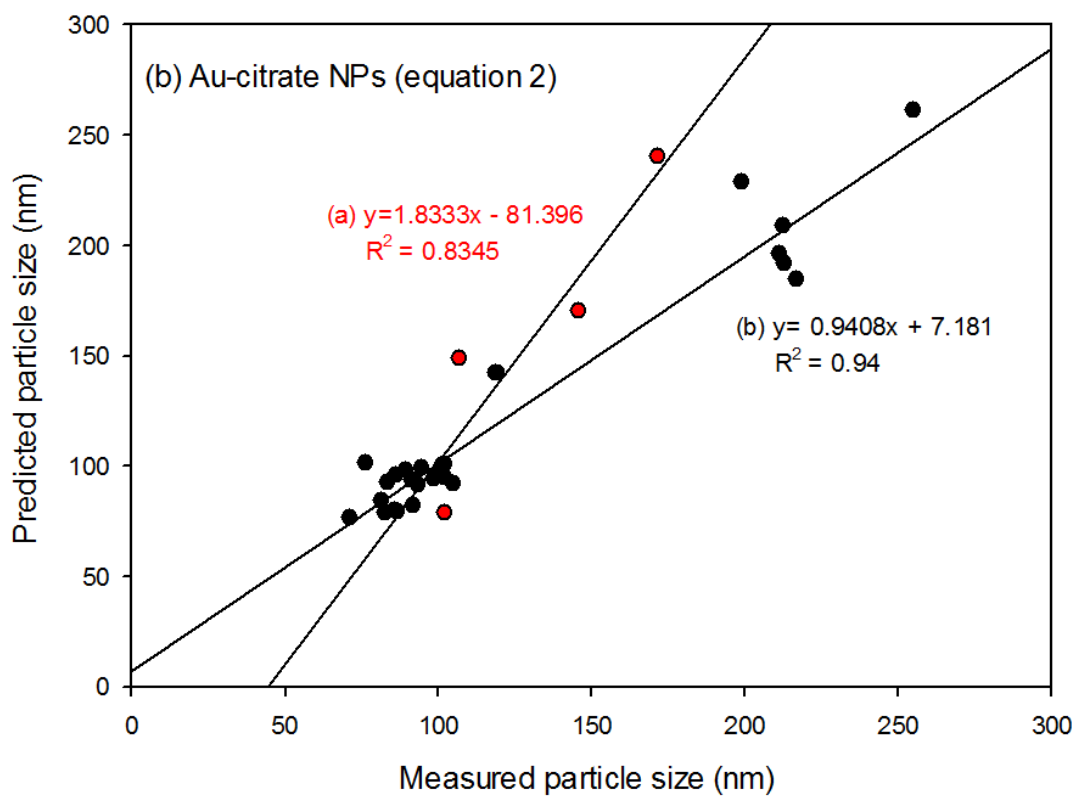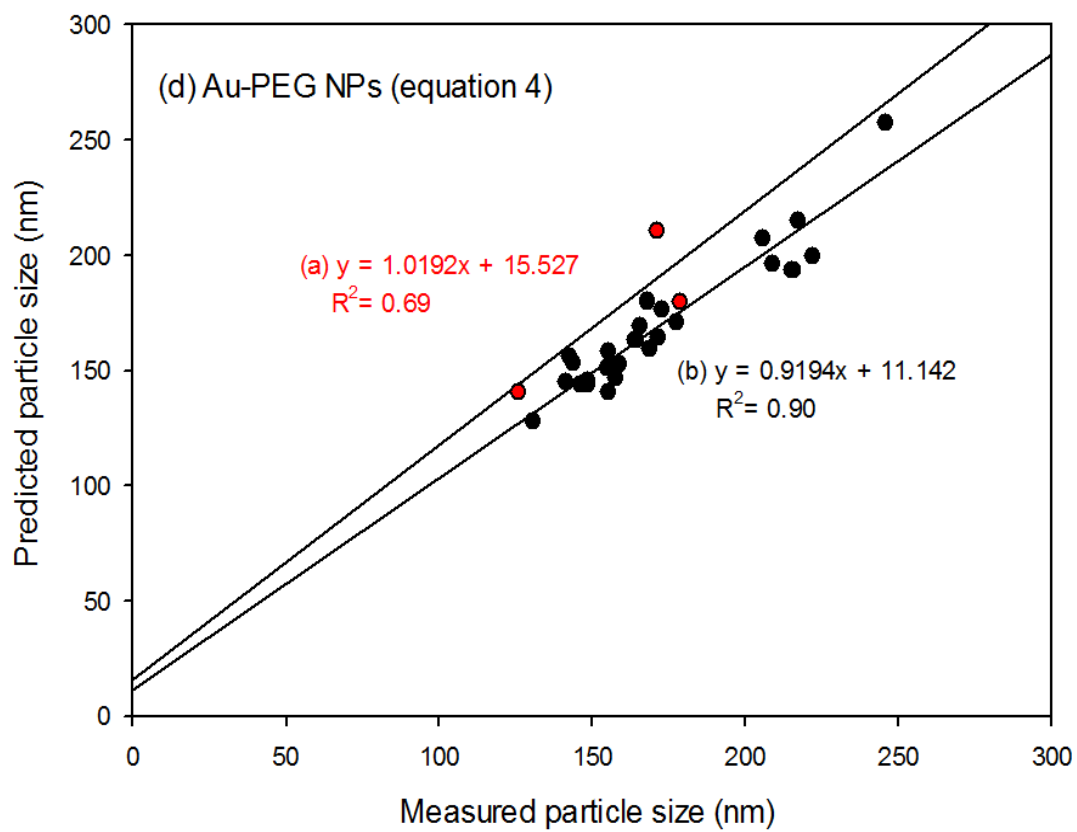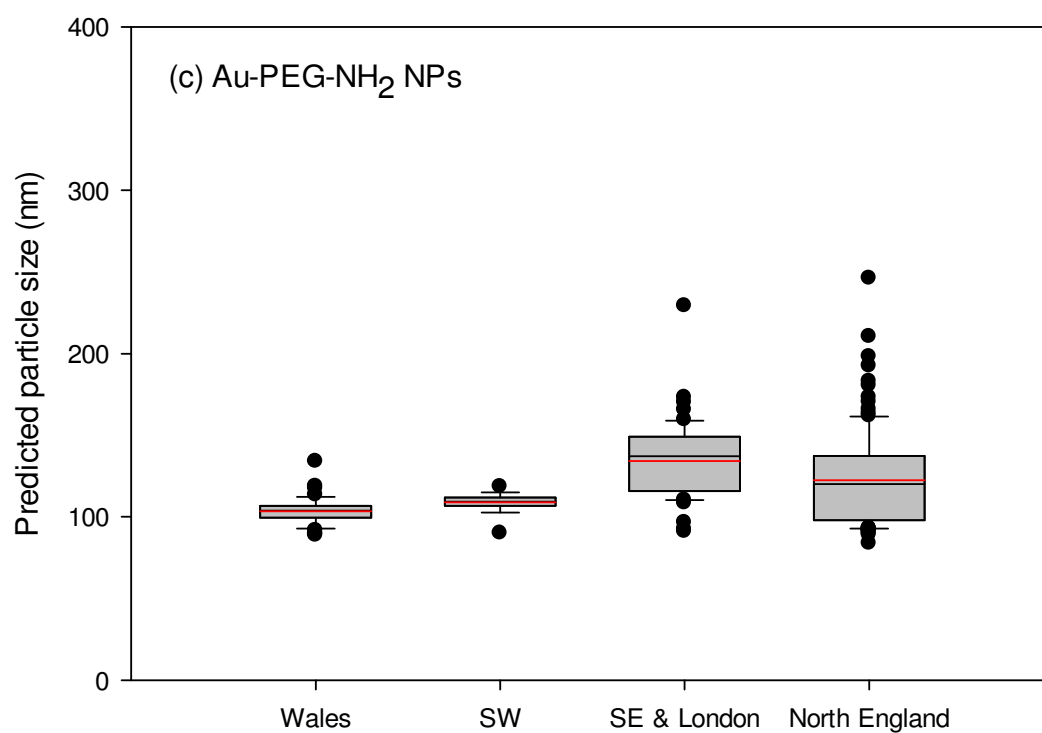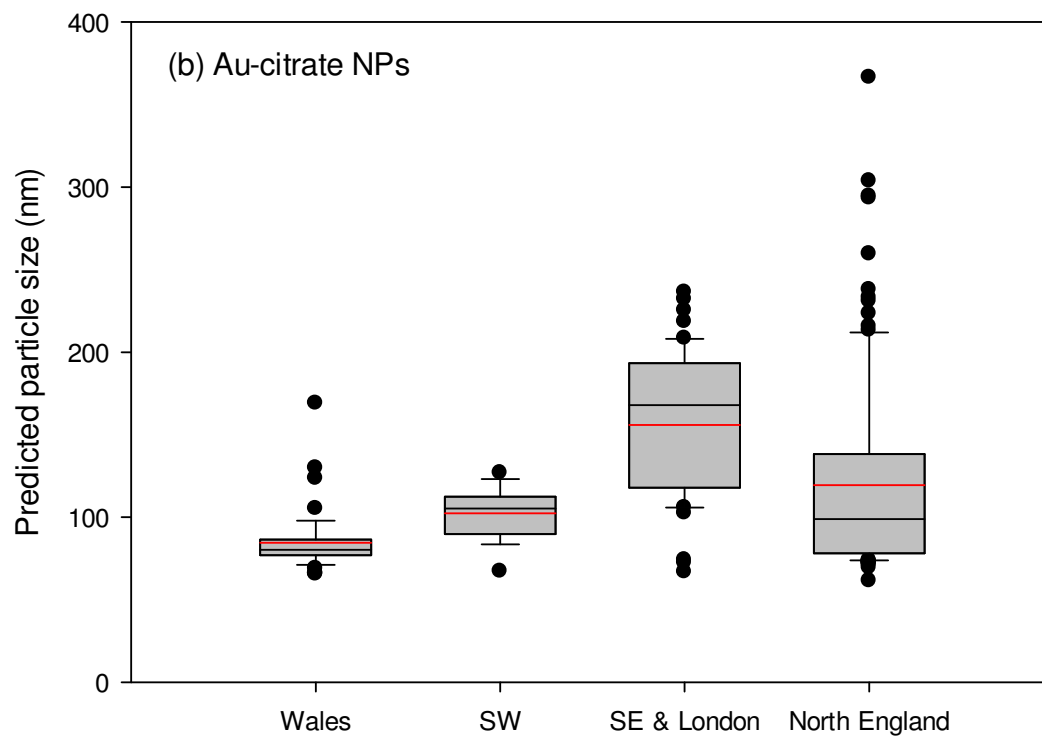
Figure14. Continued.
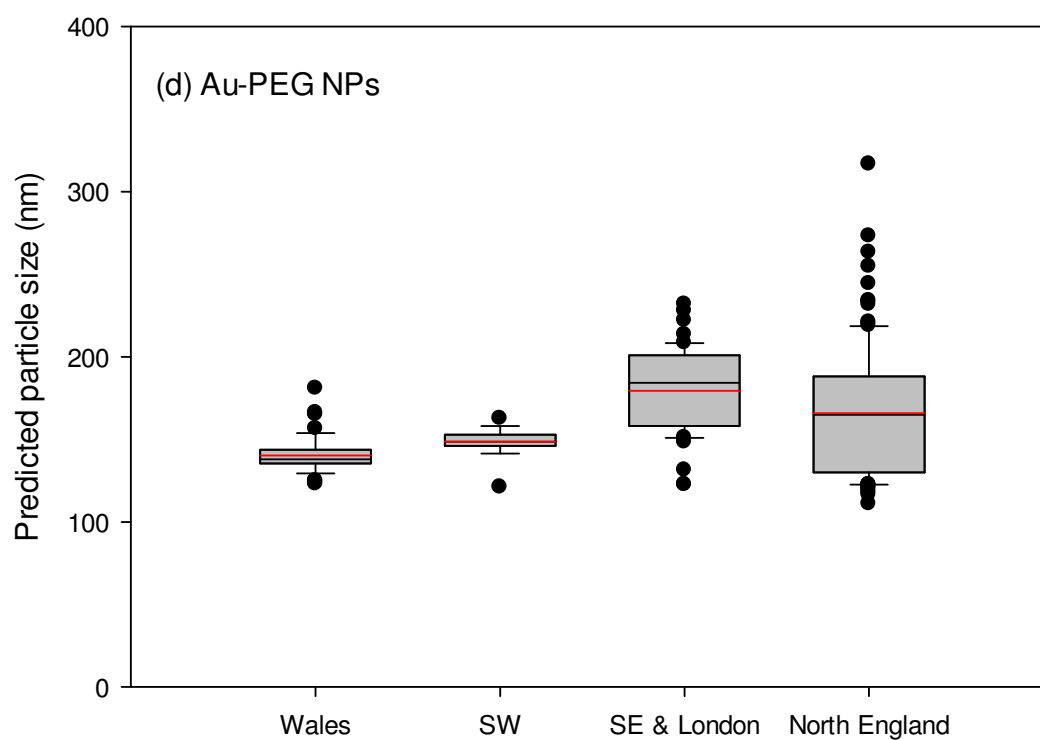
Figure14. Continued.

Model uncertainty

There was good agreement between measured and predicted particle sizes for particles with various surface coatings. These relationships were therefore used to assess the likely stability of Au nanoparticles in surface waters across the UK. However, the study had several limitations and uncertainties which should be addressed in the future. First, this study did not consider heteroaggregation in natural waters. Heteroaggregation occurs in natural aquatic systems and involves interaction of a particle with other particle types such as various naturally existing colloidal particles. Heteroaggregation is a crucial behaviour to determine transformation of ENPs and transport process from water systems to sediment. However, up to date, heteroaggregation has not been extensively considered in many of aggregation studies. It is therefore critical to consider heteroaggregation in prediction of the fate and transport of ENPs to develop a realistic model for risk assessment of ENPs in natural water systems. Second, this study was developed based on a high introductory concentration of the ENPs. These concentrations are significantly greater than compare to predicted concentrations (i.e. microgram per litre for carbon nanotube, metal nanoparticle and MeO nanoparticles) for nanomaterials in surface water resulting from typical use patterns (Mueller and Nowack, 2008; Blaser *et al.*, 2008; Gottschalk *et al.*, 2010; Johnson *et al.*, 2011). Applying high concentration to the study has potential to lead to overestimation of particle size and provide less reliable for the exposure assessment of ENPs. Finally, the study looked at pristine particles whereas in reality particles are likely to be released into the environment in a non-pristine form, e.g. they may have undergone transformation in the product or during transport to surface waters. Through further experimentation, there is no reason why this study could not be further developed to better reflect behaviour in the real environment.

Conclusion

This study has shown different aggregation behaviours of Au nanoparticles in accordance with particle types and water chemistries of natural waters. A series of methods also predicted different degree of aggregation behaviour with different surface functionalities of Au nanoparticles in real water systems. The particle size distributions of Au nanoparticles were well described in the spatial maps that indicated which Au nanoparticles were likely to undergo rapid aggregation through the UK. Applying those prediction methods therefore can provide a good prediction of the risk of ENPs in natural water systems. The methods developed herein provide a basic concept for predicting the stability of ENPs in aqueous media and can be adapted to exposure prediction methods used in risk assessment of ENPs. However, natural systems are composed with various factors so aggregation of ENPs occurs over a wide range of conditions. It is therefore required to take into consideration which factors should be considered to develop more environmentally relevant prediction model for the risk assessment.

The predictions from this study indicate that mean particle sizes for Au nanoparticles will vary widely. This could mean that uptake and effects to aquatic organisms varies widely. Therefore in the next chapter, we explore the relationships between particle size and uptake for the study ENPs.

Chapter 5

Dose Particle Size and Surface Functionality Affect Uptake and Depuration of Gold Nanoparticles by Aquatic Invertebrates?

Introduction

A number of studies have assessed the association and uptake of ENPs with/into organisms, and revealed that the uptake effects in organisms were strongly related to physico-chemical properties of ENPs. For example, the surface properties, including surface charge, chemical composition, hydrophobic, and hydrophilic properties are regarded to be major factors influencing the uptake and cytotoxicity of ENPs when compared to other properties such as core materials (Hoshino *et al.*, 2004). At a cellular level, the uptake mechanism could be adhesion of the ENPs to outer cell membranes, and subsequent internalisation into the cell. However, if the surfaces of ENPs interact with other biological molecules, e.g. corona complex, adhesion of ENPs to the cell membrane is likely to be reduced, resulting in lower cellular uptake (Lesniak *et al.*, 2013). Another study showed that the molecular structure of surface cappings on ENPs was strongly related to cell membrane injury and led to uptake of ENPs into cells (Wang *et al.*, 2013).

The size and surface area of ENPs are believed to be important factors in determining the potential uptake and toxic effects on aquatic organisms (Crane *et al.*, 2008; Nel *et al.*, 2006). The large surface area to mass ratio is thought to lead to nano-sized

118

materials being more biologically active than larger particles of the same material, even though they have the same chemical properties (Oberdörster *et al.*, 2005). For example, larger sized particles by aggregation could not penetrate smaller pores of the zebrafish embryo chorion. Therefore, size-dependent uptake effects were not observed (Chen and Elimelech, 2007). The size distribution of ENPs in a particular environment is affected by numerous factors including the physical dimensions of the particle core, the particle capping, as well as the chemistry of the surrounding environment (Fent *et al.*, 2010; Chen and Elimelech 2007). Thus, it is to be expected that the uptake and effects of an ENP to an organism vary considerably depending on the chemistry of the environment into which it released or tested.

In this context, this study aimed to explore the uptake of gold nanoparticles, with different surface functionalities, into the freshwater amphipod *G. pulex* from waters with different characteristics. The work builds upon our previous studies in Chapter 2 that demonstrated that different model Au nanoparticles show different degrees of aggregation in standard ecotoxicological test media and natural waters. Our underlying hypothesis was that the degree of uptake of gold by the invertebrates would depend on the size distribution of an ENP in the exposure medium'.

Material and Methods

Study materials

Four different Au nanoparticles samples with an average particle size of 30 nm, each bearing a different capping agent were used: 'amphoteric' 11-mercaptoundecanoic acid-capped (Au-MUDA nanoparticles); 'negative' sodium citrate tribasic dehydrate-capped (Au-citrate nanoparticles); 'Positive' amino polyethylene glycol thiol-capped (Au-PEG-NH$_2$ nanoparticles); and 'neutral' polyethylene glycol-capped (Au-PEG nanoparticles) Au nanoparticles. Au-MUDA and citrate nanoparticles were produced for the study using the methodologye described in Chapter 2. Au-PEG-NH$_2$ nanoparticles

and Au-PEG nanoparticles were purchased from Nanocs Inc. (Boston, USA). Before each uptake study, all Au nanoparticles stock solutions were ultra-sonicated in a sonication bath for 30 minutes to ensure dispersion of the ENPs.

Test organisms

Adult *G. pulex* were collected from Bishop Wilton, East Yorkshire, United Kingdom. Following collection, they were maintained in the laboratory at 13 ºC in a 5 L aquarium in artificial pond water (APW) for at least 5 d prior to use in the uptake experiments. The light cycle was 12 h light: 12 h dark. Animals were fed re-hydrated horse chestnut leaves (*Castanea sativa*) up to one day before testing. Animals were not fed during the uptake experiments.

Test medium

Uptake of the model Au nanoparticles was evaluated for standardized ecotoxicity test media and natural waters. Four different standardised test media that were shown in Chapter 2 to induce different degrees of aggregation were selected from Chapter 2. These were: APW (Naylor *et al.*, 1989), OECD *Daphnia* M4 media (OECD, 2004), moderate hard (MHW) and soft (SW) waters (U.S. EPA, 1991). The test media contained different concentrations of $CaCl_2 \cdot H_2O$, $MgSO_4 \cdot 7H_2O$, $NaHCO_3$, KCl and $CaSO_4 \cdot H_2O$. Natural water samples with different physicochemical properties were also selected based on Chapter 2 and collected from the River Etherow, Hob Moor, Bishop Wilton and Helmsley in the North of England. After collection, samples were filtered using 2.5 μm cellulose filter paper and then kept at 4 ºC prior to use. Natural water samples were analysed for pH, conductivity, dissolved organic carbon content and cation and anion concentrations. IS and hardness, expressed as equivalent of calcium carbonate, were calculated using measured cation and anion concentrations. The details of chemical analysis methods are shown in Chapter 4. The results of chemical properties of natural waters are summarised in Table 13 and Appendix 4.

Table 13. Summary of the characteristics of natural water samples used in the uptake studies

	Unit	River Etherow	Hob Moor	Bishop Wilton	Helmsley
pH	N.A	6.53	7.66	8.19	8.24
Conductivity	µS/cm	50.4	904	510	392
Ammonium-N	µg/mL	0.003	0.48	0.01	N.A
Nitrate-N	µg/mL	0.60	0.22	0.95	0.47
DOC	mg/L	4.24	2.93	1.36	1.00
SO_4^{2-}	mmole/L	0.07	1.08	0.49	0.23
Cl^-	mmole/L	0.18	2.90	0.58	0.39
NO_3^-	mmole/L	N.A	0.14	0.60	0.24
PO_4^{3-}	mmole/L	0.63	10.86	N.A	N.A
F^-	mmole/L	N.A	9.86	2.99	N.A
K^+	mmole/L	0.02	0.23	0.06	0.01
Na^+	mmole/L	0.21	1.55	0.42	0.43
Ca^{2+}	mmole/L	0.02	2.83	2.35	2.11
Mg^{2+}	mmole/L	0.05	0.74	0.21	0.13
Hardness[*]	mg/L	7.21	357.00	256.00	224.00
Ionic strength[*]	mmole/L	0.48	11.71	6.92	5.47

N.A: Not available, *: calculated value

Preliminary toxicity tests

Preliminary studies were performed to assess if the target concentrations of ENPs used in the uptake studies would result in mortality of *G. pulex*. These studies were only performed using the standard test media. Five *G. pulex* were exposed to 0.1 mg/L, 0.3 mg/L and 1 mg/L of Au-MUDA and citrate NPs and to 0.1 mg/L and 0.5 mg/L of Au-PEG-NH$_2$ and PEG NPs for 48 h. Three replicates were performed for each test media. At the end of the exposure period, the numbers of dead and living animals were counted.

Uptake and depuration studies

Uptake and depuration studies were performed using a 24 h exposure phase followed by a 24 h depuration phase for synthetic test and natural waters. Exposure concentrations of all model Au NPs were selected based upon the findings of the preliminary toxicity tests. There were three replicates each containing ten organisms in 300 mL of test water. Five organisms were taken after 24 h exposure. The remaining five organisms were rinsed with deionised water and then transferred to clean test medium for depuration. Following the uptake and depuration phases, all organisms were frozen at -20 ºC prior to analysis. The water quality parameters (pH, conductivity and dissolved oxygen) were monitored throughout.

Particle size distribution and numbers of Au NPs during the uptake/depuration experiments were measured by nanoparticle tracking analysis (NTA) using a NanoSight 2.3 LM14 instrument (NanoSight Ltd). NTA records movement of individual nanoparticles in the water samples under Brownian motion and then calculates hydrodynamic diameter of particles (nm) using the Stokes-Einstein equation: $d_p = kT /3\pi\eta D$, where d_p is hydrodynamic diameter, k is the Boltzmann constant (J K^{-1}), T is the absolute temperature (K), η is the viscosity of the medium (kg m^{-1} s^{-1}) and D is diffusion coefficient (Malloy and Carr, 2006). Aliquots (1 mL) were sampled for NTA analysis from each replicate at 0 h after Au NPs addition and at 24 h after uptake period from

test media and the natural waters. Mean concentrations for the three replicate treatments were then used in the subsequent data analyses. Before addition of the Au NPs into the test medium, samples of the test media and natural waters were also taken for NTA analysis to check background particles without ENPs. After depuration period, the number of particles in the test medium was under the NTA limits of detection. Therefore the observations of particle aggregation were made at 0 and 24 h after exposure.

Chemical analysis of organisms

Frozen samples were transferred to pre-massed 14 mL round-bottomed polypropylene tubes and oven dried at 80 ºC for 48h and re-weighed prior to acid digestion, weights were recorded. The test organisms and a number of QC materials (spikes, reagent blanks and certified reference materials which were BCR60 with certified a value of 20 ng/g Au and BCR62 with certified a value of a 2 ng/g Au) were then digested in a heating block at 100°C for 2 h in 1 mL of concentrated acid mixture (4:1 of HNO_3 and HCl). Recoveries for the standard reference materials ranged from 77-110 %. The sample digests were then made up to 10 mL with deionised water and 0.1 mL of internal standard (Rh and In at 10 ng/mL) was added into each tube. The sample digests and a matrix matched series of calibration standards were then analysed by inductively coupled plasma-mass spectrometry (ICP-MS) (Agilent 7500ce). Data obtained from the instrument were in counts per second (cps). Using an Excel spreadsheet cps data for the unknowns and calibration standards were normalised using the internal standard response. This method corrects for changes in instrument sensitivity due to physical issues e.g. matrix deposition on the sample/skimmer cones and nebulisation efficiency fluctuations. A calibration curve was constructed from the standards to characterise the response and then the unknowns were converted to concentrations in ng/mL. The data were then corrected for dilution factors, background,

spike recovery and sample weight to give a final target analyte concentration in the organism expressed in ng/g dry weight.

Derivation of uptake and depuration rate constants

The uptake and depuration rate constant were derived using the minimised approach developed by Springer *et al.* (2008) using Equations 5.1 and 5.2. Rates were calculated from the concentration of the Au in organisms at the end of the uptake phase (C_{t1}) and at the end of the depuration period (C_{t2}) and the concentration of test substance in the water during the exposure (C_w) phase (for this the nominal concentration of 0.2 µg/mL was used).

$$k_2 = \frac{\ln C_{t1} - \ln C_{t2}}{t_d} \qquad \text{(Equation 5.1)}$$

Where t_1 and t_2 are the beginning and end of the depuration period, respectively ($t_d = t_2 - t_1$).

The uptake rate constant (k_1) is then calculated based on the depuration rate constant (k_2) generated using Equation 1.

$$k_1 = \frac{k_2 \times C_{t1}}{C_w \times \left(1 - e^{-k_2 tu}\right)} \qquad \text{(Equation 5.2)}$$

Where k_2 is depuration rate constant and t_u is the length of uptake periods.

Statistical analysis

One-way ANOVA was performed using PASW (v 20; SPSS Inc.) to assess differences in particle aggregation and uptake/depuration effects in test media and natural waters. Prior to ANOVA analysis, the data were checked for normality and homogeneity using a Shapiro-Wilk or a Kolmogorov-Smirnov test. A non-parametric analysis (Mann-Whitney analysis and Kruskal-Wallis analysis) was used if the data were not normally distributed or did not satisfy the homogeneity criteria. The significance level was $p < 0.05$.

Results and Discussion

Preliminary test

In preliminary tests, no mortality was noted following exposure to any of the concentrations of the nanoparticles used in the preliminary study. NTA characterisation for the preliminary studies showed that for the 1 mg/L treatment, the particle number concentrations were above the optimum range of the NTA (i.e., between 10^7 and 10^9 total particles/mL) (Gao *et al.*, 2009). Therefore, the final concentration selected for use in the uptake studies was 0.2 mg/L.

Particle size and size distribution in test media and natural waters in the uptake and depuration studies

In the control samples, containing no Au ENPs, no particles were detected by the NTA for the standard ecotoxicity test media. Particles were however observed in the controls of the natural water treatments (Figure 15). In River Etherow, Helmsley and Bishop Wilton water samples, the concentrations of background particles were significantly lower (0.98 ± 0.05 to $4.33 \pm 0.68 \times 10^8$ particles/mL) than those of studied Au NPs (7.73 ± 0.38 to $17.11 \pm 0.60 \times 10^8$ particles/mL after 24 h uptake period) so this had no effect

on the interpretation of the NTA results (One-way ANOVA and Mann-Whitney, $p < 0.05$). However, for the Hob Moor water, with the exception of the Au-MUDA NPs, there were no differences in particle number concentrations for background particles and Au NPs (One-way ANOVA and Mann-Whitney, $p > 0.05$). The interpretation of the Hob Moor data should therefore be considered as indicative only. During the uptake study, mean particle sizes of the Au-MUDA, Au-citrate and Au-PEG-NH$_2$ NPs increased significantly in all standard test media over 24 h (One-way ANOVA and Mann-Whitney analysis, $p < 0.05$) (Table 14). The greatest particle size were detected in M4 media as 179 ± 5.6 nm, 162.4 ± 6.9 nm and 124.2 ± 7.4 nm for Au-MUDA, citrate and PEG-NH$_2$ NPs, respectively. Limited particle aggregation was observed for Au-PEG NPs in M4 media and MHW after 24 h exposure (One-way ANOVA, $p > 0.05$). In all natural waters, significant particle aggregation was seen for all tested Au NPs (One-way ANOVA and Mann-Whitney analysis, $p < 0.05$) except for Au-PEG-NH$_2$ NPs (One-way ANOVA and Mann-Whitney analysis, $p > 0.05$). Greatest aggregation was seen for the Au-PEG-NH$_2$ NPs (mean size after 24 h around 170 nm) in the Hob Moor and Bishop Wilton waters. The degree of aggregation was smallest in the River Etherow water (mean of 67.1 ± 5.2 nm) for Au-MUDA NPs. These results matched findings from Chapter 2 which showed different behaviours of the study ENPs in synthetic test media and natural waters. The differences between natural waters and test media understood in the context of interactions between coating agents and dissolve organic matter (DOC). The lower particle aggregations of Au-MUDA and citrate in the natural waters compared to synthetic media were probably caused by DOC which adsorbed onto the surface of particles and led to steric repulsion between particles (Gao *et al.*, 2009). DOC also changes the surface charge of ENPs to either negative or to neutral charges depending on the concentrations of cations in the waters (Ottofuelling *et al.*, 2011; Zhang *et al.*, 2009). The changing surface charges of Au-PEG-NH$_2$ and PEG nanoparticles could explain the greater aggregation of those nanoparticles in the natural waters compared to the standardised test medium.
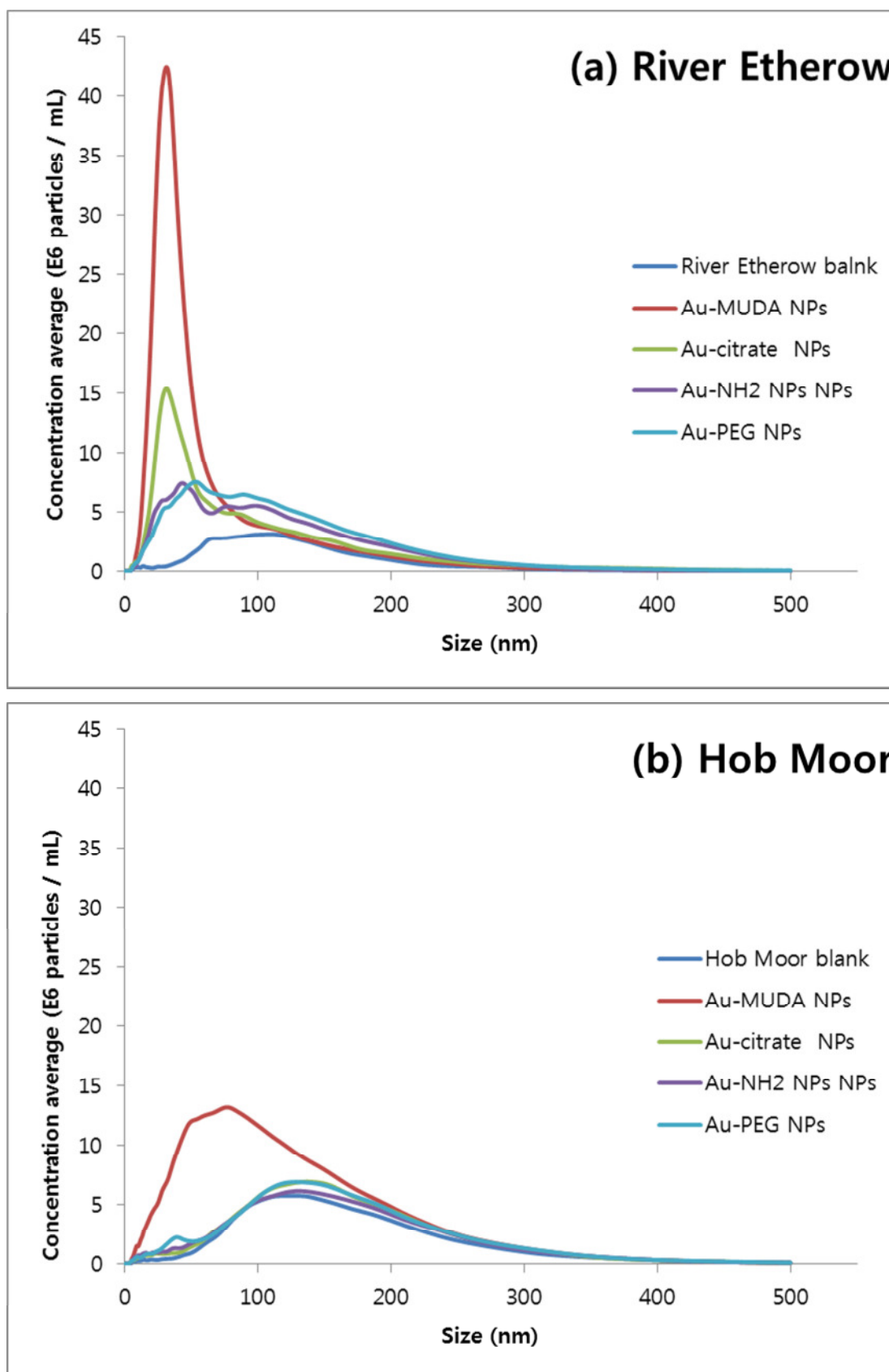
Figure 15. The mean particle concentrations in natural waters at 24 h in the uptake studies. A: River Etherow, B: Hob Moor, C: Bishop Wilton and H: Helmsley.
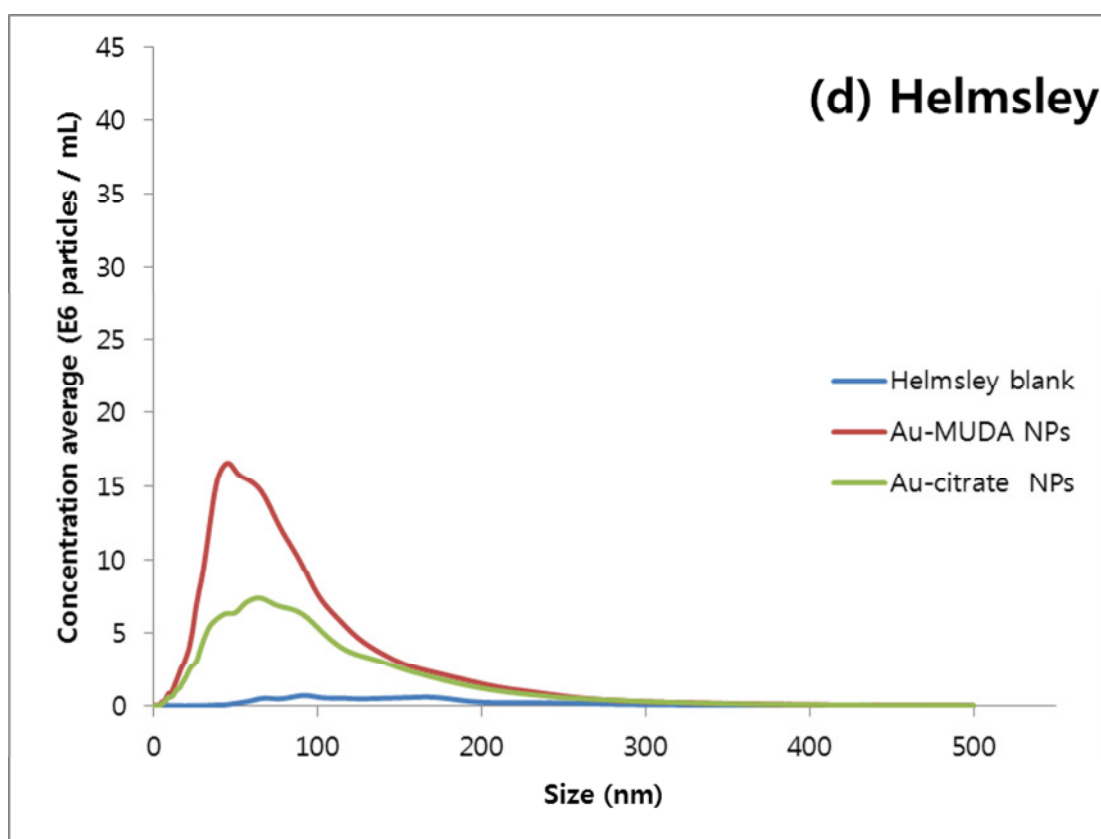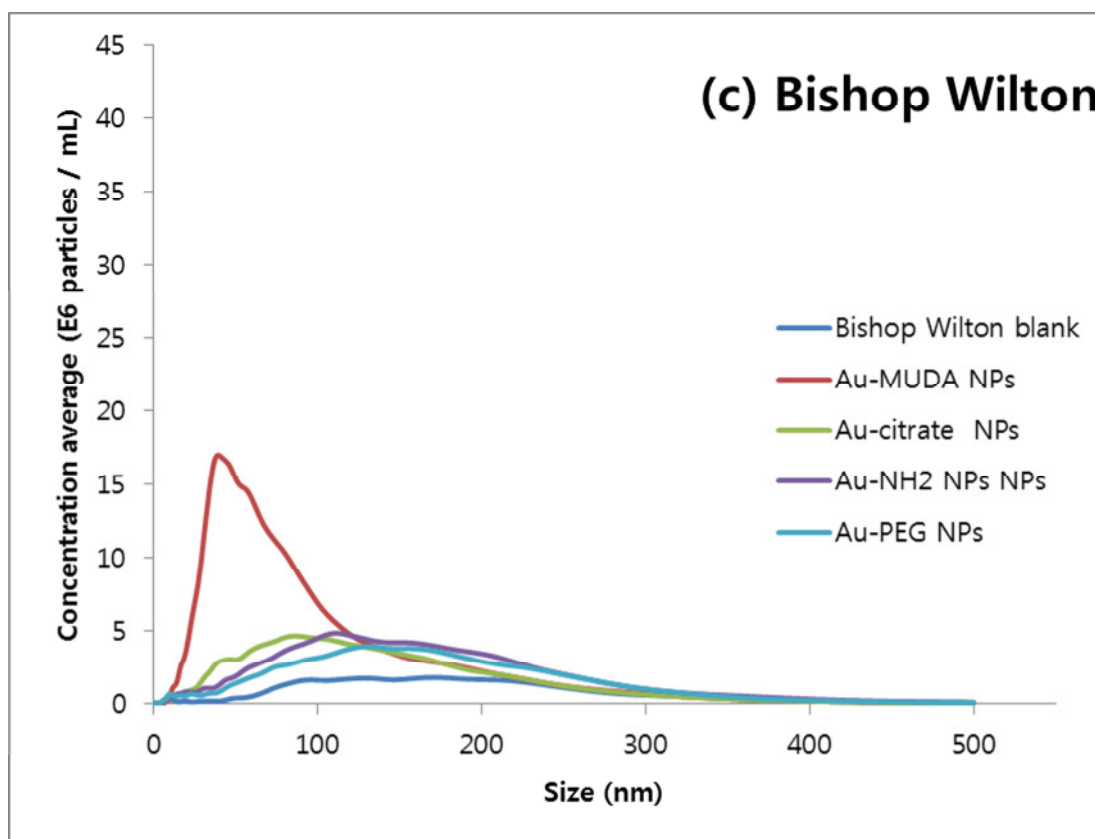
Figure 15. Continued

Table 14. Change in mean particle size and particle number concentration during

uptake period in standard test and natural waters

Au- MUDA NPs			
Particle size (nm)		Particle number concentration (× 10^8 particles/ml)	
0 h	24 h	0 h	24 h
Test media			
116.7 ± 6.9	154.2 ± 9.2*	4.74 ± 0.27	6.82 ±0.54
123.3 ± 3.0	179.0 ± 5.6*	8.24 ± 0.47	5.85 ± 0.40
55.9 ± 1.6	92.6 ± 6.0*	9.26 ± 0.45	8.15 ± 0.72
47.6 ± 1.0	93.7 ± 2.6*	11.81 ± 1.13	9.81 ± 0.99
Natural water			
51.5 ± 1.9	67.1 ± 5.2*	18.51 ± 1.00	17.11 ± 0.60
121.2 ± 2.5	130.8 ± 1.3*	19.16 ± 0.47	20.58 ± 1.15
77.3 ± 1.5	102.1 ± 1.9*	17.43 ± 0.31	15.03 ± 0.49
58.3 ± 5.1	91.9 ± 2.2*	15.32 ± 0.43	14.44 ± 0.54

Mean ± standard error, *: $p<0.05$

Table 14. Continued

Au- citrate NPs			
Particle size (nm)		Particle number concentration ($\times 10^8$ particles/ml)	
0 h	24 h	0 h	24 h
Test media			
63.1 ± 3.8	139.0 ± 3.9[*]	4.18 ± 0.46	2.48 ± 0.22
70.9 ± 4.4	162.4 ± 6.9[*]	6.22 ± 0.27	2.38 ± 0.16
68.9 ± 9.8	111.6 ± 6.2[*]	9.43 ± 1.23	5.17 ± 0.38
57.0 ± 2.3	71.7 ± 2.5[*]	5.92 ± 0.44	6.13 ± 0.43
Natural water			
76.3 ± 3.9	101.9 ± 8.3[*]	6.97 ± 0.44	10.67 ± 1.06
139.9 ± 3.1	171.6 ± 2.4[*]	18.16 ± 1.43	11.55 ± 0.38
116.0 ± 6.6	145.8 ± 2.7[*]	6.97 ± 0.50	7.89 ± 0.36
56.4 ± 1.1	106.8 ± 2.7[*]	8.64 ± 0.27	8.51 ± 0.62

Mean ± standard error, [*]: $p < 0.05$

Table 14. Continued

Au-PEG-NH$_2$ NPs			
Particle size (nm)		Particle number concentration ($\times 10^8$ particles/ml)	
0 h	24 h	0 h	24 h
Test media			
75.1 ± 4.2	106.3 ± 6.8*	1.47 ± 0.19	3.18 ± 0.22
87.8 ± 9.3	124.2 ± 7.4*	1.61 ± 0.14	2.95 ± 0.33
107.7 ± 4.4	116.4 ± 1.7*	2.92 ± 0.21	3.49 ± 0.27
89.2 ± 3.9	120.4 ± 5.4*	2.24 ± 0.24	2.50 ± 0.10
Natural water			
118.9 ± 6.0	120.8 ± 4.7	5.94 ± 0.33	9.89 ± 0.50
173.3 ± 2.9	171.7 ± 3.0	10.31 ± 0.25	10.96 ± 0.61
168.1 ± 3.5	171.5 ± 3.3	4.86 ± 0.21	9.12 ± 0.56
118.9 ± 6.0	120.8 ± 4.7	5.94 ± 0.33	9.89 ± 0.50

Mean ± standard error, *: $p<0.05$

Table 14. Continued

Au-PEG NPs			
Particle size (nm)		Particle number concentration ($\times 10^8$ particles/ml)	
0 h	24 h	0 h	24 h
Test media			
79.4 ± 7.6	99.7 ± 6.9[*]	2.02 ± 0.25	2.64 ± 0.27
76.1 ± 7.5	105.2 ± 3.1	1.73 ± 0.25	2.36 ± 0.14
94.8 ± 3.4	111.1 ± 6.4	1.94 ± 0.15	3.88 ± 0.28
97.6 ± 5.7	111.7 ± 6.5[*]	2.04 ± 0.24	3.30 ± 0.26
Natural water			
110.5 ± 3.3	125.7 ± 5.9[*]	8.44 ± 1.40	11.05 ± 0.85
157.8 ± 1.9	170.9 ± 2.5[*]	11.57 ± 0.49	11.90 ± 0.40
164.7 ± 5.2	178.8 ± 3.2[*]	4.90 ± 0.27	7.73 ± 0.38
110.5 ± 3.3	125.7 ± 5.9[*]	8.44 ± 1.40	11.05 ± 0.85

Mean ± standard error, [*]: $p < 0.05$

Uptake experiments

The uptake results and uptake rates in *G. pulex* following 24 h exposure from each standardized test medium and natural waters are shown in Figure 16 and Table 15. Surface functionality was found to affect uptake. Generally, the greatest uptake was seen for Au-MUDA NPs (8.40 ± 1.30 µg/g dry weight (River Etherow) to 29.46 ± 3.30 µg/g dry weight (APW)) followed by Au-citrate NPs (7.70 ± 1.32 µg/g dry weight (MHW) to 21.78 ± 5.39 µg/g dry weight (Bishop Wilton)), PEG (5.10 ± 2.18 µg/g dry weight (SW) to 14.84 ± 7.99 µg/g dry weight (APW)) and then PEG-NH$_2$ (6.30 ±1.48 µg/g dry weight (M4 media) to 14.19 ± 3.38 µg/g dry weight (Hob Moor)). For Au-MUDA NPs, there was a significant difference in the degree of uptake of gold observed across the different media (One-way ANOVA and Kruskal-Wallis test, $p < 0.05$). The highest uptake was seen in APW, SW and Helmsley water and lowest uptake was seen in M4 media and MHW (Figure 16 (a)). The highest concentrations of Au-citrate NPs were detected in animals exposed to the natural waters collected from Bishop Wilton and Helmsley, and uptake from these waters was significantly higher than from MHW, SW and River Etherow water (One-way ANOVA, Tukey, $p < 0.05$) (Figure 16 (b)). For Au-PEG-NH$_2$ NPs, uptake in the APW treatment was significantly higher than from the M4 media, SW and River Etherow treatments (One-way ANOVA, Tukey $p < 0.05$) (Figure 16 (c)). There was no significant difference in the uptake of Au-PEG NPs between any of the test media (Figure 16 (d)) (One-way ANOVA, $p > 0.05$).

Our study therefore shows the surface functionalisation of Au ENPs is an important factor for uptake into organisms. The effect of functionality may be particle, coating and organism specific. For example, Petersen *et al.* (2011 a; 2011b) observed the size related accumulation of multiwalled carbon nanotubes, coated with different materials in *D. magna* and the earthworm, *Eisenia fetida*. However, these studies did not show an effect of surface functionality on the uptake of the ENPs. In contrast, Feswick *et al.* (2013) observed an obvious effect of surface functionalistion of CdSe quantum dots

(QDs) in *D. magna* which were uncharged polyethylene glycol (PEG), positively charged amino terminated (PEG-NH$_2$) and negatively charged carboxyl group. Greatest uptake was seen for the carboxyl functionalised QDs which were retained and internalised in the organism (Feswick *et al.*, 2013). Bozich *et al.* (2014) did not find significant uptake effect of Au NPs in daphnia between on the surface coating types, however, different toxic effects were observed depending on the surface charge. The positive charged Au NPs were more toxic than negatively charged particles due to the high affinity potential to negative charged surface of cellular membrane after uptake. In addition negatively charged Au NPs (citrate and mercaptopropionic acid coated) affected on reproduction and body size of *D. magna* even those particles showed great aggregation in the test media. It was explained that the aggregation prevented food consumption or affected on molting or swimming behaviour.

Water chemistry is also an important factor influencing ENP uptake. Chen *et al.* (2014) and Yang *et al.* (2013) observed the effects of humic acid (HA) in test media on the uptake of fullerene (nC$_{60}$) and TiO$_2$ into *D. magna* and zebra fish. Both studies showed lower uptake of nC$_{60}$ and TiO$_2$ in *D. magna* and zebra fish in the presence HA. HA could influence the stabilisation of ENPs by changing surface charge (Park *et al.*, 2014) as well as dissolution of core materials (Liu and Hurt, 2010). Gao *et al.* (2009) found that lower toxicity of Ag NPs to *Ceriodaphnia dubia* in test media containing higher amount of Suwanee River humic acids. The organic substance reduced the Ag ion release from Ag NPs resulting in lower bioavailability and toxicity.

(a) Au-MUDA NPs
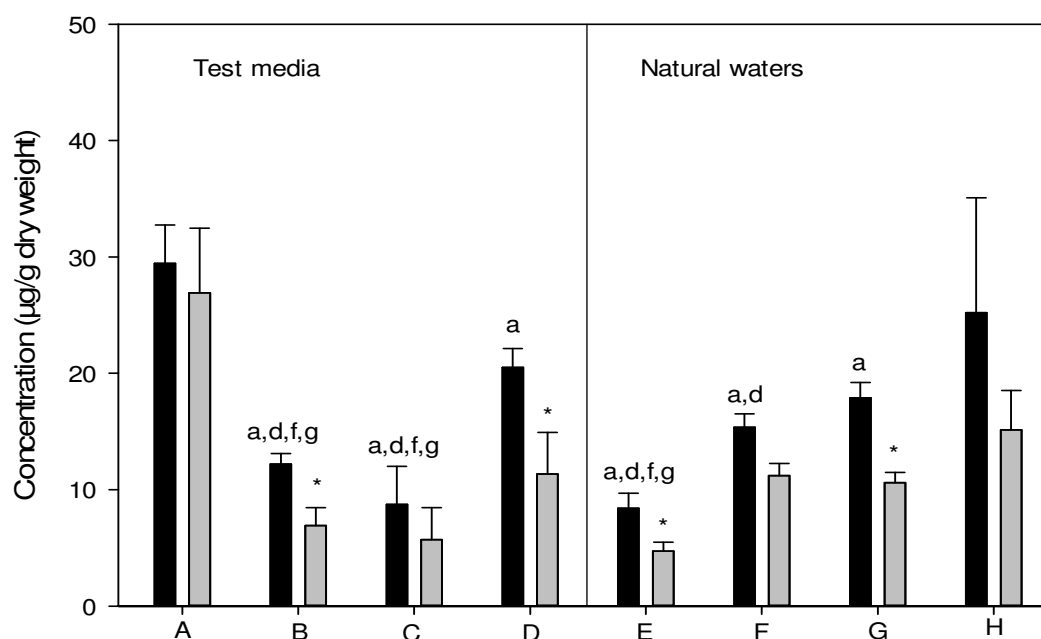
Figure 16. Concentration of Au in *G. pulex* during uptake (24 h) and depuration (48 h) periods in synthetic test water and natural waters. A: APW, B: M4 media, C: MHW, D: SW, E: River Etherow, F: Hob Moor, G: Bishop Wilton and H: Helmsley. Alphabets indicate significantly lower concentration of gold between test medium after uptake (One-way ANOVA and Kruskal-wallies test, $p < 0.05$). * presents significance on depuration compare with uptake in each test media (One way ANOVA and Mann-Whitney analysis, $p < 0.05$). Black and grey bars indicate uptake and depuration. Data shows mean ± SD.

(b) Au-citrate NPs
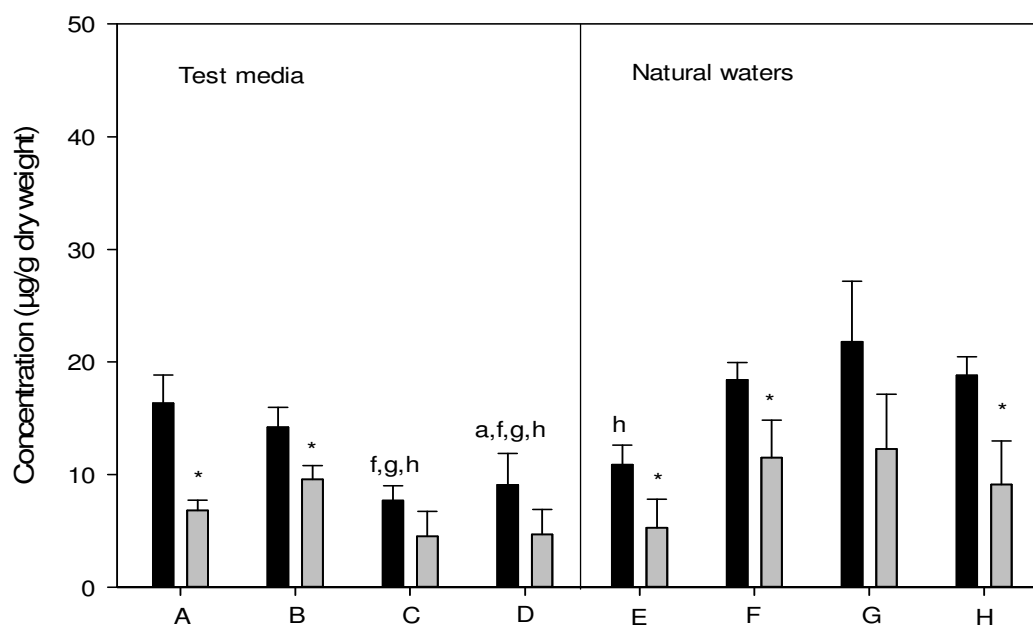
(c) Au-NH$_2$ NPs
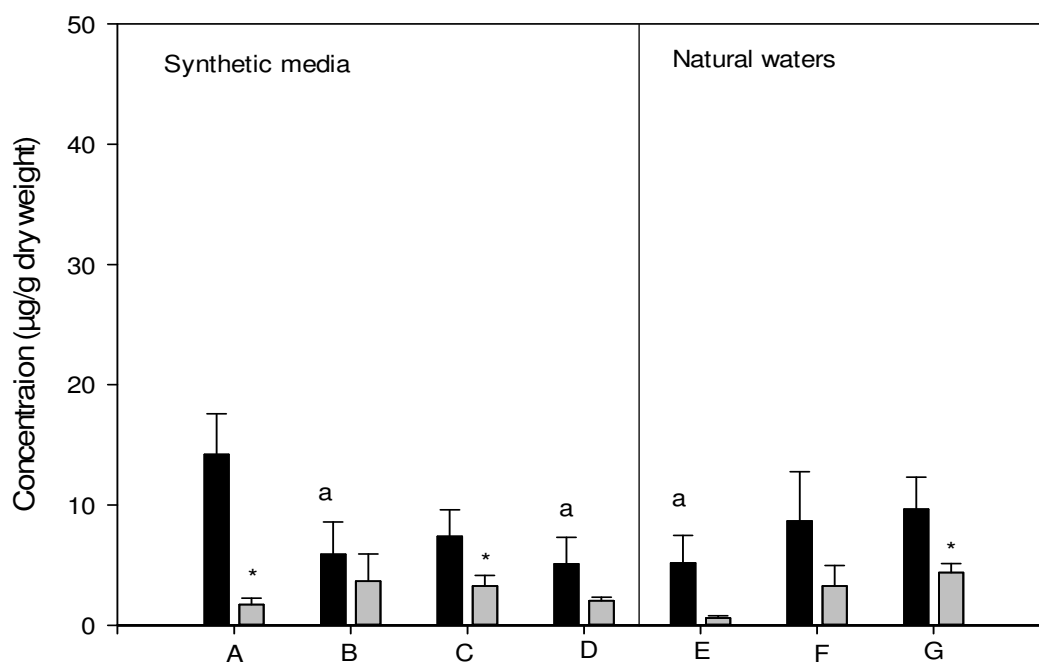
Figure 16. Continued.

(d) Au-PEG NPs
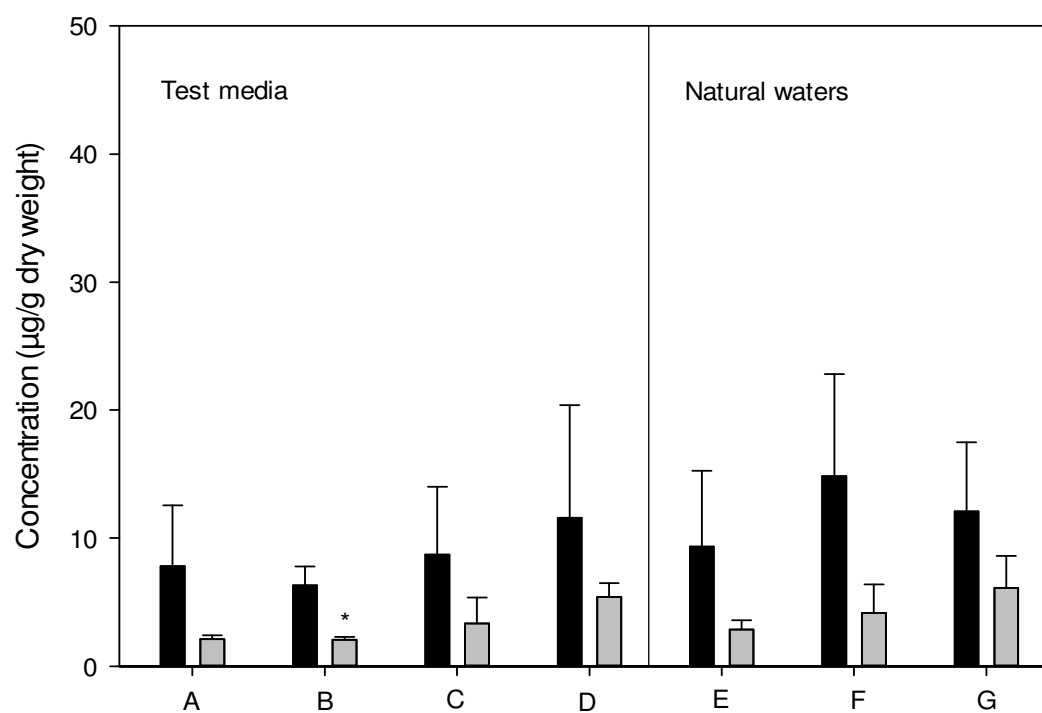
Figure 16. Continued.

Table 15. Uptake (k_1) and depuration rate (k_2) of Au nanoparticles in test media and natural waters (Mean ± standard deviation)

Au nanoparticles	Test media	k_1 (mL/g d^{-1})	k_2 (d^{-1})	Natural waters	k_1 (mL/g d^{-1})	k_2 (d^{-1})
Au-MUDA nanoparticles	APW	154.6 ± 13.9	0.1 ± 0.1	River Etherow	56.5 ± 17.5	0.6 ± 0.3
	M4	80.2 ± 2.1	0.6 ± 0.2	Hob Moor	90.0 ± 13.4	0.3 ± 0.2
	MHW	53.9 ± 18.4	0.5 ± 0.2	Bishop Wilton	115.2 ± 14.6	0.5 ± 0.1
	SW	140.0 ± 37.1	0.6 ± 0.4	Helmsley	168.0 ± 101.4	0.5 ± 0.5
Au-citrate nanoparticles	APW	130.6 ± 37.1	1.0 ± 0.2	River Etherow	81.8 ± 31.2	0.8 ± 0.6
	M4	79.3 ± 20.7	0.3 ± 0.3	Hob Moor	153.5 ± 81.2	0.5 ± 0.6
	MHW	50.1 ± 15.1	0.8 ± 0.7	Bishop Wilton	143.7 ± 26.1	0.6 ± 0.1
	SW	244.0 ± 122.9	0.7 ± 0.3	Helmsley	137.4 ± 35.0	0.8 ± 0.5
Au-PEG-NH$_2$ nanoparticles	APW	335.8 ± 218.9	2.6 ± 0.6	River Etherow	66.0 ± 40.4	2.3 ± 0.6
	M4	37.3 ± 14.1	0.5 ± 0.2	Hob Moor	76.1 ± 61.0	1.0 ± 0.5
	MHW	57.0 ± 28.5	0.8 ± 0.6	Bishop Wilton	70.5 ± 25.3	0.8 ± 0.3
	SW	40.3 ± 25.0	0.9 ± 0.4			
Au-PEG nanoparticles	APW	74.0 ± 57.3	1.2 ± 0.7	River Etherow	83.2 ± 70.0	1.1 ± 0.5
	M4	53.2 ± 19.0	1.1 ± 0.3	Hob Moor	138.3 ± 82.1	1.3 ± 0.7
	MHW	75.1 ± 65.8	1.0 ± 0.7	Bishop Wilton	91.6 ± 70.0	0.7 ± 0.7
	SW	87.7 ± 85.3	0.6 ± 0.6			

Depuration experiments

After placing the organisms into the clean water for 24 h different degrees of depuration were observed according to the type of Au NPs (Figure 16 and Table 15). For Au-MUDA NPs, the lowest depuration was seen in APW (9.12%) and Hob Moor sample (26.45%). In other test media, from 34% to 43% of MUDA coated gold were eliminated over the depuration period (Figure 16 (a)). The highest depuration of Au-citrate NPs was seen in APW followed by Helmsley water (57.69% and 50.28%) and the lowest were in M4 media and Hob Moor (31.18% and 38.05%). Similar amounts of gold were removed (nearly 40%) in MHW, SW and River Etherow (Figure 16 (b)). The greatest elimination (87.86% and 86.44%) of Au-PEG-NH_2 NPs was seen in APW and River Etherow samples. It corresponded to the highest depuration rates, 2.6 ± 0.6 and 2.3 ± 0.6, respectively (Figure 16 (c) and Table 15). Almost 50% of PEG-NH_2 coated gold was removed in other test media. For Au-PEG NPs, around 65% of gold in APW, M4 media, River Etherow and Hob Moor was depurated while slightly lower elimination was seen in MHW, SW and Bishop Wilton water (38% to 55%) (Figure 16 (d)).

Like uptake studies of ENPs, there are only a few studies in the literature that have explored the depuration of ENPs. Lovern *et al.* (2008) observed fast uptake of Au NPs into *D. magna* but, once the particles were taken up, particles formed aggregates or agglomerates inside the digestive systems of the organisms and these could not be eliminated. However, Khan *et al.* (2014) observed fast elimination of citrate coated Au NPs after a depuration period of only 1 h in the daphnids.

Previous studies have explored the depuration of ENPs in the presence and absence of natural organic matter (NOM). Depuration studies using *D. magna* and zebra fish with HA showed a significant reduction in the amount of fullerene (nC_{60}) measured in the test organisms while up to 30 % of fullerene remained after depuration in clean water (Chen *et al.*, 2014). Glover and Wood (2005) also demonstrated that NOM increases the elimination of silver from *D. magna*. It is assumed that NOM binds to

particulate substances in the gut contents of organisms and acts as a depurating ligand removing the substances via water flow when organisms consume surrounding water (Glover and Wood, 2005). However, it is assumed that NOM binds to particulate substances in the gut contents of organisms and acts as a depurating ligand removing the substances via water flow when organisms consume surrounding water.

In contrast, Oliver *et al.* (2014) observed in studies with *Lymnaea stagnalis* that dietary uptake was more relevant for bioavailability of polyvinyl pyrrolidone coated Ag NPs rather than water composition or NOM. Our study also did not show differences in depuration rates between NOM free-synthetic test media and natural waters containing NOM. The specific role of NOM in the elimination of ENPs is unknown, therefore, further investigation into the factors determining elimination of ENPs in aquatic organisms are required.

Relationship between particle size and uptake

While we expected, based on previous studies, uptake to decrease with increasing mean particle sizes in the different test media, there was actually no clear relationship between mean particle size and degree of uptake into the organisms (Figure 17). In fact for Au-citrate NPs in the test media (R^2= 0.75) and Au-PEG-NH$_2$ and PEG NPs in the natural waters (R^2= 0.96 and 0.62, respectively), greatest uptake was observed in media where the particles were some of the most aggregated (Figure 17 (b), (c) and d)). The average primary particle size of studied Au NPs in the present study was 30 nm, however, at the end of uptake period, the particle size were increased at least by a factor of two. The particle size had gradually increased within 1-6 h after dispersion (Park *et al.*, 2014). The particles could be taken up into test organisms very beginning of exposure after particles were dispersed and less aggregated. Some studies indicate fast uptake results in test organisms. Rosenkranz *et al.* (2009) and Tan et al. (2012) reported that uptake of fluorescence beads and TiO$_2$ occurred less than 1 h of exposure in the gastrointestinal tract of *D. magna*.

Many previous uptake studies have shown particle size dependence. However, some have only evaluated uptake differences between nano-sized and micro-sized particles. Rosenkranz *et al.* (2009) also demonstrated greater uptake of 20 nm to 23 nm sized fluorescent beads versus 1000 nm. In addition, Ag NPs (d = 23 nm) were taken up more quickly in *D. magna* than those with 50 nm to 1000 nm dimensions (Georgantzopoulou *et al.*, 2012). Gaiser *et al.* (2012) was observed significance uptake of Ag NPs into *Cyprinus carpio* compare with micro size Au NPs.

The mismatch between our results and the results of previous studies could be explained by a number of factors. For example the size range of particles explored in our study was not as wide as many other studies which have often looked at differences of uptake of particles <10 nm or close to 1 μm and that additional factors are driving the observed uptake.

One factor that could be important is the particle number concentration (PNC). To explore whether this was the case or not, relationships between PNC in the different media and uptake were also explored (Figure 18). For all of the study particles, uptake increased with PNC measured in the different test media, indicating that PNC is at least partly explaining the observed differences in uptake.

The previous studies have on NP uptake have explored test organisms which had different traits than our test organism, this may also explain why we don't observe some of the patterns seen by others. At a cellular level, ENPs can easily penetrate into the cell walls and/or membrane when the pore size of the cell is larger than the exposed particle size, and may cause adverse effects (Navarro *et al.*, 2008a). Filter feeding organisms (e.g. *D. magna* and mussel) could ingest the micro sized particles if they are smaller than organisms' filter sizes (Filella *et al.*, 2008; Geller *et al.*,1981; Ward *et al.*, 2009). For fish, nanoparticles could be taken up through the gill or skin by nanoparticle absorption but the dietary intake route is likely a major route for aggregated or larger sized nanoparticles (Gaiser *et al.*, 2012; Jovanovic and Palic, 2012). The feeding behaviour of *G. pulex* is mainly through shredding activity (Lahive

et al., 2014) but also uptake from the water is probably a dominant uptake route (Gross-Sorokin *et al.*, 2003).

(a) Au-MUDA NPs

(b) Au-citrate NPs
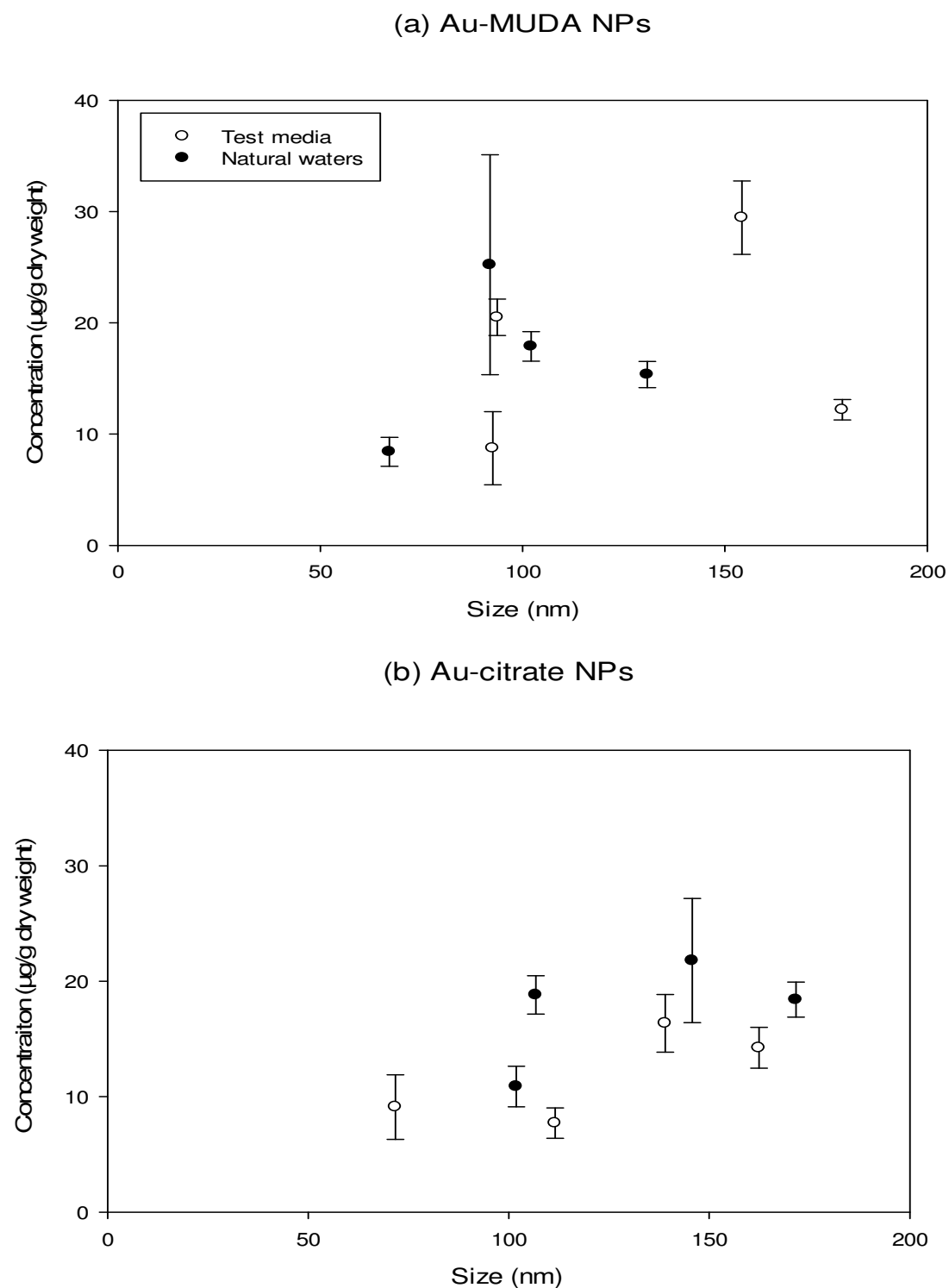
Figure 17. The mean concentration of gold in *G. pulex* and particle size of Au nanoparticles from test media and natural waters after uptake period. White and black circles are test media and natural waters. Data are mean ± SD.

(c) Au-PEG-NH$_2$ NPs
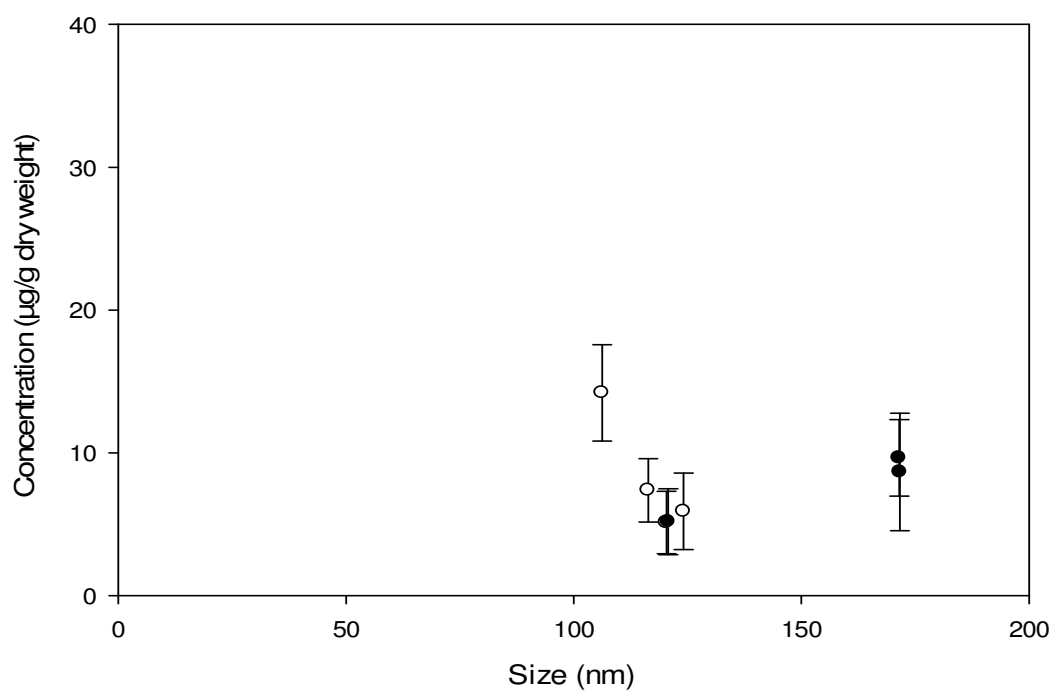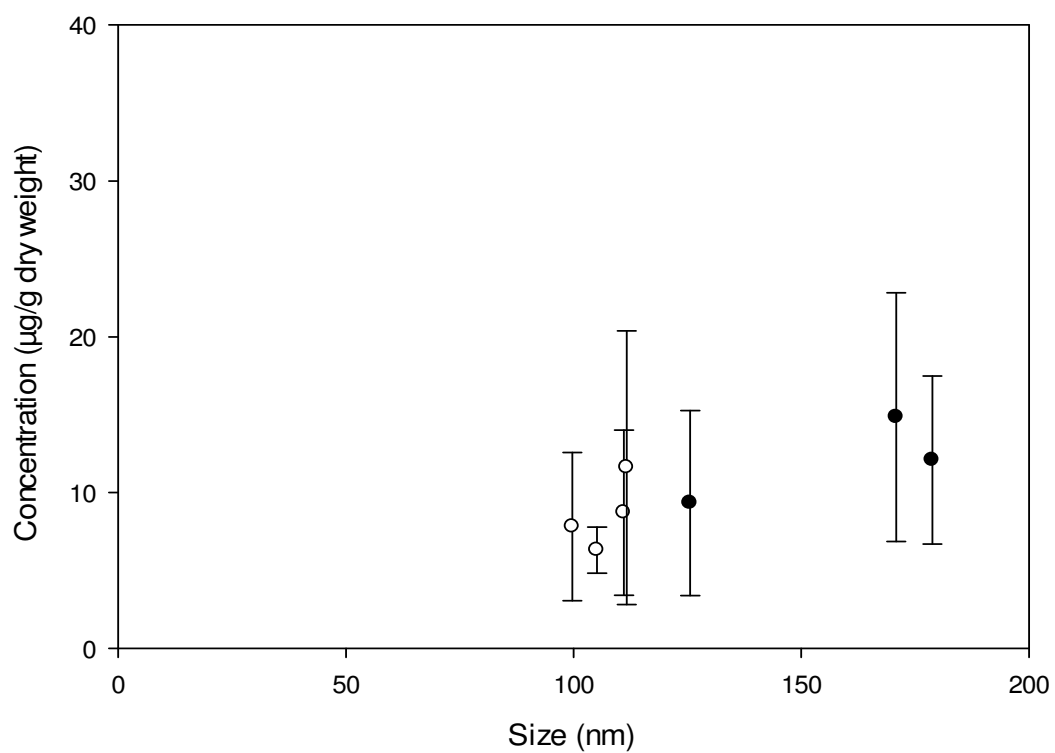
(d) Au-PEG NPs

Figure 17. Continued.

(a) Au-MUDA NPs
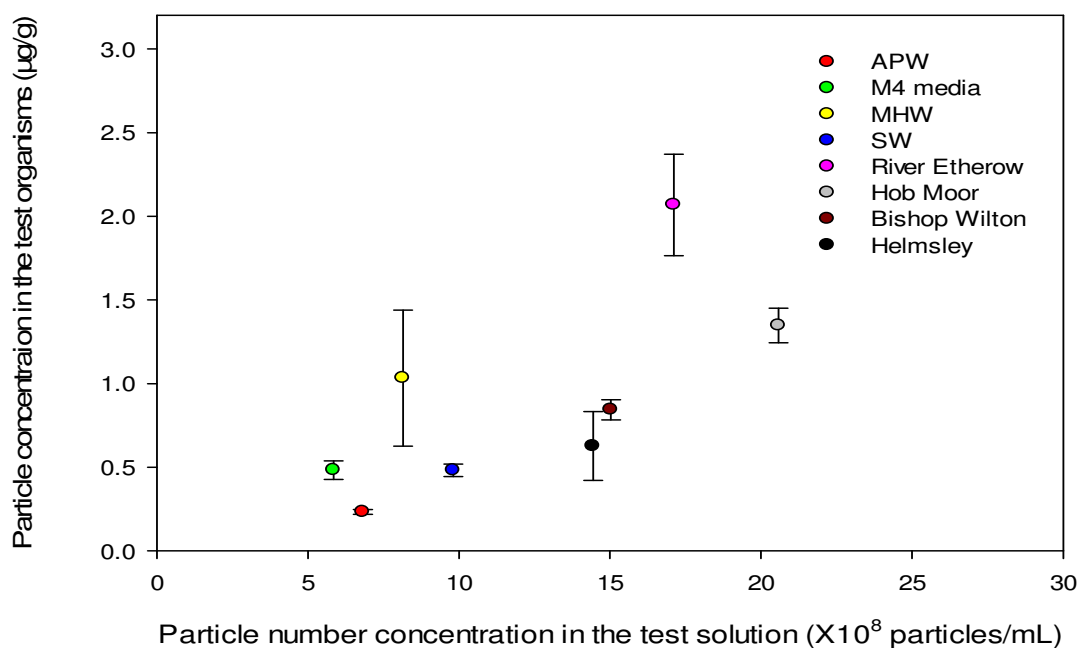
(b) Au-citrate NPs
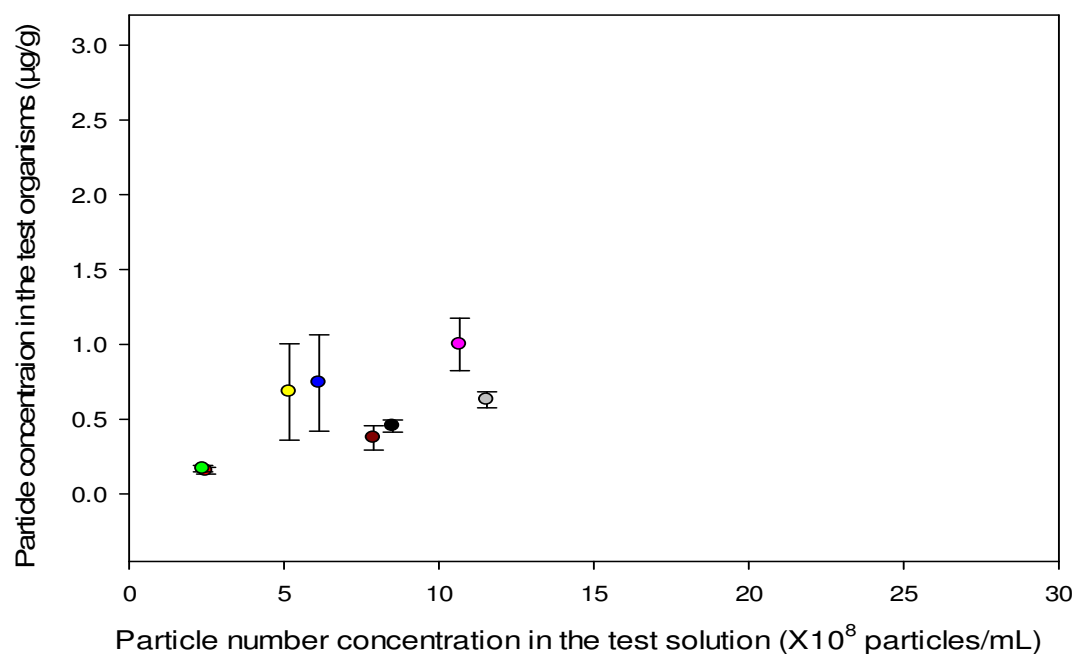
Figure 18. Relationship between particle number concentration in different media and uptake into *Gammarus pulex* for (a) Au-MUDA NPs, (b) Au-citrate NPs, (c) Au-PEG-NH_2 NPs and (d) Au-PEG NPs. Data are mean ± SD.

(c) Au-PEG-NH$_2$ NPs
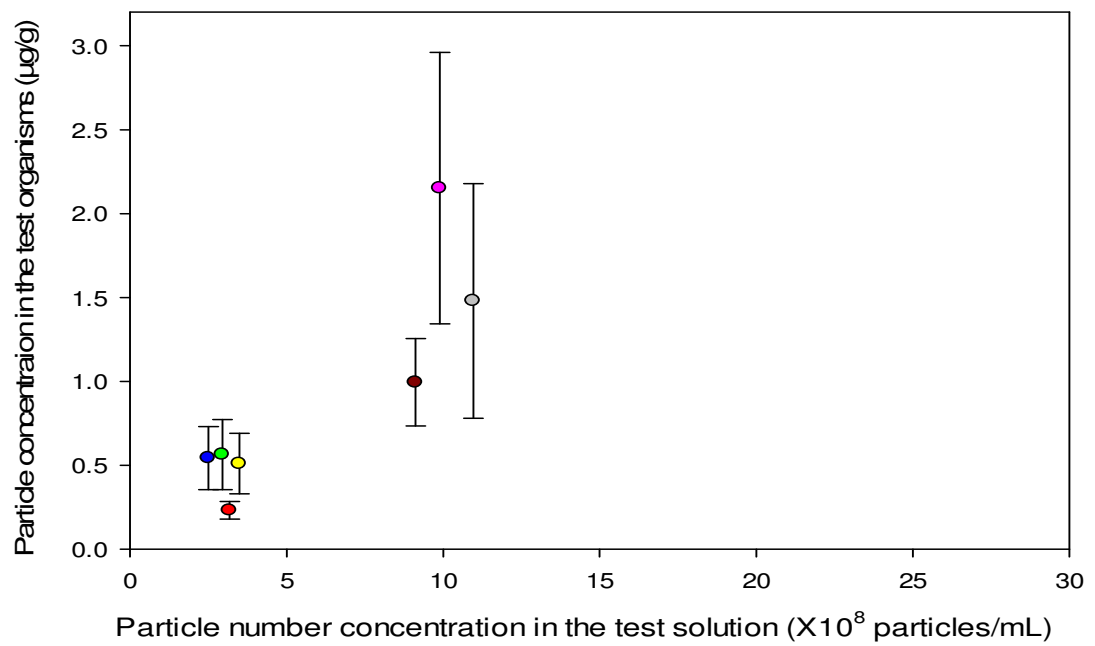
(d) Au-PEG NPs
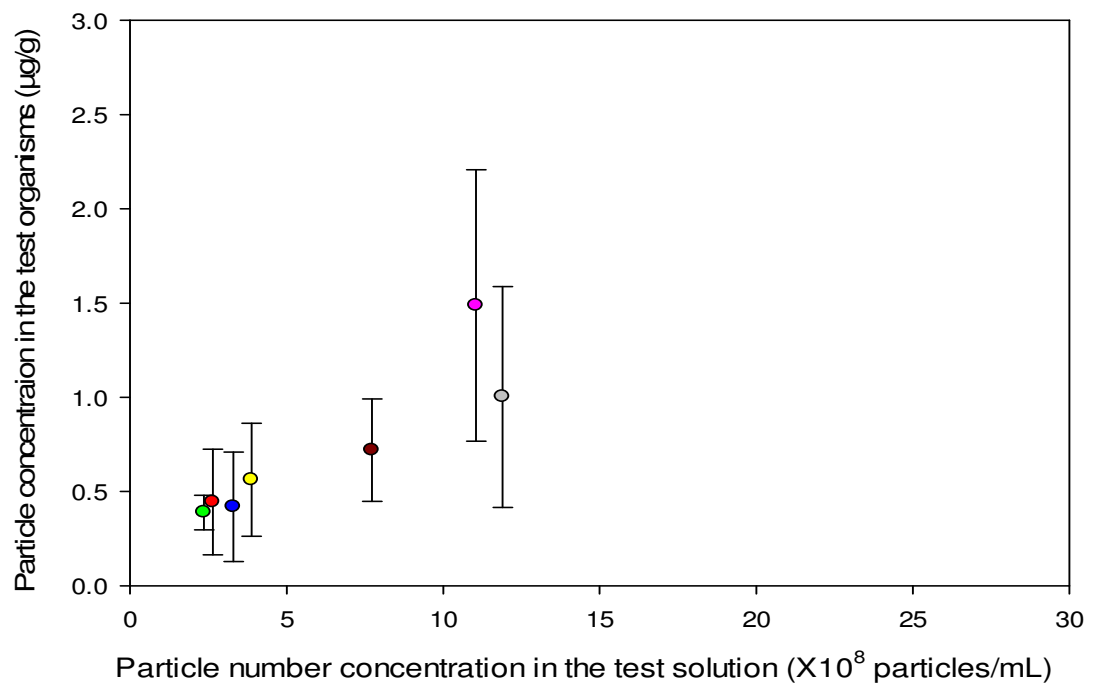
Figure 18. Continued.

Conclusion

This study observed the uptake of Au NPs with various surface functionalisations into aquatic invertebrate, *G. pulex*, from commonly used ecotoxicity test media and a range of natural waters. While, the size of ENPs was found not to be a factor in determining the degree of uptake in *G. pulex* from the test media, the PNC was found to be an important factor with greater uptake of all study NPs seen at the higher PNCs. The results suggest that environmental factors affect behaviour of ENPs in the aquatic environment as well as uptake in aquatic organisms. Previous toxicity or uptake studies of ENPs were performed without considering environmental factors such as water chemistry or NOMs and the risk of ENPs could be over/under estimated. It is therefore important to find and apply appropriate test conditions for the risk assessment of ENPs and to understand the interplay between the chemical, biological and morphological factors affecting uptake of ENPs by organisms.

Chapter 6

General discussion and conclusions

Introduction

The unique properties and new applications of ENPs have contributed to technological and economic growth in industries whose products can be advanced by using materials at the nano- scale. As it is known that ENPs are being released to, and accumulating in, various environmental matrices, the rapid growth of the nanotechnology industry has led to concerns over what risks are posed by ENPs in the environment. Despite much research effort in recent years, at present our knowledge and understanding of the impacts of ENPs on environmental and human health are limited, and many uncertainties remain. The knowledge gaps and these uncertainties make risk assessments and management of ENPs challenging.

For traditional chemical contaminants, the basic components of an environmental risk assessment include a hazard characterization and an exposure assessment. However, the behaviour and flows of ENPs in the aquatic environment are not really considered in exposure assessments due to a lack of data and information. In addition, toxicity data for the effects of ENPs on aquatic organisms are expressed in relation to mass concentration or dose response without considering the potential for ENPs to be transformed in, and interact with, the test solution. Therefore, the main aim of this PhD thesis was to improve our understanding of the behaviour of ENPs in different test solutions and how this affects uptake of ENPs in aquatic organisms. To achieve this

aim, the first priority was to investigate whether ENPs behave differently in standardized test media and natural waters. As differences in the behaviour of ENPs between natural waters and standard test media were found, the next stage was to conduct an aggregation study to determine the factors affecting aggregation, predict stabilization of ENPs in river systems through the UK, and uptake into aquatic organisms. This chapter contains a summary of the interpretation of the results presented in the experimental Chapters, and recommendations for how to take this work forward.

Summary of experimental chapters

The aggregation behaviour of Au nanoparticles with different surface functionalization was investigated in standard ecotoxicity test media and a selection of natural waters collected in Northern England (Chapter 2). Different aggregation behaviours were observed in the different test media, which could be explained by the different surface coatings of the Au nanoparticles. MUDA and citrate coated Au nanoparticles aggregated to form larger particles in most standard test media, especially APW, M4 media, ASW and HW, while positively charged PEG-NH$_2$ and neutral PEG Au nanoparticles did not show significant aggregation in any test media. The aggregation of Au nanoparticles resulted from interactions between the surface coatings and the composition of the test media. The stability of PEG-NH$_2$ and PEG charged Au nanoparticles resulted from the mainly steric repulsion, which exploits entropy to make aggregation unfavourable. Conversely, MUDA and citrate coated Au nanoparticles exhibited the greatest aggregation in test media with higher IS due to electrostatic double layer compression. In the natural water samples, aggregation behaviour of Au nanoparticles was very different with that in standardised test media. Au-MUDA and citrate nanoparticles were stable in most natural waters, while they aggregated in the standardized media. Au-PEG-NH$_2$ and PEG nanoparticles aggregated less in the natural waters than in the standard test media. It is likely that the reason for the differing behaviour of the Au nanoparticles was the higher DOC content in the natural

waters compared to the standard test media. Humic substances adsorbed to the surface of Au-MUDA and citrate nanoparticles, retarding the particle aggregation in natural waters. In the case of Au-PEG-NH$_2$ and PEG nanoparticles, the positive and neutral surface charges were changed to be either a negative or neutral, both of which interact with a number of cations in natural waters, resulting in particle aggregation. The effects of humic acid on stabilisation in natural water corresponded to stabilisation effects of humic acid in the ecotoxicity test media. The results in Chapter 2 highlighted the fact that surface functionalization can be affected by surface charge, which in turn is affected by the way the particle interacts with environmental factors.

The importance of the interaction between environmental factors and surface functionalization on the behaviour of ENPs in the environment raises the question 'how does the core material of particles affect particle aggregation?' This question was addressed in Chapter 3. For this study, the aggregation behaviour of Ag nanoparticles, coated with the same surface coatings (MUDA and citrate) as two of the Au nanoparticles used in Chapter 2, was assessed and the results obtained for the Au and Ag nanoparticles compared. Both Au and Ag nanoparticles showed similar aggregation behaviour and particle attachment efficiency, resulting from interactions of surface functionalization and ionic strength of each test medium. The aggregation of particles was found to be less affected by the core material than by the surface coating in most of the test media.

In Chapter 4, data from Chapter 2 on fate in natural water was used to develop relationships between water parameters and aggregation. Multiple regression equations were developed that were able to estimate sizes of different particles based on a range of environmental variables including pH, DOC and IS. The developed relationships were then used to explore how particle sizes of the Au study particles would vary if they were emitted to water bodies in England and Wales. Ranges of predicted particle sizes were quite large due to variations in water chemistry in different regions of the UK. For example, Welsh natural water tended to have low IS and high DOC content, thus the Au-MUDA nanoparticles were predicted to be stable in this

region (less than 50nm) whereas in areas of England the particles were predicted to have moderate to low stability.

For Au-citrate NPs, 50% of study areas were predicted to have moderately stable particles, and another 50% of areas were predicted to have unstable particles. Au-PEG-NH$_2$ and PEG nanoparticles behaviour was predicted to be geographically much less variable than that of MUDA and citrate coated nanoparticles, which were predicted to be unstable in most study areas.

In Chapter 5, the uptake of the studied Au nanoparticles by the freshwater amphipod *G. pulex* was explored using test media with different water compositions. Using the data collected in the aggregation study (Chapter 2), four standard ecotoxicity test media (APW, M4, MHW and SW) and four natural water samples, collected from four locations in Northern England (the River Etherow, Hob Moor, Bishop Wilton and Helmsley) were applied in the uptake study. Chapter 5 investigated the hypothesis that uptake of Au nanoparticles by aquatic organisms depends on the behaviour of the Au nanoparticles in the test media and natural waters. It was believed that uptake of Au nanoparticles would be different depending on the particle size, which would depend on the extent of aggregation in a particular system. Similar to the findings of Chapter 2, aggregation in the synthetic test media and natural waters, uptake and depuration were found to vary significantly across media types. In terms of uptake, MUDA and citrate coated Au nanoparticles were taken up to a greater extent in test media and natural waters than amino and PEG coated particles. Larger amounts of PEG-NH$_2$ and PEG coated Au nanoparticles were eliminated during the depuration period across all the test media compared with MUDA and citrate coated Au nanoparticles. The particle surface functionalisation and water chemistry were important factors to determine the uptake into *G. pulex.* However, there was weaker correlation between the uptake of the tested Au nanoparticles and the particle size distribution in the test media than surface waters.

Implication for risk assessment of ENPs in the environment

This thesis highlights the fact that the behaviour of ENPs is much more complex than for 'normal' chemicals and that the fate and uptake of ENPs is affected by a range of environmental factors. This complex behaviour therefore means that to establish the environmental risks of ENPs, it will probably be necessary to adopt different approaches for exposure and hazard assessment than used for traditional chemicals. This thesis has highlighted a number of issues that may need to be addressed in the environmental risk assessment process for ENPs. These are discussed below.

Relevance of existing OECD/EPA ecotoxicity testing approaches – Existing approaches recommended by e.g. OECD and EPA for testing the ecotoxicity of chemicals involve the use of surrogate species and standardised exposure media. The results of the work presented in Chapter 2 indicate that the behaviour of ENPs in the standardized media is completely different from the observed behaviour in natural waters. The use of current standardized testing approaches could therefore either over- or under-estimate the ecotoxicity of an ENP to aquatic organisms. Based on the findings of this thesis it would therefore be appropriate to develop alternative standardized test approaches that more readily reflect the behaviour of ENPs in the real environment. It may also be necessary considering developing testing approaches for other species that may be sensitive to ENP exposure.

Testing strategies for ENPs – When assessing the risks of a tradition chemical, ecotoxicity studies are typically performed on one organism type from each of the trophic levels (fish, daphnids and algae) and one media type. The results presented in Chapter 4 show that the behaviour of ENPs across England and Wales can be highly variable depending on the type of particle. An ecotoxicity test in one medium may not therefore provide an indication of how an ENP will impact organisms in different river

catchments. Therefore, when testing an ENP, it may be necessary to perform ecotoxicity studies using a range of media types. These media could be selected depending on the functionality of a particle and using some of the spatial assessment approaches presented in Chapter 4 to give information on the eotoxicity of the range of aggregation states of an ENP that are likely to occur in the system of interest.

Improved assessment of uptake into aquatic organisms – It is known that current approaches for predicting uptake of chemicals into organisms (e.g. use of the Log K_{ow}) are not appropriate for ENPs. Some researchers have suggested that uptake is related to particle size and that this could be a parameter used for risk assessment. This thesis indicates that the size of ENPs was not the principal factor contributing to the increased uptake of ENPs into the organisms tested and that uptake is probably driven by a combination of environmental and particle-related parameters. Much more work is needed on the uptake of ENPs into organisms before we can propose predictive approaches for estimating bioaccumulation as part of the risk assessment process.

Recommendations for future work

While the results in this thesis have provided new knowledge on the behaviour and uptake of ENPs in the aquatic environment, there are still many unknowns. Future work to take the findings of this thesis forward should therefore include:

Further development of models to predict the relationship water parameters and aggregation of ENPs - This thesis showed that the behaviour of ENPs could be estimated based on the water parameters in different water systems. These models should be further developed to include different ENPs sizes and surface functionalities, to allow the effect of ENP concentration to be established and to include other important fate processes such as hetero-aggregation. To do this work, fast and sensitive analytical methodologies will be required.

Further investigation of the core material effects - This study showed the core material of Au and Ag nanoparticles had less effect on aggregation of ENPs than the surface coating. This raises the prospect of developing generalised models for ENP behaviour for different surface functionalities. Before this can be done, it would be interesting to explore a wider range of core materials and surface functionalities.

Development of better datasets on water parameters around the world – In Chapter 4, we attempted to explore how the behaviour of ENPs would vary across the England and Wales landscape. This work was restricted by the availability of data on important water parameters. It would be valuable to begin to develop improved databases on water parameters for river systems around the world.

Development of models for estimating uptake of ENPs into aquatic organisms – The work in Chapter 5 indicates that particle size is not the main drive affecting the uptake of ENPs into aquatic organisms. Further work is needed to understand the actual mechanisms of uptake of ENPs into aquatic organisms and the environmental and particle properties affecting uptake. This work should ultimately aim to develop models for estimating ENP uptake. It would also be beneficial to understand the fate of the ENP within the organism, something that was not considered in this thesis.

Alongside the recommendations specific to this PhD, there are a number of broader recommendations for research that should be done so that we can fully establish the risks of ENPs in the aquatic environment. This work includes:

The development of new methods for performing ecotoxicity tests of ENPs in test media - This thesis has shown that ENPs change form and behaviour depending on aquatic chemistry. It also showed behaviour depends on the surfaces of ENPs in the test solutions. In existing testing guidelines, there are many limitations for assessing

the exact risk ENPs pose in the natural environment. The development nano-specific test systems/protocols is challenging but urgently needed. Any new test protocol should include a consideration of the role that specific physicochemical properties of ENPs play, in tandem with the pH and temperature of the exposure test media. Particle aggregation rates should be accounted for when considering timings for changing test media. The number of ions that dissolve into the test media from nanoparticles, and their behaviour, are important factors to consider, as is the concentration of nanoparticles likely to remain in suspension.

Interaction of ENPs with other pollutants - Most previous studies have investigated the effects of single ENPs on aquatic organisms, and very little information is available on how ENPs interact with other pollutants. When nanoparticles are suspended in natural water, they may come into contact with other pollutants or materials that will influence the fate and bioavailability of both the contaminant and the ENPs. Interactions with other contaminants may exacerbate the toxic effects of both contaminant and ENP to organisms through additive or synergistic mechanisms. The role nanoparticles play in transporting pollutants into aquatic organisms needs further investigation.

The development of a model to predict exposure of ENPs in aquatic systems - Detecting or measuring ENPs is difficult owing to ineffective analytical methods or complex properties of ENPs, but it is necessary to predict potential risk in the aquatic environment. Due to lack of monitoring capabilities, it is important to develop exposure models to predict the potential exposure risk. To evaluate the potential risk of ENPs to environment, the model should be able to predict concentration or quantity of ENPs, since concentration is directly linked to potential ecotoxicological effects. Furthermore, the model should be developed based on a relevant subset of properties of ENPs, including physico-chemical properties (size, size distribution, and surface reactivity), aggregation or sedimentation and possible interactions with environmental factors. It is

also imperative to consider environmental conditions arising from local geographic variation.

Uptake effects of ENPs through aquatic food chain - The uptake study using G. pulex in this thesis showed uptake effects after exposure with no elimination. The result implies that nanoparticles may move through the food chain if the organism were taken up by higher organisms. The food chain is an important system in any ecosystem, and when it is disrupted there can be drastic effects for the entire system. Nevertheless, investigating dietary uptake by predator-prey interactions and the potential migration of ENPs in the aquatic food chain have rarely been studied. We now need to develop a thorough understanding the potential effects of ENPs when they penetrate and accumulate in the body, biotranformation and migration along food chain.

Theoretically, by addressing these areas for future research it will be possible to quantify the risks ENPs pose in the environment with greater certainty than is possible at present.

Appendix 1

Visualization and characterization of engineered nanoparticles in complex environmental and food matrices using atmospheric scanning electron microscopy

P. LUO*, I. MORRISON†, A. DUDKIEWICZ*,‡, K. TIEDE‡,
E. BOYES§, P. O'TOOLE†, S. PARK* & A.B. BOXALL*

Environment Department, The University of York, Heslington, York, UK

†*Department of Biology, The University of York, Heslington, York, UK*

‡*Ecological Chemistry, The Food and Environment Research Agency, Sand Hutton, York, UK*

§*York JEOL Nanocentre, Science Park, The University of York, Heslington, York, UK*

Summary

Imaging and characterization of engineered nanoparticles (ENPs) in water, soils, sediment and food matrices is very important for research into the risks of ENPs to consumers and the environment. However, these analyses pose a significant challenge as most existing techniques require some form of sample manipulation prior to imaging and characterization, which can result in changes in the ENPs in a sample and in the introduction of analytical artefacts. This study therefore explored the application of a newly designed instrument, the atmospheric scanning electron microscope (ASEM), which allows the direct characterization of ENPs in liquid matrices and which therefore overcomes some of the limitations associated with existing imaging methods. ASEM was used to characterize the size distribution of a range of ENPs in a selection of environmental and food matrices, including supernatant of natural sediment, test medium used in ecotoxicology studies, bovine serum albumin and tomato soup under atmospheric conditions. The obtained imaging results were compared to results obtained using conventional imaging by transmission electron microscope (TEM) and SEM as well as to size distribution data derived from nanoparticle tracking analysis (NTA). ASEM analysis was found to be a complementary technique to existing methods that is able to visualize ENPs in complex liquid matrices and to provide ENP size information without extensive sample preparation. ASEM

Correspondence to: Ping Luo, Environment Department, The University of York, Heslington, *York YO10 5DD, UK*. Tel.: 0044-1904-462000 (ext 3538); fax: 0044-1904-322998; e-mail: ping.luo@live.cn.

images can detect ENPs in liquids down to 30 nm and to a level of 1 mg L^{-1} (9×10^8 particles mL^{-1}, 50 nm Au ENPs). The results indicate ASEM is a highly complementary method to existing approaches for analyzing ENPs in complex media and that its use will allow those studying to study ENP behavior *in situ*, something that is currently extremely challenging to do.

Introduction

As a result of the increase in the usage of engineered nanoparticles (ENPs) in every day products, there are growing concerns about the safety of ENPs to humans and the environment (Hristozov & Malsch, 2009). A large number of studies have and are being performed to assess the risks of ENPs in the environment and food to human and ecological health (Green & Ndegwa, 2011). In order to understand levels of exposure in the environment and food stuffs and the mechanisms driving toxicity of ENPs, precise characterization of the concentrations and properties of the ENPs in their respective media is essential, which unfortunately remains a significant challenge (Tiede *et al.,* 2009a; Boxall *et al.,* 2007; Liu *et al.,* 2012). Although conventional analytical methods, e.g. inductively coupled plasma mass spectrometry (ICP-MS) and atomic absorption spectroscopy (AAS) and light scattering techniques have been commonly used in the analysis of ENPs (Tiede *et al.,* 2009b; Gillespie, Halling, & Edwards, 2011), these techniques only provide information on mass concentrations and/or particle size distributions of ENPs. They do not however provide information on e.g. the morphology of ENPs.

Morphological information can be obtained using image-based approaches such as electron microscopy (Dudkiewicz *et al.*, 2011). In combination with methods for elemental analysis, e.g. energy dispersive X-ray spectroscopy (EDS), conventional electron microscopy can allow visualization of ENPs within a sample and can provide information on the chemical composition of the ENPs (Tiede *et al.*, 2008; Lorenz *et al.*, 2010). The vacuum environment inside the microscope chamber however dictates that samples usually need to be prepared in such a way that they are in a dry or solid state. This necessity can introduce artefacts during drying processes leading to erroneous results (Blasco & Picó, 2011). These artefacts can be avoided by e.g. using cryogenic preparation methodologies or wet scanning electron microscopy capsules (wetSEM; e.g. Tiede *et al.*, 2009b) or by the application of other imaging technologies such as environmental scanning electron microscopy (ESEM; e.g. Gatti *et al.*, 2008). However, cryogenic preparation is very time-consuming, ESEM does not work at 'real' atmospheric pressures which is very important for environmental studies, and the electron-transparent polymer QuantomiX capsule film used in wetSEM is vulnerable to electron beam damage (Tiede *et al.*, 2009b) and introduces the sample in an inverted scenario thus making sedimentary material difficult to image.

Due to the challenges around analysis of ENPs in complex media, and the limitations of different available methods, most researchers recognize that a suite of methods needs to be applied to a sample in order to produce useful data. Here we demonstrate a relatively new approach, atmospheric scanning electron microscope (ASEM), which is an instrument offering scanning electron imaging at atmospheric pressure. The use of a silicon nitride (SiN_x) membrane in the ASEM dish has drastically improved the stability of the sample enclosure when compared with the QuantomiX WetSEM capsule. It prevents the moisture from leaking into the vacuum chamber, is electron transparent, and it is stable up to $150°C$ in aqueous samples (Suga *et al.*, 2011).

An added advantage is that the system uses an inverted column, thus the samples are imaged from below. This allows for imaging of sedimentary materials. ASEM can therefore minimize artefacts introduced by sample preparation while avoiding some of the limitations and undesired sample handling problems associated with ESEM and WetSEM. So far, the method has been successfully used to visualize cell structure and nuclei (Nishiyama *et al.*, 2010), mycoplasma (Sato *et al.*, 2012), nitrate solution, silver paste, solder paste and the self-organization process of particles (Suga *et al.*, 2011). However, to the best of our knowledge, it has not yet been applied in the nanosafety research area. This study therefore investigated the application of ASEM to a range of environmental and food matrices and a range of ENPs. The results were compared to results obtained using TEM, SEM and nanoparticle tracking analysis (NTA) to evaluate the advantages and disadvantages of the method.

Methods and material

Study ENPs

Mercaptoundecanoic acid coated (MUDA) Au ENPs, with a nominal diameter of 30 nm, were obtained from Dr Jon Veinot at the University of Alberta (Edmonton, Canada). Citrate coated Au ENPs, with a nominal diameter of 50 nm, were purchased from BBInternational (Cardiff, UK; batch no. 10836). Titanium dioxide (TiO_2) nanopowder was purchased from Sigma Aldrich (UK, lot no. 637254, nominal diameter <25 nm). Spherical silica ENPs in dispersion were provided by AZ Electronic Material France SAS (Klebosol 30R50, nominal diameter 80 nm, concentration 29–31% w/w).

Study matrices

The natural sediment was selected to meet the criteria described in OECD guideline 106 (OECD, 2000) for sediment ecotoxicity testing and was collected from the river Derwent at Buttercrambe, York, UK (54° 0′59.04″ N, 0° 52′ 52.67″ W). The natural sediment had a pH value of 7.67, a composition of 4.2% clay (<2 μm), 2.8% silt (2∼50 μm) 93% sand (>50 μm). Elendt M4 Daphnia culture medium was prepared according to OECD guideline 211 (OECD, 1998). Elendt medium is mainly used to culture *Daphnia magna* for ecological tests and is composed of various trace elements, macronutrients and vitamins. Tomato soup was obtained from Dr Thomas Linsinger and Dr Ringo Grombe at the Joint Research Centre (Brussels, Belgium). The tomato soup was prepared as a reference material under laboratory conditions for further ENPs fate studies. Bovine serum albumin (BSA) powder was purchased from Sigma Aldrich (UK); 10 g L^{-1} BSA made up in water is commonly used to stabilise nanoparticles for cell culture studies. Polylysine solution (P8920) and dextran-500 (31392) for ASEM dish treatment were obtained from Sigma Aldrich (UK).

Characterization of ENPs in stock solutions and environmental and food matrices by ASEM and other techniques

Stock dispersions of the MUDA and citrate coated ENPs were characterized by ASEM, FEG-SEM, TEM and NTA. ASEM, TEM and NTA were also applied to visualize citrate Au ENPs in the supernatant of natural sediment and in M4 medium; TiO_2 ENPs in BSA; and SiO_2 particles in tomato soup. An overview of the particle-matrix combinations that were characterized, the analytical approaches used and the concentrations of particles applied is given in Table 1.

ASEM Imaging

ASEM imaging was performed using a JEOL JASM-6200 ClairScope. The ClairScope consists of an upright optical

Table 1. Overview of the particle-matrix combinations that were characterized, the analytical approaches used and the concentrations of particles applied.

Nominal diameter	30 nm	50 nm	50 nm	50 nm	<25 nm	80 nm
Core	Au	Au	Au	Au	TiO_2	SiO_2
Coating material	11-MUDA[*1]	Citrate acid	Citrate acid	Citrate acid	n.a.	n.a.
Supplier	Edmonton, Canada	BBI, UK	BBI, UK	BBI, UK	Sigma Aldrich, UK	Sigma Aldrich, UK
Matrix	Stock	Stock	Daphnia medium	Natural sediment	BSA	Tomato soup
Mass [con]	40 mg L^{-1}	50 mg L^{-1}	50 mg L^{-1}	50 mg L^{-1}	n.a.	n.a.
Applied techniques	ASEM, TEM, NTA, FEG-SEM	ASEM, TEM, NTA, FEG-SEM	ASE, TEM, NTA	ASEM, TEM, NTA	ASEM, TEM, NTA	ASEM, TEM, NTA
Pre-treatment	n.a.	n.a.	$V_{ENPs}:V_{medium} = 1:3$ leave for 0.5 hr	$M_{ENPs}:M_{sedi} = 4:1$ leave overnight	10×10^3 mg L^{-1} of TiO_2 in BSA	2×10^3 mg L^{-1} of SiO_2 in tomato soup
ASEM	Step 1. add 200 μL of 0.01% w/v poly-L-Lysine solution to the ASEM dish for 10 min then washed with DI water					
	Step 2. add 500 μL sample to ASEM dish[*2, 3]					
	Step 3. add 500 μL glutaraldehyde (this step only was applied to 30 nm AuMUDA)					
	Step 4. add 500 μL dextran 500 (20 g L^{-1})					
FEG-SEM	Dry in an oven at 50 °C over night	n.a.	n.a.	n.a.	n.a.	
NTA	200 times dilution in water	n.a.	[*4]	100× in water	5000× in water	
TEM	Step 1. coat formvar-carbon coated copper grids with 0.01% w/v poly-L-Lysine solution					
	Step 2. add 5 μL of the sample onto the treated grid, the excess moisture was blotted off using filter paper[*5].					

Note: [1] 11-MUDA, 11-mercaptoundecanoic acid.

[2] The TiO_2 ENPs in BSA solution were mixed with glucose solution in the volume ratio of 1:2 to reduce the beam damage to the BSA.

[3] Only the supernatant of the ENP-sediment system was imaged.

[4] Prior to ENPs dispersion, the sediment was pre-treated by vacuum filtration (11 μm filter pore size). After ENP spiking, the sample was centrifuged (rcf = 2000g, 2500 rpm × 5 min, Hermle Z 513K). The supernatant was sampled and further diluted with water for 100 times (HPLC fluorescence grade water, Fisher scientific, UK).

[5] The ultracentrifugation of the ENPs in the supernatant of sediment onto TEM grids was performed on a Beckman XL-100 ultracentrifuge (Beckman, California) with a SW40Ti swing bucket rotor and polymer tubes, at 20°C for 1 h, with rcf = 100×10^3 g and $\omega = 128 \times 10^3$ rpm.

microscope (OM, not used in this study) and an inverted SEM with the specimen in a thin-film windowed dish, in the observation chamber under atmospheric conditions. The dishes are produced by depositing a 100 nm SiN_x film on a silicon substrate, etching the under-surface to leave a 250 μm square window, and inserting the chip into the base of a 35 mm diameter cell culture dish (Nishiyama *et al.*, 2010). The high-energy electrons travel through the SiN_x film of the open dish to interact with the specimen and backscattered electrons (BSE) are detected in the vacuum chamber to construct a SEM image of the specimen. An optical image can be taken by OM from the other side of the specimen. The ASEM was operated at 30 kV acceleration voltages and 30 spot size (8 nm beam diameter, Nishiyama *et al.*, 2010). This spot size was selected based on a compromise between the resolutions, signal to noise and heating. Larger spot sizes can provide more signal but at risk of reduced resolution and increased heating which would shorten the ASEM dish lifespan.

Prior to imaging, 200 μL of 0.01% w/v poly-L-Lysine (Sigma-Aldrich P8920, diluted 10-fold) solution was added to the ASEM dish to give a positive charge for better adhesion of the negatively charged ENPs (Table 1, Ramachandran *et al.*, 1998; Tiede *et al.*, 2009b). The positively charged poly-L-Lysine can properly neutralize the surface charge on the ASEM film window. The poly-L-Lysine was removed after 10 min, and the dish washed with pure water. This coating can be omitted if a neutral ASEM dish is required. Approximately 500 μL of each sample was then added to the centre of the ASEM dish and left to settle at room temperature for approximately 10 min. Sample preparation was completed by adding 500 μL of dextran 500 (20 g L^{-1}) on the top of the sample. The dextran acted as a free radical scavenger thus reducing the damage to the SiN_x membrane.

Scanning Electron Microscopy (SEM)

For SEM imaging, the same specimen as used in the ASEM was deposited on a silicon slab, allowed to dry in an oven (50°C) over night and was then imaged using a JEOL 7500F field emission gun-SEM (FEG-SEM) at 5.0 kV acceleration voltage and at a 4.3 mm working distance.
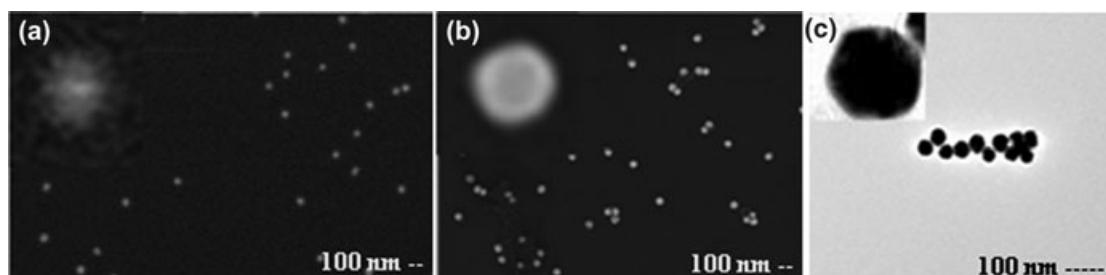
Fig. 1. Images of nominal 50 nm BBI Au obtained from ASEM (a), FEG-SEM (b) and TEM (c). Analysis showed that TEM, which has a greater resolution than ASEM and FEG-SEM gives the smallest mean particles size for a sample. Magnified images of single particles are presented in the top left corner of each image.

Transmission Electron Microscopy (TEM)

TEM images were acquired by a JEOL JEM-2010 microscope (200 kV) which was fitted with an energy dispersive X-ray spectrometer (EDS, Oxford Instruments, UK). Formvar-carbon coated copper grids (S162–4, Agar Scientific, UK) were coated with 0.1% w/v poly-L-Lysine solution (P8920, Sigma-Aldrich) to enhance the attraction of negatively charged particles. Dispersed ENPs (5 μL) were then applied to the copper grids and the excess moisture was blotted off with filter paper.

To increase the number of ENPs being visualized in the supernatant of natural sediment, ultracentrifugation, was applied to increase particle number concentration and hence improve imaging of particles. The ultracentrifugation was performed on a Beckman XL-100 ultracentrifuge (Beckman, California) with a SW40Ti swing bucket rotor and polymer tubes, at 20°C for 1 h, with rcf = 100×10^3 g and $\omega = 128 \times 10^3$ rpm. ENPs accumulated on the TEM grid located at the bottom of the centrifuge tube, with a flat bottom support of Agar 100 resin (Agar Scientific, UK).

Nanoparticle Tracking Analysis (NTA)

NTA was performed to monitor the ENP size distribution in liquid using a Nanosight-LM10 (NTA, Nanosight, UK). In order to meet the NTA ideal number concentration requirement ($1\sim25\times10^8$ particles per mL solution), samples were prepared differently. Stock solutions of the MUDA and citrate coated ENPs, TiO_2 ENPs in BSA and SiO_2 particles in tomato soup were further diluted in water prior to the analysis. A more extensive pre-treatment was carried out on the Au ENPs in natural sediment; the natural sediment was firstly treated by vacuum filtration (11 μm filter pore size). After mixing with ENPs, the ENP-sediment sample was centrifuged (rcf = 2000g, 2500 rpm × 5 min, Hermle Z 513K). The supernatant was sampled and further diluted (100 times) with water (HPLC fluorescence grade water, Fisher scientific, UK) for NTA analysis.

After sample preparation, 0.3 mL of each sample was injected into the NTA chamber using a BD Plastipak syringe (2 mL, lot number 300185, Spain) and 60 sec videos (frames per second = 60, viscosity = 0.95 at 22°C,

640 × 480 resolutions) were recorded. Videos were analyzed using NTA software 2.0 by calculating the sphere equivalent hydrodynamic diameter of each single particle via the Stokes-Einstein equation (Gillespie *et al.*, 2011).

Image Analysis

All the images acquired by TEM, ASEM and FEG-SEM were then analyzed by the eCognition Architect software (version 8.7) which has implemented solutions designed specifically for ENP characterization developed as part of the EU-FP7-funded project "Nanolyse". It is an object-based analysis software (OBIA), which groups pixels of the objects basing on color and shape (Blaschke, 2010; Tiede *et al.,* 2009c, 2010). Three representative images were collected from each sample. Each sample includes more than 50 particles that were measured for the mean equivalent circle diameter.

Result and discussion

Capability of ENP size measurement using ASEM

Images of the 50 nm Au ENPs were acquired by ASEM, FEG-SEM and TEM (Fig. 1). As expected, analysis showed that TEM, which has a greater resolution than ASEM and FEG-SEM gives the smallest mean particle size for a sample. The three methods all provide useful information for studying ENPs with various advantages and disadvantages. The ASEM images, seen in the top left corner, enables the samples to be simply imaged without any sample processing and while the ENPs are in their natural environment. However, the images of the ENPs in the ASEM appear blurry and the periphery lacks definition. This is because the electron beam scattering is broadened in solution and the electrons are absorbed during the pathway to and from a particle in a sample. Electron backscattering depends on the thickness of the scattering material, and thus differs between the centre and edge of the object. Moreover, Monte Carlo simulation shows that electron backscattering also depends on the location depth and the size of Au particles (Däbritz, Langer & Hauffe, 2001). Therefore, the beam broadening affects both the particle size and shape measurement.

Fig. 2. Imaging of the smallest ENPs by ASEM in this study. The smallest round Au ENPs (a) detected by ASEM is 30 nm Au stock solution. The size of smallest irregular shaped TiO$_2$ aggregates (b) detected in BSA is 80 nm.
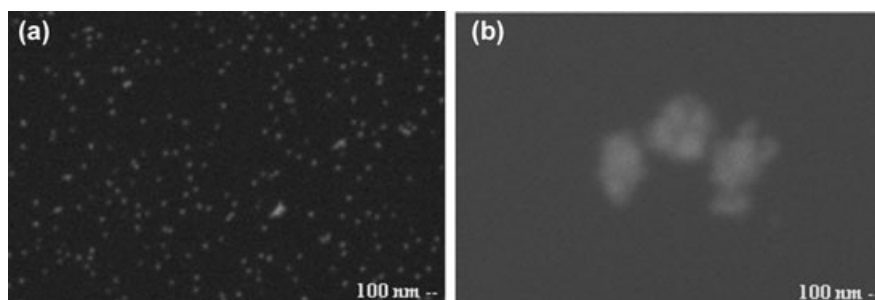
ASEM images showed an image size of 66 ± 6 nm, which is significantly larger ($p < 0.05$) than the ones acquired by the FEG-SEM (50 ± 6 nm), conventional TEM (41 ± 3 nm) and NTA (60 ± 39 nm, as shown in Fig. 3c). The difference between the NTA measurements and the TEM and SEM measurements are probably explained by the fact that NTA measures the hydrodynamic particle diameter whilst SEM and TEM detects the size of dry particle (Gittings & Saville, 1998).

The difference between FEG-SEM and TEM are probably due to the fact that high resolution FEG-SEM employs the secondary detector to acquire the image via detecting low energy secondary electrons ($\leq$50 eV, Goldstein *et al.*, 1981), primarily providing information on surface topology. Hence, both the core and coating material of the ENPs are imaged by FEG-SEM at 5 kV accelerating voltage. In a TEM, image acquisition is achieved by transmitted electrons. The core of the ENPs, Au, appears dark in the image whilst the shell regions (surface coating) of the ENPs appear grey or bright and the background appears bright at 200 kV (Fig. 1). Therefore the size of the core material and coating measured by FEG-SEM is larger than the size of the core measured by TEM.

The enlarged size measured by ASEM may be due to a range of different factors. The dominant factor is thought to be the increased electron scattering at the window and in the liquid environment, both to the incoming beam and in the BSE. Improved size measurement results could probably be obtained by deconvolution of these processes. However such estimation of particle sizes obtained from SEM in an aqueous medium behind a SiN$_x$ window is a complex problem that is beyond the scope of this study. Another reason may be that the particles in liquid are able to undergo small movements which would reduce the image resolution. Similar conclusions were made by Tiede *et al.* (2009b) when using Quantomix capsules (WetSEM) in a conventional SEM to image ENPs under fully liquid conditions.

Optimising detection of ENPs

Size detection limit. Figure 2(a) shows the smallest Au ENPs detected by ASEM is 30 nm Au stock solution. The size of smallest TiO$_2$ aggregates detected in BSA is 80 nm (Fig. 2b) although TEM imaging suggests that the TiO$_2$ aggregates are down to $\sim$30 nm (not shown). The detection limit might be improved through changes in the beam diameter and in sample preparation.

As illustrated in 'Capability of ENP size measurement using ASEM' section, electron beam broadening at the membrane and in the liquid are major factors in determination of particle size. The electron beam broadening effect is dependent on the beam diameter, sample preparation, film thickness of the ASEM dish, the operating voltage and current (Suzuki *et al.*, 2007). Theoretically, small beam diameter will enhance the electron interaction with the unit area of target sample, will limit the electron beam broadening effect, and ultimately will improve the size detection limit.

Sample preparation is another determinant of electron beam broadening. The effect of beam scattering can be minimized by using a short electron travel path. It is crucial to attract the ENPs close to the SiN$_x$ film (3 μm). This is a key advantage of the ASEM over wetSEM where in ASEM gravity permits ENPs to settle on the surface of the SiN$_x$ membrane, whereas the particles need to be physically attracted to the membrane used in wetSEM where the membrane is presented facing upwards. However to minimize movement of the particles whilst being examined, the SiN$_x$ was also charged. On the ASEM dish, the behavior of ENPs under the electron beam is determined by the competition between different forces. One is the attractive force between the SiN$_x$ membrane and ENPs, e.g. the ASEM dish was coated with positively charged poly-L-Lysine to attract the negatively charged ENPs (Ramachandran *et al.*, 1998; Tiede *et al.*, 2009b). The other force is the dispersive force of the ENP that is caused by Brownian motion, charging or thermal effects (Suga *et al.*, 2011) and the bonding force between each ENP. In this study, only a few of nominal 30 nm Au ENPs which were coated with 11-mercaptoundecanoic acid (11-MUDA) were observed using ASEM under liquid conditions. The negatively charged ENPs quickly drifted away from the position of the focused beam. Interestingly, this agrees with the phenomena reported by Suga *et al.* (2011), where the positively charged silica particles gathered toward the SiN$_x$
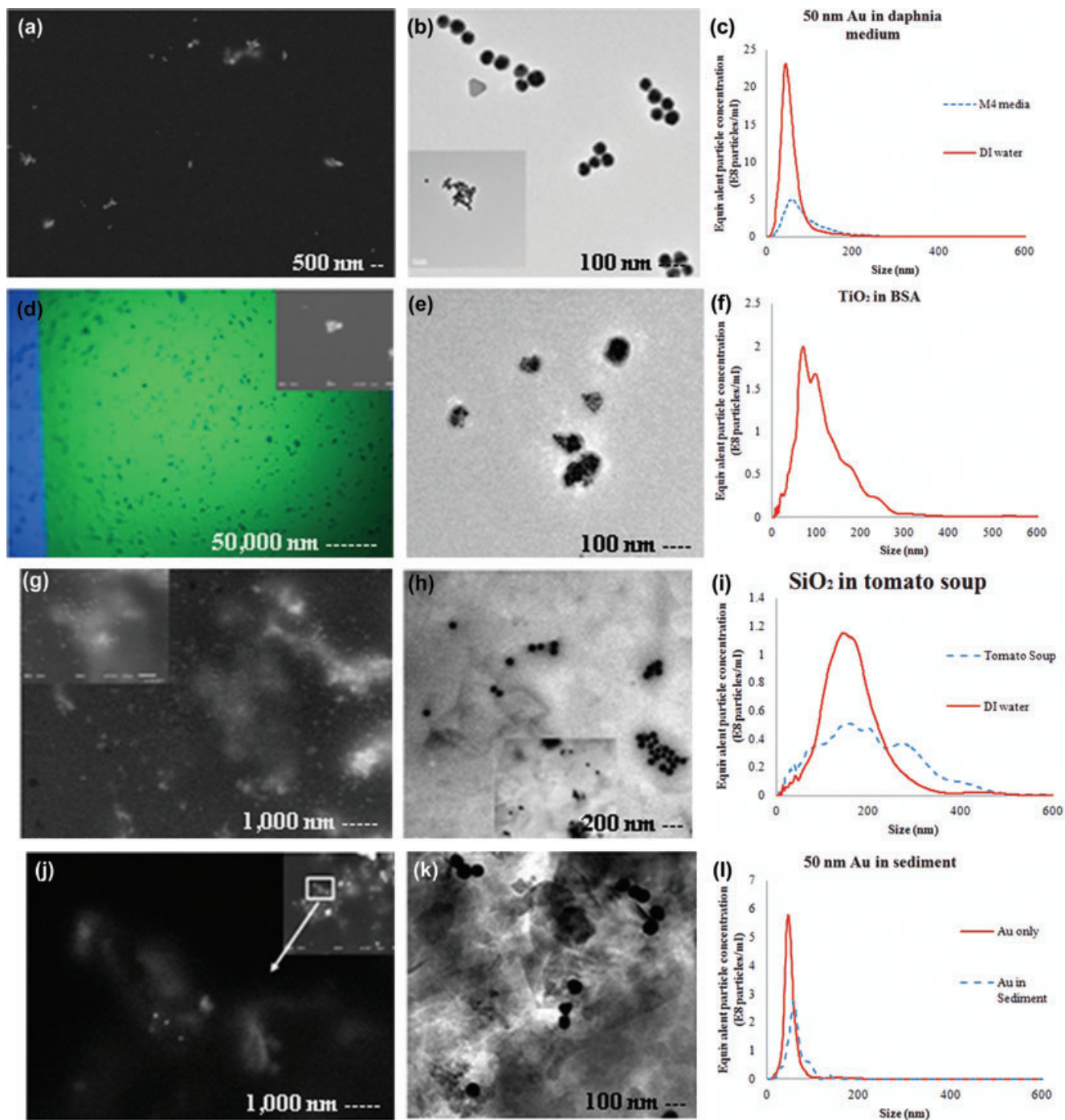
Fig. 3. Size distribution of ENPs in different sample matrices were acquired by ASEM, TEM and NTA, respectively (Fig. 3a–i). Large Au agglomerates in Daphnia culture medium is shown in the ASEM images due to the effect of gravity (Fig. 3a–c). ASEM shows the large TiO_2 aggregates in BSA which have been missed by TEM and NTA (Fig. 3d–f). The measurement of SiO_2 in tomato soup using ASEM (Fig. 3g) is slightly more difficult than TEM (Fig. 3h) and NTA (Fig. 3i) due to the low density. TEM images (Fig. 3k) mainly show Au agglomerates in sediment while ASEM images indicate that the Au ENPs associate with the natural sediment as singlets (Fig. 3j) which agrees with NTA data (Fig. 3l, 62 ± 21 nm)

film at the focus of the beam. Suga *et al.* (2011) explained that, the total sum of the secondary and BSE emitted from the SiN_x film is less than the total incident electrons which creates a potential difference in the water. This potential difference can attract the positive charged ENPs (e.g. Silica) while repel the negatively charged ENPs, e.g. 11-MUDA coated Au ENPs. If this repulsion force plus the dispersive force is weaker than the attraction force between the ENPs and ASEM dish, the

ENPs would be stable in the liquid and images of the ENPs can be obtained. The imaging of these 30 nm Au ENPs was highly improved by further treatment with glutaraldehyde. The covalent binding force between the glutaraldehyde (ENPs coating) can overcome the repulsion force and bring ENPs close to the SiN$_x$ film (Fig. 2a). Another example is when Au ENPs are immobilized by an external matrix, e.g. by fixing in biological cells, then much smaller particles can be detected (<30 nm, C.L. Dennison, private communication). It is relatively straightforward to image 20 nm particles although the signal to noise of particles is lower and the precision of the size determination is correspondingly worse.

The operating voltage and film thickness of the ASEM dish, which controls the number of electrons and their path length through the film-windowed SiN$_x$ ASEM dish, can play a role on the beam broadening. Generally the higher the voltage, the more electrons would hit the sample and minimize the broadening effect. Nishiyama *et al.* (2010) imaged 15 nm colloidal Au in liquid state through various SiN$_x$ membranes, i.e. 150 nm, 100 nm and 30 nm at various accelerating voltages (20 and 30 kV). They suggested that the combination of 30 nm SiN$_x$ film with higher voltage (30 kV) produced more sharply defined particles and the measured particle diameter is closer to the real value. However, 100 nm SiN$_x$ film deposited ASEM dishes were used in this study since it offers a reasonable resolution and a longer lifetime than 30 nm film. All the specimens in this study were imaged at 30 kV. Therefore, the observable particle size is small when the beam diameter is small, acceleration voltage is high, when the film is thin, when the distance between the target and film is small.

The dose of the generated signal depends on the acceleration voltage and spot size, target atomic number, density, size and shape. Backscattered imaging at low accelerating voltages and large spot size (high current) results in enhanced specimen surface contrast and detail since the primary electrons penetrate less deep into the target and generate BSE closer to the original irradiated area (Richards *et al.*, 1999). The backscattering image contrast is reflecting the atomic number of the specimen composition. Therefore more BSE will be acquired with Au ($Z_{Au} = 79$) than for low atomic number samples such as Ti ($Z_{Ti} = 22$) (Nishiyama *et al.*, 2010). Figure 3(a) and (j) show the images of the nominal 50 nm Au ENPs in Daphnia culture medium and an extract of natural sediment, respectively. The presence of sand/organic matter in the sediment influenced the visualization of the Au ENPs. The greater the differences between the atomic numbers of the target object and sample matrix, the better the quality of images that can be obtained from ASEM, e.g. a dried sample is better than a wet one, a purified sample matrix is better than a crude one.

In addition, the size of signal generation area also depends on the size and shape of the sample. The minimum observable size of sphere particles (e.g. 30 nm Au ENPs) is smaller than the irregular shape of aggregates (e.g. 80 nm TiO$_2$). Therefore,

the observable size is small when the acceleration voltage is low, the spot size is big, the atomic number and density of the sample is high and the sample shape is sphere. This explains smaller particle size was measured on spherical Au ENPs (30 nm) than the TiO$_2$ aggregates (80 nm).

Minimum particle number concentration

To achieve the ideal particle number concentration range for the ASEM imaging, theoretical calculations based on the experimental data were employed. Figure 1a shows an image of 5 μL of nominal 50 nm Au ENPs (50 mg L^{-1}), which is equivalent to 4.5×10^{10} particles mL^{-1}. About 50 ENPs are visible on the dish film at 50,000$\times$ nominal magnification and spot size 30. Assuming that the ideal particle number in an image for statistical analysis is between 5 and 100 particles, the ideal sample concentration for 50 nm Au ENPs would be 5–100 mg L^{-1} with a corresponding particle number concentration of 4.5×10^9–9×10^{10} particles mL^{-1} at the same magnification (50 k).

Evaluation of ASEM imaging for a range of ENPs in different sample matrices

Au ENPs in Daphnia culture medium

The elongated shape of agglomerated Au ENPs (nominal size of single ENP = 50 nm) was observed by ASEM after spiking into Daphnia culture medium for 20 min (Fig. 3a). Analysis by e-Cognition showed that the size of agglomerates was 230 ± 102 nm. This size measurement differed from results obtained by TEM imaging (85 ± 17 nm, Fig. 3b) and NTA (97 ± 73 nm, Fig. 3c). NTA analysis also showed that, after being spiked into Daphnia culture medium for 20 min, the hydrodynamic size of the ENPs increased from 60 ± 39 nm to 97 ± 73 nm along with an increased number of bigger particles (100 nm to 150 nm, Fig. 3c). It seems that ASEM indicates a larger size of agglomerates than TEM. This is possibly due to the fact that large agglomerates are easily to be seen under the effect of gravity.

TiO$_2$ ENPs in BSA solution

Results were obtained for the TiO$_2$ ENPs in BSA solution using similar methods. One of the ClairScope OM images of the TiO$_2$ ENPs (nominal <25 nm) in BSA is shown in Figure 3d (430$\times$), with an insert showing the electron image. All the TiO$_2$ ENPs were observed as round firm aggregates with the size of 3822 ± 700 nm. The large aggregates are about 6 μm across while the small aggregates are down to $\sim$80 nm. Only small aggregates were found by TEM imaging (127 ± 74 nm, Fig. 3e) and NTA (123 ± 75 nm, Fig. 3f). Various scenarios might contribute to these differences. First, NTA is incapable of detecting particles >1000 nm (Gillespie *et al.*, 2011). Second,

dilution (in deionized water) required by NTA might separate the agglomerates to constituent particles. NTA measurement of TiO$_2$ sample was performed in DI water due to the existence of large number of particles in the BSA solution. This indicates another drawback of NTA; it is unable to differentiate the target ENPs from other particles contained in the matrices. Third, the sample preparation required by TEM imaging (e.g. transferring with a pipette or blotting with filter paper) might lose the large agglomerates/aggregates. Larger particles are more likely to be lost if any part of the particles can be washed away from the grid surface during dry blotting. This is because, comparing with the smaller particles, the large ENPs have the lower surface-to-volume ratio and subsequent weak electrostatic attraction of particles toward the TEM grid. Lastly, the electron beam in ASEM might trigger the agglomeration/aggregation of ENPs in solution (Suga *et al.*, 2011), although at the used concentrations this is thought to be a low probability.

The main findings from the TiO$_2$ analysis are: (i) the nominal <25 nm TiO$_2$ nanopowders have been agglomerated into 80 nm $\sim$ 6000 nm particles after being dispersed into BSA. (ii) TEM and NTA overrated the small aggregates (up to 500 nm) whilst ASEM can provide a broad overview of the whole population ranging from nano to micro scale although it slightly overrated the large aggregates due to the effect of gravity. (iii) ASEM can provide a clear image of ENPs in a cloudy matrix which is incompatible with the NTA.

SiO$_2$ ENPs in tomato soup

The spherical SiO$_2$ ENPs were observed in tomato soup by ASEM imaging (Fig. 3g, 579 $\pm$ 370 nm). The bright cloud from the images (seen as arrow in Fig. 3g) may correspond to the loosely packed agglomerates in TEM images (Fig. 3h, 84 $\pm$ 15 nm). The large agglomerates observed by ASEM were a few μm in size, whereas the large agglomerates measured by TEM images were only about 600 nm in size. NTA showed the mean value of 126 $\pm$ 109 nm with the exception that a few agglomerates measured between 550 and 1000 nm in size. The explanation of the size differences between ASEM, TEM and NTA is similar to that given in 'TiO$_2$ ENPs in BSA Solution' section. Nevertheless, the measurement of SiO$_2$ ENPs (Fig. 3g) using ASEM is slightly difficult than TEM (Fig. 3h) and NTA (Fig. 3i) due to the low density.

Au ENPs in an extract of natural sediment

50 nm nominal size Au ENPs were imaged in an extract of natural wet pond sediment for the first time (Fig. 3j). The Au ENPs associated with the natural organic matter in the supernatant of the sediment as single particles. The size of the single ENPs in the extract was as 81 $\pm$ 3 nm, which is slightly larger than the size of the single Au ENPs measured in stock (66 $\pm$ 6 nm, Fig. 1). This is possibly due to the lower signal to noise of the ENP images as shown in section

of minimum particle number concentration. Regarding the size distribution of ENPs in the sediment, TEM images (Fig. 3k) mainly show agglomerates, ASEM images indicate that the Au ENPs associate with the natural sediment as singlets which agrees with NTA data (Fig. 3l, 62 $\pm$ 21 nm)

Advantages and limitations of ASEM

ASEM offers imaging of dry, semi-dry and liquid samples in their original state and provides a broad overview of the whole population of particles ranging from the nano to micro scale. Furthermore, the alternative OM in the ClairScope will be convenient to check large aggregates in any depth which were washed out during sample preparation for TEM and SEM and which were underestimated by NTA. Minimum sample preparation is required and can be achieved using simple approaches such as the application of poly-L-Lysine solution to attract ENPs to the ASEM dish, use of dextran 500 or glucose to neutralize the free radicals, use of glutaraldehyde to cross link the coating of ENPs. Although, it is worth noting that even this minimal preparation can potentially alter the dispersion state of the ENPs. With necessary sample preparation, the minimum measurable concentration of the ENPs in liquid is 1 mg L^{-1} (9×10^8 particles mL^{-1}) for 50 nm nominal Au ENPs.

The ASEM dish is not reusable or recyclable. Care must be taken when viewing hard materials to ensure that the fine membrane is not compromised. Similar to the Quantomix capsules in WetSEM, the ASEM dish film may deteriorate during exposure to the electron beam due to the free radical or other mechanical damages (Tiede, *et al.,* 2009b). The free radicals, which are induced by electron beam irradiation, can instigate complex chemical reactions with the SiN$_x$ dish film and eventually will cause failure of the film integrity. Addition of free radical scavengers (Dextran) to the specimen can somewhat reduce these effects. After comparison studies, these effects can be effectively minimised by the selection of a spot size of 30 which can maximize the resolution. Nevertheless, a 100 nm SiN$_x$ film is recommended which provides a <1 hr lifespan, where the beam can focus on one area for maximum 35 mins, which is enough for observation. New developments such as multi-windowed film dishes are expected to ease this restriction.

Some researchers have highlighted the need for analysis of the chemical composition of particles during imaging of samples. Current developments allow the combination of TEM and SEM with EDS, Electron energy loss spectroscopy (EELS), Selected area electron diffraction (SAED), Wavelength dispersive spectroscopy (WDS) or High angle annular dark field (HAADF) to obtain elemental information. No chemical analysis can be achieved by ASEM based on the current design. However, the OM fitted on the top of specimen does allow various kinds of fluorescent and bright-field imaging which could provide useful additional information on the

composition of a sample (Murai *et al.*, 2011), which not readily achieved using the other techniques. The OM can also be of great use to identify regions of interest prior to using the scanning electron mode and can also provide a corresponding field of view with ASEM.

Conclusions

This study has demonstrated the application of ASEM to the analysis of environmental and food samples. While measured mean sizes for the samples tested were higher than those obtained by TEM, FEG-SEM and NTA, the fact that ASEM is able to measure particles in the liquid phase with minimum preparation provides a number of advantages over the other methods and means that data can begin to be generated on the behaviour of an ENP *in situ*. With necessary sample preparations, ASEM images can provide the information of ENPs down to at least 30 nm, 1 mg L^{-1} (9×10^8 particles mL^{-1}, 50 nm Au ENPs). The ASEM was successfully applied to a range of different core/shell ENPs, e.g. metal (Au), metal oxide (TiO_2) and semiconductor oxide (SiO_2) with different coating materials in complex wet matrices, such as Daphnia culture medium, BSA and tomato soup.

Overall, we believe that ASEM is a valuable addition to the existing 'tool kit' that is available for understanding the occurrence and behaviour of ENPs in complex media. While the results are by no means perfect, the fact that ENPs can be visualised with ease in 'wet' complex samples offers a number of advantages over some of the existing techniques. When used in combination with other methods, ASEM should provide useful additional knowledge on the characteristics of ENPs in environmental matrices and food.

References

Blasco, C. & Picó, Y. (2011) Determining nanomaterials in food. *Trac-trend Anal. Chem.* **30**, 86–99.

Blaschke, T. (2010) Object based image analysis for remote sensing. *ISPRS J. Photogramm* **65**, 2–16.

Boxall A.B.A., Chaudhry, Q., Sinclair, C., Jones, A., Aitken, R., Jefferson, B. & Watts, C. (2007) *Current and Future Predicted Environmental Exposure to Engineered Nanoparticles*. Central Science Laboratory, York, UK.

Däbritz, S., Langer, E. & Hauffe, W. (2001) Kossel and pseudo Kossel CCD pattern in comparison with electron backscattering diffraction diagrams. *Appl. Surf. Sci.*, **179**, 38–44.

Dudkiewicz, A., Tiede, K., Loeschner, K., Jensen, L.H.S., Jensen, E., Wierzbicki, R., Boxall, A.B.A. & Molhave, K. (2011) Characterization of nanomaterials in food by electron microscopy. *Trac-Trend Anal. Chem.* **30**, 28–43.

Gatti, A., Kirkpatrick, J., Gambarelli, A., Capitani, F., Hansen, T., Eloy, R. & Clermont, G. (2008) ESEM evaluations of muscle/nanoparticles interface in a rat model. *J. Mater. Sci.: Mater. Med.* **19**, 1515–1522.

Gillespie, C., Halling, P. & Edwards, D. (2011) Monitoring of particle growth at a low concentration of a poorly water soluble drug using the NanoSight LM20. *Colloid Surf. A: Physicochem. Eng. Aspects*, **384** (1–3), 233–239.

Gittings M.R. & Saville D.A. (1998) The determination of hydrodynamic size and zeta potential from electrophoretic mobility and light scattering measurements. *Coll. Surf. A: Physicochem. Eng. Aspects* **141**, 111–117.

Green, C. & Ndegwa, S. (2011) *Nanotechnology*: A Review of Exposure, Health Risks and Recent Regulatory Developments, National Collaborating Centre for Environmental Health. Accessed by 20th February, 2012. [http://www.ncceh.ca/sites/default/files/Nanotechnology_Review_Aug_2011.pdf]

Goldstein J.I., Newbury D.E., Echlin P, Joy D.C., Fiori C.E. & Lifshin E. (1981) Scanning electron microscopy and X-ray microanalysis, Plenum Press, New York.

Hristozov, D. & Malsch I. (2009) Hazards and risks of engineered nanoparticles for the environment and human health, *Sustainability* **1**, 1161–1194.

Liu, J., Legros, S., Ma, G., Veinot, J.G.C., Kamme, F.v.d. & Hofmann, T. (2012) Influence of surface functionalization and particle size on the aggregation kinetics of engineered nanoparticles, *Chemosphere* **87**, 918–924.

Lorenz, C., Tiede, K., Tear S., Boxall, A.B.A., Von Goetz, N. & Hungerbühler, K. (2010). Imaging and characterisation of engineered nanoparticles in sunscreens by electron microscopy, under wet and dry conditions, *Int. J. Occup. Environ. Health* **16**, 406–428.

Murai, T., Maruyama, Y., Mio, K., Nishiyama, H., Suga, M. & Sato, C. (2011) Low cholesterol triggers membrane microdomain-dependent CD44 shedding and suppresses tumor cell migration. *J. Biol. Chem.*, **286**(3) 1999–2007.

Nishiyama, H., Suga, M., Ogura, T., Maruyama, Y., Koizumi, M., Mio, K., Kitamura, S. & Sato, C. (2010) Atmospheric scanning electron microscope observes cells and tissues in open medium through silicon nitride film. *J Struct. Biol.* **172**, 191–202.

OECD/OCDE (1998) Guideline for the testing of chemicals 211: Daphnia magna Reproduction Test.

OECD/OCDE (2000) Guideline for the testing of chemicals 106: Adsorption–Desorption Using a Batch Equilibrium Method.

Richards, R.G., Owen, G. Rh, & ap Gwynn, I. (1999) Low voltage backscattered electron imaging (<5 kV) using field emission scanning electron microscopy. *Scanning Microsc.* **13**, 55–60.

Sato, C., Manaka S., Nakane, D., Nishiyama, H., Suga, M., Nishizaka, T., Miyata, M. & Maruyama, Y. (2012) Rapid imaging of mycoplasma in solution using atmospheric scanning electron microscopy (ASEM). *Biochem. Biophys. Res. Commun.* **417**, 1213–1218.

Suga, M., Nishiyama, H., Konyuba, Y., Iwamatsu, S., Watanabe, Y., Yoshiura, C., Ueda, T. & Sato, C. (2011) The atmospheric scanning electron microscope with open sample space observes dynamic phenomena in liquid or gas. *Ultramicrocopy* **111**,1650–1658.

Suzuki,M., Kitsuki, H., Ngo, Q., *et al.* (2007) Image formation mechanisms in scanning electron microscopy of carbon nanofibers on substrate. *Microsc. Microanal.* **13**, 580–581.

Wilson, M.A., Tran, N.H., Milev, A.S., Kannangara, G.S.K., Volk H. & Lu, G.Q.M. (2008) Nanomaterials in soils. *Geoderma* **146**, 291–302.

Ramachandran,T.R., Baur, C., Bugacov, A., Madhukar, A., Koel, B.E., Requicha, A. & Gazen, C. (1998) Direct and controlled manipulation of nanometer-sized particles using the non-contact atomic force microscope. *Nanotechnology* **9**, 237–245.

Tiede, K., Boxall, A.B.A., Tear, S.P., Lewis, J., David, H. & Hassellöv, M. (2008) Detection and characterization of engineered nanoparticles in food and the environment. *Food Addit. Contam.* **25**, 795–821.

Tiede, K., Hasselló v, M., Breitbarth, E., Chaudhry, Q. & Boxall, A.B.A. (2009a) Considerations for environmental fate and ecotoxicity testing to support environmental risk assessments for engineered nanoparticles. *J. Chromatogr. A* **1216**, 503–509.

Tiede, K., Tear, S.P., David, H. & Boxall, A.B.A. (2009b) Imaging of engineered nanopartlicles and their aggregates under fully liquid conditions in environmental matrices. *Water Res.* **43**, 3335–3343.

Tiede, K., Boxall, A.B., Tiede, D., Tear S.P., David, H. & Lewis, J. (2009c) A robust size-characterisation methodology for studying nanoparticle behaviour in "real" environmental samples, using hydrodynamic chromatography coupled to ICP-MS. *J. Anal. Atom. Spectrom.* **24**, 964–972.

Tiede, K., Boxall, A.B.A., Wang, X.M., *et al.* (2010) Application of hydrodynamic chromatography-ICP-MS to investigate the fate of silver nanoparticles in activated sludge. *J. Anal. Atom. Spectrom.* **25**, 1149–1154.

Appendix 2

Spectroscopic characterization of gold nanoparticles prepared in aqueous solutions with different functional capping molecules

The capping molecules used sodium 11-mercaptoundecanoic acid and citrate tribasic dehydrate are shown as below:
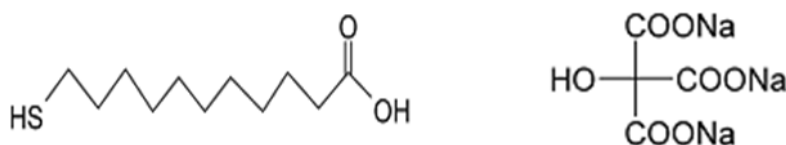
Figure A. 2. 1. Capping molecules of (a) 11-mercaptoundecanoic acid (MUDA) gold nanoparticles, (b) sodium citrate tribasic dehydrate (citrate).

The gold precursor used was solid $H_2AuCl_4 \cdot 2H_2O$. The small size nanoparticles was reduced by fresh prepared $NaBH_4$ aqueous solution using solid $NaBH_4$ at room temperature and the big size nanoparticles was reduced with citric acid at 15 times gold concentration at temperature close to the boiling water (about 90°C). After doing experiments many times, the optimized preparation procedures are summary as below:

The procedure used for the gold nanoparticles preparation:

Synthesis of 8-10 nm Au nanoparticles (Sample 1 with citric acid and Sample 2 with 11-mercaptoundecanoic acid capping):

A stock solution of gold nanoparticles was prepared in aqueous solution via reduction

of $H_2AuCl_4 \cdot 2H_2O$ (0.25 mM, 1 liter) upon addition of an aqueous $NaBH_4$ solution (0.015 g dissolved in 5 mL of distilled water containing 0.11 g sodium citrate tribasic salt) in one rapid addition. Particle growth was arrested by surface passivation with the sodium citrate tribasic salt of citrate (0.11 g) that was present in the initial $H_2AuCl_4 \cdot 2H_2O$ solution.

Purified citrate capped nanoparticles (Sample 1):

Au nanoparticle solutions were purified by dialysis. The 1000 mL stock solution was divided into two 500 mL fractions. On fraction was placed in Lot Number 3244650 dialysis tubing (approximate molecular weight cut off (MWCO) = 8,000 Daltons) and the filled tubes were submerged in distilled water for 4 d (bath water was changed at regular 12 hour intervals).

11-mercaptoundecanoic acid passivated nanoparticles (Sample 2):

The second fraction of the stock Au-nanoparticles was added directly to an ethanol solution of 11-mercaptoundecanoic acid (0.12 g, 3 mL) and the mixture was stirred in subdued light for one week. During this period, the apparent colour of the solution changed from "blood red" to "purple red". The resulting solution was dialyzed using the procedure outlined above.

Synthesis of 24-30 nm Au nanoparticles (Sample 3 with citric acid and sample 4 with 11-mercaptoundecanoic acid capping):

Au nanoparticle were prepared in aqueous solution by heating the solution of $H_2AuCl_4 \cdot 2H_2O$ (0.25 mM, 3.75 mM tribasic salt, 1 L) to approximately 90°C. The solution was heated for 1 hour and colour of solution gradually changed to gray and finally to purple red, that indicated the expected size of nanoparticles was achieved.

Purified citrate capped nanoparticles (Sample 3)

The same procedure used as Sample 1

11-mercaptoundecanoic acid passivated nanoparticles (Sample 4)

The same procedure used as Sample 2

TEM analysis of Samples 2 and 3 indicates particle diameters noted in the provided figures.   UV-vis absorption spectra indicate no detectable changes in particle diameter upon functionalization. TEM results for the 11-mercaptoundecanoic acid capped particles are pending.
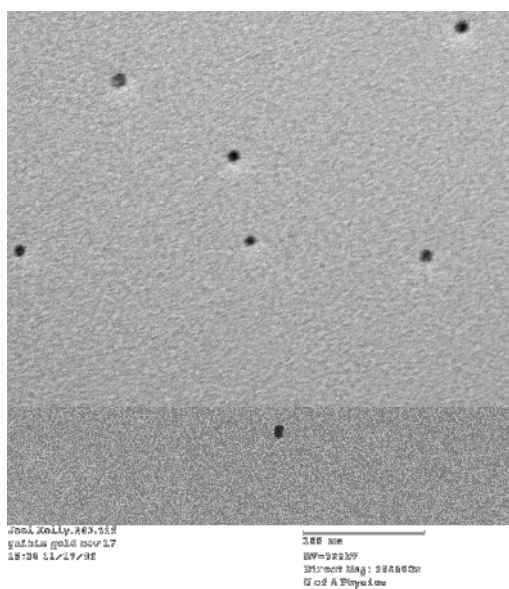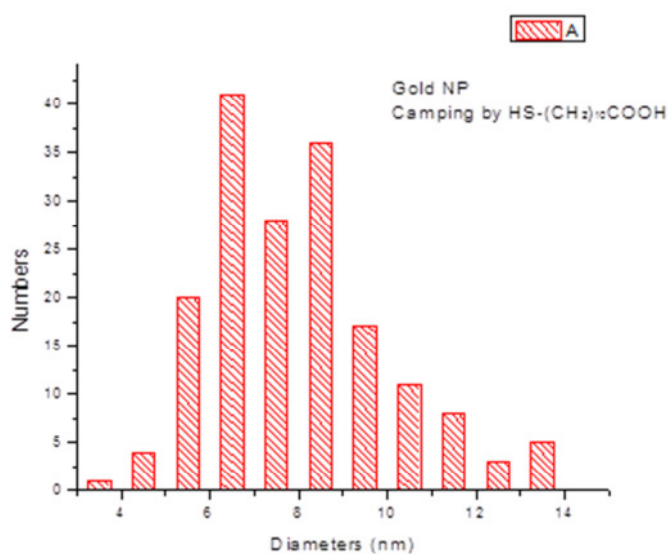
Figure A. 2. 2. 11-mercaptoundecanoic acid passivated gold nanoparticles.
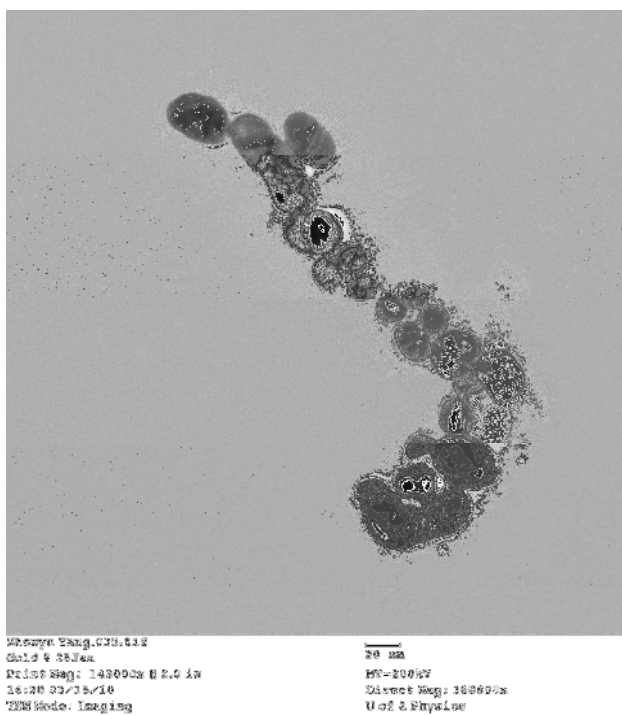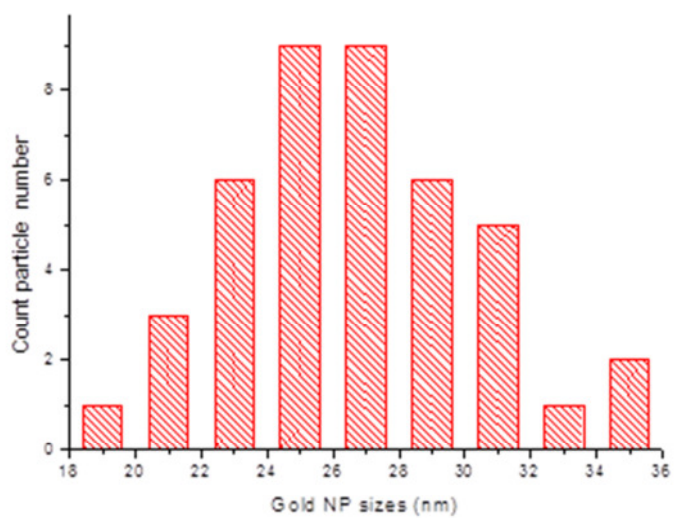
Figure A. 2. 3. Citrate capped nanoparticles gold nanoparticles.
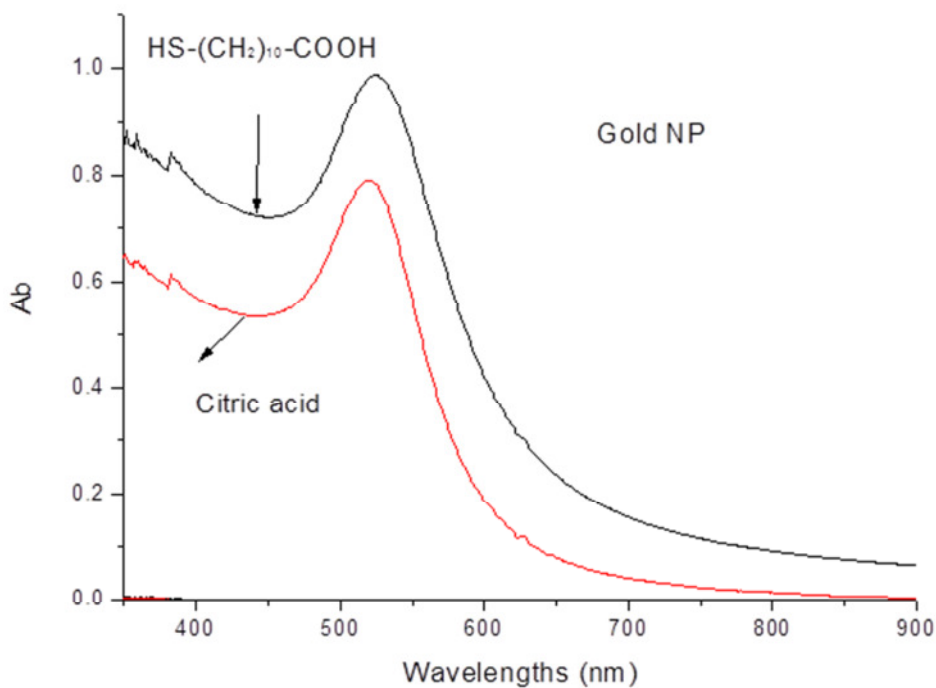
Figure A. 2.4. UV-Vis spectra of gold nanoparticles after the ligand exchange in aqueous solutions (samples 1 and 2, respectively).
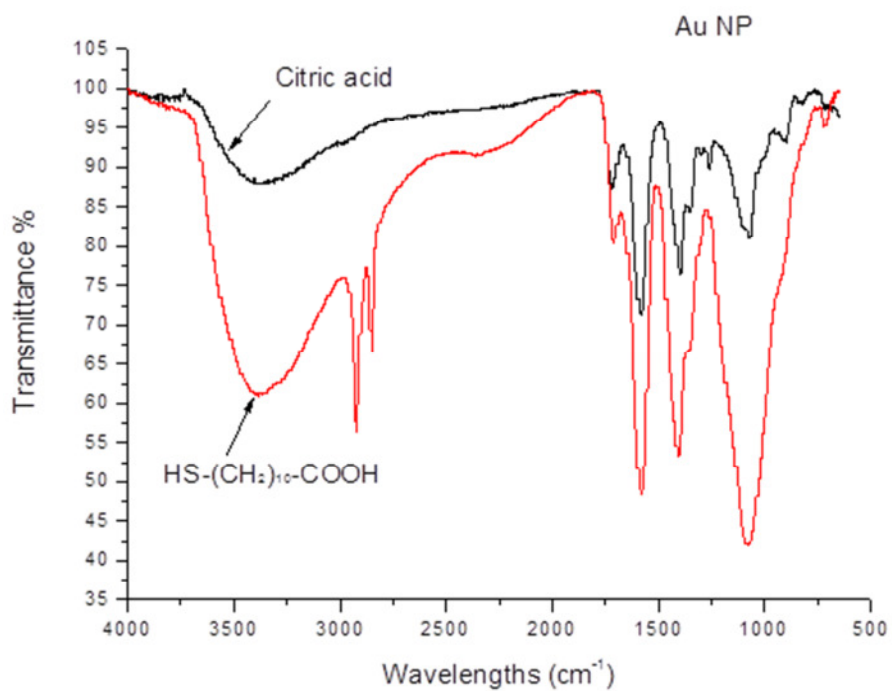
Figure A. 2. 5. FT-IR analysis of citrate (black trace) and mercaptoundecanoic acid (red trace) Functionalised Au nanoparticles.
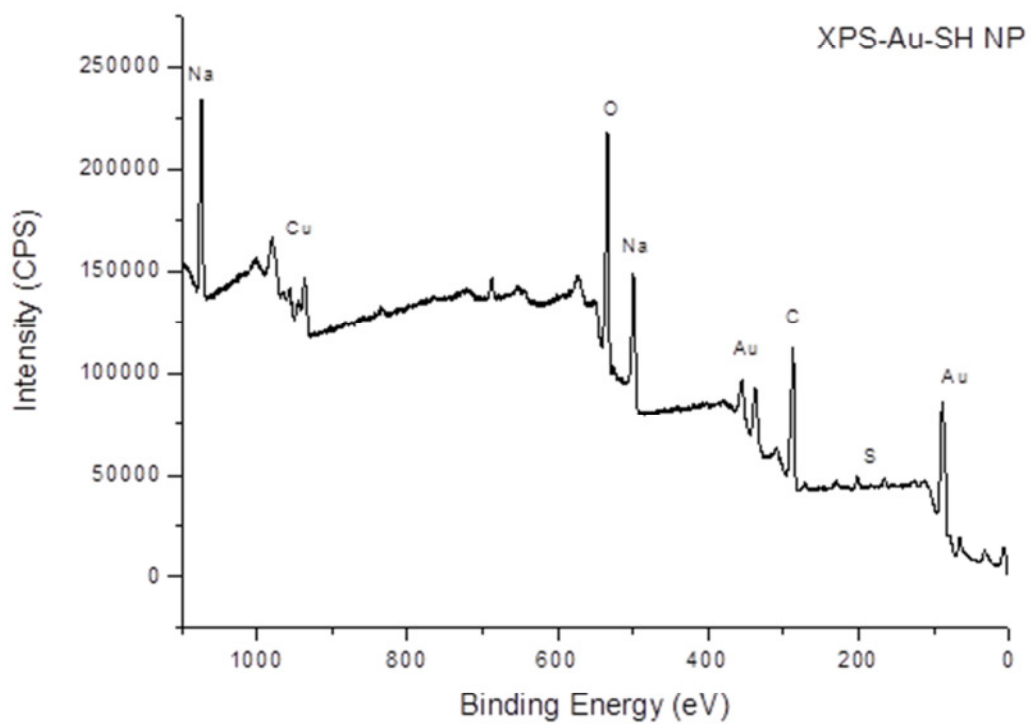
Figure A. 2. 6. XPS for gold nanoparticles (sample 2) with 11-mercaptoundecanoic acid capping groups. The sample was prepared on a copper substrate.

Appendix 3

Spectroscopic characterization of silver nanoparticles prepared in aqueous solutions with different functional capping molecules

Synthesis of citric acid and 11-MUDA stabilised 30 nm Ag nanoparticles:

Citric acid capped silver nanoparticles were prepared in aqueous solution by mixing $AgNO_3$ and citric acid in the molar ratio citric acid/$AgNO_3$ = 12 (0.25 mM of $AgNO_3$, 3.0 mM tribasic salt, 1 liter). 2 drops of 4 M NaOH base solution were added after stirring the citric acid/$AgNO_3$ solution for 10 minutes, and then the solution was heated to $70^{\circ}C$ for 1 hour. During heating the solution gradually changed to dark yellow consistent with the formation of Ag nanoparticles. 11-mercaptoundecanoic acid (11-MUDA) passivated Ag nanoparticles were prepared by a ligand exchange reaction of 11-MUDA. 11-MUDA readily displaces the surface citric acid on Ag-Citrate nanoparticles. An ethanol solution of 11-MUDA (0.12 g, 3 mL) was added dropwise to 1 liter of citric acid capped Ag-nanoparticles aqueous stock solution with rapidly stirring. The mixture was kept in subdued light and was stirred for one week.

Purification of the synthesized Ag nanoparticles samples:

All silver nanoparticles were purified using dialysis. The 200 mL of the stock solution of choice was poured into a dialysis tube. The filled tubes were submerged distilled water (4-litre capacity beaker) for 4 d (bath water was changed at regular 5 hour intervals).

Characterization the synthesized Ag nanoparticles*:*

Transmission electron microscopy (TEM) samples of Ag nanoparticleswere drop-cast from an aqueous suspension onto holey carbon coated copper grids and dried under vacuum. TEM analyses were performed using a JEOL-2010 (LaB$_6$ filament) electron microscope with an accelerating voltage of 200 keV. UV-vis spectra were recorded with a Hewlett-Packard 8453 UV-vis DAD spectrophotometer. The Ag NP diameters were determined by measuring the TEM images using the program-soft ImageJ and histogram analysis were performed using Origin 8.0.
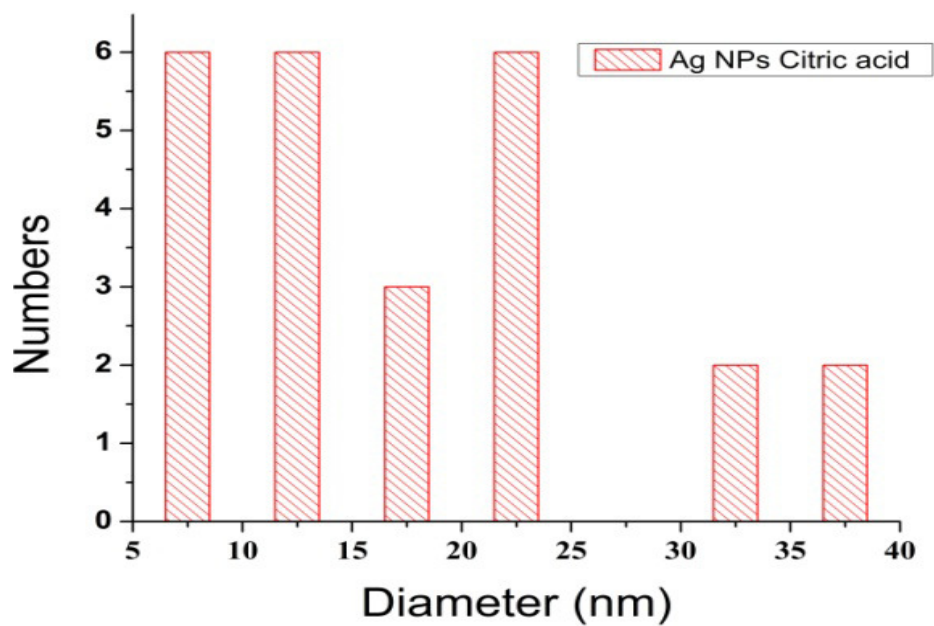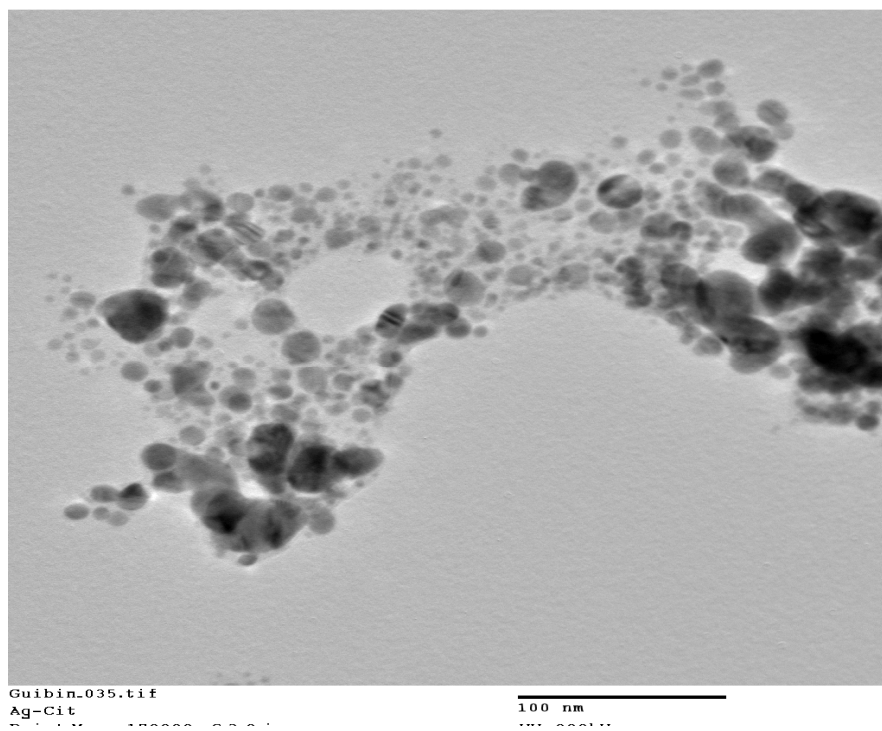
Figure A.3.1. Bright field TEM and particle size distribution of Ag-Citrate nanoparticles

(d = 17.5 ± 9.4 nm).
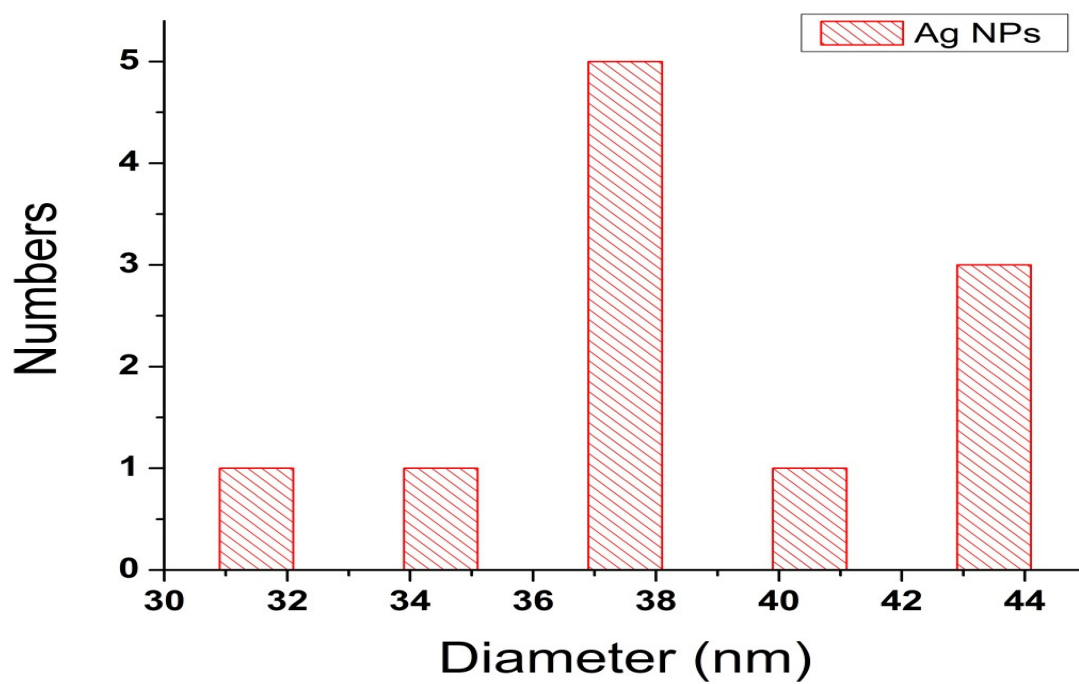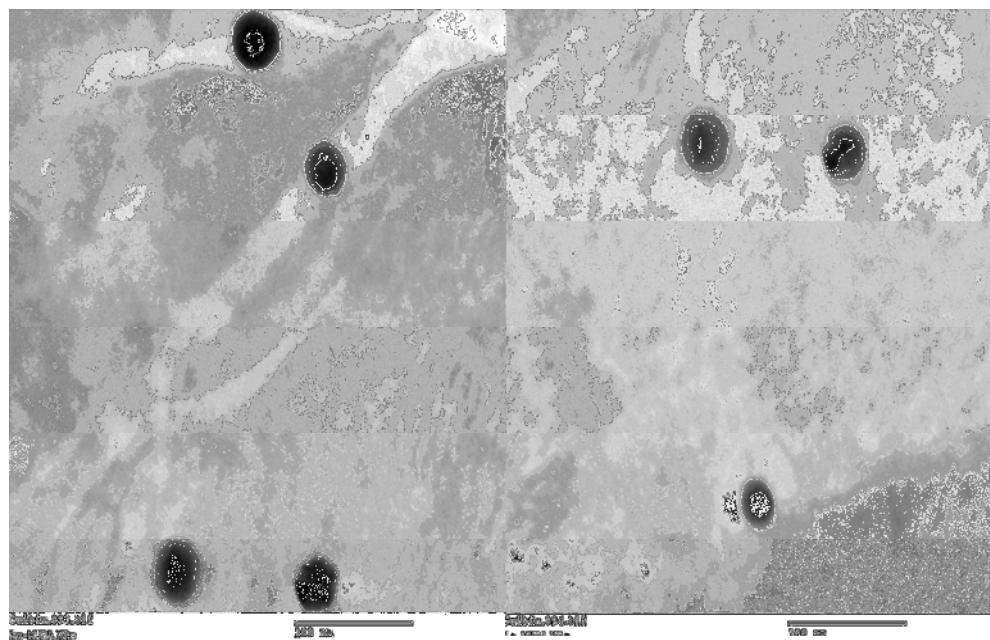
Figure A.3.2. Bright field TEM and particle size distribution of Ag-MUDA nanoparticles (d = 38.8 ± 3.6 nm).
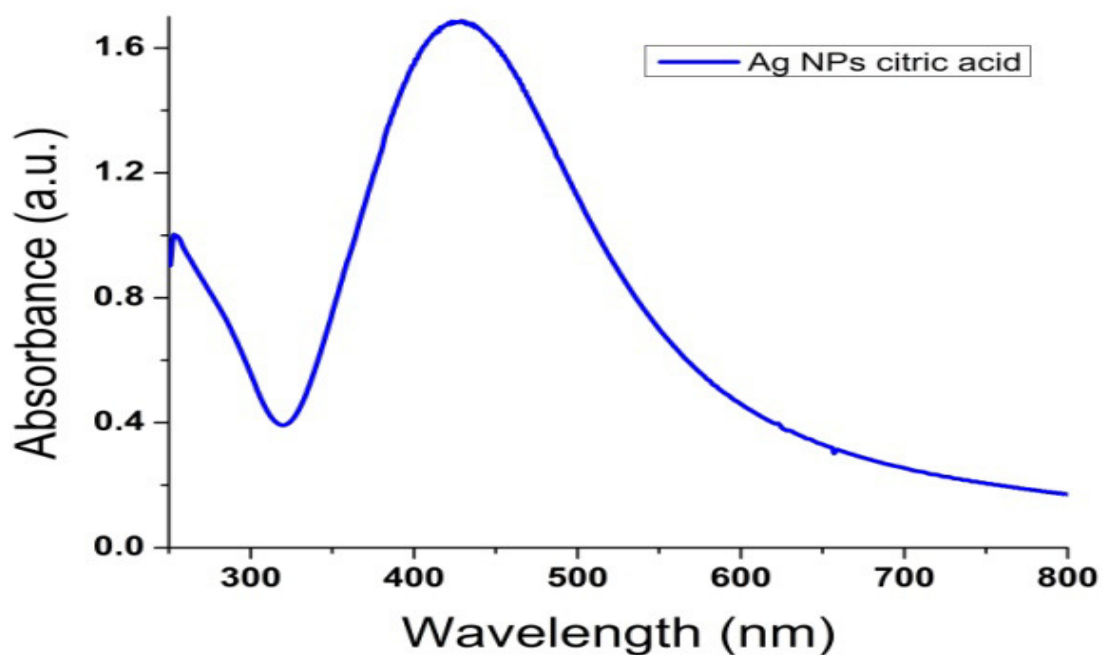
Figure A.3.3. UV-Vis spectrum of Ag-Citrate nanoparticles in aqueous solution.

DLS analyses of Ag nanoparticles with citric acid (top) and 11-MUDA (bottom) capping were carried out in aqueous solutions (See Figure A.3.4). The DLS size distribution data indicate the citric acid Ag nanoparticles (5) show two distribution peaks at 43.41 nm with intensity 84% and 5.2 nm with 16%, while for 11-MUDA at 52.2nm with intensity 89% and 5.3 nm with 11%. Zeta-potential measurements for two capping agents are -34.1 mV for citric acid and -43.9 mV for 11-MUDA, respectively. In principle DLS measured results were almost identical from aqueous solutions for these two Ag nanoparticles with citric acid and 11-MUDA capping ligands.
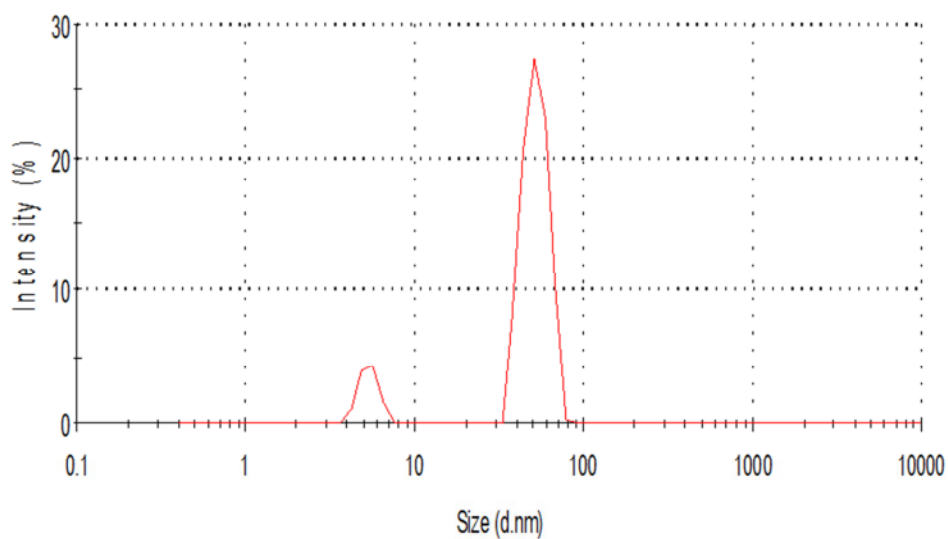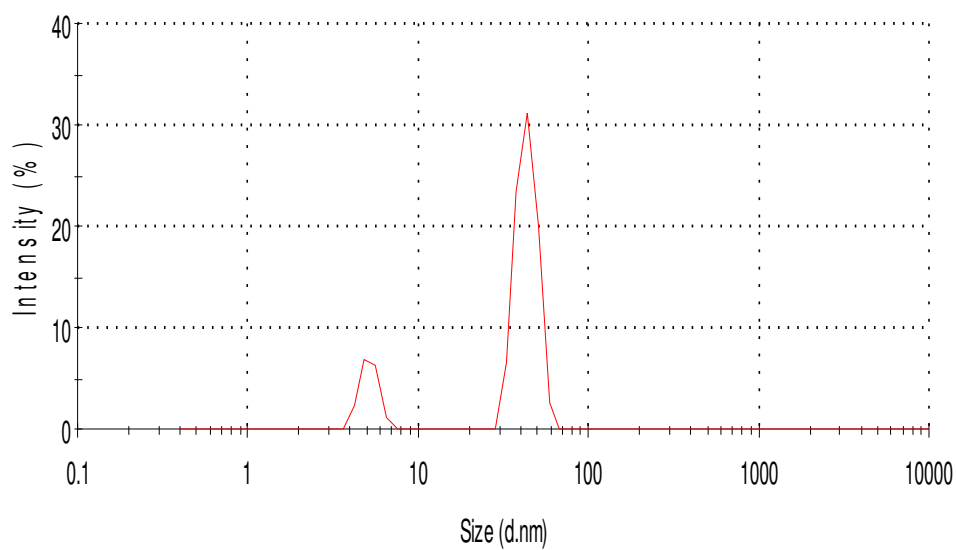
Figure A.3.4. The DLS measurements of Ag nanoparticles. Top: citric acid. Bottom: 11-MUDA capped.

Appendix 4

Table A.4.1. Summary of water chemistry in each natural water sample and particle size of Au-MUDA NPs after 8 h exposure.

Sampling time and site		Size (nm)	pH	conductivity	DOC	SO_4^{2-}	Cl^-	NO_3^-	PO_4^{3-}	F^-	K^+	Na^+	Ca^{2+}	Mg^{2+}	Hardness	IS
Mar-2012	1	37.67	7.28	54.10	3.80	0.03	0.09	0.03	N.A	0.00	0.03	0.08	0.04	0.06	9.78	0.37
Mar-2012	1	42.50	7.42	54.40	3.76	0.04	0.10	0.03	N.A	0.00	0.02	0.09	0.04	0.06	9.97	0.40
Mar-2012	1	42.83	7.29	58.30	5.36	0.05	0.09	0.02	N.A	0.00	0.01	0.10	0.08	0.06	14.11	0.48
Mar-2012	1	43.00	5.25	71.40	3.25	0.12	0.18	0.04	0.00	0.00	0.01	0.23	0.04	0.11	15.41	0.77
Mar-2012	1	43.50	7.19	54.30	3.96	0.03	0.09	0.03	N.A	0.00	0.02	0.10	0.04	0.06	10.16	0.39
Aug-2011	3	43.83	6.78	91.40	6.61	0.02	0.06	0.00	N.A	0.00	0.01	0.25	0.15	0.09	23.50	0.68
Aug-2011	2	45.33	7.06	113.90	7.88	0.03	0.10	0.00	N.A	0.00	0.12	0.16	0.13	0.09	22.50	0.70
Aug-2011	3	48.17	6.39	173.40	7.63	0.06	0.08	0.01	N.A	0.01	0.03	0.28	0.81	0.53	133.09	2.97
Mar-2012	3	48.33	7.44	203.00	4.94	0.15	0.31	0.04	N.A	0.00	0.01	0.26	0.47	0.09	55.68	1.72
Mar-2012	1	48.67	6.92	209.00	5.78	0.08	0.40	0.02	0.00	0.00	0.17	0.43	0.25	0.15	40.79	1.48
Mar-2012	1	48.83	5.41	46.10	13.14	0.05	0.15	0.05	0.00	0.00	0.01	0.14	0.02	0.04	6.16	0.41
Aug-2011	3	49.00	6.96	241.00	6.94	0.08	0.10	0.01	N.A	0.01	0.05	0.44	0.54	0.22	75.78	1.98

Site 1: River Etherow, 2, Hob Moor, 3. Helmsley, 4. Bishop Wilton

Unit: conductivity: µS/cm, DOC: mg/L, Hardness: mg/L as $CaCO_3$, IS: mmole, Cations and anions: mmole/L, NA: not available

Table A.4.1. Continued

Sampling time and site		Size (nm)	pH	conductivity	DOC	SO_4^{2-}	Cl^-	NO_3^-	PO_4^{3-}	F^-	K^+	Na^+	Ca^{2+}	Mg^{2+}	Hardness	IS
Mar-2012	1	49.33	5.33	56.50	11.66	0.07	0.16	0.03	0.00	0.00	0.01	0.17	0.03	0.08	11.51	0.56
Mar-2012	1	49.67	4.64	57.90	13.38	0.07	0.15	0.03	0.00	0.00	0.01	0.13	0.01	0.03	4.06	0.38
Aug-2011	2	50.00	7.39	234.00	9.04	0.02	0.07	N.A	0.01	0.00	0.05	0.12	0.83	0.17	100.78	2.17
Mar-2012	1	50.33	5.05	46.90	14.20	0.05	0.16	0.05	0.00	0.00	0.02	0.13	0.02	0.04	6.14	0.40
Mar-2012	3	50.33	7.52	185.60	5.21	0.18	0.43	0.01	N.A	0.00	0.02	0.38	0.29	0.14	42.96	1.63
Mar-2012	3	51.00	6.56	79.90	3.92	0.13	0.22	0.01	N.A	0.00	0.01	0.16	0.06	0.08	14.06	0.74
Mar-2012	3	51.17	7.31	150.40	4.45	0.14	0.39	0.06	0.00	0.00	0.03	0.32	0.17	0.15	31.97	1.31
Mar-2012	1	51.33	5.68	64.50	14.09	0.07	0.27	0.04	0.00	0.00	0.01	0.14	0.03	0.06	8.83	0.56
Aug-2011	3	52.00	6.73	235.00	7.27	0.09	0.15	0.01	N.A	0.01	0.04	0.63	0.41	0.24	65.26	1.90
Mar-2012	1	52.33	4.29	53.80	17.65	0.07	0.15	0.04	0.00	0.00	0.01	0.15	0.01	0.04	5.59	0.42
Mar-2012	3	52.50	6.48	191.50	4.30	0.18	0.40	0.01	N.A	0.00	0.03	0.33	0.24	0.19	42.28	1.58
Aug-2011	2	52.83	7.40	250.00	9.60	0.02	0.08	N.A	0.01	0.00	0.05	0.12	0.87	0.19	106.32	2.29
Mar-2012	3	53.67	6.47	210.00	3.76	0.19	0.53	0.01	N.A	0.00	0.03	0.45	0.23	0.20	43.20	1.76
Mar-2012	1	53.67	7.02	134.20	5.49	0.09	0.18	0.00	N.A	0.00	0.02	0.22	0.21	0.13	33.90	1.08
Aug-2011	1	54.67	4.46	83.20	23.70	0.01	0.10	0.00	N.A	0.00	0.22	0.01	0.02	0.03	5.00	0.29

Table A.4.1. Continued

Sampling time and site		Size (nm)	pH	conductivity	DOC	SO_4^{2-}	Cl^-	NO_3^-	PO_4^{3-}	F^-	K^+	Na^+	Ca^{2+}	Mg^{2+}	Hardness	IS
Aug-2011	1	54.83	4.14	79.70	23.13	0.01	0.08	0.00	N.A	0.00	0.19	0.01	0.01	0.02	3.11	0.23
Aug-2011	1	55.33	4.75	87.70	23.21	0.01	0.10	0.00	N.A	0.00	0.28	0.01	0.05	0.02	7.02	0.37
Aug-2011	1	56.00	4.34	63.00	24.74	0.01	0.07	0.00	N.A	0.00	0.13	0.01	0.00	0.02	2.26	0.18
Aug-2011	1	57.33	4.15	54.10	36.60	0.01	0.03	0.01	N.A	0.00	0.00	0.01	0.02	0.03	4.50	0.13
Aug-2011	1	60.83	3.92	88.40	42.42	0.01	0.02	0.01	N.A	0.00	0.00	0.01	0.00	0.02	1.73	0.08
Aug-2011	1	60.83	4.29	60.00	34.36	0.01	0.03	0.01	N.A	0.00	0.00	0.01	0.03	0.03	5.95	0.17
Aug-2011	1	62.50	3.79	85.30	43.49	0.01	0.02	0.01	N.A	0.00	0.00	0.01	0.00	0.02	1.56	0.08
Aug-2011	1	65.83	3.83	122.80	47.37	0.01	0.09	0.01	N.A	0.00	0.23	0.02	0.00	0.02	1.92	0.24
Aug-2011	1	67.17	3.80	93.90	49.38	0.01	0.03	0.01	N.A	0.00	0.00	0.01	0.00	0.02	2.30	0.09
Aug-2011	1	67.33	3.80	91.60	48.98	0.01	0.03	0.01	N.A	0.00	0.01	0.01	0.00	0.02	2.15	0.09
Aug-2011	1	72.83	3.83	86.50	46.53	0.02	0.02	0.00	N.A	0.00	0.00	0.01	0.01	0.01	2.05	0.09
Aug-2011	2	89.83	7.68	575.00	11.34	0.08	0.39	0.02	0.01	0.02	0.11	0.44	0.54	0.47	100.01	2.64
Aug-2011	2	103.67	7.84	883.00	8.01	0.16	0.69	0.02	0.01	0.01	0.31	2.05	2.34	0.66	299.86	7.85
Aug-2011	2	109.83	7.90	747.00	7.74	0.14	0.56	0.02	0.01	0.02	0.16	1.74	2.27	0.56	283.32	7.18
Mar-2012	3	114.17	7.11	448.00	1.84	0.23	0.43	0.03	0.00	0.00	0.01	0.31	2.03	0.12	215.86	5.16
Aug-2011	2	119.17	7.75	868.00	7.17	0.17	0.71	0.02	0.01	0.01	0.20	2.19	2.46	0.71	317.06	8.23

Table A.4.1. Continued

Sampling time and site		Size (nm)	pH	conductivity	DOC	SO_4^{2-}	Cl^-	NO_3^-	PO_4^{3-}	F^-	K^+	Na^+	Ca^{2+}	Mg^{2+}	Hardness	IS
Mar-2012	2	193.83	7.20	896.00	5.56	0.08	0.26	0.02	0.00	0.00	0.15	1.84	2.43	0.67	310.17	7.50
Mar-2012	2	194.83	7.33	974.00	6.37	0.08	0.28	0.02	0.00	0.00	0.15	2.73	2.87	0.77	365.23	9.05
Mar-2012	2	206.00	7.28	904.00	6.32	0.10	0.12	0.00	0.00	0.00	0.07	0.98	3.61	1.23	484.69	10.46
Mar-2012	2	213.33	7.27	877.00	5.78	0.08	0.28	0.02	0.00	0.00	0.16	2.96	2.46	0.74	320.26	8.27
Mar-2012	2	216.80	7.16	914.00	5.60	0.08	0.27	0.02	0.00	0.00	0.16	2.19	2.57	0.70	327.53	8.02
Mar-2012	2	236.83	7.64	1239.00	14.18	0.10	0.39	0.02	0.00	0.00	0.20	3.57	3.31	1.25	456.31	11.41
Jul-2013	4	77.25	8.19	510.00	1.36	0.49	0.58	0.60	N.A	2.99	2.38	0.42	2.35	0.21	256.00	0.01

Table A.4.2. Summary of water chemistry in each natural water sample and particle size of Au-citrate NPs after 8 h exposure.

Sampling time and site		Size (nm)	pH	conductivity	DOC	SO_4^{2-}	Cl^-	NO_3^-	PO_4^{3-}	F^-	K^+	Na^+	Ca^{2+}	Mg^{2+}	Hardness	IS
Mar-2012	1	71.17	5.25	71.40	3.25	0.12	0.18	0.04	0.00	0.00	0.01	0.23	0.04	0.11	15.41	0.77
Mar-2012	3	76.17	7.44	203.00	4.94	0.15	0.31	0.04	N.A	0.00	0.01	0.26	0.47	0.09	55.68	1.72
Mar-2012	1	81.33	7.29	58.30	5.36	0.05	0.09	0.02	N.A	0.00	0.01	0.10	0.08	0.06	14.11	0.48
Mar-2012	1	82.50	7.28	54.10	3.80	0.03	0.09	0.03	N.A	0.00	0.03	0.08	0.04	0.06	9.78	0.37
Mar-2012	1	83.50	5.33	56.50	11.66	0.07	0.16	0.03	0.00	0.00	0.01	0.17	0.03	0.08	11.51	0.56
Mar-2012	1	85.67	7.42	54.40	3.76	0.04	0.10	0.03	N.A	0.00	0.02	0.09	0.04	0.06	9.97	0.40
Mar-2012	3	86.17	6.47	210.00	3.76	0.19	0.53	0.01	N.A	0.00	0.03	0.45	0.23	0.20	43.20	1.76
Mar-2012	1	86.33	7.19	54.30	3.96	0.03	0.09	0.03	N.A	0.00	0.02	0.10	0.04	0.06	10.16	0.39
Mar-2012	1	89.33	6.92	209.00	5.78	0.08	0.40	0.02	0.00	0.00	0.17	0.43	0.25	0.15	40.79	1.48
Mar-2012	3	91.17	7.31	150.40	4.45	0.14	0.39	0.06	0.00	0.00	0.03	0.32	0.17	0.15	31.97	1.31
Mar-2012	3	91.83	6.56	79.90	3.92	0.13	0.22	0.01	N.A	0.00	0.01	0.16	0.06	0.08	14.06	0.74
Mar-2012	1	93.17	4.64	57.90	13.38	0.07	0.15	0.03	0.00	0.00	0.01	0.13	0.01	0.03	4.06	0.38

Site 1: River Etherow, 2, Hob Moor, 3. Helmsley, 4. Bishop Wilton

Unit: conductivity: µS/cm, DOC: mg/L, Cations and anions: mmole/L, Hardness: mg/L as $CaCO_3$, IS: mmole, NA: not available

Table A.4.2. Continued

Sampling time and site		Size (nm)	pH	conductivity	DOC	SO_4^{2-}	Cl^-	NO_3^-	PO_4^{3-}	F^-	K^+	Na^+	Ca^{2+}	Mg^{2+}	Hardness	IS
Mar-2012	1	94.50	5.68	64.50	14.09	0.07	0.27	0.04	0.00	0.00	0.01	0.14	0.03	0.06	8.83	0.56
Mar-2012	1	98.33	5.41	46.10	13.14	0.05	0.15	0.05	0.00	0.00	0.01	0.14	0.02	0.04	6.16	0.41
Mar-2012	1	99.00	5.05	46.90	14.20	0.05	0.16	0.05	0.00	0.00	0.02	0.13	0.02	0.04	6.14	0.40
Mar-2012	1	101.17	4.29	53.80	17.65	0.07	0.15	0.04	0.00	0.00	0.01	0.15	0.01	0.04	5.59	0.42
Mar-2012	3	102.00	7.52	185.60	5.21	0.18	0.43	0.01	N.A	0.00	0.02	0.38	0.29	0.14	42.96	1.63
Mar-2012	3	102.17	6.48	191.50	4.30	0.18	0.40	0.01	N.A	0.00	0.03	0.33	0.24	0.19	42.28	1.58
Mar-2012	1	104.67	7.02	134.20	5.49	0.09	0.18	0.00	N.A	0.00	0.02	0.22	0.21	0.13	33.90	1.08
Mar-2012	3	118.83	7.11	448.00	1.84	0.23	0.43	0.03	0.00	0.00	0.01	0.31	2.03	0.12	215.86	5.16
Mar-2012	2	199.00	7.28	904.00	6.32	0.10	0.12	0.00	0.00	0.00	0.07	0.98	3.61	1.23	484.69	10.46
Mar-2012	2	211.17	7.27	877.00	5.78	0.08	0.28	0.02	0.00	0.00	0.16	2.96	2.46	0.74	320.26	8.27
Mar-2012	2	212.50	7.33	974.00	6.37	0.08	0.28	0.02	0.00	0.00	0.15	2.73	2.87	0.77	365.23	9.05
Mar-2012	2	212.67	7.16	914.00	5.60	0.08	0.27	0.02	0.00	0.00	0.16	2.19	2.57	0.70	327.53	8.02
Mar-2012	2	216.67	7.20	896.00	5.56	0.08	0.26	0.02	0.00	0.00	0.15	1.84	2.43	0.67	310.17	7.50
Mar-2012	2	254.83	7.64	1239.00	14.18	0.10	0.39	0.02	0.00	0.00	0.20	3.57	3.31	1.25	456.31	11.41
Jul-2013	4	115.95	8.19	510.00	1.36	0.49	0.58	0.60	N.A	2.99	2.38	0.42	2.35	0.21	256.00	0.01

Table A.4.3. Summary of water chemistry in each natural water sample and particle size of Au-PEG-NH$_2$ NPs after 8 h exposure.

Sampling time and site		Size (nm)	pH	conductivity	DOC	SO$_4^{2-}$	Cl$^-$	NO$_3^-$	PO$_4^{3-}$	F$^-$	K$^+$	Na$^+$	Ca^{2+}	Mg^{2+}	Hardness	IS
Mar-2012	3	72.67	7.11	448.00	1.84	22.28	15.15	2.14	0.09	0.06	0.49	7.15	81.54	2.93	215.86	5.16
Mar-2012	1	85.50	7.42	54.40	3.76	3.68	3.72	2.05	N.A	0.09	0.92	1.99	1.74	1.37	9.97	0.40
Mar-2012	1	89.67	5.25	71.40	3.25	11.43	6.41	2.29	0.13	0.07	0.31	5.21	1.60	2.78	15.41	0.77
Mar-2012	1	91.33	7.19	54.30	3.96	3.22	3.06	1.60	N.A	0.09	0.83	2.31	1.75	1.41	10.16	0.39
Mar-2012	1	92.17	7.28	54.10	3.80	3.28	3.14	1.67	N.A	0.09	0.98	1.78	1.65	1.38	9.78	0.37
Mar-2012	3	101.33	6.48	191.50	4.30	16.84	14.11	0.81	N.A	0.15	1.14	7.54	9.52	4.51	42.28	1.58
Mar-2012	1	102.00	7.29	58.30	5.36	4.40	3.15	1.26	N.A	0.10	0.57	2.24	3.25	1.46	14.11	0.48
Mar-2012	1	112.00	6.92	209.00	5.78	7.56	14.05	1.52	0.37	0.12	6.60	9.78	10.15	3.76	40.79	1.48
Mar-2012	3	116.00	7.31	150.40	4.45	13.24	13.81	3.41	0.09	0.13	1.00	7.30	6.91	3.58	31.97	1.31
Mar-2012	1	116.50	5.33	56.50	11.66	6.73	5.83	1.88	0.08	0.07	0.30	3.86	1.34	1.99	11.51	0.56
Mar-2012	3	117.00	6.47	210.00	3.76	18.41	18.84	0.90	N.A	0.15	1.18	10.31	9.25	4.90	43.20	1.76
Mar-2012	3	118.50	7.44	203.00	4.94	14.21	10.87	2.48	N.A	0.07	0.53	5.96	18.74	2.15	55.68	1.72

Site 1: River Etherow, 2, Hob Moor, 3. Helmsley, 4. Bishop Wilton

Unit: conductivity: µS/cm, DOC: mg/L, Cations and anions: mmole/L, Hardness: mg/L as CaCO$_3$,IS: mmole, NA: not available

Table A.4.3. Continued

Sampling time and site		Size (nm)	pH	conductivity	DOC	SO_4^{2-}	Cl^-	NO_3^-	PO_4^{3-}	F^-	K^+	Na^+	Ca^{2+}	Mg^{2+}	Hardness	IS
Mar-2012	1	120.67	4.64	57.90	13.38	6.58	5.17	1.79	0.10	0.07	0.39	3.05	0.43	0.72	4.06	0.38
Mar-2012	1	121.17	4.29	53.80	17.65	6.63	5.38	2.43	0.12	0.07	0.27	3.47	0.59	1.01	5.59	0.42
Mar-2012	1	123.00	7.02	134.20	5.49	8.88	6.53	0.30	N.A	0.11	0.65	5.14	8.23	3.25	33.90	1.08
Mar-2012	1	123.67	5.05	46.90	14.20	4.97	5.52	3.24	0.08	0.06	0.63	3.01	0.76	1.03	6.14	0.40
Mar-2012	1	130.17	5.41	46.10	13.14	5.02	5.48	3.34	0.09	0.07	0.40	3.27	0.75	1.05	6.16	0.41
Mar-2012	1	130.83	5.68	64.50	14.09	7.00	9.74	2.38	0.09	0.07	0.55	3.32	1.23	1.40	8.83	0.56
Mar-2012	3	131.33	7.52	185.60	5.21	16.88	15.27	0.59	N.A	0.10	0.95	8.68	11.68	3.36	42.96	1.63
Mar-2012	3	141.83	6.56	79.90	3.92	12.46	7.94	0.83	N.A	0.09	0.47	3.61	2.60	1.84	14.06	0.74
Mar-2012	2	154.00	7.27	877.00	5.78	7.87	9.78	1.31	0.64	0.15	6.15	68.10	98.55	18.02	320.26	8.27
Mar-2012	2	155.17	7.33	974.00	6.37	7.82	9.89	1.20	0.40	0.16	5.73	62.79	115.21	18.83	365.23	9.05
Mar-2012	2	157.83	7.16	914.00	5.60	7.69	9.64	1.28	0.71	0.15	6.14	50.45	103.23	16.94	327.53	8.02
Mar-2012	2	166.00	7.28	904.00	6.32	9.18	4.29	0.14	0.36	0.12	2.67	22.59	144.94	29.84	484.69	10.46
Mar-2012	2	168.83	7.20	896.00	5.56	7.85	9.37	1.00	0.69	0.14	5.82	42.41	97.32	16.31	310.17	7.50
Mar-2012	2	177.00	7.64	1239.00	14.18	9.62	13.97	1.12	0.15	0.20	7.91	82.15	132.65	30.41	456.31	11.41
Jul-2013	4	168.12	8.19	510.00	1.36	0.49	0.58	0.60	N.A	2.99	2.38	0.42	2.35	0.21	256.00	0.01

Table A.4.4. Summary of water chemistry in each natural water sample and particle size of Au-PEG NPs after 8 h exposure.

Sampling time and site		Size (nm)	pH	conductivity	DOC	SO$_4^{2-}$	Cl$^-$	NO$_3^-$	PO$_4^{3-}$	F$^-$	K$^+$	Na$^+$	Ca^{2+}	Mg^{2+}	Hardness	IS
Mar-2012	3	95.17	7.11	448.00	1.84	22.28	15.15	2.14	0.09	0.06	0.49	7.15	81.54	2.93	215.86	5.16
Mar-2012	1	130.67	5.25	71.40	3.25	11.43	6.41	2.29	0.13	0.07	0.31	5.21	1.60	2.78	15.41	0.77
Mar-2012	1	141.33	7.42	54.40	3.76	3.68	3.72	2.05	N.A	0.09	0.92	1.99	1.74	1.37	9.97	0.40
Mar-2012	1	142.50	6.92	209.00	5.78	7.56	14.05	1.52	0.37	0.12	6.60	9.78	10.15	3.76	40.79	1.48
Mar-2012	1	143.50	7.02	134.20	5.49	8.88	6.53	0.30	N.A	0.11	0.65	5.14	8.23	3.25	33.90	1.08
Mar-2012	1	146.17	7.28	54.10	3.80	3.28	3.14	1.67	N.A	0.09	0.98	1.78	1.65	1.38	9.78	0.37
Mar-2012	3	148.50	7.19	54.30	3.96	3.22	3.06	1.60	N.A	0.09	0.83	2.31	1.75	1.41	10.16	0.39
Mar-2012	3	148.50	6.47	210.00	3.76	18.41	18.84	0.90	N.A	0.15	1.18	10.31	9.25	4.90	43.20	1.76
Mar-2012	1	154.67	7.29	58.30	5.36	4.40	3.15	1.26	N.A	0.10	0.57	2.24	3.25	1.46	14.11	0.48
Mar-2012	3	155.17	7.44	203.00	4.94	14.21	10.87	2.48	N.A	0.07	0.53	5.96	18.74	2.15	55.68	1.72
Mar-2012	3	155.33	6.56	79.90	3.92	12.46	7.94	0.83	N.A	0.09	0.47	3.61	2.60	1.84	14.06	0.74
Mar-2012	3	157.50	6.48	191.50	4.30	16.84	14.11	0.81	N.A	0.15	1.14	7.54	9.52	4.51	42.28	1.58

Site 1: River Etherow, 2, Hob Moor, 3. Helmsley, 4. Bishop Wilton

Unit: conductivity: µS/cm, DOC: mg/L, Cations and anions: mmole/L, Hardness: mg/L as CaCO$_3$,IS: mmole, NA: not available

Table A.4.4. Continued

Sampling time and site		Size (nm)	pH	conductivity	DOC	SO_4^{2-}	Cl^-	NO_3^-	PO_4^{3-}	F^-	K^+	Na^+	Ca^{2+}	Mg^{2+}	Hardness	IS
Mar-2012	3	158.83	7.31	150.40	4.45	13.24	13.81	3.41	0.09	0.13	1.00	7.30	6.91	3.58	31.97	1.31
Mar-2012	1	164.17	5.33	56.50	11.66	6.73	5.83	1.88	0.08	0.07	0.30	3.86	1.34	1.99	11.51	0.56
Mar-2012	1	165.67	5.41	46.10	13.14	5.02	5.48	3.34	0.09	0.07	0.40	3.27	0.75	1.05	6.16	0.41
Mar-2012	1	167.83	4.29	53.80	17.65	6.63	5.38	2.43	0.12	0.07	0.27	3.47	0.59	1.01	5.59	0.42
Mar-2012	3	168.67	7.52	185.60	5.21	16.88	15.27	0.59	N.A	0.10	0.95	8.68	11.68	3.36	42.96	1.63
Mar-2012	1	171.33	4.64	57.90	13.38	6.58	5.17	1.79	0.10	0.07	0.39	3.05	0.43	0.72	4.06	0.38
Mar-2012	1	172.67	5.68	64.50	14.09	7.00	9.74	2.38	0.09	0.07	0.55	3.32	1.23	1.40	8.83	0.56
Mar-2012	1	177.50	5.05	46.90	14.20	4.97	5.52	3.24	0.08	0.06	0.63	3.01	0.76	1.03	6.14	0.40
Mar-2012	2	205.50	7.33	974.00	6.37	7.82	9.89	1.20	0.40	0.16	5.73	62.79	115.21	18.83	365.23	9.05
Mar-2012	2	208.83	7.16	914.00	5.60	7.69	9.64	1.28	0.71	0.15	6.14	50.45	103.23	16.94	327.53	8.02
Mar-2012	2	215.33	7.20	896.00	5.56	7.85	9.37	1.00	0.69	0.14	5.82	42.41	97.32	16.31	310.17	7.50
Mar-2012	2	217.00	7.28	904.00	6.32	9.18	4.29	0.14	0.36	0.12	2.67	22.59	144.94	29.84	484.69	10.46
Mar-2012	2	221.83	7.27	877.00	5.78	7.87	9.78	1.31	0.64	0.15	6.15	68.10	98.55	18.02	320.26	8.27
Mar-2012	2	245.83	7.64	1239.00	14.18	9.62	13.97	1.12	0.15	0.20	7.91	82.15	132.65	30.41	456.31	11.41
Jul-2013	4	164.73	8.19	510.00	1.36	0.49	0.58	0.60	N.A	2.99	2.38	0.42	2.35	0.21	256.00	0.01

References

Aitken,R., Chaudhry, M., Boxall, A. & Hull, M. (2006). Manufacture and use of nanomaterials: current status in the UK and global trends. *Occ Med,* 56 (5), 300-306.

Ajayan, P. & Zhou, O. (2001). Applications of carbon nanotubes. In *Carbon Nanotubes*, Springer Berlin Heidelberg, 391-425.

Alkilany, A. & Murphy, C. (2010). Toxicity and cellular uptake of gold nanoparticles: what we have learned so far? *J Nanopar Res,* 12 (7), 2313-2333.

Aruoja, V., Dubourguier, H, Kasemets, K., & Kahru, A. (2009). Toxicity of nanoparticles of CuO, ZnO and TiO_2 to microalgae *Pseudokirchneriella subcapitata*. *Sci Total Environ,* 407 (4), 1461-1468.

Baalousha, M., Manciulea, A., Cumberland, S., Kendall, K., & Lead, J. R. (2008). Aggregation and surface properties of iron oxide nanoparticles: influence of pH and natural organic matter. *Environ Toxicol Chem,* 27 (9), 1875-1882.

Banfield, J. F., & Zhang, H. (2001). Nanoparticles in the environment. *Rev Mineral. Geochem,* 44 (1), 1-58.

Baun, A., Hartmann, N. B., Grieger, K., & Kusk, K. O. (2008a). Ecotoxicity of engineered nanoparticles to aquatic invertebrates: a brief review and recommendations for future toxicity testing. *Ecotoxicology,* 17(5), 387-395.

Baun, A., Sørensen, S., Rasmussen, R., Hartmann, N., & Koch, C. (2008b). Toxicity and bioaccumulation of xenobiotic organic compounds in the presence of aqueous suspensions of aggregates of nano-C_{60}. *Aquat Toxicol,* 86(3), 379-387.

Benn, T., & Westerhoff, P. (2008). Nanoparticle silver released into water from commercially available sock fabrics. *Environ Sci Technol,* 42(11), 4133-4139.

Bian, S., Mudunkotuwa, I., Rupasinghe, T., & Grassian, V. (2011). Aggregation and dissolution of 4 nm ZnO nanoparticles in aqueous environments: influence of pH, ionic strength, size, and adsorption of humic acid. *Langmuir,* 27(10), 6059-6068.

Bigall, N. & Eychmüller, A. (2010). Synthesis of noble metal nanoparticles and their non-ordered superstructures. *Phil Trans Math Phys Eng Sci, 368* (1915), 1385-1404.

Blaser, S., Scheringer, M., MacLeod, M., & Hungerbühler, K. (2008). Estimation of cumulative aquatic exposure and risk due to silver: Contribution of nano-functionalized plastics and textiles. *Sci Total Environ,* 390(2), 396-409.

Bosi, S., Da Ros, T., Spalluto, G., & Prato, M. (2003). Fullerene derivatives: an attractive tool for biological applications. *Eur. J. Med. Chem,* 38(11), 913-923.

Boxall, A., Chaudhry, Q., Sinclair, C., Jones, A., Aitken, R., Jefferson, B., & Watts, C. (2007). Current and future predicted environmental exposure to engineered nanoparticles. Central Science Laboratory, Department of the Environment and Rural Affairs, London, UK.

Bozich, S., Lohse, E., Torelli, D., Murphy, J., Hamers, J., Klaper D. (2014). Surface chemistry, charge and ligand type impact the toxicity of gold nanoparticles to *Daphnia magna. Environ Sci: Nano*, *1*(3): 260-270.

Brayner, R., Dahoumane, S., Yéprémian, C., Djediat, C., Meyer, M., Couté, A., & Fiévet, F. (2010). ZnO nanoparticles: synthesis, characterization, and ecotoxicological studies. *Langmuir,* 26(9), 6522-6528.

Bronstein, L. & Shifrina, Z. (2009). Nanoparticles in dendrimers: From synthesis to application. *Nanotechnologies in Russia,* 4(9-10), 576-608.

Burns, C. (1968). Relationship between body size of filter-feeding *Cladocera* and maximum size of particle Ingested. *Limnol. Oceanography,* 13(4), 675-678.

Buzea, C., Pacheco, I. & Robbie, K. (2007). Nanomaterials and nanoparticles: sources and toxicity. *Biointerphases*, *2*(4), MR17-MR71.

Chae, Y., Pham, C., Lee, J., Bae, E., Yi, J. & Gu, M. B. (2009). Evaluation of the toxic impact of silver nanoparticles on Japanese medaka (*Oryzias latipes*). *Aquat toxicol,* 94(4), 320-327.

Chaudret, B., & Philippot, K. (2007). Organometallic nanoparticles of metals or metal Oxides. *Oil & Gas Science and Technology-Revue de l'IFP,* 62(6), 799-817.

Chen, K., & Elimelech, M. (2006). Aggregation kinetics of alginate-coated hematite nanoparticles in monovalent and divalent electrolytes. *Environ Sci Technol,* 40(5), 1516-1523.

Chen, K., & Elimelech, M. (2007). Influence of humic acid on the aggregation kinetics of fullerene (C_{60}) nanoparticles in monovalent and divalent electrolyte solutions. *J Colloid Interf Sci*, 309(1), 126-134.

Chen, Q., Yin, D., Li, J., & Hu, X. (2014). The effects of humic acid on the uptake and depuration of fullerene aqueous suspensions in two aquatic organisms. *Environ Toxicol Chem,* 33(5), 1090–1097.

Chithrani, B., Ghazani, A., & Chan, W. (2006). Determining the size and shape dependence of gold nanoparticle uptake into mammalian cells. *Nano Lett,* 6(4), 662-668.

Christian, P., Von der Kammer, F., Baalousha, M., & Hofmann, T. (2008). Nanoparticles: structure, properties, preparation and behaviour in environmental media. *Ecotoxicology,* 17(5), 326-343.

Clark, K., Gobas, F., & Mackay, D. (1990). Model of organic chemical uptake and clearance by fish from food and water. *Environ Sci Technol,* 24(8), 1203-1213.

Coello, W., & Khan, M. (1996). Protection against heavy metal toxicity by mucus and scales in fish. *Arch Environm Contam Toxicol,* 30(3), 319-326.

COMMISSION, E. 2006. Directive 2006/121/EC of the European Parliament and of the Council of 18 December 2006 amending Council Directive 67/548/EEC on the approximation of laws, regulations and administrative provisions relating to the classification, packaging and labelling of dangerous substances in order to adapt it to Regulation (EC) No 1907/2006 concerning the Registration, Evaluation, Authorisation and Restriction of Chemicals (REACH) and establishing a European Chemicals Agency.

Cronholm, P., Karlsson, H., Hedberg, J., Lowe, T., Winnberg, L., Elihn, K., Wallinder, I., & Möller, L. (2013). Intracellular uptake and toxicity of Ag and CuO nanoparticles: a

comparison between nanoparticles and their corresponding metal ions. *Small,* 9(7), 970-982.

Dabrunz, A., Duester, L., Prasse, C., Seitz, F., Rosenfeldt, R., Schilde, C., Schaumann, G.,& Schulz, R. (2011). Biological surface coating and molting inhibition as mechanisms of TiO_2 nanoparticle toxicity in *Daphnia magna*. *PLoS One,* 6(5), e20112.

Dickson, D., Liu, G., Li, C., Tachiev, G., & Cai, Y. (2012). Dispersion and stability of bare hematite nanoparticles: Effect of dispersion tools, nanoparticle concentration, humic acid and ionic strength. *Sci Total Environ,* 419, 170-177.

Duncan, R., & Izzo, L. (2005). Dendrimer biocompatibility and toxicity. *Adv drug delivery rev,* 57(15), 2215-2237.

Dytham, C. 2011. *Choosing and using statistics: a biologist's guide*, John Wiley & Sons.

El Badawy, A., Luxton, P., Silva, R., Scheckel, K., Suidan, M., & Tolaymat, T. (2010). Impact of environmental conditions (pH, ionic strength, and electrolyte type) on the surface charge and aggregation of silver nanoparticles suspensions. *Environ Sci Technol,* 44(4), 1260-1266.

El Badawy, A., Silva, R., Morris, B., Scheckel, K., Suidan, M., & Tolaymat, T. (2011). Surface charge-dependent toxicity of silver nanoparticles. *Environ Sci Technol,* 45(1), 283-287.

El Badawy, A., Scheckel, K., Suidan, M., & Tolaymat, T. (2012). The impact of stabilization mechanism on the aggregation kinetics of silver nanoparticles. *Sci Total Environ,* 429, 325-331.

Emerging, S. & Risks, N. (2007). Opinion on the appropriateness of the risk assessment methodology in accordance with the technical guidance documents for new and existing substances for assessing the risks of nanomaterials. *Scientific Committee on Emerging and Newly Identified Health Risks*.

Endo, M., Strano, M., & Ajayan, P. (2008). Potential applications of carbon nanotubes. *Carbon Nanotubes*, 13-61.

Esawi, A., & Farag, M. (2007). Carbon nanotube reinforced composites: potential and current challenges. *Mater Design,* 28(9), 2394-2401.

Fabrega, J., Luoma, S., Tyler, C., Galloway, T., & Lead, J. (2011). Silver nanoparticles: behaviour and effects in the aquatic environment. *Environ Int,* 37(2), 517-31.

Farkas, J., Christian, P., Gallego-Urrea, J., Roos, N., Hassellöv, M., Tollefsen, K., & Thomas, K. (2011). Uptake and effects of manufactured silver nanoparticles in rainbow trout (*Oncorhynchus mykiss*) gill cells. *Aquat toxicol,* 101(1), 117-125.

Farré, M., Gajda-Schrantz, K., Kantiani, L., & Barceló, D. (2009). Ecotoxicity and analysis of nanomaterials in the aquatic environment. *Anal Bioanal Chem,* 393(1), 81-95.

Feldheim, D. (2007). The new face of catalysis. *Science,* 316(5825), 699-700.

Fent, K., Weisbrod, C., Wirth-Heller, A., & Pieles, U. (2010). Assessment of uptake and toxicity of fluorescent silica nanoparticles in zebrafish (*Danio rerio*) early life stages. *Aquat toxicol,* 100(2), 218-228.

Feswick, A., Griffitt, R., Siebein, K., & Barber, S. (2013). Uptake, retention and internalization of quantum dots in Daphnia is influenced by particle surface functionalization. *Aquat toxicol,* 130, 210-218.

Filella, M., Rellstab, C., Chanudet, V., & Spaak, P. (2008). Effect of the filter feeder Daphnia on the particle size distribution of inorganic colloids in freshwaters. *Water Res,* 42(8), 1919-1924.

Franklin, M., Rogers, J., Apte, C., Batley, E., Gadd, E., & Casey, S. (2007). Comparative toxicity of nanoparticulate ZnO, bulk ZnO, and ZnCl2 to a freshwater microalga (*Pseudokirchneriella subcapitata*): the importance of particle solubility. *Environ Sci Technol,* 41(24), 8484-8490.

French, R., Jacobson, R., Kim, B., Isley, L., Penn, L., & Baveye, C. (2009). Influence of ionic strength, pH, and cation valence on aggregation kinetics of titanium dioxide nanoparticles. *Environ Sci Technol,* 43(5), 1354-1359.

Gaiser, B., Biswas, A., Rosenkranz, P., Jepson, M., Lead, J., Stone, V., Tyler, C., & Fernandes, T. (2011). Effects of silver and cerium dioxide micro- and nano-sized particles on *Daphnia magna. J Environ Monitor,* 13(5), 1227-1235.

Gaiser, B., Fernandes, T., Jepson, M., Lead, J., Tyler, C., Baalousha, M., Biswa,s A., Britton, G., Cole, P., Johnston, B. (2012). Interspecies comparisons on the uptake and toxicity of silver and cerium dioxide nanoparticles. *Environ Toxicol Chem,* 31,144-154.

Gao, J., Youn, S., Hovsepyan, A., Llaneza, V., Wang, Y., Bitton, G., & Bonzongo, J. (2009). Dispersion and toxicity of selected manufactured nanomaterials in natural river water samples: effects of water chemical composition. *Environ Sci Technol,* 43(9), 3322-3328.

Geller, W., & Müller, H. (1981). The Filtration Apparatus of Cladocera - Filter Mesh-Sizes and Their Implications on Food Selectivity. *Oecologia,* 49(3), 316-321.

Georgantzopoulou, A., Balachandran, Y. L., Rosenkranz, P., Dusinska, M., Lankoff, A., Wojewodzka, M., Kruszewski, M., Guignard, C., Audinot J., & Girija, S. (2012). Ag nanoparticles: size-and surface-dependent effects on model aquatic organisms and uptake evaluation with NanoSIMS. *Nanotoxicology,* 7(7), 1168-1178.

Geranio, L., Heuberger, M., & Nowack, B. (2009). The behavior of silver nanotextiles during washing. *Environ Sci Technol,* 43(21), 8113-8118.

Ghasemi, Y., Peymani, P., & Afifi, S. (2009). Quantum dot: Magic nanoparticle for imaging, detection and targeting. *Acta Biomed,* 80(2), 156-165.

Ghosh Chaudhuri, R., & Paria, S. (2011). Core/shell nanoparticles: classes, properties, synthesis mechanisms, characterization, and applications. *Chem Rev,* 112(4), 2373-433.

Gibson, K., & Pula, D. (2009). Nanoparticles: Environmental risk and regulation. *Environ Qual Manage,* 18(13), 1-7.

Glover, N., & Wood, M. (2005). Accumulation and elimination of silver in *Daphnia magna* and the effect of natural organic matter. *Aquat Toxicol,* 73(4), 406-417.

Gottschalk, F., Sonderer, T., Scholz, R., & Nowack, B. (2010). Possibilities and limitations of modeling environmental exposure to engineered nanomaterials by probabilistic material flow analysis. *Environ Toxicol Chem,* 29(5), 1036-1048.

Gross-Sorokin, M., Grist, E., Cooke, M., Crane, M. (2003). Uptake and depuration of 4-nonylphenol by the benthic invertebrate Gammarus pulex: how important is feeding rate? *Environ Sci Technol,* 37, 2236-2241.

Goulden, C., & Hornig, L. (1980). Population oscillations and energy reserves in planktonic *Cladocera* and their consequences to competition. *Proc Natl Acad Sci,* 77(3), 1716-1720.

Griffitt, J., Luo, J., Gao, J., Bonzongo, J., & Barber, D. (2008). Effects of particle composition and species on toxicity of metallic nanomaterials in aquatic organisms. *Environ Toxicol Chem,* 27(9), 1972-1978.

Griffitt, J., Hyndman, K., Denslow, N., & Barber, D. (2009). Comparison of molecular and histological changes in Zebrafish gills exposed to metallic nanoparticles. *Toxicol Sci,* 107(2), 404-415.

Handy, R., Henry, T., Scown, T., Johnston, B., & Tyler, C. (2008a). Manufactured nanoparticles: their uptake and effects on fish—a mechanistic analysis. *Ecotoxicology,* 17(5), 396-409.

Handy, R., von der Kammer, F., Lead, J., Hassellöv, M., Owen, R., & Crane, M. (2008b). The ecotoxicology and chemistry of manufactured nanoparticles. *Ecotoxicology,* 17(4), 287-314.

Hassellöv, M., Readman, J., Ranville, J., & Tiede, K. (2008). Nanoparticle analysis and characterization methodologies in environmental risk assessment of engineered nanoparticles. *Ecotoxicology,* 17(5), 344-361.

He, D., Bligh, M., & Waite, T. (2013). Effects of aggregate structure on the dissolution kinetics of citrate-stabilized silver nanoparticles. *Environ Sci Technol,* 47(16), 9148-9156.

Heinlaan, M., Ivask, A., Blinova, I., Dubourguier, H., & Kahru, A. (2008). Toxicity of nanosized and bulk ZnO, CuO and TiO_2 to bacteria *Vibrio fischeri* and crustaceans *Daphnia magna* and *Thamnocephalus platyurus. Chemosphere,* 71(7), 1308-1316.

Heinlaan, M., Kahru, A., Kasemets, K., Arbeille, B., Prensier, G., & Dubourguier, H. (2011). Changes in the *Daphnia magna* midgut upon ingestion of copper oxide nanoparticles: A transmission electron microscopy study. *Water Res,* 45(1), 179-190.

Hoecke, K., Quik, J., Mankiewicz-Boczek, J., Schamphelaere, K., Elsaesser, A., Meeren, P., Barnes, C., Mckerr, G., Howard, D., & Meent, D. (2009). Fate and effects of CeO_2 nanoparticles in aquatic ecotoxicity tests. *Environ Sci Technol,* 43(12), 4537-4546.

Hoecke, K., De Schamphelaere, K., Van der Meeren, P., Lcucas, S., & Janssen, C. (2008). Ecotoxicity of silica nanoparticles to the green alga *Pseudokirchneriella subcapitata*: Importance of surface area. *Environ Toxicol Chem,* 27(9), 1948-1957.

Hoecke, K., De Schamphelaere, K., Van der Meeren, P., Smagghe, G., & Janssen, C. (2011). Aggregation and ecotoxicity of CeO_2 nanoparticles in synthetic and natural waters with variable pH, organic matter concentration and ionic strength. *Environ Pollut,* 159(4), 970-976.

Hotze, E., Phenrat, T., & Lowry, G. (2010). Nanoparticle aggregation: challenges to understanding transport and reactivity in the environment. *J Environ Qual,* 39(6), 1909-1924.

Huynh, K., & Chen, K. (2011). Aggregation kinetics of citrate and polyvinylpyrrolidone coated silver nanoparticles in monovalent and divalent electrolyte solutions. *Environ Sci Technol,* 45(13), 5564-5571.

Hyung, H., Fortner, J., Hughes, J., & Kim, J. (2007). Natural organic matter stabilizes carbon nanotubes in the aqueous phase. *Environ Sci Technol,* 41(1), 179-184.

Jain, P., Huang, X., El-Sayed, I., & El-Sayed, M. (2008). Noble metals on the nanoscale: optical and photothermal properties and some applications in imaging, sensing, biology, and medicine. *Acc Chem Res,* 41(12), 1578-1586.

Jeong, S., & Kim, S. (2009). Aggregation and transport of copper oxide nanoparticles in porous media. *J Environ Monitor,* 11(9), 1595-1600.

Jiang, W., Kim, B., Rutka, J., & Chan, W. (2008). Nanoparticle-mediated cellular response is size-dependent. *Nat Nanotechnol,* 3(3), 145-150.

Jiang, J., Oberdörster, G., & Biswas, P. (2009a). Characterization of size, surface charge, and agglomeration state of nanoparticle dispersions for toxicological studies. *J Nanopart Res,* 11(1), 77-89.

Jiang, L., Guan, J., Zhao, L., Li, J., & Yang, W. (2009b). pH-dependent aggregation of citrate-capped Au nanoparticles induced by Cu^{2+} ions: The competition effect of hydroxyl groups with the carboxyl groups. *Coll Surf A,* 346(1), 216-220.

Johnson, A., Bowes, M., Crossley, A., Jarvie, H., Jurkschat, K., Jürgens, M., Lawlor, A., Park, B., Rowland, P., Spurgeon, D., Svendsen, C., Thompson, I., Barnes, R., Williams, R., Xu, N. (2011). An assessment of the fate, behaviour and environmental risk associated with sunscreen TiO_2 nanoparticles in UK field scenarios. *Sci Total Environ,* 409(3), 2503-2510.

Johnston, B., Scown, T., Moger, J., Cumberland, S., Baalousha, M., Linge, K., van Aerle R, Jarvis, K., Lead, J., Tyler, C. (2010). Bioavailability of Nanoscale Metal Oxides TiO_2, CeO_2, and ZnO to Fish. *Environ Sci Technol* 44, 1144-1151.

Joner, E., Hartnik, T., & Amundsen, C. (2008). Environmental fate and ecotoxicity of engineered nanoparticles. *Final Report. TA,* 2304, 2007.

Jovanovic, B., & Palic, D. (2012). Immunotoxicology of non-functionalized engineered nanoparticles in aquatic organisms with special emphasis on fish--review of current knowledge, gap identification, and call for further research. *Aquat Toxicol,* 118-119, 141-151.

Ju-Nam, Y., & Lead, J. (2008). Manufactured nanoparticles: An overview of their chemistry, interactions and potential environmental implications. *Sci Total Environ,* 400(1), 396-414.

Kümmerer, K., Menz, J., Schubert, T., & Thielemans, W. (2011). Biodegradability of organic nanoparticles in the aqueous environment. *Chemosphere,* 82(10), 1387-1392

Kaegi, R., Ulrich, A., Sinnet, B., Vonbank, R., Wichser, A., Zuleeg, S., Simmler, H., Brunner, S., Vonmont, H., & Burkhardt, M. 2008. Synthetic TiO_2 nanoparticle emission from exterior facades into the aquatic environment. *Environ Pollut,* 156(2), 233-239.

Kashiwada, S. (2006). Distribution of nanoparticles in the see-through medaka (*Oryzias latipes*). *Environmen Health Persp,* 114, 1697–1702.

Keller, A., Wang, H., Zhou, D., Lenihan, H., Cherr, G., Cardinale, B., Miller, R., & Ji, Z. (2010). Stability and aggregation of metal oxide nanoparticles in natural aqueous matrices. *Environ Sci Technol,* 44(6), 1962-1967.

Kester, D., Duedall, I., Connors, D., & Pytkowicz, R. (1967). Preparation of Artificial Seawater. *Limnol Oceanogr,* 12(1), 176-179.

Khan, F., Kennaway, M., Croteau, M., Dybowska, A., Smith, B., Nogueira, A., Rainbow, P., Luoma, S., Valsami-Jones, E. (2014). *In vivo* retention of ingested Au NPs by *Daphnia magna*: No evidence for trans-epithelial alimentary uptake. *Chemosphere* 100, 97-104.

Klaine, S., Alvarez, P., Batley, G., Fernandes, T., Handy, R., Lyon, D., Mahendra, S., Mclaughlin, M. & Lead, J. (2008). Nanomaterials in the environment: behavior, fate, bioavailability, and effects. *Environ Toxicol Chem,* 27(9), 1825-1851.

Klajnert, B., & Bryszewska, M. (2001). Dendrimers: properties and applications. *Acta Biochim Pol,* 48(1), 199-208.

Kleinow, K., Nichols, J., Hayton, W., McKim, J., & Barron, M. (2008). *Toxicokinetics in fishes*, CRC Press: Boca Raton (FL).

Kuhl, A., & Lorenzen, H. (1964). Handling and Culturing of Chlorella. *Method Cell Biol,* 1, 159-187.

Laaksonen, T., Ahonen, P., Johans, C., & Kontturi, K. (2006). Stability and electrostatics of mercaptoundecanoic acid-capped gold nanoparticles with varying counterion size. *Chemphyschem,* 7(10), 2143-9.

Lee, K., Nallathamby, P., Browning, L., Osgood, C., & Xu, X. (2007). *In vivo* imaging of transport and biocompatibility of single silver nanoparticles in early development of zebrafish embryos. *ACS Nano,* 1(2), 133-143.

Lewinski, N., Zhu, H., Jo, H., Pham, D., Kamath, R., Ouyang, C., Vulpe, C., Colvin, V., & Drezek, R. (2010). Quantification of water solubilized CdSe/ZnS quantum dots in *Daphnia magna*. *Environ Sci Technol,* 44(5), 1841-1846.

Lahive, E., O'Halloran, J., Jansen, M. (2014). A marriage of convenience; a simple food chain comprised of *Lemna minor* and *Gammarus pulex* to study the dietary transfer of zinc. *Plant Biology*.

Lesniak, A., Fenaroli, F., Monopoli, M., Aberg, C., Dawson, K., & Salvati, A. (2012). Effects of the presence or absence of a protein corona on silica nanoparticle uptake and impact on cells. *ACS nano*, *6*(7), 5845-5857.

Li, M., & Huang, C. (2011). The responses of *Ceriodaphnia dubia* toward multi-walled carbon nanotubes: Effect of physical–chemical treatment. *Carbon,* 49(5), 1672-1679.

Lesniak, A., Salvati, A., Santos-Martinez, M., Radomski, M., Dawson, K., & Aberg, C. (2013). Nanoparticle adhesion to the cell membrane and its effect on nanoparticle uptake efficiency. *J Am Chem Soc*, *135*(4), 1438-1444.

Li, X., & Lenhart, J. (2012). Aggregation and dissolution of silver nanoparticles in natural surface water. *Environ Sci Technol,* 46(10), 5378-5386.

Lin, D., & Xing, B. (2008). Root uptake and phytotoxicity of ZnO nanoparticles. *Environ Sci Technol,* 42(15), 5580-5585.

Lin, D., Liu, N., Yang, K., Xing, B., & Wu, F. (2010). Different stabilities of multiwalled carbon nanotubes in fresh surface water samples. *Environ Pollut,* 158(5), 1270-1274.

Liu, J., von der Kammer, F., Zhang, B., Legros, S., & Hofmann, T. (2013). Combining spatially resolved hydrochemical data with in-vitro nanoparticle stability testing: assessing environmental behavior of functionalized gold nanoparticles on a continental scale. *Environ Int,* 59, 53-62.

Liu, J., Legros, S., Ma, G., Veinot, J., von der Kammer, F., & Hofmann, T. (2012). Influence of surface functionalization and particle size on the aggregation kinetics of engineered nanoparticles. *Chemosphere,* 87(8), 918-924.

Lovern, S., & Klaper, R. (2006). *Daphnia magna* mortality when exposed to titanium dioxide and fullerene (C_{60}) nanoparticles. *Environ Sci Technol,* 25(4), 1132-1137.

Lovern, S., Owen, H., & Klaper, R. (2008). Electron microscopy of gold nanoparticle intake in the gut of *Daphnia magna*. *Nanotoxicology,* 2(1), 43-48.

Lynch, I., & Dawson, K. (2008). Protein-nanoparticle interactions. *Nano Today*, *3*(1), 40-47.

Malloy, A., & Carr, B. (2006). Nanoparticle tracking analysis–the Halo™ system. *Part Part Syst Char,* 23(2), 197-204.

Meredith-Williams, M., Carter, L., Fussell, R., Raffaelli, D., Ashauer, R., & Boxall, A. (2012). Uptake and depuration of pharmaceuticals in aquatic invertebrates. *Environ Pollut,* 165, 250-258.

Miao, A. J., Luo, Z., Chen, C., Chin, W., Santschi, P., & Quigg, A. (2010). Intracellular uptake: A possible mechanism for silver engineered nanoparticle toxicity to a freshwater Alga *Ochromonas danica. PloS one,* 5, e15196

Mudunkotuwa, I., Rupasinghe, T., Wu, C., & Grassian, V. (2011). Dissolution of ZnO nanoparticles at circumneutral pH: a study of size effects in the presence and absence of citric acid. *Langmuir,* 28(1), 396-403.

Mueller, N., & Nowack, B. (2008). Exposure modeling of engineered nanoparticles in the environment. *Environ Sci Technol,* 42(12), 4447-4453.

Murayama, H., Tomonoh, S., Alford, J., & Karpuk, M. (2005). Fullerene production in tons and more: from science to industry. *Fuller Nanotub Car N,* 12(1-2), 1-9.

Murphy, C., Sau, T., Gole, A., Orendorff, C., Gao, J., Gou, L., Hunyadi, S., & Li, T. (2005). Anisotropic metal nanoparticles: Synthesis, assembly, and optical applications. *J Phys Chem B,* 109(29), 13857-13870.

Nason, J., McDowell, S., & Callahan, T. (2012). Effects of natural organic matter type and concentration on the aggregation of citrate-stabilized gold nanoparticles. *J Environ Monitor,* 14(7), 1885-1892.

Navarro, E., Baun, A., Behra, R., Hartmann, N. B., Filser, J., Miao, A. J., Quigg, A., Santschi, P. & Sigg, L. (2008a). Environmental behavior and ecotoxicity of engineered nanoparticles to algae, plants, and fungi. *Ecotoxicology,* 17 (5), 372-386.

Navarro, E., Piccapietra, F., Wagner, B., Marconi, F., Kaegi, R., Odzak, N., Sigg, L., & Behra, R. (2008b). Toxicity of silver nanoparticles to *Chlamydomonas reinhardtii. Environ Sci Technol,* 42(23), 8959-8964.

Navarro, D., Watson, D., Aga, D., & Banerjee, S. (2009). Natural organic matter-mediated phase transfer of quantum dots in the aquatic environment. *Environ Sci Technol,* 43(3), 677-682.

Naylor, C., Maltby, L., & Calow, P. (1989). Scope for growth in *Gammarus pulex*, a freshwater benthic detritivore. *Hydrobiologia,* 188, 517-523.

Neal, C., Bowes, M., Jarvie, H. P., Scholefield, P., Leeks, G., Neal, M., Rowland, P., Wicham, H., Harman, S. & Armstrong, L. (2012). Lowland river water quality: a new UK data resource for process and environmental management analysis. *Hydrol Process,* 26(6), 949-960.

Nowack, B., & Bucheli, T. (2007). Occurrence, behavior and effects of nanoparticles in the environment. *Environ Pollut,* 150 (1), 5-22.

O'Brien, N., & Cummins, E. (2011). A risk assessment framework for assessing metallic nanomaterials of environmental concern: aquatic exposure and behavior. *Risk Anal,* 31(5), 706-726.

OECD (1992). *OECD Guidelines for the Testing of Chemicals, Section 2: Effects on Biotic Systems, Test No. 203: Fish, Acute Toxicity Test*, OECD Publishing.

OECD (2004). *OECD Guidelines for the Testing of Chemicals, Section 2: Effects on Biotic Systems, Test No. 202: Daphnia sp. Acute Immobilisation Test,* Paris: OECD Publishing.

OECD (2006). *OECD Guidelines for the Testing of Chemicals, Section 2: effects on biotic systems,Test No. 221: Lemna sp. Growth Inhabition Test,* Paris, OECD Publishing.

OECD (2011). *OECD Guidelines for the Testing of Chemicals, Section 2: Effects on Biotic Systems, Test No. 201: Alga, Growth Inhibition Test,* Paris: OECD Publishing.

Oliver, A., Croteau, M., Stoiber, T., Tejamaya, M., Römer, I., Lead, J., Luoma, N. (2014). Does water chemistry affect the dietary uptake and toxicity of silver nanoparticles by the freshwater snail Lymnaea stagnalis? *Environ Pollut,*189, 87-91.

Ottofuelling, S., Von Der Kammer, F., & Hofmann, T. (2011). Commercial titanium dioxide nanoparticles in both natural and synthetic water: Comprehensive

multidimensional testing and prediction of aggregation behavior. *Environ Sci Technol,* 45(23), 10045-10052.

Park, B., Donaldson, K., Duffin, R., Tran, L., Kelly, F., Mudway, I., Guest, R., Jenkinson, P., Samaras, Z., Giannouli, M., Kouridis, H., & Martin, P. (2008). Hazard and risk assessment of a nanoparticulate cerium oxide-based diesel fuel additive - a case study. *Inhal Toxicol,* 20(6), 547-566.

Park S & Choi J. (2010). Geno-and ecotoxicity evaluation of silver nanoparticles in freshwater crustacean *Daphnia magna*. *Environ Eng Res*,15(1), 23–27.

Park, S., Woodhall, J., Ma, G., Veinot, J., Cresser, M., & Boxall, A. (2014). Regulatory ecotoxicity testing of engineered nanoparticles: are the results relevant to the natural environment? *Nanotoxicology,* 8(5), 583-592.

Patra, M., Ma, X., Isaacson, C., Bouchard, D., Poynton, H., Lazorchak, J., & Rogers, K. (2011). Changes in agglomeration of fullerenes during ingestion and excretion in *Thamnocephalus Platyurus*. *Environ Toxicol Chem,* 30(4), 828-835.

Petersen, E., Akkanen, J., Kukkonen, J., & Weber Jr, W. (2009). Biological uptake and depuration of carbon nanotubes by *Daphnia magna*. *Environ Sci Technol,* 43(8), 2969-2975.

Petersen, E., Pinto, R., Mai, D., Landrum, P., Weber, W. (2011a). Influence of polyethyleneimine graftings of multi-walled carbon nanotubes on their accumulation and elimination by and toxicity to *Daphnia magna*. *Environ Sci Technol*, 45, 1133-1138.

Petersen, E., Pinto, RA., Zhang, L., Huang, Q., Landrum, P., Weber, W. (2011b). Effects of polyethyleneimine-mediated functionalization of multi-walled carbon nanotubes on earthworm bioaccumulation and sorption by soils. *Environ Sci Technol*, 45, 3718-3724.

Petosa, A., Jaisi, D., Quevedo, I., Elimelech, M., & Tufenkji, N. (2010). Aggregation and deposition of engineered nanomaterials in aquatic environments: role of physicochemical interactions. *Environ Sci Technol,* 44(17), 6532–6549.

Peyrot, C., Gagnon, C., Gagné, F., Willkinson, K., Turcotte, P., & Sauvé, S. (2009). Effects of cadmium telluride quantum dots on cadmium bioaccumulation and

metallothionein production to the freshwater mussel, *Elliptio complanata*. *Comp Biochem and Physiol C: Toxicol Pharmacol,* 150(2), 246-251.

Pronk, M., Wijnhoven, S., Bleeker, E., Heugens, E., Peijnenburg, W., Luttik, R., & Hakkert, B. (2009). Nanomaterials under REACH. *Nanosilver as a case study. RIVM rapport,* 601780003.

Qi, L., & Gao, X. (2008). Emerging application of quantum dots for drug delivery and therapy. *Expert Opin Drug Deliv,* 5, 263-267.

Qu, F., Oliveira, R., & Morais, P. (2004). . Effects of nanocrystal shape on the surface charge density of ionic colloidal nanoparticles. *J magn and magn mater,* 272, 1668-1669.

Quik, J., Lynch, I., Hoecke, K., Miermans, C., De Schamphelaere, K., Janssen, C., Dawson, K., Stuart, M., & Meent, D. (2010). Effect of natural organic matter on cerium dioxide nanoparticles settling in model fresh water. *Chemosphere,* 81(6), 711-715.

Rahman, M., Laurent, S., Tawil, N., Yahia, L, & Mahmoudi, M. (2013). Nanoparticle and protein corona. In *Protein-Nanoparticle Interactions*, 21-44. Springer Berlin Heidelberg.

Rayavarapu, R., Petersen, W., Ungureanu, C., Post, J., van Leeuwen, T., & Manohar, S. (2007). Synthesis and bioconjugation of gold nanoparticles as potential molecular probes for light-based imaging techniques. *J Biomed Imaging,* 2007(1), 5-5.

Roberts, A. P., Mount, A. S., Seda, B., Souther, J., Qiao, R., Lin, S., Ke, P., Rao, A. & Klaine, S. (2007). *In vivo* biomodification of lipid-coated carbon nanotubes by *Daphnia magna. Environ Sci Technol,* 41(8), 3025-3029.

Robichaud, C., Uyar, A., Darby, M., Zucker, L., & Wiesner, M. (2009). Estimates of upper bounds and trends in nano-TiO_2 production as a basis for exposure assessment. *Environ Sci Technol,* 43(12), 4227-4233.

Rodea-Palomares, I., Boltes, K., Fernández-Piñas, F., Leganés, F., García-Calvo, E., Santiago, J., & Rosal, R. (2011). Physicochemical characterization and ecotoxicological assessment of CeO_2 nanoparticles using two aquatic microorganisms. *Toxicol Sci,* 119(1), 135-145.

Rogers, N., Franklin, N., Apte, S., Batley, G., Angel, B., Lead, J., & Baalousha, M. (2010). Physico-chemical behaviour and algal toxicity of nanoparticulate CeO_2 in freshwater. *Environ Chem,* 7(1), 50-60.

Rosenkranz, P., Chaudhry, Q., Stone, V., & Fernandes, T. (2009). A Comparison of nanoparticle and fine particle uptake by *Daphnia magna*. *Environ Toxicol Chem,* 28(10), 2142-2149.

Sakthivel, T., & Florence, A. (2003). Dendrimers and dendrons: facets of pharmaceutical nanotechnology. *Drug Deliv Technol*, 3(5), 50-60.

Sayre, P., Prothero, S., & Alwood, J. (2011). Nanomaterial risk assessment and management experiences related to worker health under the toxic substances control act. *J Occup Environ Med,* 53, S98-S102.

SCENIHR 2005. The appropriateness of existing methodologies to assess the potential risks associated with engineered and adventitious products of nanotechnologies. *Scientific Committee on Emerging Newly Identified Health Risks, EUROPEAN COMMISSION.*

Schaller, M., & Fan, Y. (2009). River basins as groundwater exporters and importers: Implications for water cycle and climate modeling. *J Geophys Rea,* 114(D4), D04103.

Scown, T., Van Aerle, R., & Tyler, C. (2010). Review: Do engineered nanoparticles pose a significant threat to the aquatic environment? *Crit Re Toxicol,* 40(7), 653-670.

Seaton, A., Tran, L., Aitken, R., & Donaldson, K. (2009). Nanoparticles, human health hazard and regulation. *J R Soc Interface,* 7 Suppl 1, S119-29.

Sharma, V. (2009). Aggregation and toxicity of titanium dioxide nanoparticles in aquatic environment-A Review. *J Environ Sci Health Part A,* 44(14), 1485-1495.

Siegfried, B., & Som, C. (2007). Nanotextiles: functions, nanoparticles and commercial applications. *Semester thesis in the frame of Nanosafe Textiles Project, TVS Textilverband and Empa.*

Sillanpää, M., Paunu, T. M., & Sainio, P. (2011). Aggregation and deposition of engineered TiO2 nanoparticles in natural fresh and brackish waters. In *Journal of Physics: Conference Series* (Vol. 304, No. 1, p. 012018). IOP Publishing.

Simon-Deckers, A., Loo, S., Mayne-L'hermite, M., Herlin-Boime, N., Menguy, N., Reynaud, C., Gouget, B., & Carrière, M. (2009). Size-, composition-and shape-dependent toxicological impact of metal oxide nanoparticles and carbon nanotubes toward bacteria. *Environ Sci Technol,* 43(21), 8423-8429.

Simonet, B., & Valcárcel, M. (2009). Monitoring nanoparticles in the environment. *Anal and Bioanal Chem,* 393(1), 17-21.

Smith, C., Shaw, B., & Handy, R. (2007) Toxicity of single walled carbon nanotubes to rainbow trout (*Oncorhynchus mykiss*): Respiratory toxicity, organ pathologies, and other physiological effects. *Aquat toxicol,* 82(2), 94-109.

Solomon, K., Giesy, J., & Jones, P. (2000). Probabilistic risk assessment of agrochemicals in the environment. *Crop Prot,* 19(8), 649-655.

Springer, T., Guiney, P., Krueger, H., & Jaber, M. (2008). Assessment of an approach to estimating aquatic bioconcentration factors using reduced sampling. *Environ Toxicol Chem,* 27(11), 2271-2280.

Stankus, D., Lohse, S., Hutchison, J., & Nason, J. (2011). Interactions between natural organic matter and gold nanoparticles stabilized with different organic capping agents. *Environ Sci Technol,* 45(8), 3238-3244.

Stone, V., Nowack, B., Baun, A., van den Brink, N., von der Kammer, F., Dusinska, M., Handy, R., Hankin, S., Hassell, M., & Fernandes, T. (2010). Nanomaterials for environmental studies: classification, reference material issues, and strategies for physico-chemical characterisation. *Sci Total Environ,* 408(7), 1745-1754.

Suttiponparnit, K., Jiang, J., Sahu, M., Suvachittanont, S., Charinpanitkul, T., & Biswas, P. (2011). Role of surface area, primary particle size, and crystal phase on titanium dioxide nanoparticle dispersion properties. *Nanoscale Res lett,* 6(1), 1-8.

Tan, C., Fan, WH., Wang, W. (2012). Role of titanium dioxide nanoparticles in the elevated uptake and retention of cadmium and zinc in *Daphnia magna*. *Environ Sci Technol*, 46, 469-476.

Tao, X., Fortner, J. D., Zhang, B., He, Y., Chen, Y., & Hughes, J. B. (2009). . Effects of aqueous stable fullerene nanocrystals (nC$_{60}$) on *Daphnia magna*: Evaluation of sub-lethal reproductive responses and accumulation. *Chemosphere,* 77(11), 1482-1487.

Terrones, M. (2003). Science and technology of the twenty-first century: synthesis, properties, and applications of carbon nanotubes. *Annu Rev Mater Res,* 33(1), 419-501.

Thio, B., Zhou, D., & Keller, A. (2011). Influence of natural organic matter on the aggregation and deposition of titanium dioxide nanoparticles. *J Hazard Mater,* 189(1), 556-563.

Tiede, K. (2008). *Detection and fate of engineered nanoparticles in aquatic systems.* Ph.D. thesis, University of York.

Tiede, K., Hassellöv, M., Breitbarth, E., Chaudhry, Q., & Boxall, A. (2009). Considerations for environmental fate and ecotoxicity testing to support environmental risk assessments for engineered nanoparticles. *J Chromatogr A,* 1216(3), 503-509.

Tufenkji, N., & Elimelech, M. (2004) Deviation from the classical colloid filtration theory in the presence of repulsive DLVO interactions. *Langmuir,* 20(25), 10818-10828.

UNEP 2007 *Chapter 7: Emerging challenges-nanotechnology and the environment* Nairobi, Kenya, United Nations Environment Programme Division of Early Warning and Assessment.

USEPA 1991. *Methods for measuring the acute toxicity of effluents and receiving waters to freshwater and marine organisms*, Environmental Monitoring Systems Laboratory, Office of Research and Development, US Environmental Protection Agency.

Wang, Z., Li, J., Zhao, J., & Xing, B. (2011). Toxicity and internalization of CuO nanoparticles to prokaryotic alga *Microcystis aeruginosa* as affected by dissolved organic matter. *Envirom Sci Technol,* 45(14), 6032-6040.

Wang GZ, Chen J, Li X, Shao J, Peijnenbrug WJGM. 2012. Aquatic toxicity of nanosilver colloids to different trophic organisms: Contributions of particles and free silver ion. *Environ Toxicol Chem*, 31(10), 2408–2413.

Wang, Y., Miao, A.J., Luo, J., Wei, Z. B., Zhu, J. J., & Yang, L. Y. (2013). Bioaccumulation of CdTe quantum dots in a freshwater alga *Ochromonas danica*: A kinetics study. *Environ Sci Technol*, *47*(18), 10601-10610.

Ward, J., & Kach, D. (2009). Marine aggregates facilitate ingestion of nanoparticles by suspension-feeding bivalves. *Mar environ Res,* 68(3), 137-142.

Wiench, K., Wohlleben, W., Hisgen, V., Radke, K., Salinas, E., Zok, S., & Landsiedel, R. (2009). Acute and chronic effects of nano- and non-nano-scale TiO_2 and ZnO particles on mobility and reproduction of the freshwater invertebrate *Daphnia magna*. *Chemosphere,* 76(10), 1356-1365.

Wigginton, N., Haus, K., & Hochella M. (2007). Aquatic environmental nanoparticles. *J Environ Monitor,* 9(12), 1306-1316.

Yang, S., Bar-Ilan, O., Peterson, R., Heideman, W., Hamers, R., & Pedersen, J. (2013). Influence of humic acid on titanium dioxide nanoparticle toxicity to developing Zebrafish. *Environ Sci Technol,* 47(9), 4718-4725.

Zhang, L., & Monteiro-Riviere, N. (2009). Mechanisms of quantum dot nanoparticle cellular uptake. *Toxicol Sci,* 110(1), 138-155.

Zhang, Y., Chen, Y., Westerhoff, P., & Crittenden, J. (2009). Impact of natural organic matter and divalent cations on the stability of aqueous nanoparticles. *Water Res,* 43(17), 4249-57.

Zhao, C., & Wang, W. (2010). Biokinetic uptake and efflux of silver nanoparticles in *Daphnia magna. Environ Sci Technol,* 44(19), 7699-7740.

Zhu, X., Zhu, L., Chen, Y., & Tian, S. (2009). Acute toxicities of six manufactured nanomaterial suspensions to *Daphnia magna. J Nanopart Res,* 11(1), 67-75.

Zhu, X., Chang, Y., & Chen, Y. (2010). Toxicity and bioaccumulation of TiO_2 nanoparticle aggregates in *Daphnia magna. Chemosphere,* 78(3), 2009-2021.